frontiers | Research Topics

Novel insights into the pathophysiology of diabetes-related complications: Implications for improved therapeutic strategies

Edited by
Jian Ma, Wenxiang Hu, Chunjie Jiang, Xuebin Fu, Jun Chen and Lin Yuan

Published in
Frontiers in Endocrinology

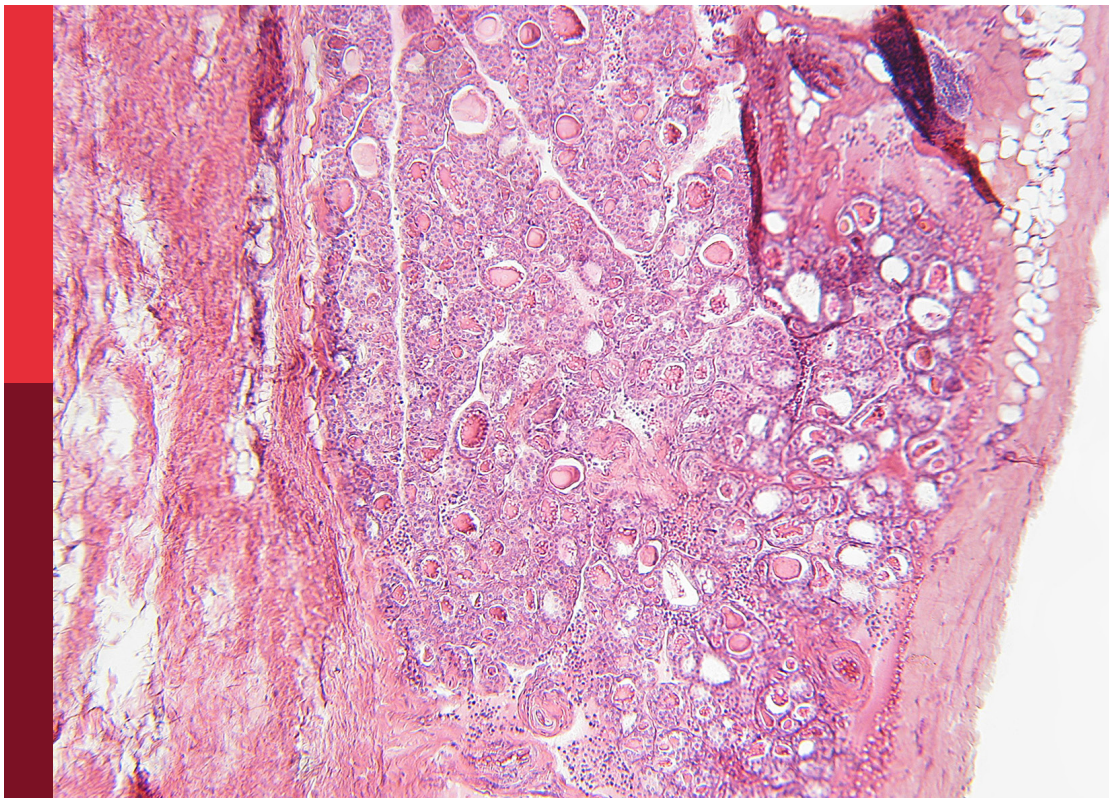

ISSN 1664-8714
ISBN 978-2-83251-927-1
DOI 10.3389/978-2-83251-927-1

About Frontiers

Frontiers is more than just an open access publisher of scholarly articles: it is a pioneering approach to the world of academia, radically improving the way scholarly research is managed. The grand vision of Frontiers is a world where all people have an equal opportunity to seek, share and generate knowledge. Frontiers provides immediate and permanent online open access to all its publications, but this alone is not enough to realize our grand goals.

Frontiers journal series

The Frontiers journal series is a multi-tier and interdisciplinary set of open-access, online journals, promising a paradigm shift from the current review, selection and dissemination processes in academic publishing. All Frontiers journals are driven by researchers for researchers; therefore, they constitute a service to the scholarly community. At the same time, the *Frontiers journal series* operates on a revolutionary invention, the tiered publishing system, initially addressing specific communities of scholars, and gradually climbing up to broader public understanding, thus serving the interests of the lay society, too.

Dedication to quality

Each Frontiers article is a landmark of the highest quality, thanks to genuinely collaborative interactions between authors and review editors, who include some of the world's best academicians. Research must be certified by peers before entering a stream of knowledge that may eventually reach the public - and shape society; therefore, Frontiers only applies the most rigorous and unbiased reviews. Frontiers revolutionizes research publishing by freely delivering the most outstanding research, evaluated with no bias from both the academic and social point of view. By applying the most advanced information technologies, Frontiers is catapulting scholarly publishing into a new generation.

What are Frontiers Research Topics?

Frontiers Research Topics are very popular trademarks of the *Frontiers journals series*: they are collections of at least ten articles, all centered on a particular subject. With their unique mix of varied contributions from Original Research to Review Articles, Frontiers Research Topics unify the most influential researchers, the latest key findings and historical advances in a hot research area.

Find out more on how to host your own Frontiers Research Topic or contribute to one as an author by contacting the Frontiers editorial office: frontiersin.org/about/contact

Novel insights into the pathophysiology of diabetes-related complications: Implications for improved therapeutic strategies

Topic editors

Jian Ma — Harbin Medical University, China
Wenxiang Hu — Guangzhou Laboratory, China
Chunjie Jiang — University of Pennsylvania, United States
Xuebin Fu — Ann & Robert H. Lurie Children's Hospital of Chicago, United States
Jun Chen — Shandong University, China
Lin Yuan — China Medical University, China

Citation

Ma, J., Hu, W., Jiang, C., Fu, X., Chen, J., Yuan, L., eds. (2023). *Novel insights into the pathophysiology of diabetes-related complications: Implications for improved therapeutic strategies*. Lausanne: Frontiers Media SA.
doi: 10.3389/978-2-83251-927-1

Table of contents

frontiers | Frontiers in Endocrinology

TYPE Editorial
PUBLISHED 01 March 2023
DOI 10.3389/fendo.2023.1157807

OPEN ACCESS

EDITED AND REVIEWED BY
Jared Rutter,
The University of Utah, United States

*CORRESPONDENCE
Jian Ma
jma@hrbmu.edu.cn

SPECIALTY SECTION
This article was submitted to Diabetes: Molecular Mechanisms, a section of the journal Frontiers in Endocrinology

RECEIVED 03 February 2023
ACCEPTED 13 February 2023
PUBLISHED 01 March 2023

CITATION
Ma J, Jiang C, Fu X, Chen J, Hu W and Yuan L (2023) Editorial: Novel insights into the pathophysiology of diabetes-related complications: Implications for improved therapeutic strategies.
Front. Endocrinol. 14:1157807.
doi: 10.3389/fendo.2023.1157807

Editorial: Novel insights into the pathophysiology of diabetes-related complications: Implications for improved therapeutic strategies

Jian Ma[1]*, Chunjie Jiang[2], Xuebin Fu[3,4], Jun Chen[5], Wenxiang Hu[6] and Lin Yuan[7]

[1]Department of Immunology, Harbin Medical University, Harbin, China, [2]Department of Genome, University of Texas MD Anderson Cancer Center, Houston, TX, United States, [3]Department of Cardiovascular-Thoracic Surgery, Northwestern University Feinberg School of Medicine, Chicago, IL, United States, [4]Department of Pediatrics, Ann & Robert H. Lurie Children's Hospital, Chicago, IL, United States, [5]Department of Endocrinology, Qilu Hospital, Cheeloo College of Medicine, Shandong University, Jinan, China, [6]Department of Basic Research, Guangzhou Laboratory, Guangzhou, China, [7]Laboratory of Research in Parkinson's Disease and Related Disorders, Health Science Institute, China Medical University, Shenyang, China

KEYWORDS

diabetes, complications, pathophysiology, molecular mechanism, insight

Editorial on the Research Topic

Novel insights into the pathophysiology of diabetes-related complications: Implications for improved therapeutic strategies

Globally, diabetes mellitus (DM) is a significant and prevalent health problem. It is increasingly apparent that not only a cure for the current worldwide diabetes epidemic is required, but also a cure for its major complications, including heart disease, chronic kidney disease, and nerve damage (1). In addition, other problems with feet, oral health, vision, hearing, reproduction, and mental health also need to be explored (2–6). Understanding the underlying mechanisms of these diabetic complications would help prevent or delay the occurrence of complications and to improve the overall health condition of people with DM. To promote the understanding, we were invited by the journal editorial team to organize A Research Topic titled "*Novel Insights into the Pathophysiology of Diabetes-related Complications: Implications for Improved Therapeutic Strategies*". This topic aims to recruit high-quality original research and review articles that contribute to uncovering the intracellular signaling pathways with the development of diabetic complications, or exploring the possible role of genetic issues, metabolic regulation, and inflammation mechanisms. The topic was initiated last spring, May 5th, and closed on Sept 22nd, 2022. During these five months, total 37 submissions, including 25 manuscripts and 12 abstracts, were received. And finally, 10 peer-reviewed articles with high quality were selected and published. These 10 articles cover different issues on diabetes and complications, i.e., diabetic retinopathy (DR), diabetic neuropathy (DN), type 2 diabetes mellitus (T2DM)-associated periodontitis, diabetic oxidative liver damage, diabetic-related wound healing, etc.

To DR, a common and serious microvascular complication of DM, Li et al. performed a study on investigating the correlation between methylation of *THBS1* transcription regulation area and DR occurred. Based on the detection data from recruited patients diagnosed with DR and DM patients without retinal problems, they observed that THBS1 mRNA expression in peripheral blood was significantly higher in DR patients than in DM patients and concluded that *THBS1* overexpression is related to *THBS1* transcription regulation area hypomethylation and may be genetically controlled in DR patients. To another microvascular complication of DM, DN, one research article delineated the underlying mechanisms of dapagliflozin as a potent drug for DN. In this study, Bai et al., revealed that many lncRNA and mRNA expression levels were significantly altered in kidney tissues of dapagliflozin-treated *db/db* mice by combing transcriptome analysis and a network pharmacology approach. Network pharmacology analysis further identified that several genes including SMAD9, PPARG, CD36, and CYP4A12A might be the pivotal targets of dapagliflozin for treating diabetic nephropathy. Taken together, this study provides novel insights into the protective mechanism of dapagliflozin for treating nephropathy. Also, for DN, a study from Cao et al., revealed the role of S-palmitoylation in DN. In the research, the authors analyzed the proteomic data of lumbar dorsal root ganglia (DRG) of diabetic mice and palmitoylation profiling data of the HUVEC cell line, demonstrating that the S-palmitoylation status of Cys47 could affect the interaction between PRDX6 and the C-terminal domain of AE3, thereby regulating the activity of AE3 anion exchanger enzyme in the nervous system, revealing a potential association between activating protein palmitoylation and DN.

In addition, we have one article focused on T2DM-associated periodontitis, a common disease with high prevalence featuring persistent infection and complicated manifestations. Wang et al. used the rat model to mimic T2DM-associated periodontitis, which was found to have an intense inflammatory response and decreased autophagy. In the treatment group, the application of calcitriol, a common supplement, had shown a significant inhibition effect of inflammation and increased autophagy. The study provided a piece of evidence that an easy and daily supplement of calcitriol may provide effective treatment against T2DM-associated periodontitis.

For diabetic-related wound healing issue, Mu et al. focused on the role of pyroptosis in promoting diabetic complications and summarized the underlying mechanisms of pyroptosis in the recovery of diabetic wounds, such as the activation of the NLRP3 inflammasome and other pyroptosis-related signaling pathways, and highlights the potential therapeutic approaches to promoting diabetic-related wound healing *via* targeting these signaling pathways. Besides, a research article from Li et al. comprehensively analyzed differential expression genes in diabetes and depression based on several RNA sequencing datasets from the GEO database and found an interesting target molecule NK1R in the overlapping set. They further designed *in vitro* and *in vivo* experiments to confirm the function of NK1R in angiogenesis, epithelial-mesenchymal transition (EMT), collagen deposition, and inflammation in diabetes and depression. Of note, the *in vivo* experiment data suggested that the downregulation of NK1R promoted vascular proliferation and enhance diabetic wound healing, providing a potential therapeutic target for the management of diabetic non-healing wounds and depression.

Given that the disruption of circadian rhythm is associated with the development of T2DM, Jiang et al., did a comprehensive bioinformatics analysis about the rhythmicity of gene transcription, mature RNA abundance, protein abundance, and DBP activity, presenting a global view of the oscillating genes in multiple layers and indicating the complexity of regulatory mechanisms across different layers for further functional study. In addition, m6A has been demonstrated to be crucial to the development of DM and its complications. To plot the knowledge maps and predict the hotspots and trends in m6A related studies on DM, Zhang et al., used the CiteSpace software to perform a retrospective bibliometric analysis and science mapping. They provided an overview of the trend of publication outputs, countries/regions and institutions distribution, authors, cited authors, cited journals, as well as hotspots and frontiers, which may help us better understand the studies in the field. And most interestingly, one study of current topic show different result from previous research. It's well known that long-term treatment with omega-3 PUFAs, which are CYP2E1 substrates, may affect CYP2E1 expression in the liver, and result in the development of diabetic oxidative liver damage. However, Maksymchuk et al., observed that long-term treatment of diabetic rats with omega-3 PUFAs does not increase the risk of CYP2E1-dependent oxidative stress and development of liver pathology but prevents some diabetic ultrastructural damage to hepatocytes *via* using streptozotocin-induced rat model of type 1 diabetes.

In a word, we believed that the above review or research articles could reflect the research progresses on diabetes and complications and contribute to the academic community. With a limited number of submissions in current topic, we are looking forward to seeing many more academic articles on diabetic complications studies in the future, particulars at other research targets, such as DM-related heart disease, a reproductive disorder in diabetic women (7, 8) or the relationship between diabetes and the development of Alzheimer's disease (9), etc.

Author contributions

All authors listed have made a substantial, direct, and intellectual contribution to the work and approved it for publication.

Conflict of interest

The authors declare that the research was conducted in the absence of any commercial or financial relationships that could be construed as a potential conflict of interest.

Publisher's note

References

1. Zheng Y, Ley SH, Hu FB. Global aetiology and epidemiology of type 2 diabetes mellitus and its complications. *Nat Rev Endocrinol* (2018) 14(2):88–98. doi: 10.1038/nrendo.2017.151

2. Armstrong DG, Boulton AJM, Bus SA. Diabetic foot ulcers and their recurrence. *N Engl J Med* (2017) 376(24):2367–75. doi: 10.1056/NEJMra1615439

3. Northridge ME, Kumar A, Kaur R. Disparities in access to oral health care. *Annu Rev Public Health* (2020) 41:513–35. doi: 10.1146/annurev-publhealth-040119-094318

4. Wong TY, Cheung CM, Larsen M, Sharma S, Simó R. Diabetic retinopathy. *Nat Rev Dis Primers* (2016) 2:16012. doi: 10.1038/nrdp.2016.12

5. Johns EC, Denison FC, Norman JE, Reynolds RM. Gestational diabetes mellitus: Mechanisms, treatment, and complications. *Trends Endocrinol Metab* (2018) 29 (11):743–54. doi: 10.1016/j.tem.2018.09.004

6. Feldman EL, Callaghan BC, Pop-Busui R, Zochodne DW, Wright DE, Bennett DL, et al. Diabetic neuropathy. *Nat Rev Dis Primers* (2019) 5(1):41. doi: 10.1038/s41572-019-0092-1

7. Travers JG, Tharp CA, Rubino M, McKinsey TA. Therapeutic targets for cardiac fibrosis: From old school to next-gen. *J Clin Invest* (2022) 132(5):e148554. doi: 10.1172/jci148554

8. Rajaobelina K, Dow C, Romana Mancini F, Dartois L, Boutron-Ruault MC, Balkau B, et al. Population attributable fractions of the main type 2 diabetes mellitus risk factors in women: Findings from the French E3n cohort. *J Diabetes* (2019) 11 (3):242–53. doi: 10.1111/1753-0407.12839

9. Biessels GJ, Despa F. Cognitive decline and dementia in diabetes mellitus: Mechanisms and clinical implications. *Nat Rev Endocrinol* (2018) 14(10):591–604. doi: 10.1038/s41574-018-0048-7

frontiers | Frontiers in Endocrinology

TYPE Original Research
PUBLISHED 22 July 2022
DOI 10.3389/fendo.2022.955070

OPEN ACCESS

EDITED BY
Yanshan Dai,
Bristol Myers Squibb, United States

REVIEWED BY
Hongyi Zhang,
University of Texas Southwestern Medical Center, United States
Qi Su,
University of California, San Diego, United States
Peng Hu,
Shanghai Ocean University, China

*CORRESPONDENCE
Dongyin Guan
dongyin.guan@bcm.edu

SPECIALTY SECTION
This article was submitted to Diabetes: Molecular Mechanisms, a section of the journal Frontiers in Endocrinology

RECEIVED 28 May 2022
ACCEPTED 27 June 2022
PUBLISHED 22 July 2022

CITATION
Jiang C, Liu P, La CM and Guan D (2022) *In silico* integrative analysis of multi-omics reveals regulatory layers for diurnal gene expression in mouse liver.
Front. Endocrinol. 13:955070.
doi: 10.3389/fendo.2022.955070

In silico integrative analysis of multi-omics reveals regulatory layers for diurnal gene expression in mouse liver

Chunjie Jiang, Panpan Liu, Cam Mong La and Dongyin Guan*

Division of Diabetes, Endocrinology, and Metabolism, Department of Medicine, Baylor College of Medicine, Houston, TX, United States

Diurnal oscillation persists throughout the body and plays an essential role in maintaining physiological homeostasis. Disruption of diurnal rhythm contributes to many diseases including type 2 diabetes. The regulatory mechanism of the transcription-translation feedback loop (TTFL) of core clock genes is well-established, while a systematic study across all regulatory layers of gene expression, including gene transcription, RNA translation, and DNA binding protein (DBP) activities, is still lacking. We comprehensively bioinformatics analyzed the rhythmicity of gene transcription, mature RNA abundance, protein abundance and DBP activity using publicly available omic-datasets from mouse livers. We found that the core clock genes, *Bmal1* and *Rev-erbα*, persistently retained rhythmicity in all stages, which supported the essential rhythmic function along with the TTFL. Interestingly, there were many layer-specific rhythmic genes playing layer-specific rhythmic functions. The systematic analysis of gene transcription rate, RNA translation efficiency, and post-translation modification of DBP were incorporated to determine the potential mechanisms for layer-specific rhythmic genes. We observed the gene with rhythmic expression in both mature RNA and protein layers were largely due to relatively consistent translation rate. In addition, rhythmic translation rate induced the rhythms of protein whose mature RNA levels were not rhythmic. Further analysis revealed a phosphorylation-mediated and an enhancer RNA-mediated cycling regulation between the corresponding layers. This study presents a global view of the oscillating genes in multiple layers *via* a systematical analysis and indicates the complexity of regulatory mechanisms across different layers for further functional study.

KEYWORDS

diurnal rhythm, multi-omics analysis, liver, gene expression, regulatory layer

Introduction

Diurnal rhythms are approximate 24-hour cycles in which there are regular light and dark periods (1). These rhythms are critical to maintaining physiological homeostasis *via* aligning the internal clock with daily environmental changes, such as light and temperature (2, 3). The disruption of diurnal rhythms due to shift work or sedentary lifestyle leads to many diseases, including metabolic disorders and various cancers (4–6) and is associated with the development of type 2 diabetes, a global health problem (7, 8). Understanding the regulatory mechanism underlying diurnal rhythms could shed light on potential chrono-therapeutic strategies and druggable targets.

Several transcription activators and repressors form the transcription-translation feedback loop (TTFL). The transcription activators include brain and muscle ARNT-like 1 (BAML1) and circadian locomotor output cycles kaput (CLOCK), and transcription repressors include REV-ERB (9–12). Due to the central role of TTFL in the expression of core clock genes, TTFL is considered to be the universal building block of circadian clocks (13). In addition to core clock genes, the question of how oscillating genes are regulated is still largely unknown.

With advanced technologies of next-generation sequencing and mass spectrometry, emerging studies established genome-wide datasets regarding oscillating enhancer activity (4, 14), gene transcription (14), mature RNA abundance (15), protein level (16–18), and DNA binding protein (DBP) activity (18). Moreover, the rhythms of mature RNA translation rate (19) and phosphorylation (20) have been recently measured. These datasets provide us an opportunity to systematically determine the conservativity and specificity of diurnal rhythm for gene expression in various layers, including RNA transcription, processing translation, and protein post-translation modification and activities. The pathways enriched in layer-specific rhythmic genes and related regulators from the current integrative analysis of multi-omics will facilitate our further understanding on the regulatory mechanism of diurnal rhythms in the liver.

Materials and methods

Data source

To determine the rhythmicity of gene expression in different layers, we obtained raw datasets of gene transcription (14) and mature RNA (15) and collected expression of protein (16–18). Moreover, we also gathered the ribosome profiling (Ribo-seq) dataset for qualifying RNA translation rate (19) and proteomic datasets for DBP (18) and protein phosphorylation (20). Only proteins detected in all three independent datasets (14–16) were considered for downstream analysis to get highly confident expressed proteins in the liver. The raw data was extracted from publicly available sources, as indicated in Table 1. All datasets were selected from mouse liver tissue that was harvested from multiple time points across light-dark cycles.

Global run-on sequencing data processing

Raw reads were trimmed using fastp v0.23.1 (21). Clean reads were then mapped to the mouse genome (mm10) using Bowtie2 v2.4.1 (22). Samtools v1.14 (23) was used to extract unique mapped reads, followed by the generation of bigwig files using Homer v4.9 (24), which were further visualized on Integrative Genomics Viewer (IGV) (25).

RNA-seq data processing

RNA-seq data was processed following the pipeline described previously (9, 26, 27). Briefly, raw reads were trimmed using fastp v0.23.1 (21). Clean reads were then mapped to the mouse genome (mm10) using Hisat2 v2.1.0 (28) with default parameters. Unique reads were extracted using samtools v1.14 (23). Read counts were calculated and normalized to reads per kilobase of exon per million reads mapped (RPKM) using Homer v4.9 (24).

TABLE 1 Omics data sets across TTFL.

Profile	Library	Time point	Reference
Transcription	GRO-seq	8	(14)
Mature RNA	RNA-seq	8	(15)
Protein	MS	8, 8, 8	(16–18)
DBP	CatTFRE pull-down +MS	8	(18)
Enhancer RNA	GRO-seq	8	(14)
Translation rate	RNA-seq; Ribo-seq	8;12	(15, 19)
Phosphorylation	MS	8	(20)

GRO-seq, Global Run-On Sequencing. MS, Mass spectrometry. DBP, DNA binding protein. CatTFRE, concatenated tandem array of the consensus TFREs. Ribo-seq, Ribosome profiling.

Ribo-seq data processing

Ribo-seq data was processed following the pipeline described previously (19). Briefly, adapter sequences were removed using cutadapt v4.0 (29) with parameters, -a ;AGATCGGAAGAGCACACGTCTGAACTCCAGTCAC –match-read-wildcards -m 6, followed by further trimming and size-filtered (lengths 26-35 nt) using fastp v0.23.1 (21). Trimmed reads were mapped to the mouse genome (mm10) using Bowtie2 v2.4.1 (22). Unique reads were extracted using samtools v1.14 (23). Read counts were calculated and normalized to reads per kilobase of exon per million reads mapped (RPKM) using Homer v4.9 (24). The translation rate was calculated using an in-house Perl script which has been deposited on GitHub at https://github.com/ChunjieJiang/Multi-Omics_CircadianRhythm_RegulatoryLayers.

Quantification of transcription rate

We used pre-RNA abundance to quantify the transcription rate. The pre-RNA identified from GRO-Seq was measured following the pipeline described previously (14, 15). Briefly, transcripts were measured using GRO-Seq unique mapped reads. For genes with annotated body length > 12kb, a 10kb window (+2kb to 12kb) was considered for quantification. Genes with annotated body length between 2kb and 12kb were quantified using the window from +2kb to the transcription end site (TES). While for genes shorter than 2kb, the whole gene body was used to do the quantification. Reads from each gene were normalized to reads per kb per ten million reads (RPKTM).

Quantification of protein from western blot

As a technological limitation of mass spectrometry, some clock genes (e.g., *Bmal1* and *Rev-erb*) could not be detected. The diurnal rhythms of these proteins were indicated by western blot from multiple studies (30–32). Image J (version 1.51, NIH) was used to quantify the relative expression in protein levels across light-dark cycles based on the data from Western Blot.

De novo identification of enhancer RNA

Enhancer RNAs were identified following the pipeline described previously (14, 33). Briefly, unique mapped reads from GRO-Seq were separated into the reads mapped to the plus and minus strands, followed by peak calling using Homer v4.9 (24). Peaks with FDR < 0.001 and fold changes > 3 were considered. Sites located within 300bp of annotated TSSs were excluded. Reads mapped within 500bp away from an enhancer RNA locus center were extracted and normalized to RPKTM.

Identification of oscillation genes

To determine the rhythmic transcription, mature RNA, protein, DNA binding protein (DBP), enhancer RNA, and translational rate, JTK_CYCLE tests (34) were performed with period range 20-28 h and the amplitude and phase as free parameters. The JTK_CYCLE algorithm calculates the p-value using Kendall's tau correlation, and then the p-values would be adjusted by Bonferroni correction. This allowed for thorough identification of circadian patterns. Rhythmic transcription, mature RNA, enhancer RNA, and translational rate were defined as those with JTK_CYCLE adj-p value < 0.05. For protein and DNA-binding protein, the statistical cut-off of JTK_CYCLE adj-p value < 0.1 was used as suggested by Wang et al. (18).

Results

Strategy to dissect regulatory layers for diurnal gene expression

To systematically investigate the complexity and specificity of diurnal gene expression in different regulatory layers, we first quantified the expression level of RNA transcription, mature RNA abundance, and protein abundance, as well as DNA binding activity of DBP (Figure 1). The rhythmicity analysis pipeline was uniformed by using JKT_CYCLE. To explore the potential mechanisms of the specificity of oscillating genes in each layer, we determined the impacts of enhancer activity, translation efficiency, and protein post-translational modification in the counterpart adjacent layers. In sum, this pipeline allows us to globally investigate the full spectrum of gene expression regulatory layers.

Identification of rhythmic genes in each regulatory layer

With the above pipeline, the rhythmic gene transcription, mature RNA abundance, protein abundance, and DPB with rhythmic DNA binding activity were identified (Figure 2A). The rhythms of these genes in these four layers were further confirmed using principal component analysis (PCA). The temporally annotated samples in each layer were correctly ordered with non-supervised information (Figures 2B–E).

Interestingly, we observed 60% of genes with rhythmic transcription stayed rhythmic as mature RNA and 56% of

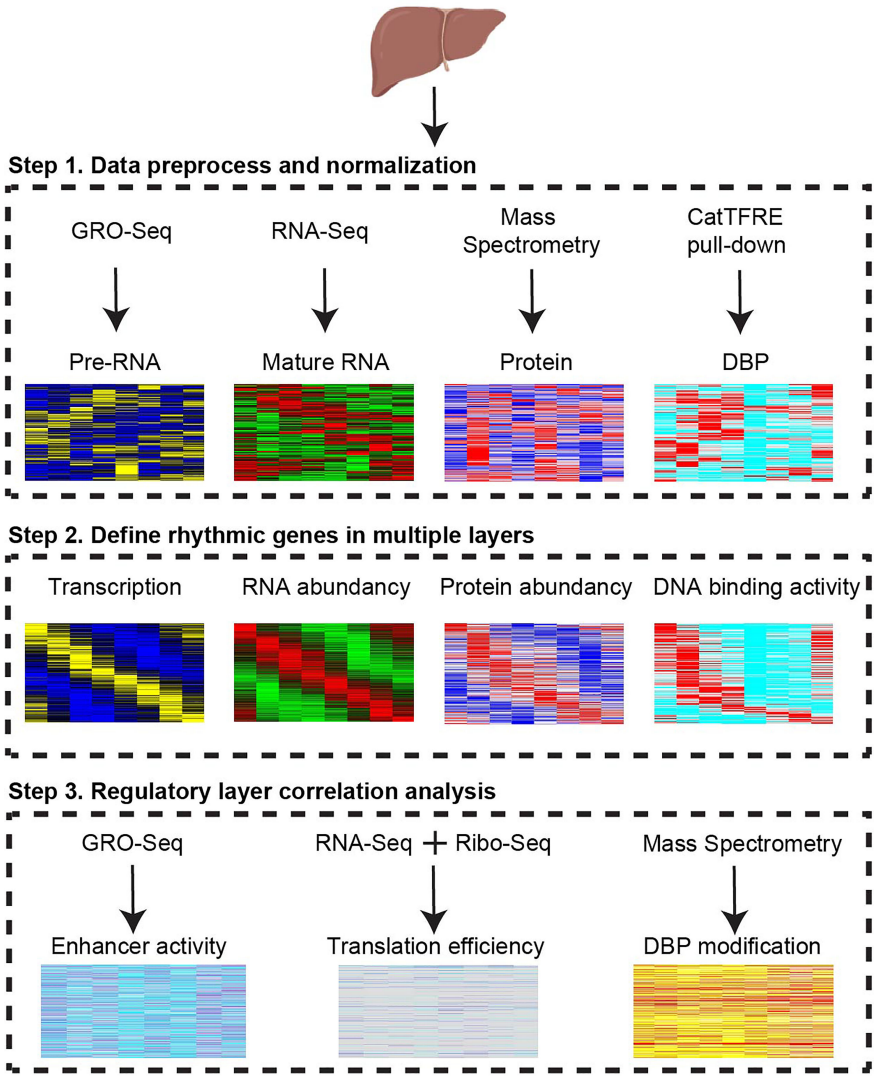

FIGURE 1
Strategy to dissect regulatory layers for diurnal gene expression. Multi-omics profiles from transcription, mature RNA, protein, DNA binding protein, enhancer RNA, translation rate, and phosphorylation were integrated to reveal multiple rhythmic regulatory layers. CatTFRE, concatenated tandem array of the consensus TFREs. DBP, DNA binding protein. GRO-seq, Global Run-On Sequencing. Ribo-seq, Ribosome profiling.

rhythmic protein retained rhythmicity from mature RNA, while only 30% of DBP kept rhythmic DNA binding activity (Figure 3A). The core clock genes exampled by *Bmal1* and *Rev-erbα* maintain their rhythmicity across all four layers (Figures 3B, C). To further check the function of the reserved rhythmic genes between adjacent layers, functional enrichment analysis was performed using Enrichr (35) based on BioPlanet (36). As expected, pathways involving circadian rhythm and lipid metabolism were enriched for genes with reserved rhythmicity between pre-RNA and mature RNA levels, as well as the ones between mature RNA and protein levels (Figures 3D, E).

Layer-specific rhythmic genes support the layer-specific function

Remarkably, besides the conserved rhythmic genes between adjacent layers, we also observed many rhythmic disrupted or enhanced genes in a specific layer. Moreover, genes with rhythmic signals in transcription rate, and non-rhythmic signals in mature RNA level (Figure 4A, left panel) were involved in the pathway related to transcription, endocytosis, etc. (Figure 4B, upper panel). Conversely, genes with enhanced rhythmic signals in mature RNA level (Figure 4A, right panel) were enriched in metabolism and amino acids metabolism

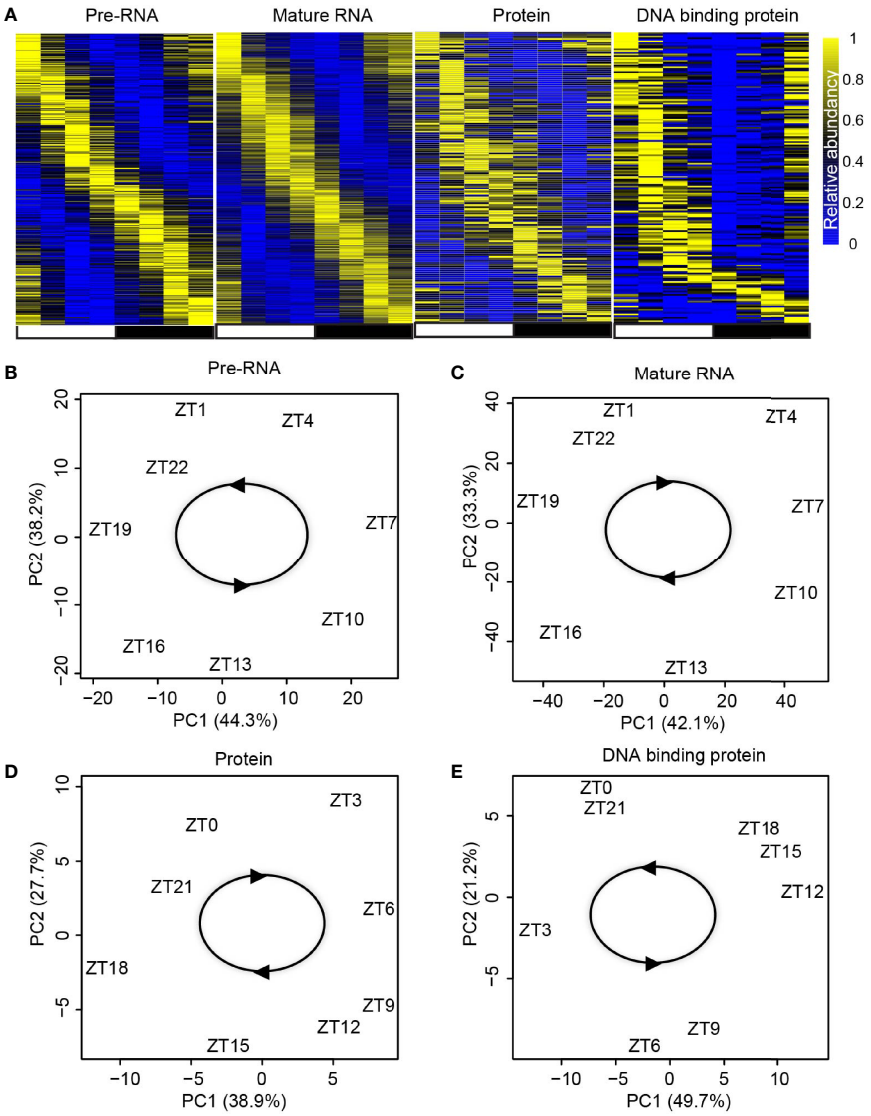

FIGURE 2
Identification of rhythmic genes in each regulatory layer. **(A)** Heatmap shows the expression/activity of rhythmic genes at transcription, mature RNA, protein, and DBP levels. **(B–E)** Principal component analysis (PCA) for the dataset from transcription **(B)**, mature RNA **(C)**, protein **(D)**, and DBP **(E)** levels.

biological process (Figure 4B, bottom panel). Further analysis on the comparison between mature RNA and protein levels showed that genes playing a function in biological processes such as metabolism and amino acids metabolism (Figure 4D, upper panel) were rhythm disrupted genes in protein level (Figure 4C, left panel), whereas rhythm enhanced genes (Figure 4C, right panel) were involved in TCA cycle and mitochondrial fatty acid metabolism (Figure 4D, bottom panel). Altogether, in addition to the rhythmic conserved genes and pathways, there are other regulatory mechanisms mediating the layer-specific oscillating genes.

Translation rate, post-translational modification, and epigenetic effect contribute to the layer-specific diurnal rhythm

To extend our understanding on the changes of rhythmic expression between mature RNA and protein levels, bulk RNA-seq and Mass Spectrometry data were integrated with Ribo-seq, a technique that can be used to determine translation efficiency (37, 38). The genes with conserved rhythmic expression in both levels showed a much lower variation of translation rate

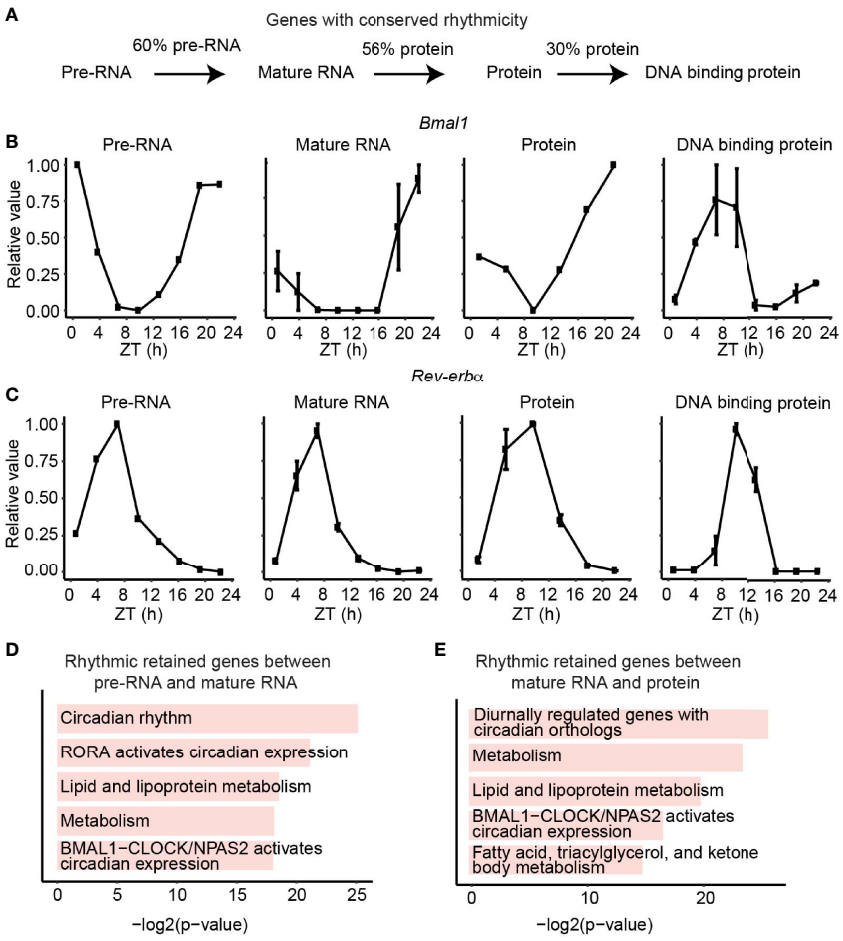

FIGURE 3
Rhythmic retained genes between adjacent layers. **(A)** The fraction of conserved rhythmic genes between adjacent layers. **(B, C)** The expression/activity of conserved rhythmic gene *Bmal1* **(B)** and *Rev-erbα* (C) at transcription, mature RNA, protein, and DBP level. **(D, E)** Bar plots show the enriched pathways of conserved rhythmic genes between transcription and mature RNA levels **(D)**, and the conserved rhythmic genes between mature RNA and protein levels **(E)**. Only genes detected in both adjacent layers were considered.

compared to the ones with disrupted rhythmic expression in protein level (Figure 5A), implying that genes with rhythmic expression in both mature RNA and protein layers were largely due to the relatively consistent translation rate. Moreover, 45% of the protein-specific rhythmic genes were rhythmic translational rate dependent (Figure 5B), indicating that rhythmic translational rate induces the rhythms of protein whose mature RNA levels were not rhythmic.

Protein undergoes post-translational modifications (e.g., phosphorylation) to control its stability, activity, interaction, nuclear localization, and function in different biological processes (39, 40). By integrating the phosphorylation profile, we found that 62% of DBP-specific rhythmic genes are phosphorylation-dependent (Figure 5C). Enhancers are known to initiate the transcription of nearby or distal genes together with DBP (e.g., transcriptional factors). To interpret the rhythmic gap from DBP to transcription, enhancer RNA profile from the GRO-seq dataset was investigated. We found there were many rhythmic DBP regulating rhythmic transcription rate through rhythmic enhancer activities (Figure 5D). This data indicated a phosphorylation-dependent and an enhancer-dependent regulation on rhythmic expression between the adjacent layers.

Discussion

Oscillating gene expression is essential for diurnal rhythmic physiology (41, 42). Previous studies on the regulation of oscillating gene expression focused on the regulatory

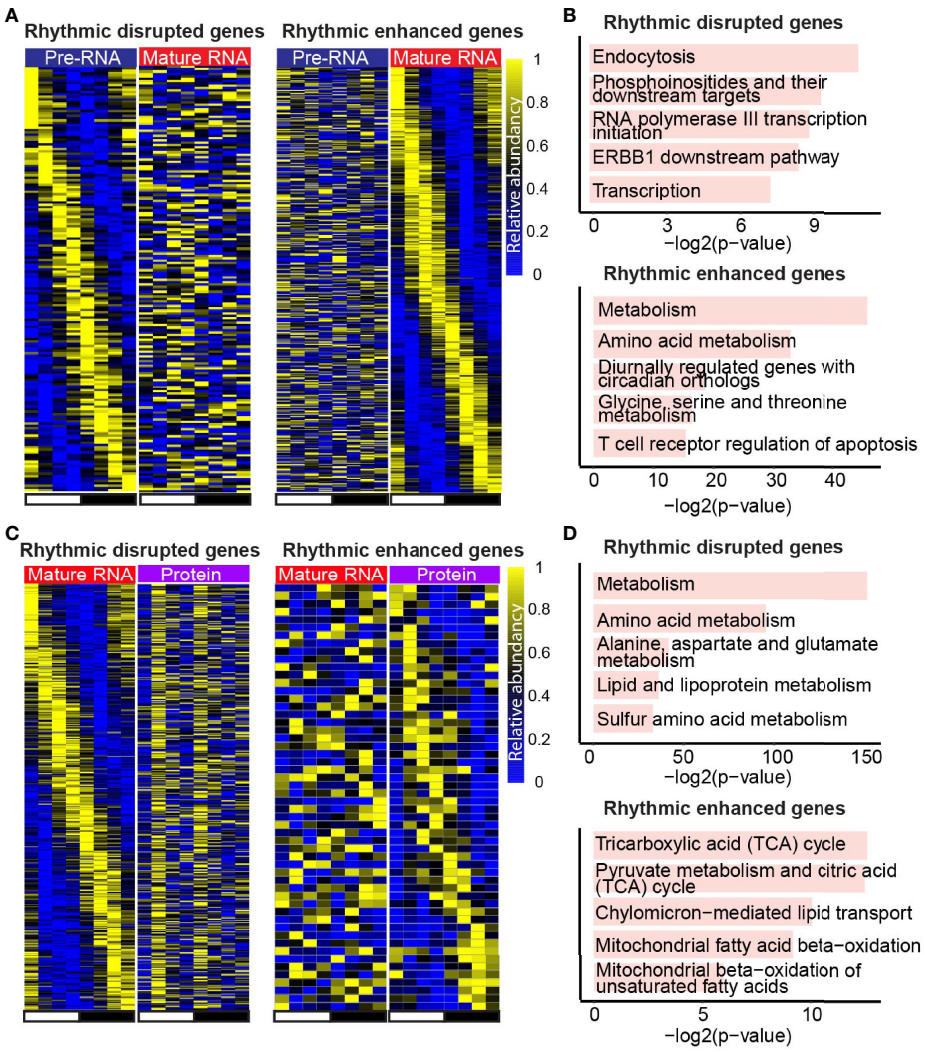

FIGURE 4
Layer-specific rhythmic genes support the layer-specific function. **(A, C)** Heatmaps show the expression of rhythmic disrupted genes (left panel) and rhythmic enhanced genes (right panel) at mature RNA level compared with transcription **(A)**, and the ones in protein level compared with mature RNA **(C)**. **(B, D)** Bar plots show the enriched pathways of rhythmic disrupted genes (top panel) and rhythmic enhanced genes (bottom panel) in mature RNA level compared with transcription **(B)**, and the ones in protein level compared with mature RNA **(D)**. Only genes detected in both adjacent layers were considered.

mechanisms between adjacent layers, including transcription rate-mature RNA (19), mature RNA-protein abundance (17), and protein-DNA binding actives pairs (18). The current study provided a full spectrum of regulatory layers on oscillating gene expression, from enhancer activity, transcription, translation, and post-translation modification to the DNA binding activity of DBP. The identification of layer-specific oscillating genes indicates the underlying layer-specific regulatory mechanisms, including RNA-processing, translation efficiency control, post-translational modification, and enhancer actives. Further global studies about RNA stability and protein stability could provide additional insights for layer-specific regulation of oscillating gene expression.

Our integrative analysis of multiple omics represents an example of an in-depth dissection of the complexity and specificity of diurnal rhythms. This comprehensive pipeline has proved to be a powerful tool and enabled us to identify related pathways and potential regulators in each layer. These results are supported by different oscillating omics datasets in mouse livers: (1) epigenomics and transcriptomics profiling identified the regulatory layers between enhancer and gene transcription; (2) transcriptomics and proteomics profiling

10.3389/fendo.2022.955070

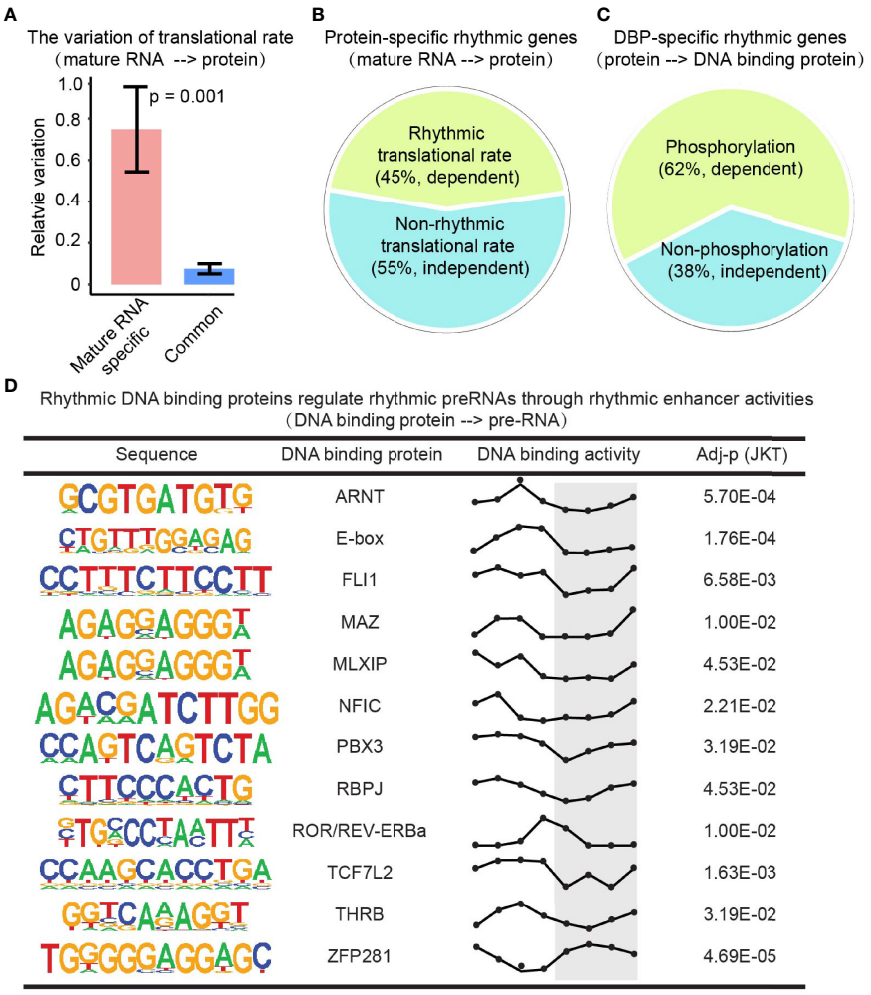

FIGURE 5
Translation rate, post-translational modification, and epigenetic effect contribute to the layer-specific diurnal rhythm. **(A)** Bar plot shows the variation of translation rates of mature RNA-specific rhythmic genes and the conserved rhythmic genes. P value comes from Student's t-test. **(B)** Protein-specific rhythmic genes with rhythmic (olive green) or non-rhythmic (cadet blue) translational rate. **(C)** DBP-specific rhythmic genes that were phosphorylated (olive green) or not (cadet blue). **(D)** The DBPs with rhythmic activities regulate rhythmic transcription through rhythmic enhancer activities. The Y axis in the third column present the DNA binding activities. And the X axis present the Zeitgeber time (ZT), a standardized 24-hour notation of the phase in an entrained circadian cycle. ZT0 is the time that light is turned on and ZT12 is the time that light is turned off.

defined the regulatory layers between mature RNA and protein; (3) ribosome profiling was integrated to determine the potential mechanism for the rhythmic remodeling between above two layers; (4) protein, DBP, and phosphoproteomics profiling comprehensively indicated the role of post-translational modification of DBP activities; 5) DBP proteomics and epigenomics profiling determined the rhythmic regulation of transcription factors on enhancer activities. These omics form a regulatory loop for diurnal rhythmic gene expression. Future hypothesis-driven functional studies are required to determine the layer-specific regulators, which could provide novel targets for the manipulation of diurnal rhythms.

Data availability statement

The datasets presented in this study can be found in publications. The full citations of these publications can be found in the article/supplementary material.

Author contributions

CJ and DG conceptualized the study, interpreted data, and wrote the manuscript, which was approved by all authors. PL helped generate part of the omics profiles. CL assisted with

writing and technical support. All authors contributed to the article and approved the submitted version.

Funding

This work was supported by Cancer Prevention and Research Institute of Texas (RR210029, DG), as well as by National Institutes of Health grants (K01-DK125602, DG and pilot award DK056338, DG).

Acknowledgments

We thank H. Xu and S. Yu for their technical support and valuable discussions.

Conflict of interest

The authors declare that the research was conducted in the absence of any commercial or financial relationships that could be construed as a potential conflict of interest.

Publisher's note

References

1. Bass J, Lazar MA. Circadian time signatures of fitness and disease. *Science* (2016) 354:994–9. doi: 10.1126/SCIENCE.AAH4965

2. Gerhart-Hines Z, Feng D, Emmett MJ, Everett LJ, Loro E, Briggs ER, et al. The nuclear receptor rev-erbα controls circadian thermogenic plasticity. *Nature* (2013) 503:410–3. doi: 10.1038/nature12642

3. Bunger MK, Wilsbacher LD, Moran SM, Clendenin C, Radcliffe LA, Hogenesch JB, et al. Mop3 is an essential component of the master circadian pacemaker in mammals. *Cell* (2000) 103:1009–17. doi: 10.1016/S0092-8674(00)00205-1

4. Guan D, Xiong Y, Borck PC, Jang C, Doulias PT, Papazyan R, et al. Diet-induced circadian enhancer remodeling synchronizes opposing hepatic lipid metabolic processes. *Cell* (2018) 174:831–42.e12. doi: 10.1016/j.cell.2018.06.031

5. Sutton EF, Beyl R, Early KS, Cefalu WT, Ravussin E, Peterson CM. Early time-restricted feeding improves insulin sensitivity, blood pressure, and oxidative stress even without weight loss in men with prediabetes. *Cell Metab* (2018) 27:1212–21.e3. doi: 10.1016/J.CMET.2018.04.010

6. Masri S, Papagiannakopoulos T, Kinouchi K, Liu Y, Cervantes M, Baldi P, et al. Lung adenocarcinoma distally rewires hepatic circadian homeostasis. *Cell* (2016) 165:896–909. doi: 10.1016/J.CELL.2016.04.039

7. Vetter C, Dashti HS, Lane JM, Anderson SG, Schernhammer ES, Rutter MK, et al. Night shift work, genetic risk, and type 2 diabetes in the UK biobank. *Diabetes Care* (2018) 41:762–9. doi: 10.2337/DC17-1933

8. Mokhlesi B, Temple KA, Tjaden AH, Edelstein SL, Utzschneider KM, Nadeau KJ, et al. Association of self-reported sleep and circadian measures with glycemia in adults with prediabetes or recently diagnosed untreated type 2 diabetes. *Diabetes Care* (2019) 42:1326–32. doi: 10.2337/DC19-0298

9. Dierickx P, Emmett MJ, Jiang C, Uehara K, Liu M, Adlanmerini M, et al. SR9009 has REV-ERB–independent effects on cell proliferation and metabolism. *Proc Natl Acad Sci U S A* (2019) 116:12147–52. doi: 10.1073/pnas.1904226116

10. McDearmon EL, Patel KN, Ko CH, Walisser JA, Schook AC, Chong JL, et al. Dissecting the functions of the mammalian clock protein BMAL1 by tissue-specific rescue in mice. *Sci (1979)* (2006) 314:1304–8. doi: 10.1126/SCIENCE.1132430

11. Nakahata Y, Kaluzova M, Grimaldi B, Sahar S, Hirayama J, Chen D, et al. The NAD+-dependent deacetylase SIRT1 modulates CLOCK-mediated chromatin remodeling and circadian control. *Cell* (2008) 134:329–40. doi: 10.1016/J.CELL.2008.07.002

12. Asher G, Gatfield D, Stratmann M, Reinke H, Dibner C, Kreppel F, et al. SIRT1 regulates circadian clock gene expression through PER2 deacetylation. *Cell* (2008) 134:317–28. doi: 10.1016/J.CELL.2008.06.050

13. Brown SA, Kowalska E, Dallmann R. (Re)inventing the circadian feedback loop. *Dev Cell* (2012) 22:477–87. doi: 10.1016/J.DEVCEL.2012.02.007

14. Fang B, Everett LJ, Jager J, Briggs E, Armour SM, Feng D, et al. Circadian enhancers coordinate multiple phases of rhythmic gene transcription *in vivo*. *Cell* (2014) 159:1140–52. doi: 10.1016/j.cell.2014.10.022

15. Guan D, Xiong Y, Trinh TM, Xiao Y, Hu W, Jiang C, et al. The hepatocyte clock and feeding control chronophysiology of multiple liver cell types. *Sci (1979)* (2020) 369:1388–95. doi: 10.1126/SCIENCE.ABA8984

16. Mauvoisin D, Wang J, Jouffe C, Martin E, Atger F, Waridel P, et al. Circadian clock-dependent and -independent rhythmic proteomes implement distinct diurnal functions in mouse liver. *Proc Natl Acad Sci U S A* (2014) 111:167–72. doi: 10.1073/pnas.1314066111

17. Robles MS, Cox J, Mann M. *In-vivo* quantitative proteomics reveals a key contribution of post-transcriptional mechanisms to the circadian regulation of liver metabolism. *PLoS Genet* (2014) 10:e1004047. doi: 10.1371/journal.pgen.1004047

18. Wang Y, Song L, Liu M, Ge R, Zhou Q, Liu W, et al. A proteomics landscape of circadian clock in mouse liver. *Nat Commun* (2018) 9:1553. doi: 10.1038/s41467-018-03898-2

19. Janich P, Arpat AB, Castelo-Szekely V, Lopes M, Gatfield D. Ribosome profiling reveals the rhythmic liver translatome and circadian clock regulation by upstream open reading frames. *Genome Res* (2015) 25:1848–59. doi: 10.1101/gr.195404.115

20. Robles MS, Humphrey SJ, Mann M. Phosphorylation is a central mechanism for circadian control of metabolism and physiology. *Cell Metab* (2017) 25:118–27. doi: 10.1016/j.cmet.2016.10.004

21. Chen S, Zhou Y, Chen Y, Gu J. Fastp: an ultra-fast all-in-one FASTQ preprocessor. *Bioinformatics* (2018) 34:i884–90. doi: 10.1093/BIOINFORMATICS/BTY560

22. Langmead B, Salzberg SL. Fast gapped-read alignment with bowtie 2. *Nat Methods* (2012) 9:357–9. doi: 10.1038/nmeth.1923

23. Li H, Handsaker B, Wysoker A, Fennell T, Ruan J, Homer N, et al. The sequence Alignment/Map format and SAMtools. *Bioinformatics* (2009) 25:2078. doi: 10.1093/BIOINFORMATICS/BTP352

24. Heinz S, Benner C, Spann N, Bertolino E, Lin YC, Laslo P, et al. Simple combinations of lineage-determining transcription factors prime cis-regulatory elements required for macrophage and b cell identities. *Mol Cell* (2010) 38:576–89. doi: 10.1016/J.MOLCEL.2010.05.004

25. Robinson JT, Thorvaldsd Ottir H, Wenger AM, Zehir A, Mesirov JP. Variant review with the integrative genomics viewer. *Cancer Res* (2017) 77:e31-e34. doi: 10.1158/0008-5472.CAN-17-0337

26. Hu W, Jiang C, Guan D, Dierickx P, Zhang R, Moscati A, et al. Patient adipose stem cell-derived adipocytes reveal genetic variation that predicts antidiabetic drug response. *Cell Stem Cell* (2019) 24:299–308.e6. doi: 10.1016/j.stem.2018.11.018

27. Hu W, Jiang C, Kim M, Yang W, Zhu K, Guan D, et al. Individual-specific functional epigenomics reveals genetic determinants of adverse metabolic effects of glucocorticoids. *Cell Metab* (2021) 33:1592–609.e7. doi: 10.1016/j.cmet.2021.06.004

28. Kim D, Paggi JM, Park C, Bennett C, Salzberg SL. Graph-based genome alignment and genotyping with HISAT2 and HISAT-genotype. *Nat Biotechnol* (2019) 37:907–15. doi: 10.1038/S41587-019-0201-4

29. Martin M. Cutadapt removes adapter sequences from high-throughput sequencing reads. *EMBnet J* (2011) 17:10–2. doi: 10.14806/EJ.17.1.200

30. Feng D, Liu T, Sun Z, Bugge A, Mullican SE, Alenghat T, et al. A circadian rhythm orchestrated by histone deacetylase 3 controls hepatic lipid metabolism. *Sci (1979)* (2011) 331:1315–9. doi: 10.1126/SCIENCE.1198125

31. Patel SA, Velingkaar N, Makwana K, Chaudhari A, Kondratov R. Calorie restriction regulates circadian clock gene expression through BMAL1 dependent and independent mechanisms. *Sci Rep 2016 6:1* (2016) 6:1–10. doi: 10.1038/srep25970

32. Bugge A, Feng D, Everett LJ, Briggs ER, Mullican SE, Wang F, et al. Rev-erbα and rev-erbβ coordinately protect the circadian clock and normal metabolic function. *Genes Dev* (2012) 26:657–67. doi: 10.1101/gad.186858.112

33. Fang B, Guan D, Lazar MA. Using GRO-seq to measure circadian transcription and discover circadian enhancers. *Methods Mol Biol* (2021) 2130:127–48. doi: 10.1007/978-1-0716-0381-9_10

34. Hughes ME, Hogenesch JB, Kornacker K. JTK_CYCLE: an efficient nonparametric algorithm for detecting rhythmic components in genome-scale data sets. *J Biol Rhythms* (2010) 25:372–80. doi: 10.1177/0748730410379711

35. Kuleshov MV, Jones MR, Rouillard AD, Fernandez NF, Duan Q, Wang Z, et al. Enrichr: a comprehensive gene set enrichment analysis web server 2016 update. *Nucleic Acids Res* (2016) 44:W90–7. doi: 10.1093/NAR/GKW377

36. Huang R, Grishagin I, Wang Y, Zhao T, Greene J, Obenauer JC, et al. The NCATS BioPlanet – an integrated platform for exploring the universe of cellular signaling pathways for toxicology, systems biology, and chemical genomics. *Front Pharmacol* (2019) 10:445/BIBTEX. doi: 10.3389/FPHAR.2019.00445/BIBTEX

37. Heiman M, Schaefer A, Gong S, Peterson JD, Day M, Ramsey KE, et al. A translational profiling approach for the molecular characterization of CNS cell types. *Cell* (2008) 135:738–48. doi: 10.1016/J.CELL.2008.10.028

38. Dougherty JD. The expanding toolkit of translating ribosome affinity purification. *J Neurosci* (2017) 37:12079–87. doi: 10.1523/JNEUROSCI.1929-17.2017

39. Mehra A, Baker CL, Loros JJ, Dunlap JC. Post-translational modifications in circadian rhythms. *Trends Biochem Sci* (2009) 34:483–90. doi: 10.1016/J.TIBS.2009.06.006

40. Gallego M, Virshup DM. Post-translational modifications regulate the ticking of the circadian clock. *Nat Rev Mol Cell Biol 2007 8:2* (2007) 8:139–48. doi: 10.1038/nrm2106

41. Zhang R, Lahens N. HB-p of the, 2014 undefined. a circadian gene expression atlas in mammals: implications for biology and medicine. *Natl Acad Sci USA* (2014) 111:16219–24. doi: 10.1073/pnas.1408886111

42. Schibler U. The daily timing of gene expression and physiology in mammals. *Dialogues Clin Neurosci* (2007) 9:257–72. doi: 10.31887/DCNS.2007.9.3/USCHIBLER

frontiers | Frontiers in Endocrinology

TYPE Review
PUBLISHED 05 August 2022
DOI 10.3389/fendo.2022.950798

OPEN ACCESS

EDITED BY
Jian Ma,
Harbin Medical University, China

REVIEWED BY
Ziyue Li,
Dana–Farber Cancer Institute, United States
Chen Li,
Free University of Berlin, Germany

*CORRESPONDENCE
Xuqiang Nie
niexuqiang@126.com

SPECIALTY SECTION
This article was submitted to Diabetes: Molecular Mechanisms, a section of the journal Frontiers in Endocrinology

RECEIVED 23 May 2022
ACCEPTED 19 July 2022
PUBLISHED 05 August 2022

CITATION
Mu X, Wu X, He W, Liu Y, Wu F and Nie X (2022) Pyroptosis and inflammasomes in diabetic wound healing. *Front. Endocrinol.* 13:950798. doi: 10.3389/fendo.2022.950798

Pyroptosis and inflammasomes in diabetic wound healing

Xingrui Mu[1,2], Xingqian Wu[1,2], Wenjie He[1,2], Ye Liu[1,2], Faming Wu[1,2] and Xuqiang Nie[1,2]*

[1]College of Pharmacy, Zunyi Medical University, Zunyi, China, [2]Key Laboratory of Basic Pharmacalogy of Ministry of Education and Joint International Research Laboratory of Ethnomedicine of Ministry of Education, Zunyi, China

Diabetic wound is one of the complications of diabetes and is not easy to heal. It often evolves into chronic ulcers, and severe patients will face amputation. Compared with normal wounds, diabetic wounds have an increased proportion of pro-inflammatory cytokines that are detrimental to the normal healing response. The burden of this disease on patients and healthcare providers is overwhelming, and practical solutions for managing and treating diabetic wounds are urgently needed. Pyroptosis, an inflammatory type of programmed cell death, is usually triggered by the inflammasome. The pyroptosis-driven cell death process is primarily mediated by the traditional signaling pathway caused by caspase -1 and the non-classical signaling pathways induced by caspase -4/5/11. Growing evidence that pyroptosis promotes diabetic complications, including diabetic wounds. In addition, inflammation is thought to be detrimental to wound healing. It is worth noting that the activation of the NLRP3 inflammasome plays a crucial role in the recovery of diabetic wounds. This review has described the mechanisms of pyroptosis-related signaling pathways and their impact on diabetic wounds. It has discussed new theories and approaches to promote diabetic wound healing, as well as some potential compounds targeting pyroptosis and inflammasome signaling pathways that could be new approaches to treating diabetic wounds.

KEYWORDS

pyroptosis, inflammasome, signaling pathways, NLRP3, diabetic wound

Introduction

Diabetes is a metabolic disease caused by a variety of etiologies, and the number of people suffering from type 2 diabetes mellitus (T2DM) is growing every year (1). By 2045, the number of people with diabetes is expected to exceed 700 million (7.8% of the global population) (2). Diabetes has over 100 complications, making it the most well-known disease. These complications include cardiovascular disease, peripheral neuropathy, chronic renal failure, stroke, and diabetic wounds or ulcers (3). Diabetic wounds are a

condition that affects about 20% of patients with diabetes (4). Diabetic wounds are characterized by impaired healing responses, prolonged inflammation, and reduced epithelialization kinetics in diabetic patients (5).

Wound healing is a physiological response to structural tissue injury, which includes skin damage. Wound healing is a multi-stage process that includes hemostasis, inflammation, proliferation, and remodeling (6). Diabetic wounds heal slower than normal wounds due to the production of pro-inflammatory mediators, ischemia induced by microvascular problems, particular metabolic deficiencies, and decreased production of healing-related components, among other causes (7). As a result, diabetic wounds have a longer course and more complex mechanisms than normal wounds, affecting patients' morbidity, mortality, and quality of life significantly (8).

Pyroptosis, an type of programmed cell death, is usually associated with inflammatory responses (9). According to new research, cell death pathways include apoptosis, necroptosis, autophagy, ferroptosis, cuproptosis, pyroptosis, and necrosis, and the regulators and effectors of these pathways remain promising therapeutic targets (10). When germs, pathogens, or endotoxins stimulate cells, the caspase family becomes active, triggering pyroptosis, also known as inflammatory cell death. As a result of this process, cell swelling, cell membrane pore formation, cell membrane rupture, inflammasome activation, and finally the release of cell contents and inflammatory mediators all occur, culminating in severe inflammatory responses (11, 12).

In conclusion, this review summarizes the research progress on the relationship between pyroptosis and diabetic wounds. The primary purpose of this review is to clarify the mechanism of pyroptosis-related signaling pathways and their impact on diabetic wound, explore new therapeutic approaches and identify potential therapeutic targets.

Pyroptosis and inflammasome

Cell death dependent on caspase-1 was originally called apoptosis (13). In 2000, Cookson introduced the term "pyroptosis". Pyroptosis differs from apoptosis in the morphological features and inflammatory nature of cell death (14, 15). Pyroptosis is involved in the pathogenesis of various diseases, such as tumors, cardiovascular diseases, COVID-19, diabetes and its complications. The mechanism of pyroptosis is regulated by many protein or protein complexes, such as caspase, inflammasome, and Gasdermin. Typically, caspases exist in an inactive precursor form, a pro-caspase. After activation by the inflammasome, caspases cleave Gasdermin and generate a hydrophilic C-terminal domain and a lipophilic N-terminal domain. The N-terminal lipophilic domain oligomerizes and binds to the cell membrane to form a pyroptotic pore, ultimately triggering pyroptosis.

Caspases, a group of proteases with similar structures present in the cytoplasm, are known to drive apoptosis or pyroptosis and play a key role in programmed cell death and inflammation (16). Mammalian caspases fall into two broad categories: apoptotic and inflammatory caspases. Among them, caspase-1, -4, -5, -11, and -12 belong to the family of inflammatory caspases, which are closely related to pyroptosis (17). According to the latest research, the signaling pathways of pyroptosis can be split into four kinds based on different activation modalities: canonical inflammasome signaling pathways (caspase-1), non-canonical inflammasome signaling pathways (caspase-4/5/11), and pyroptotic pathways depending on caspase-3 and caspase-8 (18–20).

The inflammasome is a multi-protein complex assembled by intracellular pattern recognition receptors (PRRs) and is an essential part of the innate immune system (21, 22). Damage-associated molecular patterns (DAMPs), endogenous molecules released by the body's cell death, namely endogenous danger signals, originate from immune cells activated by damaged or necrotic tissue. Pathogen-associated molecular patterns (PAMPs) are ligand receptors that PRRs recognize and bind, mainly referring to some highly conserved molecular structures shared on the surface of pathogenic microorganisms, such as lipopolysaccharide of G-bacteria. Generally, both PAMPs and DAMPs induce inflammasome activation *via* PRRs. Inflammasomes can recognize PAMPs or DAMPs and recruit and activate the pro-inflammatory protease caspase-1, thereby inducing cell death under pathological conditions of inflammation and stress. It is known that this process can promote the maturation and secretion of pro-IL-1β and pro-IL-18 during innate immune defense (23–25).

Current research indicates that there are five common inflammasomes, including NLRP1, NLRP3, NLRC4, Pyrin, and AIM2 (26). The NLRP3 inflammasome, in particular, has been widely investigated and is involved in a number of diseases, including type 2 diabetes and diabetic wounds (22, 27). NLRP3 may promote interaction with the pyrin domain (PYD) in ASC in response to immune activators (e.g., PAMPs, DAMPs), other exogenous invaders, or environmental stimuli. Subsequently, the caspase recruitment domain (CARD) of ASC binds to the CARD domain on pro-caspase-1 to generate the NLRP3 inflammasome. The creation of this complex causes pro-caspase-1 to self-cleave, resulting in an active caspase-1 p10/p20 tetramer, and the maturation of the pro-inflammatory cytokines IL-1β and IL-18 from their immature "pro" versions.

Activation of the NLRP3 inflammasome appears to proceed in two steps. The first step involves priming or initiation signals, and many PAMPs or DAMPs are recognized, leading to the activation of NF-κB-mediated signaling that upregulates the transcription of inflammasome-related components, including inactive NLRP3, pro-IL-1β, and pro -IL-18. The second step is the oligomerization of NLRP3 and the subsequent assembly of NLRP3, ASC, and pro-caspase-1 into a complex (28). Based on

the available evidence and research results, pro-caspase-1 conversion to caspase-1 is accompanied by the release of mature IL-1β and IL-18. Furthermore, triggering PAMPs and DAMPs causes the creation of ROS, which promotes the assembly and activation of the NLRP3 inflammasome (Figure 1). Therefore, as the center of the inflammatory response, the NLRP3 inflammasome could be a potential therapeutic target for inflammatory illnesses. However, non-canonical inflammasome activation pathways mediated by mouse caspase-11 or human caspase-4/5 are independent of inflammasome activation. Pyroptosis was also successfully induced in response to intracellular lipopolysaccharide (LPS) detection (29). ASC (also known as PYCARD) is a protein containing pyran and CARD domains that aid in inflammasome assembly (30).

The six members of the gasdermins are Gasdermin A–E and DFNB59 (31). Except for DFNB59, other components have been reported to be associated with the pyroptotic process. A peptide linker connects an N-terminal domain (effector domain that creates the transmembrane pore) to a C-terminal domain (with auto-inhibitory effects). Among gasdermins, gasdermin D (GSDMD) and gasdermin E(GSDME) are the most well-characterized in terms of activation and function (32). Gasdermin family members are mainly expressed in skin, gastrointestinal tract, and immune cells to actively eliminate infected cells through pyroptosis (33, 34). GSDMD is a substrate of caspase-1, a component of the inflammasome responsible for executing pyroptosis and secreting mature IL-1β (35). When caspase cleaves the gasdermin-N domain free, it binds to the lipids on the cell membrane and encourages the creation of pores, which causes the membrane to rapidly lose its integrity and allow the contents of the cell to flow out. Pore-forming activity and pyroptosis are therefore reduced in the absence of GSDMD activation (36). Of course, two critical steps in pyroptosis are inflammasome activation and GSDMD cleavage. Recent studies have found that disruption of mitochondrial membrane potential (MMP) and reactive oxygen species (ROS) production is commonly associated with macrophage pyroptosis (37).

Signaling pathways of pyroptosis

Canonical inflammasome signaling pathway (Caspase-1)

In most cases, the formation of the inflammasome requires pattern recognition receptors (PRRs) as sensors, the adaptor protein ASC (CARD-containing apoptosis-associated speck-like protein) and caspase1 (38). The assembly of inflammasomes triggers the hydrolysis of inactive pro-caspase-1 to active caspase-1, which converts the cytokines pro-IL-1β and pro-IL-18 into mature and bioactive IL-1β and IL-18, respectively (39, 40). Caspase-1 cleaves GSDMD, which is involved in membrane pore formation. Membrane pores cause the production of inflammatory molecules, including IL-1β and IL-18, which

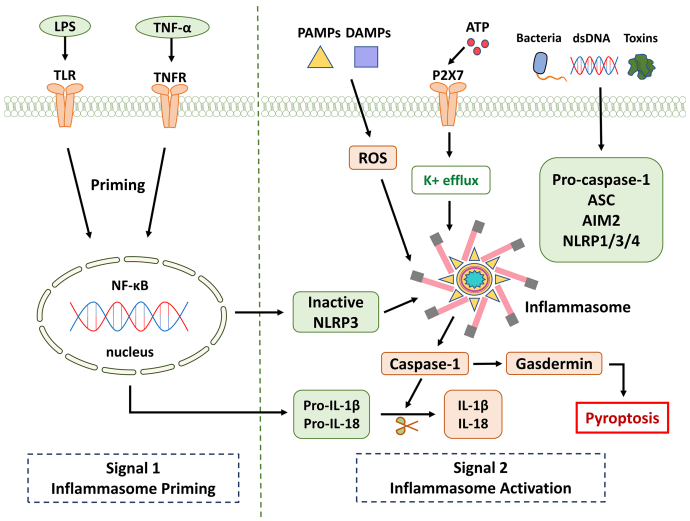

FIGURE 1
NLRP3 inflammasome signaling pathway. It is known that the activation of NLRP3 is divided into two key steps: priming and activation. Signal 1 (priming; left): When pathogens and their products, injury, stress, and other signals stimulate cells, TLR, TNFR, and other receptors can be activated. NF-κB is activated through different pathways, which in turn promotes NLRP3, pro-IL-1β, and pro-IL-18. Provide a material basis for the activation and function of NLRP3 inflammasome. Signal 2 (activation; right): Multiple upstream signaling events are activated by PAMPs and DAMPs. These include K^+ efflux, reactive oxygen species (ROS) production, etc. Inflammasome formation activates caspase-1, which cleaves pro-IL-1β and pro-IL-18. Gasdermin is also cleaved and inserted into membranes, forming pores and inducing pyroptosis.

causes the cells to expand and eventually develop into pyroptosis (Figure 2).

Many multifactorial diseases, such as gouty arthritis, atherosclerosis, and type 2 diabetes, are exacerbated by NLRP3-mediated inflammation. PAMPs/DAMPs that activate NLRP3 include hyperglycemia, fatty acids, protein aggregates, and extracellular ATP, among many others (41, 42). The mechanism of activation of the NLRP3 inflammasome is clearly described in paragraph 2 (Figure 1). The inflammasome effector cytokines IL-1β and IL-18, due to NLRP3 activation, are major effector molecules that exacerbate these diseases. As a result, maintaining optimal cellular homeostasis and health requires fine-tuning NLRP3 inflammasome activity (43).

Non-canonical inflammasome signaling pathway (Caspase-4/5/11)

Mouse caspase-11 and its human orthologs caspase-4 and -5 are involved in non-canonical inflammasome signaling, and investigations of mouse caspase-11 have led to various findings concerning their immunological role (44). The TLR4/MD2 complex identified the pathogen-associated molecular pattern to activate inflammatory responses as lipopolysaccharide (LPS), a significant component of Gram-negative bacteria's outer membrane (45). Myeloid differentiation factor 2 (MD2) is a key mediating protein required for the dimerization/activation of TLR4 (Toll-like receptor 4). LPS activates pro-caspase-4/5/11, and pro-caspase-4/5/11 initiates pyroptosis-mediated cell death (46). Caspase-4/5/11 binds to LPS and cleaves the 53-kDa precursor form of the GSDMD protein molecule, resulting in the formation of the N-terminus of the mature GSDMD p30 fragment. Thus, the formation of pores in the cell membrane results in the release of IL-1β and IL-18 from the cells and induction of pyroptosis (47, 48). Caspase-4/5/11 can also stimulate NLRP3-mediated caspase-1 initiation and IL-1β/IL-18 *via* GSDMD cleavage. GSDMD has been identified as an important downstream component of both canonical and non-canonical inflammasome pathways involved in pyroptosis (49, 50) (Figure 2).

Caspase-3-dependent pyroptosis pathway

Caspase-3, an apoptosis-executing protein, is the main protein responsible for the cleavage and activation of GSDME. In addition to GSDMD, GSDME also plays a crucial role in pyroptosis (51). Caspase-3 is activated by the mitochondrial and death receptor pathways and cleaves GSDME to form GSDME-N fragments, which lead to plasma membrane pore formation, cell swelling, and pyroptosis (52). GSDME protein molecules can

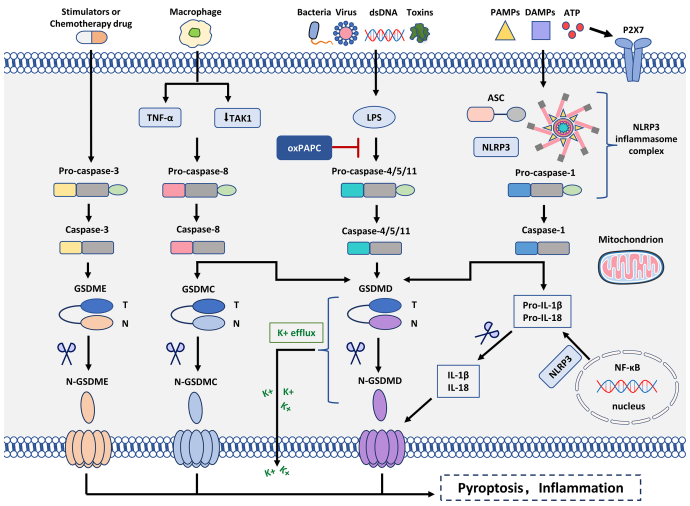

FIGURE 2
Molecular mechanism of pyroptosis. In the canonical inflammasome signaling pathway, PAMPs, DAMPs, and extracellular ATP are stimulated by intracellular signaling molecules and assembled with pro-caspase-1 and ASC to form inflammasomes and activated caspase-1. N-GSDMD perforates cell membranes by forming non-selective pores. In addition, IL-1β and IL-18 were secreted in the pores formed by N-GSDMD. In the non-canonical inflammasome signaling pathway, intracytoplasmic LPS activates caspase-4/5/11, which triggers pyroptosis by cleaving GSDMD. However, oxPAPC competes with LPS for binding to caspase-4, thereby inhibiting pyroptosis. Cleavage of GSDMD leads to K+ efflux that ultimately mediates the assembly of the NLRP3 inflammasome. Moreover, cleavage of GSDMD leads to cleavage of pro-IL-1β and pro-IL-18. In the caspase-3-mediated pathway, active caspase-3 cleaves GSDME to form N-GSDME, inducing pyroptosis. In the caspase-8-mediated pathway, inhibition of TAK1 induces the activation of caspase-8, which cleaves GSDMD, leading to pyroptosis. In addition, under hypoxia, TNF-α activates caspase-8 after apoptosis to pyroptosis, which can regulate the transcription of GSDMC.

be cleaved into N-terminal and C-terminal fragments by caspase-3. GSDME-N components are equivalent in function and purpose to GSDMD-N components (53). GSDME directly induces tumor cell pyroptosis through Caspase-3 and indirectly acts on T lymphocytes through Granzyme B, acting as a tumor suppressor gene (54). Furthermore, when chemotherapeutic drugs activate Caspase-3, primary human cells exhibit GSDME-dependent pyroptosis, providing new insights into cancer chemotherapy (54). These findings indicate that different caspase substrates, rather than activated caspases, influence the type of cell death induced.

Caspase-8-dependent pyroptosis pathway

Recent research has revealed unexpected roles for caspase-8's enzymatic activity and scaffold function in inflammasome activation and pyroptosis induction (55). The activation of the ASC-caspase-1 inflammasome is caused by the production of catalytically inactive caspase-8, leading to GSDMD-mediated pyroptosis (56). In the presence of inhibitors, activation of caspase-8 cleaves GSDMD leading to pyroptosis. More research is needed to see if caspase-8 can directly cleave GSDMD or if other intermediary substrates, other than caspase-1/11, are necessary to produce the pore-forming p30 subunit (57). However, pure active caspase-8 has been demonstrated to cleave recombinant mouse GSDMD creating p30 pore-forming fragments (58). Following caspase-8 activation in tumor cells, GSDMC has been found to mediate tumor necrosis. The pyrogenic cell death mediated by GSDMC/caspase-8 provides essential insights into the pyroptotic pathway in cancer cells (59). Based on the current research results, the mechanism of pyroptosis induced by caspase-8 is not clear enough, and the research on its mechanism is a direction worthy of attention in the future.

Role of pyroptosis and inflammasomes in wound healing

Acute wound healing includes four stages: hemostasis, inflammation, proliferation, and remodeling (60). Excessive or long-term inflammation is one of the main characteristics of chronic wounds, since this condition negatively affects wound healing and leaves scars behind (61). The NLRP3 inflammasome is expressed in epithelial tissues, such as skin. As the first line of defense against external threats, it can participate in the skin's innate immunity (62, 63).

The role of the NLRP3 inflammasome in the early stages of cutaneous wound healing is increasingly being investigated. Results of studies have demonstrated the effect of mulberry leaf and fruit extract (MLFE) on skin wound healing and the involvement of the NLRP3 inflammasome (64). Concurrently, research has revealed the function of the NLRP3 inflammasome in the proliferative and remodeling phases of wound healing (65). A combination of mulberry leaf and fruit extract (MLFE) provided better anti-obesity and anti-inflammatory benefits than mulberry leaf extract alone. Under obese conditions, the expression of the NLRP3 inflammasome and its associated markers (pro-caspase-1, IL-1β-precursor and IL-1β-mature) is higher than basal levels. Among them, the NLRP3 inflammasome is inhibited during the inflammatory phase of skin wound healing (66). The results showed that the addition of MLFE reduced body fat mass, fasting blood glucose levels, blood lipid levels, and hepatotoxicity. Therefore, body fat mass and fasting blood glucose may be potential indicators of delayed wound healing in obese patients. Although the exact activator or mechanism of the NLRP3 inflammasome is not known, it can be determined that MLFE normalizes the levels of the NLRP3 inflammasome and suppresses skin inflammatory responses during the early stages of wound healing in obesity (67). Deletion of the NLRP3 inflammasome will result in a decrease in proinflammatory cytokines such as IL-1β and TNF-α and delayed angiogenesis (68). MLFE may have potential therapeutic value in treating obesity and obesity-related complications, and NLRP3 might be a promising target in the fight against obesity wounds since it may promote the early healing of wounds. However, this study focused on detecting NLRP3-related proteins and ignored the close relationship between the inflammasome and pyroptosis. The article only detects pro-caspase-1 is not enough. If the expression of GSDMD and caspase-1 protein is detected, it is enough to show that it is related to pyroptosis, which may be another way to explore.

DNA nanomaterials with distinctive spatial configurations are known as tetrahedral framework nucleic acids (TFNAs) (69). TFNAs have excellent biosafety with anti-inflammatory, antioxidant, anti-fibrotic, angiogenic, and skin wound healing activities with little toxicity (70). *In vitro* and *in vivo* research have uncovered that TFNAs increase corneal transparency, speed wound reepithelialization, and play a positive role in corneal epithelial wound healing (71). TFNAs are not only beneficial for corneal wound healing but also for skin wound healing. The results of the study showed that treatment with TFNAs accelerated the healing process of skin wounds and reduced scarring. This is the first report that nanophase materials with nucleic acid biological properties can accelerate wound healing and reduce scarring, suggesting that TFNA can be used to promote skin tissue regeneration (72).

In addition, studies have shown that TFNA can promote diabetic wound healing by accelerating processes such as angiogenesis, epithelialization, and collagen deposition. Through their antioxidant activity *via* the PI3K/Akt/Nrf2/HO-1 signaling pathway, TFNAs can protect endothelial cell function, reduce inflammation, and prevent oxidative damage. The PI3K/Akt/Nrf2/HO-1 signaling pathway is regulated by

metformin and plays a key role in metformin-induced osteogenesis. Therefore, the use of TFNAs could help diabetic wounds recover faster (73). As various local or systemic diseases promote skin inflammation, fibrosis (the result of a dysregulated tissue repair response) begins to dominate the repair process when the intensity or duration of skin damage exceeds the ability of the tissue to repair. As a result, medicines that substantially prevent skin fibrosis while also reducing immunogenicity, inflammation, apoptosis, and pyroptosis are required. TFNA inhibits the pyroptotic pathway and reduces inflammatory cytokine levels and skin collagen content in studies. Both NLRP3 inflammasome and pro-caspase-1 levels were down-regulated after TFNA treatment, indicating that the inflammasome was reduced and the active form of caspase-1 was reduced, resulting in a subsequent down-regulation of N-terminal GSDMD levels. The results showed that TFNA has anti-inflammatory and anti-fibrotic abilities without cytotoxicity (74). In this study, proteins related to pyroptosis and inflammasome signaling pathways were detected, including pro-caspase-1, caspase-1, NLRP3, GSDMD, etc. In a nutshell, TFNAs have important research significance for skin wound healing and have been confirmed to be closely related to pyroptosis and inflammasome pathways.

The research progress of bioactive glass (BG) in soft tissue repair is relatively rapid, especially in wound healing. The findings suggest that BG may accelerate wound closure, granulation development, collagen deposition, and angiogenesis (75). The method used in this study is that BG inhibits endothelial cell pyroptosis and promotes wound healing by regulating the Cx43/ROS signaling pathway. Therefore, BG inhibits the activation of caspase-1 by the NLRP3 inflammasome, attenuate the perforation activity of GSDMD, and ultimately inhibit the pyroptosis of endothelial cells (76). In addition, BG inhibits the production of ROS while regulating the expression of connexin 43 (Cx43) (77). Subsequently, BG promotes the formation of blood vessels resulting in accelerated wound healing. The study also made further proofs showed that BG could reduce the expression of Cx43 and the level of ROS, which strongly suggested that BG could inhibit the pyroptosis of endothelial cells (78). It has been shown that inhibiting pyroptosis enhances angiogenesis in many animal models, implying that BG also enhances angiogenesis. It can be concluded that BG can promote wound healing by impeding pyroptosis through the Cx43/ROS signaling pathway. Even though this study did not directly regulate pyroptosis and inflammasome signaling pathways, it did confirm their close relationship. It inspires us is that fewer drugs and methods inhibit pyroptosis, but it can be achieved by modulating other signaling pathways.

While the wound healing process is complex and dynamic, the pyroptosis and inflammasome pathways also have complex connections. There is currently a lack of studies on the crosstalk between multiple signaling pathways in wound healing or on pyroptosis and changes in the NLRP3 inflammasome at different phases of wound healing. Therefore, further in-depth study of other factors in the wound healing process will also provide us with new insights into the mechanism of wound healing. New treatment methods such as new carriers and new Chinese herbal extracts have been evaluated and will be used in the clinic in the future. How to optimize individualized treatment strategies while improving chronic inflammatory and pyroptotic states during wound healing needs to be considered.

Role of pyroptosis and inflammasomes in diabetic wound healing

Diabetic wound pathogenesis is complicated and involves numerous pathways. There is some evidence that suggests that the local hyperglycemic environment is the main factor leading to diabetic wounds, but recent research shows that factors such as oxidative stress damage, accumulation of advanced glycation end products (AGEs), and chronic inflammation are closely related to diabetic wounds (79, 80). Persistent inflammatory activation is the leading cause of chronic refractory diabetic wound, and an essential factor leading to diabetic foot ulcer (DFU), gangrene, amputations, and even the root cause of prolonged hospital stays and increased wound management costs (81).

Targeting the NLRP3 inflammasome, which plays a role in the pathophysiology of numerous inflammatory disorders, could be a potential target for enhancing diabetic wound healing. Neutrophils release extracellular traps (NETs) to defend against pathogens that induce tissue damage (82). NETs have been detected in diabetic wounds and have been associated with impaired healing processes, but the mechanism by which NETs pause wound healing and their role in promoting inflammatory dysregulation remain unclear (83). Overproduced NETs in diabetic wounds trigger NLRP3 inflammasome activation and IL-1β release in macrophages (84). Meanwhile, NETs up-regulates the levels of NLRP3 and pro-IL-1β through the TLR-4/TLR-9/NF-κB signaling pathway, triggering the production of ROS, and activating the NLRP3 inflammasome (85). Furthermore, in a diabetic rat model, NET digestion by DNase I reduced NLRP3 inflammasome activation, altered immune cell infiltration, and expedited wound healing (86).

In recent years, most studies have focused on the role of the inflammasome, especially NLRP3 and pyroptosis, on wound healing. The NLRP3 inflammasome has been characterized in a corneal epithelial wear model in which wound healing and non-regeneration of diabetic corneal wounds have been studied. Recent studies suggest that the NLRP3 inflammasome-mediated inflammation and pyroptosis contribute to the pathogenesis of diabetic keratopathy (DK) (87). NLRP3 is necessary for corneal wound healing and nerve regeneration in

physiological circumstances (88). In diabetics, however, prolonged activation of the NLRP3 inflammasome causes corneal wound healing to be delayed and nerve regeneration to be hindered. In addition, inhibiting the AGEs/ROS/NLRP3 inflammasome axis genetically and pharmacologically greatly accelerates diabetic corneal epithelial wound closure and nerve regeneration (87). The study highlighted that ocular surface damage in diabetic mice might be related to ROS/NLRP3/Caspase-1/IL-1β signaling pathway (89, 90). Activation of the NLRP3 inflammasome by high glucose-induced P2X7R (purinergic ligand-gated ion channel 7 receptor) affects the pathogenesis of diabetic retinopathy (DR) (91). Therefore, it is known that NLRP3 inflammasome and pyroptosis play critical roles in DK and DR. In addition, NLRP3 and pyroptosis also have significant effects on diabetic wounds (Table 1).

Glyburide is a commonly used sulfonylurea drug to treat type 2 diabetes (92). The capacity to suppress the NLRP3 inflammasome through a mechanism different from its ability to enhance insulin release from pancreatic beta-cells was recently discovered, and glyburide improves wound healing in diabetic mice (98). Cryopyrin/NALP3/NLRP3 is an essential component of the inflammasome triggered by PAMPs, DAMPs, and crystalline substances (99). Glyburide is the first chemical able to block PAMPs, DAMPs, and crystal-induced IL-1β production by acting upstream of cryoproteins. Inflammasome activity was persistent in macrophages (mø) isolated from diabetes and db/db mice wounds, which was associated with low expression levels of endogenous inflammasome inhibitors. Because a wound-conditioned medium activates caspase-1 and stimulates the production of IL-1β and IL-18 in cultured cells through a ROS-mediated route, soluble components in these wound biochemical conditions are sufficient to activate the inflammasome (100). Inhibiting inflammasome activity in wounds of db/db mice by topical application of pharmacological inhibitors improves wound healing. This treatment shifts from a pro-inflammatory state to a pre-healing state and increases pre-healing growth factor levels.

Bacillus subtilis is a probiotic that modulates immune responses and reshapes the gut flora (101). *Bacillus subtilis* (WB800N) has the ability to activate TLRs (Toll-like receptors) and enhance immune responses (102). In recent years, there has been evidence that diabetic wounds are associated with gut microbiota. Studies have shown that amoxicillin can reduce the alpha and beta diversity of the intestinal microbiota in mice, leading to intestinal microbiota disturbances, thereby alleviating diabetic wounds (103). It is also significant that *Bacillus subtilis* (WB800N) can relieve diabetic wounds by regulating Toll-like receptor-2 (TLR2) (93). TLR2 is a major innate immune response factor, and of immune response activation benefits diabetic wound healing (104). The results showed that *Bacillus subtilis* (WB800N) could increase the expression of TLR2, NLRP3, ASC and Caspase-1 in diabetic wound mice. However, the TLR2 antagonist SsnB could reduce the expression of TLR2, NLRP3, ASC and Caspase-1 in diabetic wound mice. NLRP3/ASC is required for Caspase-1 activation and pro-IL-1β cleavage to generate mature IL-1β. In conclusion, *Bacillus subtilis* (WB800N) promotes inflammatory response in diabetic wound mice by activating TLR2. This study only explored the NLRP3 inflammasome signaling pathway but lacked the detection of pyroptosis-related proteins. The authors believe that *Bacillus subtilis* (WB800N) promotes cell apoptosis, but it is actually more likely to be pyroptosis, which is worth exploring in the future.

Skin infections and the spread of *Staphylococcus aureus* (*S. aureus*) in mice are limited by perforin-2, an innate immune molecule against intracellular bacteria (105). The study showed the accumulation of *S. aureus* within the epidermal cells of DFU without clinical signs of infection due to significant inhibition of perforin-2 (106). Evidence from studies shows that *S. aureus* within the epidermis of DFU triggers AIM2 inflammasome activation and pyroptosis. From the results, increased induction of AIM2 inflammasome, ASC-pyroptosome, and IL-1β was found in non-healing DFU (107). The correlation of AIM2 with healing outcomes suggests that AIM2 has a central function in regulating the inflammatory response to DFU. There is evidence that the increase in IL-1β involved in pyroptosis is accompanied by an increase in the AIM2 inflammasome, resulting in the oligomerization of ASCs into pyroptosomes which then triggers the activation of pro-caspase-1 resulting in the cleavage of porins such as Gasdermin D, and the lysis of cells

TABLE 1 Compounds or Molecules Inhibiting the Pyroptosis Signaling Pathway for the Treatment and Management of Diabetic Wound.

Classification	Mechanism of Pyroptosis Inhibition	References
Glyburide	NLRP3/caspase-1/IL-1β/IL-18/ASC	(92)
Bacillus subtilis (WB800N)	NLRP3/caspase-1/IL-1β/IL-37/TLR2/ASC	(93)
Perforin-2	AIM2/GSDMD/IL-1β/ASC	(94)
Bletilla striata polysaccharide	NLRP3/IL-1β/TNF-α/ROS	(95)
Paeoniflorin	NLRP3/caspase-1/IL-1β/IL-18/TNF-α/ASC	(96)
Heparan sulfate	NLRP3/IL-1β/IL-18/TNF-α/ASC	(97)

NLRP3, NOD-like receptor family pyrin domain containing 3; AIM2, Absent in melanoma 2; ASC, CARD-containing apoptosis-associated speck-like protein; IL-1β, interleukin-1beta; IL-18, interleukin-18; IL-37, interleukin-37; TLR2, Toll-like receptor-2; GSDMD, gasdermin D; TNF-α, Tumour Necrosis Factor alpha; ROS, reactive oxygen species.

involved in inflammation (108). In patients with DFU, the inhibition of perforin-2, intracellular accumulation of *S. aureus*, and related blepharoptosis lead to the inhibition of wound healing and the persistence of inflammation (94). Intracellular *S. aureus* accumulates in the DFU epidermis as a result of perforin-2 suppression, triggering activation of the AIM2 inflammasome, which results in caspase-1-mediated IL-1β activation and proteolysis of the pore-forming gasdermin D processing. As a consequence of this cascade, holes are formed in the plasma membrane, opening up a pathway for pyroptosis and for the release of intracellular components. As a result, inflammatory mediators and accumulated intracellular S. aureus are released, leading to chronic inflammation and direct inhibition of wound healing. Further, it was determined that gasdermin D, one of the substrates of caspase-1, is also cleaved and activated by DFU (109). This study is the first to demonstrate that intracellular *S. aureus* can inhibit perforin-2 in DFU. Pyroptosis is the predominant form of cell death in DFU, but the possibility of other forms of cell death such as necroptosis, ferroptosis, and cuproptosis remains to be tested.

Pyroptosis inhibitors for the treatment and management of diabetic wounds

A growing body of research suggests that *Bletilla striata* polysaccharide (BSP), the main active ingredient in Bletilla striata, promotes normal or diabetic wound healing (110). This is due to the fact that BSP improves diabetic wound healing by infiltrating fibroblasts and enhancing collagen synthesis in the skin wound tissue. Furthermore, BSP is suitable for medical applications, including wound dressings, hydrogels, tissue engineering scaffolds, and drug delivery vehicles (111–113). This study has demonstrated that the therapeutic effect of BSP on DFU is mediated by inhibiting HG-induced NLRP3 inflammasome activation in macrophages, which increases insulin sensitivity in endothelial cells (95). The results showed that the expressions of TXNIP, NLRP3, pro-caspase-1, cleaved-caspase-1, pro-IL-1β and cleaved-IL-1β were increased in diabetic skin wounds. However, BSP treatment resulted in decreased levels of some proteins, such as pro-caspase-1, cleaved-caspase-1, pro-IL-1β, and cleaved-IL-1β. In addition, the sensitivity of BSP to insulin was improved.

BSP has a protective effect on macrophages and can significantly reduce the amount of ROS produced by HG, thereby preventing macrophages from being induced by HG. In addition to this, IL-1β secretion and NLRP3 inflammasome activation were also inhibited (114, 115). Additionally, BSP is thought to play an important role in preventing HG-induced endothelial cell inactivation and ROS homeostasis imbalance (116). The results showed that BSP more effectively protected BMDMs (Bone marrow-derived macrophages) from the HG-induced ROS production, inhibited NLRP3 inflammasome activation and reduced IL-1β secretion. It also reduced the abnormal production of ROS in CMECs (cardiac microvascular endothelial cells) while maintaining cell viability (114). Macrophage infiltration and angiogenesis in DFU are inhibited by IL-1β, TNF-α, and monocyte chemoattractant protein 1, which ultimately interfere with wound healing (117). This study showed that the dosing regimen of BSP affects the local production of TNF-α and IL-1β (especially in skin tissue), excluding serum levels.

BSP reduced macrophage infiltration and increased angiogenesis in cutaneous wound tissue. These results are in line with increased TNF-α and IL-1β levels in skin wound tissue. The potential of BSP to improve diabetic wound healing may be due to its inhibition of NLRP3 inflammasome activation in macrophages. Although the study did not explicitly mention that BSP inhibits the pyroptotic pathway, it is closely related to NLRP3. In addition to promoting the maturation and release of IL-1β, the over-activation of the NLRP3 inflammasome also leads to the over-activation of pyroptosis. In future research, we can consider detecting the expression of ASC-pyroptosome and GSDMD and explore the molecular mechanism of the pyroptosis and inflammasome pathway.

Paeoniflorin is one of the main active components in Paeonia alba Radix, with antioxidant and anti-inflammatory effects (118). The use of paeoniflorin can alleviate diabetic nephropathy by inhibiting the release of inflammatory cytokines and chemokines (TNF-α, IL-1β, and MCP-1) through toll-like receptor 2 (TLR2) inactivation (119). In recent years, traditional Chinese medicine has been recommended as adjuvant therapy for DFU patients (120). Herbal products containing phenolic compounds, terpenoids, or glycosides have positively affected managing diabetic complications (121). Activation of NLRP3 inflammasome in diabetic wounds can maintain inflammation and delay the wound healing process, so inhibiting the activation of NLRP3 inflammasome and the production of IL-1β can effectively promote the healing of diabetic wounds. Paeoniflorin treatment reduced inflammatory cells and decreased the expression levels of NLRP3 and cleaved-caspase-1. In addition, paeoniflorin significantly down-regulated IL-1β, IL-18 and TNF-α levels in DFU.

Paeoniflorin efficiently suppressed NLRP3 and NF-B-mediated DFU inflammation by inhibiting CXCR2, according to *in vitro* findings (122). CXCR2 is a neutrophil receptor that is activated by chemokines like CXCL1 and CXCL2. The activation of the NF-κB pathway in response to IL-1β drives the production of these chemokines. Additionally, studies have shown that TNF-α can regulate the chemokine network in inflammation-related diseases through the NF-κB signaling pathway (123, 124). CXCR2 has critical functions in neutrophil activation and recruitment at inflammatory sites, which provides a reference for positioning CXCR2 as a drug

target for many inflammatory diseases. In HG-treated HaCaT cells, blockade of CXCR2 blunts NLPR3/ASC inflammasome activation. In conclusion, paeoniflorin inhibits the formation of NLRP3/ASC/caspase-1 inflammasome and the NF-κB transcription by blocking CXCR2, inhibiting the release of pro-inflammatory cytokines, and promoting the healing of diabetic wounds (96). Although the current evidence is insufficient and further exploration is needed, studies have shown that paeoniflorin is a potential drug for the treatment of DFU.

Heparan sulfate (HS) is a structural element of tissue scaffold and regulates activities of locally synthesized proteolytic enzymes, morphogens, chemokines and growth factors (125, 126). Morphogens are proteins that encode transcription factors, receptors and regulate translation. HS was shown to improve the healing of diabetic wounds in rats by reducing the inflammatory response (127). DAMPs are increased during diabetes to act as activators of the NLRP3 inflammasome and these activators promote inflammasome assembly leading to insulin resistance and organ dysfunction (128). Based on the existing results, it is speculated that HS may promote wound healing by reducing neutrophil infiltration and accumulation of macrophages (129). Moreover, diabetic wounds are more prone to inflammation than different types of wounds. Cleaved-IL-1β and IL-18 play key roles in wound inflammation through interactions with pro-inflammatory cytokines. Research evidence indicates that antagonists of cleaved-IL-1β or IL-18 may be used to treat inflammatory diseases such as gout, arthritis, or arthritic pain. Among them, TNF-α is a representative pro-inflammatory factor, and high levels of TNF-α can amplify and prolong the inflammatory response. The study found that HS significantly reduced Cleaved-IL-1β, IL-18 and TNF-α levels in diabetic rats (130). In addition, it may be possible for HS to work as an anti-inflammatory mechanism by inhibiting the NLRP3 inflammasome activity, so that controlling the level of NLRP3 inflammasome activity can be a method for treating diabetic wounds (97). In the process of wound healing, HS can promote wound healing in diabetic rats. The activation of Cleaved-IL-1β, IL-18 and TNF-α was decreased, and the expressions of NLRP3 and ASC were decreased in the HS group. HS inhibits the inflammatory response and promotes wound healing during diabetic wound healing by down-regulating NLRP3 inflammasome and Cleaved-IL-1β. Therefore, reducing the production of inflammatory factors and the reduction of neutrophil infiltration in the diabetic wound will improve the diabetic wound environment and ultimately shorten the wound healing time (Figure 3).

The NLRP3 inflammasome plays an essential physiological role in skin wound healing. Therefore, targeting NLRP3 inflammasome activity and its effectors may be an effective therapeutic strategy to reduce chronic inflammation and promote healing in diabetic wounds. During wound healing, the transient activity of the inflammasome promotes the propagation of wound inflammation and is critical for both epidermis and dermis healing (131). Among the strategies for inhibiting pyroptosis and the NLRP3 inflammasome signaling pathway, drugs such as glyburide and metformin are the closest to clinical translation. In published studies, a variety of

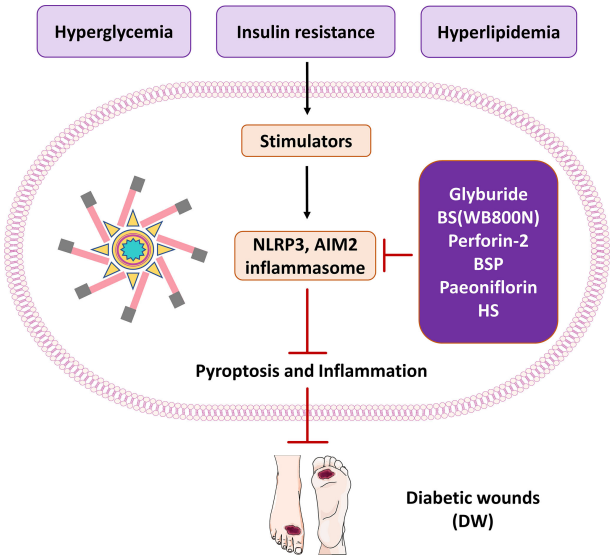

FIGURE 3
The therapeutic significance of potential molecules or materials for diabetic wound by inhibiting pyroptosis and inflammasome NLRP3 and AIM2.

compounds can be used to directly or indirectly inhibit NLRP3 inflammasome activity in diabetic wounds. Improves diabetic wound healing by affecting pyroptosis and NLRP3 inflammasome or upstream and downstream signaling. Most researchers are now keen to inhibit the inflammasome pathway to improve diabetic wounds. However, it is often overlooked that inflammation and pyroptosis are closely related. The research horizon should be broadened, and more attention should be paid to pyroptosis while detecting the inflammasome pathway, which may lead to surprising results.

Conclusion and future prospectives

In recent years, numerous studies have demonstrated that pyroptosis plays a vital role in developing diabetes and its complications. This article has reviewed the impact and role of pyroptosis in diabetic wound healing and the inflammasome is a crucial player in pyroptosis. Danger signals or stimuli cause the activation of caspase-1/4/5/11/3/8 and release IL-1β, IL-18 and other inflammatory factors, resulting in cell pyroptosis. Pyroptosis inhibits wound healing and prolongs the inflammatory response in diabetic wounds, and multiple studies have demonstrated that inhibition of pyroptosis improves wound healing. This review has described some potential drugs and molecules that may be helpful to targets for managing and treating diabetic wounds in the future.

At present, there are few studies on pyroptosis in diabetic wounds, and extensive research is needed to deeply analyze and elucidate the mechanisms and pathophysiological roles of pyroptosis and inflammasome in diabetic wounds. Furthermore, unlike common cell death mechanisms, ferroptosis and cuproptosis have become research hotspots in recent years. Among the forms of cell death in wound healing or diabetic wound healing, the possibility of other forms of cell death (such as necroptosis, ferroptosis, and cuproptosis) remains to be confirmed and is an area worthy of future attention and research. A more in-depth examination of the various modes of cell death could provide new insights into the pathogenesis and development of diabetic wounds.

Author Contributions

XM was responsible for the literature review and writing. XW, WH and YL were responsible for proofreading. XN and FW were responsible for correction. All authors contributed to the article and approved the submitted version.

Funding

This work was supported by the National Natural Science Foundation of China (82160770, 81960741, 82060687), the Guizhou Provincial Natural Science Foundation (QKH-J-2020-1Z070), Outstanding Young Scientific and Technological Talents Project of Guizhou Province (2021-5639), *Dendrobium* Specialized Class Project of Guizhou Province (QSKH-2019003).

Conflict of interest

The authors declare that the research was conducted in the absence of any commercial or financial relationships that could be construed as a potential conflict of interest.

Publisher's note

References

1. IDF releases report of global survey on access to medicines and supplies for people with diabetes. *Diabetes Res Clin Pract* (2017) 129:224–5. doi: 10.1016/j.diabres.2017.06.001

2. Saeedi P, Petersohn I, Salpea P, Malanda B, Karuranga S, Unwin N, et al. Global and regional diabetes prevalence estimates for 2019 and projections for 2030 and 2045: Results from the international diabetes federation diabetes atlas, 9th edition. *Diabetes Res Clin Pract* (2019) 157:107843. doi: 10.1016/j.diabres.2019.107843

3. Nathan DM. Long-term complications of diabetes mellitus. *N Engl J Med* (1993) 328:1676–85. doi: 10.1056/NEJM199306103282306

4. Siegel KR, Ali MK, Zhou X, Ng BP, Jawanda S, Proia K, et al. Cost-effectiveness of interventions to manage diabetes: Has the evidence changed since 2008? *Diabetes Care* (2020) 43:1557–92. doi: 10.2337/dci20-0017

5. Alavi A, Sibbald RG, Mayer D, Goodman L, Botros M, Armstrong DG, et al. Diabetic foot ulcers: Part i. pathophysiology and prevention. *J Am Acad Dermatol* (2014) 70:e1–18:1. doi: 10.1016/j.jaad.2013.06.055

6. Guo S, DiPietro LA. Factors affecting wound healing. *J Dent Res* (2010) 89:219–29. doi: 10.1177/0022034509359125

7. Burgess JL, Wyant WA, Abdo Abujamra B, Kirsner RS, Jozic I. Diabetic wound-healing science. *Med (Kaunas)* (2021) 57:1072. doi: 10.3390/medicina57101072

8. Sanapalli BKR, Yele V, Singh MK, Thaggikuppe Krishnamurthy P, Karri VVSR. Preclinical models of diabetic wound healing: A critical review. *Biomed Pharmacother* (2021) 142:111946. doi: 10.1016/j.biopha.2021.111946

9. Bergsbaken T, Fink SL, Cookson BT. Pyroptosis: host cell death and inflammation. *Nat Rev Microbiol* (2009) 7:99–109. doi: 10.1038/nrmicro2070

10. Moujalled D, Strasser A, Liddell JR. Molecular mechanisms of cell death in neurological diseases. *Cell Death Differ* (2021) 28:2029–44. doi: 10.1038/s41418-021-00814-y

11. Man SM, Karki R, Kanneganti T-D. Molecular mechanisms and functions of pyroptosis, inflammatory caspases and inflammasomes in infectious diseases. *Immunol Rev* (2017) 277:61–75. doi: 10.1111/imr.12534

12. Song H, Yang B, Li Y, Qian A, Kang Y, Shan X. Focus on the mechanisms and functions of pyroptosis, inflammasomes, and inflammatory caspases in infectious diseases. *Oxid Med Cell Longevity* (2022) 2022:1–21. doi: 10.1155/2022/2501279

13. Hilbi H, Moss JE, Hersh D, Chen Y, Arondel J, Banerjee S, et al. Shigella-induced apoptosis is dependent on caspase-1 which binds to IpaB. *J Biol Chem* (1998) 273:32895–900. doi: 10.1074/jbc.273.49.32895

14. Brennan MA, Cookson BT. Salmonella induces macrophage death by caspase-1-dependent necrosis. *Mol Microbiol* (2000) 38:31–40. doi: 10.1046/j.1365-2958.2000.02103.x

15. Cookson BT, Brennan MA. Pro-inflammatory programmed cell death. *Trends Microbiol* (2001) 9:113–4. doi: 10.1016/S0966-842X(00)01936-3

16. Kesavardhana S, Malireddi RKS, Kanneganti T-D. Caspases in cell death, inflammation, and gasdermin-induced pyroptosis. *Annu Rev Immunol* (2020) 38:567–95. doi: 10.1146/annurev-immunol-073119-095439

17. Man SM, Kanneganti T-D. Converging roles of caspases in inflammasome activation, cell death and innate immunity. *Nat Rev Immunol* (2016) 16:7–21. doi: 10.1038/nri.2015.7

18. Mandal R, Barrón JC, Kostova I, Becker S, Strebhardt K. Caspase-8: The double-edged sword. *Biochim Biophys Acta Rev Cancer* (2020) 1873:188357. doi: 10.1016/j.bbcan.2020.188357

19. Jiang M, Qi L, Li L, Li Y. The caspase-3/GSDME signal pathway as a switch between apoptosis and pyroptosis in cancer. *Cell Death Discovery* (2020) 6:112. doi: 10.1038/s41420-020-00349-0

20. Jorgensen I, Rayamajhi M, Miao EA. Programmed cell death as a defence against infection. *Nat Rev Immunol* (2017) 17:151–64. doi: 10.1038/nri.2016.147

21. Broz P, Dixit VM. Inflammasomes: mechanism of assembly, regulation and signalling. *Nat Rev Immunol* (2016) 16:407–20. doi: 10.1038/nri.2016.58

22. Guo H, Callaway JB, Ting JP-Y. Inflammasomes: mechanism of action, role in disease, and therapeutics. *Nat Med* (2015) 21:677–87. doi: 10.1038/nm.3893

23. Qiu Z, He Y, Ming H, Lei S, Leng Y, Xia Z-Y. Lipopolysaccharide (LPS) aggravates high glucose- and Hypoxia/Reoxygenation-induced injury through activating ROS-dependent NLRP3 inflammasome-mediated pyroptosis in H9C2 cardiomyocytes. *J Diabetes Res* (2019) 2019:8151836. doi: 10.1155/2019/8151836

24. Huang Y, Xu W, Zhou R. NLRP3 inflammasome activation and cell death. *Cell Mol Immunol* (2021) 18:2114–27. doi: 10.1038/s41423-021-00740-6

25. Kovacs SB, Miao EA. Gasdermins: Effectors of pyroptosis. *Trends Cell Biol* (2017) 27:673–84. doi: 10.1016/j.tcb.2017.05.005

26. Li Y, Huang H, Liu B, Zhang Y, Pan X, Yu X-Y, et al. Inflammasomes as therapeutic targets in human diseases. *Signal Transduct Target Ther* (2021) 6:247. doi: 10.1038/s41392-021-00650-z

27. Anand PK. Lipids, inflammasomes, metabolism, and disease. *Immunol Rev* (2020) 297:108–22. doi: 10.1111/imr.12891

28. Ozaki E, Campbell M, Doyle SL. Targeting the NLRP3 inflammasome in chronic inflammatory diseases: current perspectives. *J Inflammation Res* (2015) 8:15–27. doi: 10.2147/JIR.S51250

29. Kayagaki N, Wong MT, Stowe IB, Ramani SR, Gonzalez LC, Akashi-Takamura S, et al. Noncanonical inflammasome activation by intracellular LPS independent of TLR4. *Science* (2013) 341:1246–9. doi: 10.1126/science.1240248

30. Masumoto J, Taniguchi S, Ayukawa K, Sarvotham H, Kishino T, Niikawa N, et al. ASC, a novel 22-kDa protein, aggregates during apoptosis of human promyelocytic leukemia HL-60 cells. *J Biol Chem* (1999) 274:33835–8. doi: 10.1074/jbc.274.48.33835

31. Shi J, Gao W, Shao F. Pyroptosis: Gasdermin-mediated programmed necrotic cell death. *Trends Biochem Sci* (2017) 42:245–54. doi: 10.1016/j.tibs.2016.10.004

32. Be B, Esparza AN, Zhu H, Wang S. Gasdermin d in pyroptosis. *Acta Pharm Sin B* (2021) 11(9):2768–82. doi: 10.1016/j.apsb.2021.02.006

33. Feng S, Fox D, Man SM. Mechanisms of gasdermin family members in inflammasome signaling and cell death. *J Mol Biol* (2018) 430:3068–80. doi: 10.1016/j.jmb.2018.07.002

34. Shi J, Zhao Y, Wang K, Shi X, Wang Y, Huang H, et al. Cleavage of GSDMD by inflammatory caspases determines pyroptotic cell death. *Nature* (2015) 526:660–5. doi: 10.1038/nature15514

35. He W, Wan H, Hu L, Chen P, Wang X, Huang Z, et al. Gasdermin d is an executor of pyroptosis and required for interleukin-1β secretion. *Cell Res* (2015) 25:1285–98. doi: 10.1038/cr.2015.139

36. Kuang S, Zheng J, Yang H, Li S, Duan S, Shen Y, et al. Structure insight of GSDMD reveals the basis of GSDMD autoinhibition in cell pyroptosis. *Proc Natl Acad Sci USA* (2017) 114:10642–7. doi: 10.1073/pnas.1708194114

37. Wang Y, Shi P, Chen Q, Huang Z, Zou D, Zhang J, et al. Mitochondrial ROS promote macrophage pyroptosis by inducing GSDMD oxidation. *J Mol Cell Biol* (2019) 11:1069–82. doi: 10.1093/jmcb/mjz020

38. He Y, Hara H, Núñez G. Mechanism and regulation of NLRP3 inflammasome activation. *Trends Biochem Sci* (2016) 41:1012–21. doi: 10.1016/j.tibs.2016.09.002

39. Martinon F, Burns K, Tschopp J. The inflammasome: a molecular platform triggering activation of inflammatory caspases and processing of proIL-beta. *Mol Cell* (2002) 10:417–26. doi: 10.1016/s1097-2765(02)00599-3

40. Wang L, Manji GA, Grenier JM, Al-Garawi A, Merriam S, Lora JM, et al. PYPAF7, a novel PYRIN-containing Apaf1-like protein that regulates activation of NF-kappa b and caspase-1-dependent cytokine processing. *J Biol Chem* (2002) 277:29874–80. doi: 10.1074/jbc.M203915200

41. Jo E-K, Kim JK, Shin D-M, Sasakawa C. Molecular mechanisms regulating NLRP3 inflammasome activation. *Cell Mol Immunol* (2016) 13:148–59. doi: 10.1038/cmi.2015.95

42. Elliott EI, Sutterwala FS. Monocytes take their own path to IL-1β. *Immunity* (2016) 44:713–5. doi: 10.1016/j.immuni.2016.03.015

43. Zheng M, Kanneganti T-D. The regulation of the ZBP1-NLRP3 inflammasome and its implications in pyroptosis, apoptosis, and necroptosis (PANoptosis). *Immunol Rev* (2020) 297:26–38. doi: 10.1111/imr.12909

44. Zhao Y, Shi J, Shao F. Inflammatory caspases: Activation and cleavage of gasdermin-d *In vitro* and during pyroptosis. *Methods Mol Biol* (2018) 1714:131–48. doi: 10.1007/978-1-4939-7519-8_9

45. An J, Kim SH, Hwang D, Lee KE, Kim MJ, Yang EG, et al. Caspase-4 disaggregates lipopolysaccharide micelles *via* LPS-CARD interaction. *Sci Rep* (2019) 9:826. doi: 10.1038/s41598-018-36811-4

46. Kayagaki N, Stowe IB, Lee BL, O'Rourke K, Anderson K, Warming S, et al. Caspase-11 cleaves gasdermin d for non-canonical inflammasome signalling. *Nature* (2015) 526:666–71. doi: 10.1038/nature15541

47. Yang J, Zhao Y, Shao F. Non-canonical activation of inflammatory caspases by cytosolic LPS in innate immunity. *Curr Opin Immunol* (2015) 32:78–83. doi: 10.1016/j.coi.2015.01.007

48. Linder A, Hornung V. Irgm2 and gate-16 put a break on caspase-11 activation. *EMBO Rep* (2020) 21:e51787. doi: 10.15252/embr.202051787

49. Chen S, Jin P, Chen H, Wu D, Li S, Zhang Y, et al. Dual function of a turbot inflammatory caspase in mediating both canonical and non-canonical inflammasome activation. *Dev Comp Immunol* (2021) 121:104078. doi: 10.1016/j.dci.2021.104078

50. Man SM, Karki R, Sasai M, Place DE, Kesavardhana S, Temirov J, et al. IRGB10 liberates bacterial ligands for sensing by the AIM2 and caspase-11-NLRP3 inflammasomes. *Cell* (2016) 167:382–396.e17. doi: 10.1016/j.cell.2016.09.012

51. Shen X, Wang H, Weng C, Jiang H, Chen J. Caspase 3/GSDME-dependent pyroptosis contributes to chemotherapy drug-induced nephrotoxicity. *Cell Death Dis* (2021) 12:186. doi: 10.1038/s41419-021-03458-5

52. Rogers C, Fernandes-Alnemri T, Mayes L, Alnemri D, Cingolani G, Alnemri ES. Cleavage of DFNA5 by caspase-3 during apoptosis mediates progression to secondary necrotic/pyroptotic cell death. *Nat Commun* (2017) 8:14128. doi: 10.1038/ncomms14128

53. Rogers C, Erkes DA, Nardone A, Aplin AE, Fernandes-Alnemri T, Alnemri ES. Gasdermin pores permeabilize mitochondria to augment caspase-3 activation during apoptosis and inflammasome activation. *Nat Commun* (2019) 10:1689. doi: 10.1038/s41467-019-09397-2

54. Wang Y, Gao W, Shi X, Ding J, Liu W, He H, et al. Chemotherapy drugs induce pyroptosis through caspase-3 cleavage of a gasdermin. *Nature* (2017) 547:99–103. doi: 10.1038/nature22393

55. Fritsch M, Günther SD, Schwarzer R, Albert M-C, Schorn F, Werthenbach JP, et al. Caspase-8 is the molecular switch for apoptosis, necroptosis and pyroptosis. *Nature* (2019) 575:683–7. doi: 10.1038/s41586-019-1770-6

56. Schwarzer R, Laurien L, Pasparakis M. New insights into the regulation of apoptosis, necroptosis, and pyroptosis by receptor interacting protein kinase 1 and caspase-8. *Curr Opin Cell Biol* (2020) 63:186–93. doi: 10.1016/j.ceb.2020.02.004

57. Sarhan J, Liu BC, Muendlein HI, Li P, Nilson R, Tang AY, et al. Caspase-8 induces cleavage of gasdermin d to elicit pyroptosis during yersinia infection. *Proc Natl Acad Sci USA* (2018) 115:E10888–97. doi: 10.1073/pnas.1809548115

58. Orning P, Weng D, Starheim K, Ratner D, Best Z, Lee B, et al. Pathogen blockade of TAK1 triggers caspase-8-dependent cleavage of gasdermin d and cell death. *Science* (2018) 362:1064–9. doi: 10.1126/science.aau2818

59. Hou J, Zhao R, Xia W, Chang C-W, You Y, Hsu J-M, et al. PD-L1-mediated gasdermin c expression switches apoptosis to pyroptosis in cancer cells and

facilitates tumour necrosis. *Nat Cell Biol* (2020) 22:1264–75. doi: 10.1038/s41556-020-0575-z

60. Mirza RE, Koh TJ. Contributions of cell subsets to cytokine production during normal and impaired wound healing. *Cytokine* (2015) 71:409–12. doi: 10.1016/j.cyto.2014.09.005

61. Thomay AA, Daley JM, Sabo E, Worth PJ, Shelton LJ, Harty MW, et al. Disruption of interleukin-1 signaling improves the quality of wound healing. *Am J Pathol* (2009) 174:2129–36. doi: 10.2353/ajpath.2009.080765

62. Feldmeyer L, Werner S, French LE, Beer H-D. Interleukin-1, inflammasomes and the skin. *Eur J Cell Biol* (2010) 89:638–44. doi: 10.1016/j.ejcb.2010.04.008

63. Faustin B, Reed JC. Sunburned skin activates inflammasomes. *Trends Cell Biol* (2008) 18:4–8. doi: 10.1016/j.tcb.2007.10.004

64. Eo H, Lim Y. Combined mulberry leaf and fruit extract improved early stage of cutaneous wound healing in high-fat diet-induced obese mice. *J Med Food* (2016) 19:161–9. doi: 10.1089/jmf.2015.3510

65. Bitto A, Altavilla D, Pizzino G, Irrera N, Pallio G, Colonna MR, et al. Inhibition of inflammasome activation improves the impaired pattern of healing in genetically diabetic mice. *Br J Pharmacol* (2014) 171:2300–7. doi: 10.1111/bph.12557

66. Artlett CM. Inflammasomes in wound healing and fibrosis. *J Pathol* (2013) 229:157–67. doi: 10.1002/path.4116

67. Chen F, Wei G, Xu J, Ma X, Wang Q. Naringin ameliorates the high glucose-induced rat mesangial cell inflammatory reaction by modulating the NLRP3 inflammasome. *BMC Complement Altern Med* (2018) 18:192. doi: 10.1186/s12906-018-2257-y

68. Weinheimer-Haus EM, Mirza RE, Koh TJ. Nod-like receptor protein-3 inflammasome plays an important role during early stages of wound healing. *PloS One* (2015) 10:e0119106. doi: 10.1371/journal.pone.0119106

69. Li Y, Tang Y, Shi S, Gao S, Wang Y, Xiao D, et al. Tetrahedral framework nucleic acids ameliorate insulin resistance in type 2 diabetes mellitus *via* the PI3K/Akt pathway. *ACS Appl Mater Interfaces* (2021) 13:40354–64. doi: 10.1021/acsami.1c11468

70. Chen Y, Shi S, Li B, Lan T, Yuan K, Yuan J, et al. Therapeutic effects of self-assembled tetrahedral framework nucleic acids on liver regeneration in acute liver failure. *ACS Appl Mater Interfaces* (2022) 14:13136–46. doi: 10.1021/acsami.2c02523

71. Liu N, Zhang X, Li N, Zhou M, Zhang T, Li S, et al. Tetrahedral framework nucleic acids promote corneal epithelial wound healing in vitro and in vivo. *Small* (2019) 15:e1901907. doi: 10.1002/smll.201901907

72. Zhu J, Zhang M, Gao Y, Qin X, Zhang T, Cui W, et al. Tetrahedral framework nucleic acids promote scarless healing of cutaneous wounds *via* the AKT-signaling pathway. *Signal Transduct Target Ther* (2020) 5:120. doi: 10.1038/s41392-020-0173-3

73. Lin S, Zhang Q, Li S, Zhang T, Wang L, Qin X, et al. Antioxidative and angiogenesis-promoting effects of tetrahedral framework nucleic acids in diabetic wound healing with activation of the Akt/Nrf2/HO-1 pathway. *ACS Appl Mater Interfaces* (2020) 12:11397–408. doi: 10.1021/acsami.0c00874

74. Jiang Y, Li S, Zhang T, Zhang M, Chen Y, Wu Y, et al. Tetrahedral framework nucleic acids inhibit skin fibrosis *via* the pyroptosis pathway. *ACS Appl Mater Interfaces* (2022) 14(13):15069–79. doi: 10.1021/acsami.2c02877

75. Zhou Y, Gao L, Peng J, Xing M, Han Y, Wang X, et al. Bioglass activated albumin hydrogels for wound healing. *Adv Healthc Mater* (2018) 7:e1800144. doi: 10.1002/adhm.201800144

76. Dai W, Wang X, Teng H, Li C, Wang B, Wang J. Celastrol inhibits microglial pyroptosis and attenuates inflammatory reaction in acute spinal cord injury rats. *Int Immunopharmacol* (2019) 66:215–23. doi: 10.1016/j.intimp.2018.11.029

77. Ma J-W, Ji D-D, Li Q-Q, Zhang T, Luo L. Inhibition of connexin 43 attenuates oxidative stress and apoptosis in human umbilical vein endothelial cells. *BMC Pulm Med* (2020) 20:19. doi: 10.1186/s12890-019-1036-y

78. Zhang K, Chai B, Ji H, Chen L, Ma Y, Zhu L, et al. Bioglass promotes wound healing by inhibiting endothelial cell pyroptosis through regulation of the connexin 43/reactive oxygen species (ROS) signaling pathway. *Lab Invest* (2022) 102:90–101. doi: 10.1038/s41374-021-00675-6

79. Aitcheson SM, Frentiu FD, Hurn SE, Edwards K, Murray RZ. Skin wound healing: Normal macrophage function and macrophage dysfunction in diabetic wounds. *Molecules* (2021) 26:4917. doi: 10.3390/molecules26164917

80. Louiselle AE, Niemiec SM, Zgheib C, Liechty KW. Macrophage polarization and diabetic wound healing. *Transl Res* (2021) 236:109–16. doi: 10.1016/j.trsl.2021.05.006

81. Geng K, Ma X, Jiang Z, Huang W, Gao C, Pu Y, et al. Innate immunity in diabetic wound healing: Focus on the mastermind hidden in chronic inflammatory. *Front Pharmacol* (2021) 12:653940. doi: 10.3389/fphar.2021.653940

82. Hu Q, Shi H, Zeng T, Liu H, Su Y, Cheng X, et al. Increased neutrophil extracellular traps activate NLRP3 and inflammatory macrophages in adult-onset still's disease. *Arthritis Res Ther* (2019) 21:9. doi: 10.1186/s13075-018-1800-z

83. Lee MKS, Sreejit G, Nagareddy PR, Murphy AJ. Attack of the NETs! NETosis primes IL-1β-mediated inflammation in diabetic foot ulcers. *Clin Sci (Lond)* (2020) 134:1399–401. doi: 10.1042/CS20200240

84. He S, Li L, Chen H, Hu X, Wang W, Zhang H, et al. PRRSV infection induces gasdermin d-driven pyroptosis of porcine alveolar macrophages through NLRP3 inflammasome activation. *J Virol* (2022) 96(14):e0212721. doi: 10.1128/jvi.02127-21

85. Wong SL, Demers M, Martinod K, Gallant M, Wang Y, Goldfine AB, et al. Diabetes primes neutrophils to undergo NETosis, which impairs wound healing. *Nat Med* (2015) 21:815–9. doi: 10.1038/nm.3887

86. Liu D, Yang P, Gao M, Yu T, Shi Y, Zhang M, et al. NLRP3 activation induced by neutrophil extracellular traps sustains inflammatory response in the diabetic wound. *Clin Sci* (2019) 133:565–82. doi: 10.1042/CS20180600

87. Wan L, Bai X, Zhou Q, Chen C, Wang H, Liu T, et al. The advanced glycation end-products (AGEs)/ROS/NLRP3 inflammasome axis contributes to delayed diabetic corneal wound healing and nerve regeneration. *Int J Biol Sci* (2022) 18:809–25. doi: 10.7150/ijbs.63219

88. Gu C, Draga D, Zhou C, Su T, Zou C, Gu Q, et al. miR-590-3p inhibits pyroptosis in diabetic retinopathy by targeting NLRP1 and inactivating the NOX4 signaling pathway. *Invest Ophthalmol Vis Sci* (2019) 60:4215–23. doi: 10.1167/iovs.19-27825

89. Liu X, Liu H, Lu X, Zhao S. N-acetylcysteine alleviates ocular surface damage in STZ-induced diabetic mice by inhibiting the ROS/NLRP3/Caspase-1/IL-1β signaling pathway. *Exp Eye Res* (2021) 209:108654. doi: 10.1016/j.exer.2021.108654

90. Liu H, Xu R, Kong Q, Liu J, Yu Z, Zhao C. Downregulated NLRP3 and NLRP1 inflammasomes signaling pathways in the development and progression of type 1 diabetes mellitus. *BioMed Pharmacother* (2017) 94:619–26. doi: 10.1016/j.biopha.2017.07.102

91. Yang K, Liu J, Zhang X, Ren Z, Gao L, Wang Y, et al. H3 relaxin alleviates migration, apoptosis and pyroptosis through P2X7R-mediated nucleotide binding oligomerization domain-like receptor protein 3 inflammasome activation in retinopathy induced by hyperglycemia. *Front Pharmacol* (2020) 11:603689. doi: 10.3389/fphar.2020.603689

92. Lamkanfi M, Mueller JL, Vitari AC, Misaghi S, Fedorova A, Deshayes K, et al. Glyburide inhibits the Cryopyrin/Nalp3 inflammasome. *J Cell Biol* (2009) 187:61–70. doi: 10.1083/jcb.200903124

93. Mi J, Xie C, Zeng L, Zhu Z, Chen N, He Q, et al. Bacillus subtilis WB800N alleviates diabetic wounds in mice by regulating gut microbiota homeostasis and TLR2. *J Appl Microbiol* (2022). doi: 10.1111/jam.15547

94. Pastar I, Sawaya AP, Marjanovic J, Burgess JL, Strbo N, Rivas KE, et al. Intracellular *Staphylococcus aureus* triggers pyroptosis and contributes to inhibition of healing due to perforin-2 suppression. *J Clin Invest* (2021) 131:e133727. doi: 10.1172/JCI133727

95. Zhao Y, Wang Q, Yan S, Zhou J, Huang L, Zhu H, et al. Bletilla striata polysaccharide promotes diabetic wound healing through inhibition of the NLRP3 inflammasome. *Front Pharmacol* (2021) 12:659215. doi: 10.3389/fphar.2021.659215

96. Sun X, Wang X, Zhao Z, Chen J, Li C, Zhao G. Paeoniflorin inhibited nod-like receptor protein-3 inflammasome and NF-kappa b-mediated inflammatory reactions in diabetic foot ulcer by inhibiting the chemokine receptor CXCR2. *Drug Dev Res* (2021) 82:404–11. doi: 10.1002/ddr.21763

97. Wang T, Zhao J, Zhang J, Mei J, Shao M, Pan Y, et al. Heparan sulfate inhibits inflammation and improves wound healing by downregulating the NLR family pyrin domain containing 3 (NLRP3) inflammasome in diabetic rats. *J Diabetes* (2018) 10:556–63. doi: 10.1111/1753-0407.12630

98. Mirza RE, Fang MM, Weinheimer-Haus EM, Ennis WJ, Koh TJ. Sustained inflammasome activity in macrophages impairs wound healing in type 2 diabetic humans and mice. *Diabetes* (2014) 63:1103–14. doi: 10.2337/db13-0927

99. Sutterwala FS, Ogura Y, Szczepanik M, Lara-Tejero M, Lichtenberger GS, Grant EP, et al. Critical role for NALP3/CIAS1/Cryopyrin in innate and adaptive immunity through its regulation of caspase-1. *Immunity* (2006) 24. doi: 10.1016/j.immuni.2006.02.004

100. Tschopp J, Schroder K. NLRP3 inflammasome activation: The convergence of multiple signalling pathways on ROS production? *Nat Rev Immunol* (2010) 10:210–5. doi: 10.1038/nri2725

101. Earl AM, Losick R, Kolter R. Ecology and genomics of bacillus subtilis. *Trends Microbiol* (2008) 16:269–75. doi: 10.1016/j.tim.2008.03.004

102. Yang Y, Jing Y, Yang J, Yang Q. Effects of intranasal administration with bacillus subtilis on immune cells in the nasal mucosa and tonsils of piglets. *Exp Ther Med* (2018) 15:5189–98. doi: 10.3892/etm.2018.6093

103. Huon J-F, Montassier E, Leroy A-G, Grégoire M, Vibet M-A, Caillon J, et al. Phages versus antibiotics to treat infected diabetic wounds in a mouse model: a microbiological and microbiotic evaluation. *mSystems* (2020) 5:e00542–20. doi: 10.1128/mSystems.00542-20

104. Dasu MR, Thangappan RK, Bourgette A, DiPietro LA, Isseroff R, Jialal I. TLR2 expression and signaling-dependent inflammation impair wound healing in diabetic mice. *Lab Invest* (2010) 90:1628–36. doi: 10.1038/labinvest.2010.158

105. Ramirez HA, Pastar I, Jozic I, Stojadinovic O, Stone RC, Ojeh N, et al. *Staphylococcus aureus* triggers induction of miR-15B-5P to diminish DNA repair and deregulate inflammatory response in diabetic foot ulcers. *J Invest Dermatol* (2018) 138:1187–96. doi: 10.1016/j.jid.2017.11.038

106. Yuan L, Sun Y, Xu M, Zeng F, Xiong X. miR-203 acts as an inhibitor for epithelial-mesenchymal transition process in diabetic foot ulcers *via* targeting interleukin-8. *Neuroimmunomodulation* (2019) 26:239–49. doi: 10.1159/000503087

107. Miller LS, Pietras EM, Uricchio LH, Hirano K, Rao S, Lin H, et al. Inflammasome-mediated production of IL-1beta is required for neutrophil recruitment against *Staphylococcus aureus in vivo*. *J Immunol* (2007) 179:6933–42. doi: 10.4049/jimmunol.179.10.6933

108. Chen S, Li R, Cheng C, Xu J-Y, Jin C, Gao F, et al. Pseudomonas aeruginosa infection alters the macrophage phenotype switching process during wound healing in diabetic mice. *Cell Biol Int* (2018) 42:877–89. doi: 10.1002/cbin.10955

109. Jiang S, Zhang H, Li X, Yi B, Huang L, Hu Z, et al. Vitamin D/VDR attenuate cisplatin-induced AKI by down-regulating NLRP3/Caspase-1/GSDMD pyroptosis pathway. *J Steroid Biochem Mol Biol* (2021) 206:105789. doi: 10.1016/j.jsbmb.2020.105789

110. Zhang C, He Y, Chen Z, Shi J, Qu Y, Zhang J. Effect of polysaccharides from bletilla striata on the healing of dermal wounds in mice. *Evid Based Complement Alternat Med* (2019) 2019:9212314. doi: 10.1155/2019/9212314

111. He X, Wang X, Fang J, Zhao Z, Huang L, Guo H, et al. Bletilla striata: Medicinal uses, phytochemistry and pharmacological activities. *J Ethnopharmacol* (2017) 195:20–38. doi: 10.1016/j.jep.2016.11.026

112. Luo Y, Diao H, Xia S, Dong L, Chen J, Zhang J. A physiologically active polysaccharide hydrogel promotes wound healing. *J BioMed Mater Res A* (2010) 94:193–204. doi: 10.1002/jbm.a.32711

113. Ding L, Shan X, Zhao X, Zha H, Chen X, Wang J, et al. Spongy bilayer dressing composed of chitosan-Ag nanoparticles and chitosan-bletilla striata polysaccharide for wound healing applications. *Carbohydr Polym* (2017) 157:1538–47. doi: 10.1016/j.carbpol.2016.11.040

114. Zheng T, Wang Q, Dong Y, Ma W, Zhang Y, Zhao Y, et al. High glucose-aggravated hepatic insulin resistance: Role of the NLRP3 inflammasome in kupffer cells. *Obes (Silver Spring)* (2020) 28:1270–82. doi: 10.1002/oby.22821

115. Li Y, Xu S, Mihaylova MM, Zheng B, Hou X, Jiang B, et al. AMPK phosphorylates and inhibits SREBP activity to attenuate hepatic steatosis and atherosclerosis in diet-induced insulin-resistant mice. *Cell Metab* (2011) 13:376–88. doi: 10.1016/j.cmet.2011.03.009

116. Zheng T, Yang X, Li W, Wang Q, Chen L, Wu D, et al. Salidroside attenuates high-fat diet-induced nonalcoholic fatty liver disease *via* AMPK-dependent TXNIP/NLRP3 pathway. *Oxid Med Cell Longev* (2018) 2018:8597897. doi: 10.1155/2018/8597897

117. Dinh T, Tecilazich F, Kafanas A, Doupis J, Gnardellis C, Leal E, et al. Mechanisms involved in the development and healing of diabetic foot ulceration. *Diabetes* (2012) 61:2937–47. doi: 10.2337/db12-0227

118. Chen LC, Lee MH, Chou MH, Lin MF, Yang LL. Pharmacokinetic study of paeoniflorin in mice after oral administration of paeoniae radix extract. *J Chromatogr B BioMed Sci Appl* (1999) 735:33–40. doi: 10.1016/s0378-4347(99)00408-9

119. Shao Y-X, Xu X-X, Wang K, Qi X-M, Wu Y-G. Paeoniflorin attenuates incipient diabetic nephropathy in streptozotocin-induced mice by the suppression of the toll-like receptor-2 signaling pathway. *Drug Des Devel Ther* (2017) 11:3221–33. doi: 10.2147/DDDT.S149504

120. Kulprachakarn K, Ounjaijean S, Wungrath J, Mani R, Rerkasem K. Micronutrients and natural compounds status and their effects on wound healing in the diabetic foot ulcer. *Int J Low Extrem Wounds* (2017) 16:244–50. doi: 10.1177/1534734617737659

121. Mamun AA, Wu Y, Nasrin F, Akter A, Taniya MA, Munir F, et al. Role of pyroptosis in diabetes and its therapeutic implications. *J Inflammation Res* (2021) 14:2187–206. doi: 10.2147/JIR.S291453

122. Mirza RE, Fang MM, Ennis WJ, Koh TJ. Blocking interleukin-1β induces a healing-associated wound macrophage phenotype and improves healing in type 2 diabetes. *Diabetes* (2013) 62:2579–87. doi: 10.2337/db12-1450

123. Baggiolini M. Chemokines in pathology and medicine. *J Intern Med* (2001) 250:91–104. doi: 10.1046/j.1365-2796.2001.00867.x

124. Boro M, Balaji KN. CXCL1 and CXCL2 regulate NLRP3 inflammasome activation *via* G-Protein-Coupled receptor CXCR2. *J Immunol* (2017) 199:1660–71. doi: 10.4049/jimmunol.1700129

125. Chang Z, Meyer K, Rapraeger AC, Friedl A. Differential ability of heparan sulfate proteoglycans to assemble the fibroblast growth factor receptor complex in situ. *FASEB J* (2000) 14:137–44. doi: 10.1096/fasebj.14.1.137

126. Bosman FT, Stamenkovic I. Functional structure and composition of the extracellular matrix. *J Pathol* (2003) 200:423–8. doi: 10.1002/path.1437

127. Tong M, Tuk B, Shang P, Hekking IM, Fijneman EMG, Guijt M, et al. Diabetes-impaired wound healing is improved by matrix therapy with heparan sulfate glycosaminoglycan mimetic OTR4120 in rats. *Diabetes* (2012) 61:2633–41. doi: 10.2337/db11-1329

128. Eming SA, Krieg T, Davidson JM. Inflammation in wound repair: molecular and cellular mechanisms. *J Invest Dermatol* (2007) 127:514–25. doi: 10.1038/sj.jid.5700701

129. Tong M, Tuk B, Hekking IM, Pleumeekers MM, Boldewijn MB, Hovius SER, et al. Heparan sulfate glycosaminoglycan mimetic improves pressure ulcer healing in a rat model of cutaneous ischemia-reperfusion injury. *Wound Repair Regener* (2011) 19:505–14. doi: 10.1111/j.1524-475X.2011.00704.x

130. Luo B, Li B, Wang W, Liu X, Xia Y, Zhang C, et al. NLRP3 gene silencing ameliorates diabetic cardiomyopathy in a type 2 diabetes rat model. *PloS One* (2014) 9:e104771. doi: 10.1371/journal.pone.0104771

131. Cavalcante-Silva J, Koh TJ. Targeting the NOD-like receptor pyrin domain containing 3 inflammasome to improve healing of diabetic wounds. *Adv Wound Care (New Rochelle)* (2022). doi: 10.1089/wound.2021.0148

frontiers | Frontiers in Endocrinology

TYPE Original Research
PUBLISHED 02 September 2022
DOI 10.3389/fendo.2022.992875

OPEN ACCESS

EDITED BY
Chunjie Jiang,
University of Pennsylvania,
United States

REVIEWED BY
Yunfeng Zhao,
Ochsner LSU Health, United States
Zeguo Sun,
Icahn School of Medicine at Mount Sinai, United States
Yanni Li,
Virginia Tech, United States

*CORRESPONDENCE
Yitong Zhang
zhangyitong@bit.edu.cn

SPECIALTY SECTION
This article was submitted to Diabetes: Molecular Mechanisms, a section of the journal Frontiers in Endocrinology

RECEIVED 13 July 2022
ACCEPTED 11 August 2022
PUBLISHED 02 September 2022

CITATION
Cao Y, Wang W, Zhan X and Zhang Y (2022) PRDX6: A protein bridging S-palmitoylation and diabetic neuropathy.
Front. Endocrinol. 13:992875.
doi: 10.3389/fendo.2022.992875

PRDX6: A protein bridging S-palmitoylation and diabetic neuropathy

Yan Cao[1], Wantao Wang[2], Xiaorong Zhan[3] and Yitong Zhang[4]*

[1]Department of Anesthesiology, Sun Yat-sen University Cancer Center, State Key Laboratory of Oncology in South China, Collaborative Innovation Center for Cancer Medicine, Guangzhou, China, [2]Department of Spine Surgery, The First Affiliated Hospital of Sun Yat-sen University, Guangzhou, China, [3]Department of Endocrinology, Southern University of Science and Technology Hospital, Shenzhen, China, [4]School of Life Science, Beijing Institute of Technology, Beijing, China

Diabetic neuropathy is regarded as one of the most debilitating outcomes of diabetes. It can affect both the peripheral and central nervous systems, leading to pain, decreased motility, cognitive decline, and dementia. S-palmitoylation is a reversible posttranslational lipid modification, and its dysregulation has been implicated in metabolic syndrome, cancers, neurological disorders, and infections. However, the role of S-palmitoylation in diabetic neuropathy remains unclear. Here we demonstrate a potential association between activating protein palmitoylation and diabetic neuropathy. We compared the proteomic data of lumbar dorsal root ganglia (DRG) of diabetes mice and palmitoylome profiling data of the HUVEC cell line. The mapping results identified peroxiredoxin-6 (PRDX6) as a novel target in diabetic neuropathy, whose biological mechanism was associated with S-palmitoylation. Bioinformatic prediction revealed that PRDX6 had two palmitoylation sites, Cys47 and Cys91. Immunofluorescence results indicated PRDX6 translocating between the cytoplasm and cell membrane. Protein function analysis proposed that increased palmitoylation could competitively inhibit the formation of disulfide-bond between Cys47 and Cys91 and change the spatial topology of PRDX6 protein. Cl^-HCO3^- anion exchanger 3 (AE3) was one of the AE family members, which was proved to express in DRG. AE3 activity evoked Cl^- influx in neurons which was generally associated with increased excitability and susceptibility to pain. We demonstrated that the S-palmitoylation status of Cys47 could affect the interaction between PRDX6 and the C-terminal domain of AE3, thereby regulating the activity of AE3 anion exchanger enzyme in the nervous system. The results highlight a central role for PRDX6 palmitoylation in protection against diabetic neuropathy.

KEYWORDS

diabetic neuropathy, DRG, S-palmitoylation, PRDX6, AE3, Cl^- influx, pain

Introduction

Diabetes mellitus (DM), with an increasing prevalence, has systemic implications for health and quality of life. Among the various complications of diabetes, diabetic neuropathy (DN) is of the most importance, which can affect the peripheral nervous system, central nervous system, pain receptors, gastrointestinal systems, etc. Diabetic peripheral neuropathy (DPN), is characterized by mechanical allodynia, spontaneous pain, and paresthesia (tingling, shooting, or electric shock sensations), affecting 25 to 30% of patients with diabetes over the course of the disease (1, 2). In central nervous systems, DN can lead to decreased motility, cognitive decline, and dementia. However, currently, no treatment could clearly or effectively reverse DN in clinical. It is thus of great significance to study its molecular pathogenesis and aid in development of novel treatments for this condition.

Although the precise cellular mechanisms of DN remain poorly understood, some promising clues have emerged. Recently, various ion channels are promising topics on the mechanisms of pain inducing. The dynamic of ion channels, including sodium, potassium, calcium and chloride channels, can regulate transmission and processing of pain signals (3–5). Among those, calcium-activated chloride channels (CaCCs) intrigued us, for expressing in the neurons. Using of CaCCs current blockers can inhibit bradykinin-induced acute nociceptive pain in dorsal root ganglia (DRG) neurons (6). However, the Cl^-HCO3^- ion channel, which can cause chloride influx as CaCCs, is rarely studied in diabetic neuropathic pain.

S-Palmitoylation is a dynamic and reversible posttranslational modification of palmitate onto cysteine residue of a protein, which is catalyzed by palmitoyltransferases (PATs), a family of integral membrane enzymes (7). The human PATs comprise a family of 23 zinc-Asp-His-His-Cys (ZDHHC). S-Palmitoylation regulates a variety of intracellular functions (8–10), including protein localization, protein trafficking, protein sorting, protein stability, protein-protein interaction, etc. The development of click-chemistry-based mass spectrometry technology facilitates palmitoylome profiling, revealing that palmitoylation plays a crucial role in the occurrence and development of a large number of human diseases, such as cancer, neurodegenerative diseases, inflammatory bowel disease and immune diseases (11, 12). Excitingly, emerging evidence prove that S-palmitoylation is involved in insulin functions of resistance and secretion (13). However, the mechanism of S-palmitoylation in the occurrence and development of DN is uncovered and worth exploring.

In this study, we investigated the potential role of S-palmitoylation in DN by the proteomic and palmitoylomic data, and we identified PRDX6 as a novel candidate of S-palmitoylation in diabetic lumbar dorsal root ganglia (D-DRG). Furthermore, we analyzed the gene expression of PRDX6 in human nervous system. The results also showed that S-palmitoylation modified the Cys47 of PRDX6, and this modification enhanced its interaction with anion exchanger 3 (AE3) and activated the $Cl^-/HCO3^-$ flux inducing pain in D-DRG. This study will advance our understanding of S-palmitoylation in diabetes and will provide a new nutritional approach for diabetes associated neuropathy.

Manuscript formatting

Identifying S-palmitoylation candidates in DRG

The D-DRG protein set was obtained from Marc's research (14). They first established BKS-db/db mice contain a mutation of the leptin receptor, and then performed tandem mass tag labelling and mass spectrometry analysis of lumbar DRG in type 2 diabetes model. They performed functional cluster analysis of differential expression proteins and revealed 88 distinguished proteins (Supplementary Table 1). The data of palmitoylome in the human umbilical vein endothelial cells (HUVECs) was obtained from Wei's research (13). They used acyl-biotin exchange chemistry technique to screen the proteins modified by S-palmitoylation in HUVECs. Proteins with a threshold of stable isotope labeling by amino acids in cell culture (SILAC) ratio of >1.5 were palmitoylation candidates. They screened out 100 S-palmitoylation candidates, and we chose these proteins for analysis in this study (Supplementary Table 2). We mapped and visualized those two protein-sets by Hiplot (https://hiplot.org).

RNA-seq database

The RNA-sequencing (RNA-seq) data of the AEs family for 55 tissue types was obtained from the Consensus dataset, which was based on a combination of RNA-seq data from Internally generated Human Protein Atlas (HPA) and the Genotype-Tissue Expression (GTEx) project. The transcript per million (TPM) was normalized separately using Trimmed mean of M values (TMM) to allow for between-sample comparisons. The normalized expression (nTPM) levels were calculated for each gene in every sample.

The single cell RNA-sequencing (scRNA-seq) dataset was retrieved from the Single Cell Type Section of HPA. The data of scRNA-seq was performed on single cell suspension from tissues without pre-enrichment of cell types, and pseudo-bulk gene expression profiles were highly correlated with bulk RNA-seq profiles. The protein-coding genes were classified according to specificity into cell type enriched genes, group enriched genes and cell type enhanced genes. The cell type enriched genes were at least fourfold higher expression levels in one cell type as compared with any other analyzed cell type. The group enriched genes were enriched expression in 2-10 cell types. The cell type

enhanced genes were only moderately elevated expression. These cluster results were visualized by the UMAP plot.

The construction of PPI network

We performed the protein-protein interaction (PPI) analysis by STRING 11.5 (15). The input data was the 88 D-DRG proteins and 23 members of the ZDHHC family. We constructed full STRING network, which protein interactions included both functional and physical protein associations. The active interaction sources contained Text mining, Experiments, Databases, Co-expression, Neighborhood, Gene Fusion, and Co-occurrence. We set 0.400, indicating medium confidence, as the minimum required interaction score.

MCL clustering

We clustered the nodes (proteins) in the PPI network by the Markov Cluster Algorithm (MCL) using the STRING tool. The MCL inflation parameter was set as 3. Edges between clusters were shown in dotted line, and each dot color was coded by its cluster.

Enrichment analysis

We performed the Gene Ontology (GO) Functional annotation and Kyoto Encyclopedia of Genes and Genomes (KEGG) pathway enrichment for the 88 D-DRG proteins and the 23 ZDHHCs. We defined Strength as *Strength = lg (b/e)*, which was used to describe the enrichment effect. Here *b* refers to the number of proteins in the D-DRG network that were enriched in a term; *e* denotes the number of proteins that we expected to be enriched with this term in a random network of the same size from the genome. We used the False Discovery Rate *(FDR)* to describe the significance of the enrichment. FDR was the *p-values* corrected for multiple testing within each category using the Benjamini–Hochberg procedure.

S-palmitoylation site prediction

We used the CSS-Palm software (version 4.0) to predict the S-palmitoylation site of PRDX6 and CANX based on their protein sequence in FASTA format. CSS-Palm 4.0 included a forth-generation of Group-based Prediction System (GPS) algorithm and the training data set contained 583 palmitoylation sites from 277 distinct proteins. The Particle Swarm Optimize (PSO) was also integrated to GPS. The leave- one-out validation and 4-, 6-, 8-, 10-fold cross-validations were performed to evaluate the prediction performance and system robustness.

Protein domain analysis

We performed protein domain analysis for PRDX6 based on its protein sequence by the HMMER tool. HMMER was a tool for biosequence analysis using profile hidden Markov models. The functional domain analysis of the AE family was performed based on their protein sequence in the InterPro protein families and domains database (16).

Immunohistochemistry

The Immunochemistry (IHC) data of PRDX6 was obtained from the HPA database. We chose the IHC results of PRDX6 stained by the antibody of CAB008663. The antibody staining in the cell types of glial cells and neuronal cells in the human brain was reported as not detected, low, medium, or high. This score was based on the staining intensity and fraction of stained cells.

Immunofluorescence Staining

The indirect immunofluorescence (IF) microscopy was used to determine the subcellular location of PRDX6 and CANX (species-specific secondary antibodies labelled by Alexa Fluor 488, green) in human cancer cell lines. The staining of nuclei was labeled by 4',6-diamidino-2-fenylindol (DAPI) in blue, and the endoplasmic reticulum (ER) was labeled by Alexa Fluor 647 staining for calreticulin (yellow). All IF data was obtained from the HPA database.

Results

PRDX6 is a palmitoylated candidate in diabetic DRG

Marc et al. have established type 2 diabetes model (BKS-db/db mice) and characterized the proteome of D-DRG by tandem mass tag labelling and mass spectrometry analysis (14). In the human body, S-palmitoylation is catalyzed by the ZDHHCs family. To explore the association between diabetic neuropathy and S-palmitoylation, we performed PPI analysis for Marc's D-DRG proteome data and 23 ZDHHCs. Since clustering analysis of the nodes in the PPI network can further mine the potential relationships of the nodes in the network, we performed MCL clustering for the nodes of the PPI network. As shown in Figure 1A, the edge and cluster between CANX and ZDHHC6 was the only interaction between D-DRG proteins and ZDHHCs. Wei and colleges performed quantitative proteomic profiling of human endothelial cells using stable isotope labeling by amino

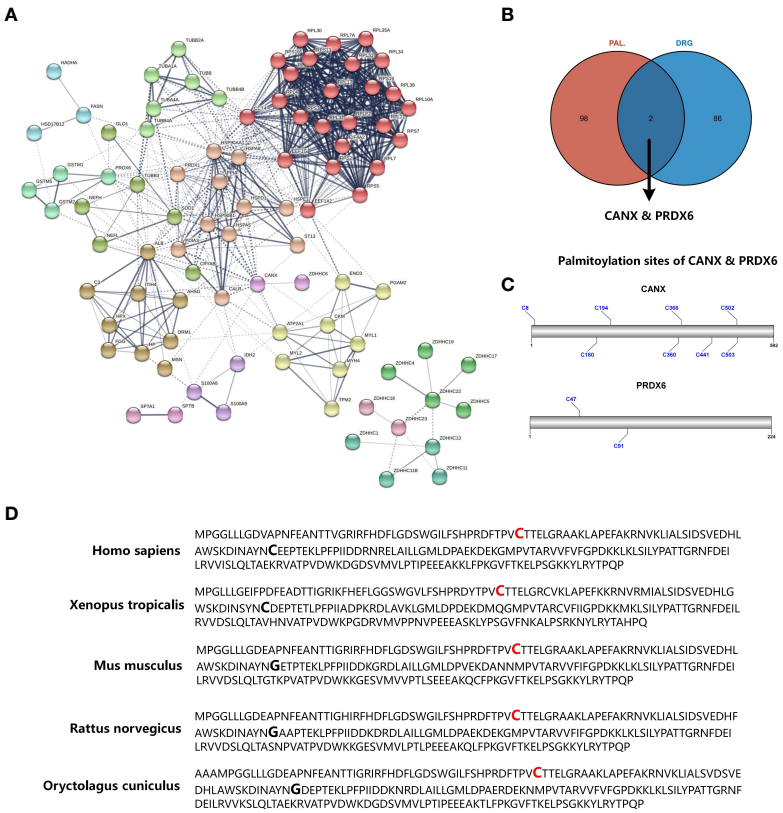

FIGURE 1
Identifying significant proteins modified by S-palmitoylation in DRG proteome of diabetic mice. **(A)** PPI network analysis of differential expression proteins in diabetic mice DRG and the ZDHHC protein family. The edges between each node indicate both functional and physical protein associations, and the line thickness indicates the strength of data support. The edges between MCL clusters were set as dotted lines. **(B)** Venn diagram showed the mapping results of DRG proteins and S-palmitoylation candidates identified by acyl-biotin exchange and mass spectrometry. **(C)** The prediction results of CANX and PRDX6 S-palmitoylation sites. **(D)** Sequence alignment among the PRDX6 amino residues of Homo sapiens, Xenopus tropicalis, mus musculus, Rattus norvegicus, and Oryctolagus cuniculus. Palmitoylation sites of Cys47 that are conserved in all species are shown in red bold type, and Cys91, not conserved in all species, are shown in bold type only. PPI, protein-protein interaction; MCL, Markov Cluster; DRG, dorsal root ganglia; Cys, cysteine.

acids combined with acyl-biotin exchange chemistry in cell culture and identified ≈ 380 putative palmitoylated proteins (13). To further discover D-DRG associated S-palmitoylation candidates, we mapped the palmitoylome data of HUVEC and the D-DRG proteome data. The Venn diagram showed CANX and Peroxiredoxin 6 (PRDX6) were the intersection proteins (Figure 1B). CANX and PRDX6 were significant proteins in D-DRG, which biological function could be regulated by the posttranslation modification of S-palmitoylation. By using the CSS-Palm software, we analyzed the FASTA data of amino sequence to predict the palmitoylation sites of CANX and PRDX6. The protein architectures revealed that CANX had eight palmitoylation sites and PRDX6 had two predicted novel palmitoylation sites of Cys47 and Cys91 (Figure 1C). It has been reported that ZDHHC6 was responsible for the Cys502 of CANX S-palmitoylation modification (17). However, the S-palmitoylation of PRDX6 has not been reported before. As a result, we chose PRDX6, but not CANX, for further study. Since conserved amino acid sites among species often have important biological functions, we compared the amino acid sequence of PRDX6 in five species of Homo sapiens, Xenopus tropicalis, Mus musculus, Rattus norvegicus, and Oryctolagus cuniculus. The Cys47 was conserved among species, but not Cys91 (Figure 1D). PRDX6 contains only one conserved cysteine residue (Cys47) rather than the two found in other six members of the PRDX family (18). These results indicated that the S-palmitoylation modification of Cys47 may play an important role in the biological function of PRDX6 in D-DRG.

PRDX6 expression in central nervous system

DM can affect not only the peripheral nervous system such as the DRG, but also the central nervous system. We analyzed the gene expression of PRDX6 in the brain, to explored whether PRDX6 could play a certain molecular function in the central nervous system. The bar-plot showed PRDX6 mRNA expression distributed in all the 13 regions of human brain sample (the HPA Human brain dataset), but there was low region specificity (Figure 2A). The UMAP plot visualized the scRNAseq data of PRDX6 in the brain cell type clusters (the HPA Human brain dataset), and PRDX6 was significantly upregulated in the astrocyte cluster (Figure 2B), which was similar to the expression levels of astrocyte markers of ALDH1L1, GFAP, and SLC1A3 (Supplementary Figure 1). Immunohistochemistry (IHC) results of human brain tissue also revealed that PRDX6 was overexpressed in the Glial cells than the neuron (Figure 2C), which cross proved the scRNAseq results.

The subcellular location of PRDX6

We performed GO functional annotation of Cellular component (CC) for the D-DRG protein set and the ZDHHCs family (Supplementary Table 3). There were 18 CC terms including PRDX6, as shown in the bubble plot (Figure 3A). The immunofluorescence (IF) results (Figure 3B) indicated that PRDX6 detected in the Plasma membrane and Cytosol in the human cancer cell lines of A-431 (Epidermoid carcinoma), U-2OS (Osteosarcoma), and U-251 MG (Glioblastoma). However, CANX localized to the Endoplasmic reticulum (Supplementary Figure 2). The schematic showed the subcellular localization of PRDX6 to Plasma membrane and Cytosol (Figure 3C).

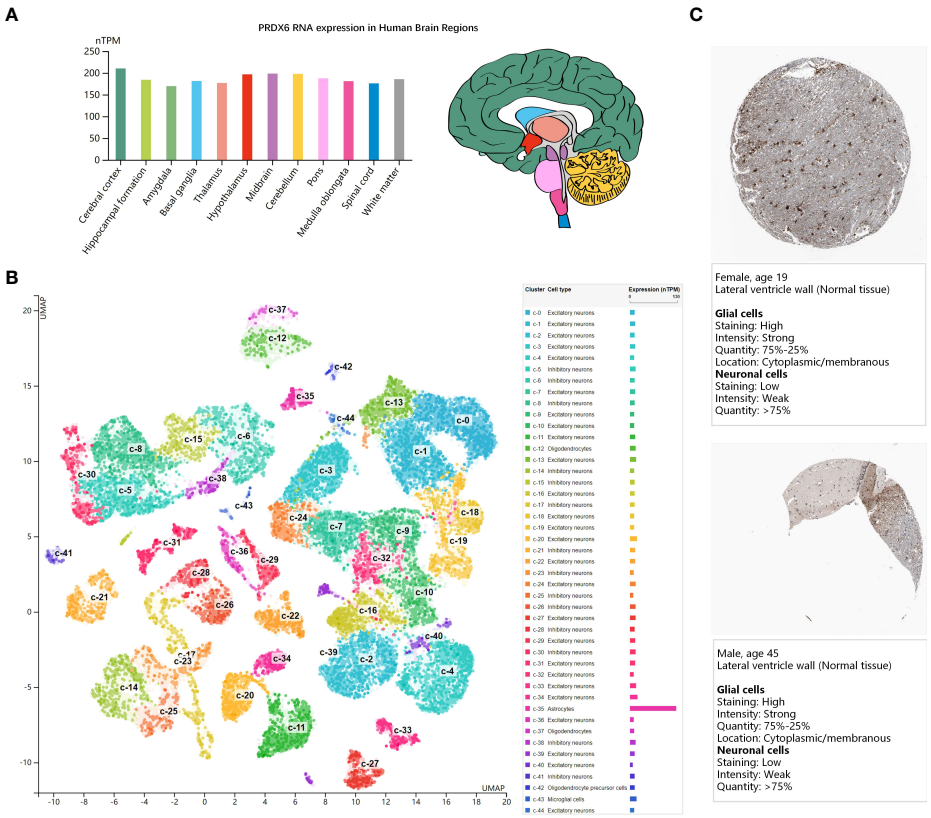

FIGURE 2
PRDX6 expression in human brain (the HPA database). **(A)** The bar-plot shows normalized RNA expression levels of PRDX6 in the 13 human brain regions. Color coding is based on brain region and the bar shows the highest expression among the subregions included. The bar-plot in red shows the distribution of PRDX6 mRNA expression in subregions of Hypothalamus. **(B)** The UMAP plot shows mRNA expression of PRDX6 in the single cell type clusters identified in brain tissue, and each dot corresponds to a cell. The bar-plot shows the mRNA expression levels of PRDX6 in each cell type cluster. The unique color assigns to each cluster. **(C)** The immunohistochemistry results of PRDX6 in histological sections from normal human brain tissues. nTPM, normalized transcript per million.

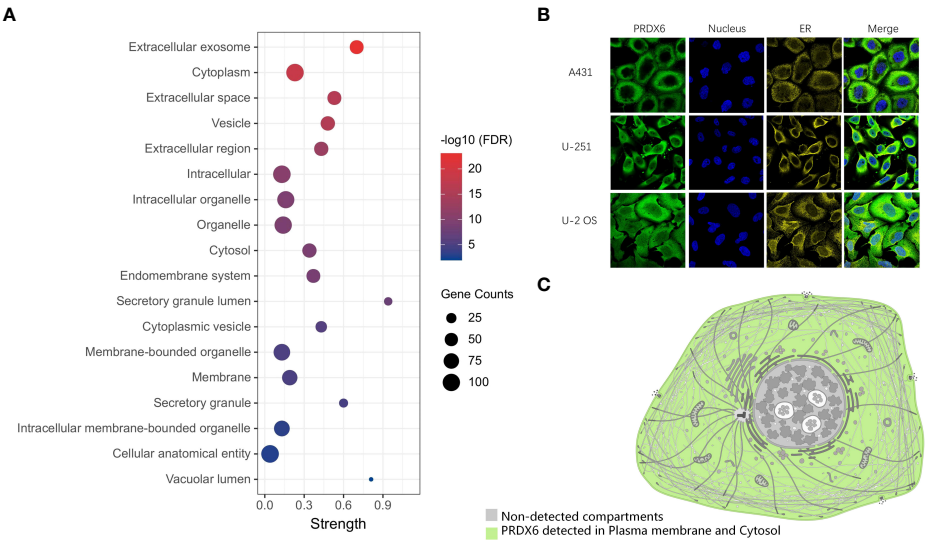

FIGURE 3
The distribution of PRDX6 in cellular components. **(A)** The GO functional categories of DRG proteins and ZDHHCs were performed by STRING. The CC terms including PRDX6 were selected and visualized in the bubble plot. **(B)** The Immunofluorescence results of PRDX6 in human cell lines indicate PRDX6 localizes in the plasma membrane and cytoplasm. **(C)** The schematic of PRDX6 subcellular localization. GO, Gene Ontology; CC, Cellular Component. A-431, Epidermoid carcinoma cell line; U-2OS, Osteosarcoma cell line; U-251 MG, Glioblastoma cell line.

The biological function of PRDX6

To discover the biological function of PRDX6, the GO functional enrichment of Biological Process (BP) and Molecular Function (MF) was also performed for the D-DRG proteins and the ZDHHC family (Figure 4A). BP results revealed that PRDX6 was involved in 25 biological processes (Supplementary Table 4). It was reported that PRDX6 translocation to the plasma membrane can increase its PLA2 activity (19), and PRDX6 was one of the D-DRG protein. Thus, we focused on BP terms of Establishment of localization in cell, Cellular localization, Transport, Localization, Organic substance metabolic process, Metabolic process, Cellular metabolic process, Primary metabolic process, and Regulation of metabolic process, which associated with localization and metabolic were identified and visualized in the bubble plot. PRDX6 was involved in six MF terms, including Catalytic activity, Antioxidant activity, Cell adhesion molecule binding, Cadherin binding, Identical protein binding, and Protein binding (Supplementary Table 5). We also performed KEGG pathway enrichment analysis (Supplementary Table 6), and found PRDX6 was only enriched in the Glutathione Metabolism Pathway (Figure 4B). To validate the molecular function of PRDX6, we analyzed the sequence of PRDX6 by the HMMER webserver which was based on hidden Markov models. As shown in Figure 4C, PRDX6 had two domains of AhpC-TSA (Alkyl hydroperoxide reductase subunit C/Thiol specific antioxidant) and 1-cysPrx_C (C-terminal domain of 1-Cys peroxiredoxin). The AhpC-TSA domain had two active sites of Cys47 and Asp140, including the conserved S-palmitoylation site of Cys47, indicating the S-palmitoylation modification of Cys47 may involve in the antioxidant function of PRDX6.

PRDX6 interacts with AE3 in nervous system

Previously, Sara et al. demonstrated that PRDX6 is a binding partner of the C-terminal tail of anion exchanger 1 (AE1), a Cl^-/$HCO3^-$exchanger, and conformed that PRDX6-AE1 interaction could be disrupted by the Cys47Ala (alanine) mutation of PRDX6 (18). However, AE1 only expressed in erythrocytes (eAE1) and at the basolateral surface of intercalated cells in the kidney (kAE1), not detected in the nervous system. Since the AE (gene symbol Slc4) family of $HCO3^-$ transporters consists of four members, we analyzed the expression of the four AEs in human tissues by RNA-seq data to identify the significant AEs in the nervous system. As shown in the bar-plots (Figure 5A), AE2, AE3 and AE4 were detected in the brain. Then we analyzed the functional domain of AEs to explore the protein structure in the C-terminal of them each. Figure 5B revealed that all of the AEs had a $HCO3^-$transport domain in the C-terminal. Although the protein sequence of $HCO3^-$transpont-like transmembrane domain of AE1 has a gap of 4 amino acids (aa 555-558), the four AEs have the same domain in the C-terminal. However, only AE3 has been proved to present in DRG; AE3 expression enhanced during short and long-lasting formalin-

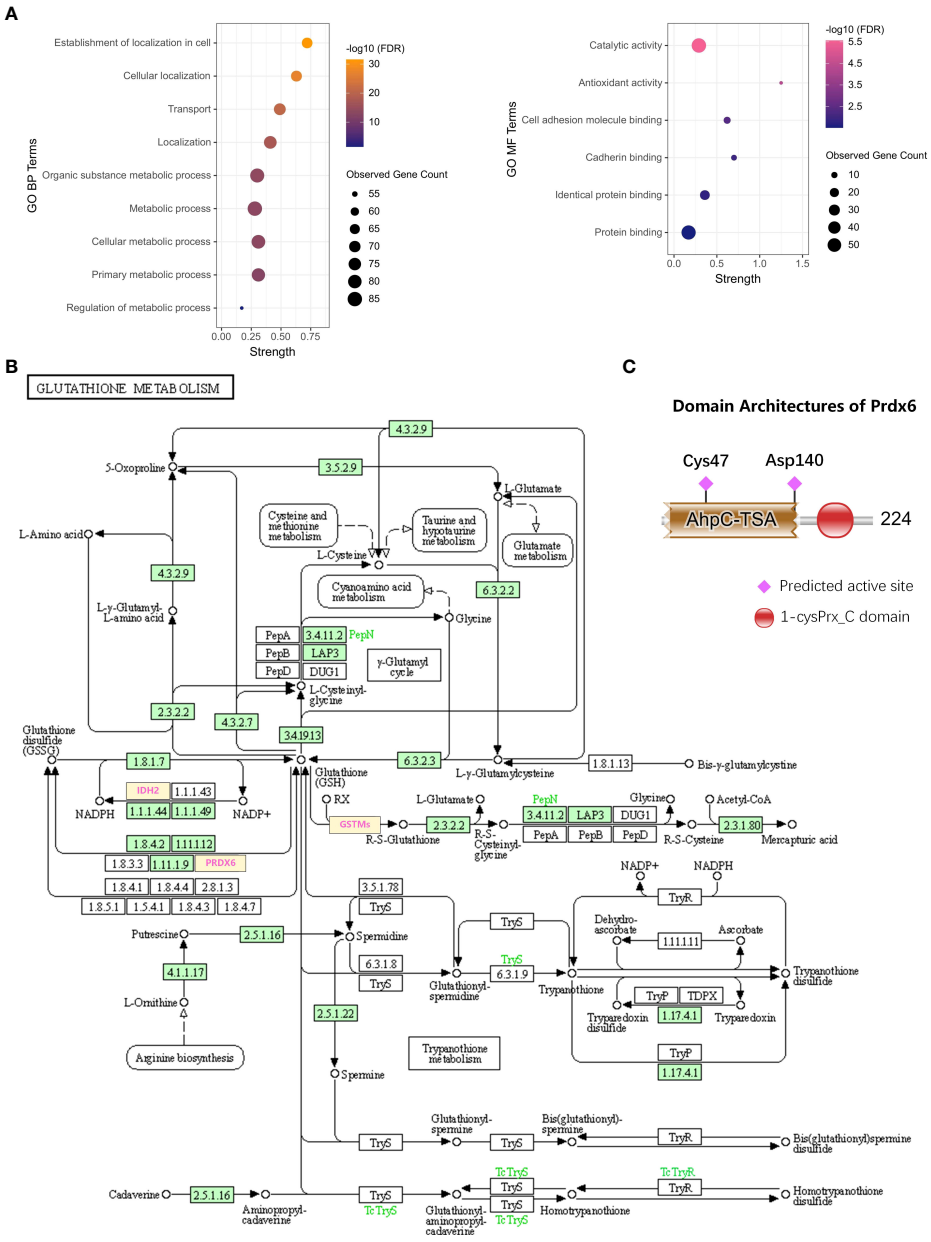

FIGURE 4
The biological function of PRDX6. **(A)** The bubble plots show the BP and MF terms of GO functional enrichment including PRDX6. **(B)** The DRG proteins of GSTM2, GSTM5, GSTM1, IDH2, and PRDX6 participate in the KEGG pathway of Glutathione metabolism (hsa00480). **(C)** The domain analysis and visualization were performed by the HMMER database. The architecture of PRDX6 protein shows the two domains of AhpC-TSA and 1-cysPrx_C, and there are two active sites of Cys47 and Asp140 in AhpC-TSA. BP, Biological Process; MF, Molecular Function; KEGG, Kyoto Encyclopedia of Genes and Genomes. Asp, aspartic.

induced nociception (19), and spared nerve injury enhanced base-line AE3 expression in L4 and L5 DRGs (20). Since PRDX6 overexpressed in the D-DRG and could be modified by S-palmitoylation, we demonstrated that the palmitoylation of PRDX6 participated in the interaction between PRDX6 and the C-terminal tail of AE3 in DRG, which could activate the influx of Cl^- and extra-flux of $HCO3^-$, resulting in pain and decrease of pH (Figure 6).

Discussion

As a diabetic complication with high incidence, DN has brought a huge impact on the prognosis and life quality of individual. Since pain is the most common DN symptom, the mechanism of ion channels has attracted more attention of scholars. At present, researches on the mechanism of pain

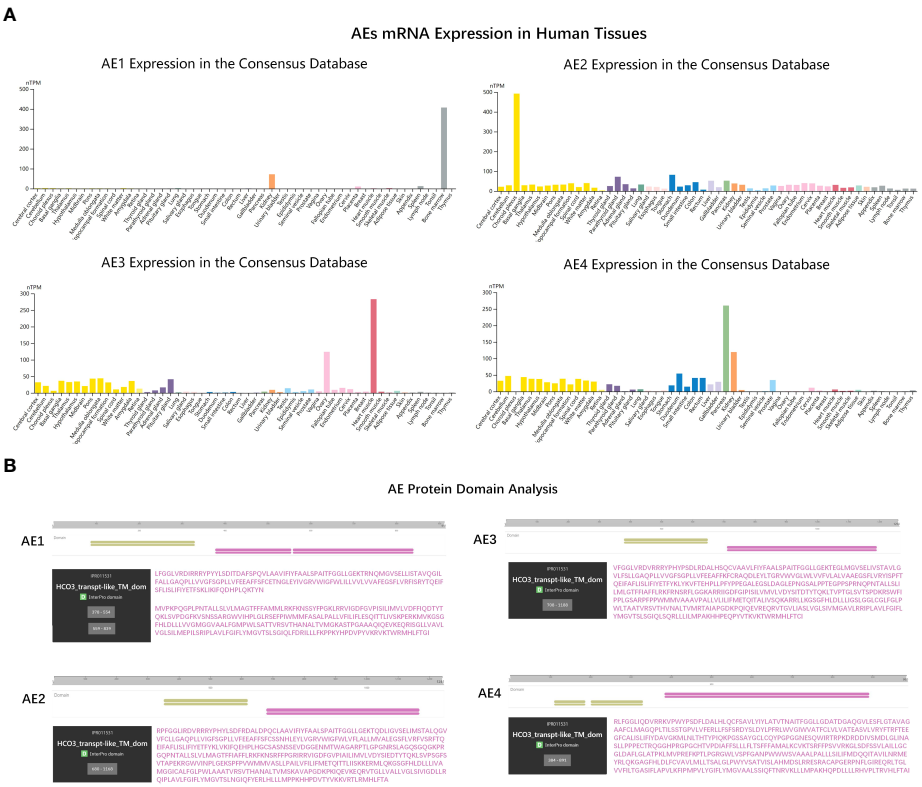

FIGURE 5
The gene expression and molecular function analysis of AEs. **(A)** The bar-plots showed tissue specificity of AEs mRNA expression in human based on RNA-sequencing data from the consensus dataset. **(B)** The protein domain analysis of the AE family (AE1-4). The amino acid sequences of key domains are shown in purple. $HCO3^-$transpt-like_TM_dom, Bicarbonate transporter-like transmembrane domain.

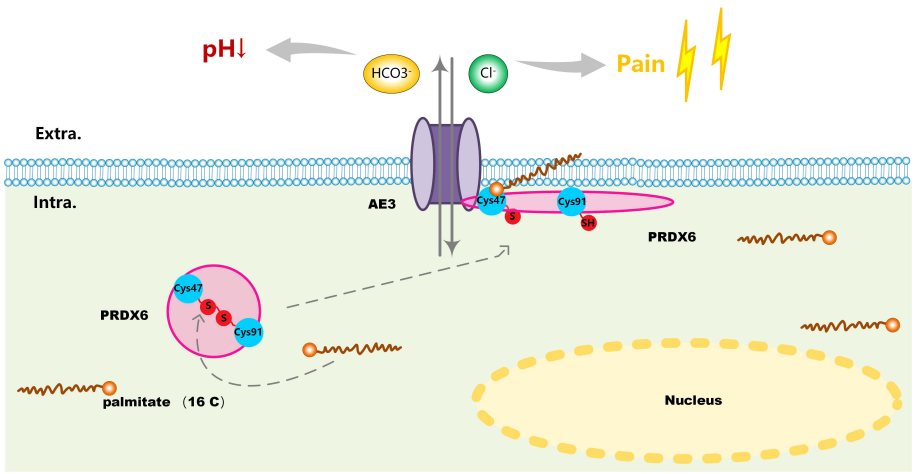

FIGURE 6
A schematic of the involved molecular mechanism that S-palmitoylation mediated reduction of disulfide bond (Cys47-Cys91) on PRDX6 activated its interaction with AE3 and induced its translocation from the cytoplasm to the plasma membrane. PRDX6-AE3 interaction enhanced the Cl^- influx and $HCO3^-$ extra flux, causing pain and decline of pH in D-DRG.

caused by DN mainly focuses on sodium and potassium channels (21–23). Recently, the role of chloride ion channels in pain has gradually attracted people's attention. Specific chloride flux participates in signal transduction and amplification at the peripheral nerve terminal, conduce to excitability and action potential generation of sensory neurons, or crucially shape synaptic transmission in the spinal dorsal horn. Besides, inflammatory mediators can modify the chloride channels through protein-protein interaction and signaling cascades, affecting them directly. Since chloride fluxes, modulated by chloride channels, can regulate pain disorders and contribute to nociceptor excitation and sensitization, their role in nociceptive primary afferents is critical. DRG neurons express several types of chloride channel belonging to different channel families, including ligand-gated, GABA, $Ca2^+$-activated chloride channels of the anoctamin (also known as TMEM16), CLC chloride channels and transporters, CFTR (cystic fibrosis transmembrane conductance regulator), Best1 (bestrophin) family, as well as VRACs (volume-regulated anion channels). Besides, Na^+-independent Cl^-HCO3^-anion exchanger, which is proved for the intracellular Cl^- accumulation, is expressed in 60% of peptidergic and 30% of non-peptidergic DRG neurons (20). However, the Cl^-HCO3^-ion channel is rarely studied in diabetic neuropathic pain.

AEs, members of solute carrier families 4 (SLC4) family, including AE1, AE2, AE3, and AE4, are transporters exchanging one intracellular $HCO3^-$ for one extracellular Cl^-. In our results, we found AE1 was not detected in the nervous system and AE2 together with AE4 were widely expressed in various tissues with no tissue specificity. AE3 mainly distributed in the brain, heart and ovary. There were evidences that AE3 was present in DRG and participates in the development and maintenance of short and long-lasting formalin-induced nociception (19). Furthermore, it also contributed to mechanical allodynia and thermal hyperalgesia in neuropathic rats (20). Therefore, we speculate that AE3 is also related to the occurrence of diabetic neuropathy pain, and its mechanism is more worthy of our study. Previous research had shown that PRDX6 and AE1 were co-localized in human kidney by immunostaining. PRDX6-AE1 interaction at cysteine residue (Cys47) conduced to preserve AE1 function during cellular stress such as during metabolic acidosis. In this research, we analyzed the functional domain of AEs to explore the protein structure and found the four AEs had the same domain in the C-terminal. Our results proposed that the S-palmitoylation of Cys47 was associated with PRDX6-AE3 interaction and activated the influx of chloride ions caused by AE3, which could promote the occurrence of pain in DN.

The PRDX family, with peroxidase and antioxidant activity, was comprised of six members. Among those, PRDX6 was distributed in tissues of the brain, heart, kidney, lung and testis. Recently, studies had proved that PRDX6 was involved in cancer (24), inflammatory diseases (25), ischemic stroke (26), traumatic brain injury (27) and neural degenerative diseases (28). Also, PRDX6 was unique for its containing only one conserved cysteine residue (Cys47) rather than the two found in other PRDXs (29) and Cys47 was evolutionally conserved in PRDX6 among most species. Furthermore, we predicted Cys47 and Cys91 were S-palmitoylation sites of PRDX6, but only Cys47 was the active site of functional domain in PRDX6. The results of our analysis showed that PRDX6 could bind with AE3 in the DRG, as the physical interaction of PRDX6-AE1 had been proved in human kidney. However, it is not yet known the underlying mechanism of PRDX6-AE3 interaction.

We demonstrated that the S-palmitoylation of Cys47 and Cys91 could affect the steric structure of PRDX6 and promote the PRDX6-AE3 interaction. On the one hand, the Cys47 and Cys91 sites of PRDX6 could form a disulfide bond, and mutation of Cys91 alone suppressed the formation of disulfide bond without affecting the function of the Cys47 site for PRDX6 (30). As S-palmitoylation on the Cys site could reduce disulfide bond formation (31), the S-palmitoylation of Cys47 and Cys91 could change the spatial topology of PRDX6 and expose its functional domain. On the other hand, S-palmitoylation could stabilize the location of a protein on cellular membrane. As AE3 was a transmembrane ion channel, the S-palmitoylation of PRDX6 could facilitate the colocalization of AE3 and PRDX6 on the cellular membrane. Taken together, S-palmitoylation of PRDX6 at Cys47 influences its interaction with AE3 and promotes chloride influx, which is a new mechanism of DN pain.

Previous researches had shown that PRDX6 had multiple functions including glutathione peroxidase (GPx) activity, lysophosphatidylcholine acyl transferase activity and phospholipaseA2 (PLA2) activity (32). The current research mainly focused on the PLA2 activity of PRDX6. NADPH oxidase (Nox) was an important activator of inflammatory signaling pathway, which was widely reported as one of the mechanisms of diabetes. Studies had confirmed that the PLA2 activity of Prdx6 was related to Nox activation (33). The PLA2 activity inhibitor MJ33 also inhibited the activity of Nox1, suggesting that Nox1 function was related to the PLA2 activity of Prdx6 (34). Experiments had confirmed that Prdx6 overexpression could lead to inactivation of p38, MAPK and JNK signaling pathways (35). Some scholars confirmed through *in vitro* and *in vivo* studies that the PLA2 activity of Prdx6 was related to the secretion of neuroinflammatory factors IL-1β, IL-17 and IL-23, and could upregulate the expression of TLR2/4 and induce the activation of NF-κB (36). Current studies uncovered that the activity regulation of Prdx6 was affected by factors such as subcellular localization, substrate binding and post-translational modification. As one of the post-translational modifications, the S-palmitoylation of PRDX6 stabilizes its localization on the membrane, which enhanced its PLA2 activity and promoted the release of inflammatory factors (37). However, no direct effect of PRDX6 with onion channel function inducing pain had been reported. Those functions of PRDX6

TABLE 1 The subcellular location and nervous system expression of ZDHHCs. (The HPA database).

	Subcellular location	Expression in nervous system
ZDHHC1	Cytosol	NA'
ZDHHC2	Plasma membrane	√
ZDHHC3	Golgi apparatus	√
ZDHHC4	NA'	√
ZDHHC5	Plasma membrane, Nucleoplasm	√
ZDHHC6	NA'	√
ZDHHC7	Golgi apparatus	√
ZDHHC8	Cytosol, Nucleoplasm	√
ZDHHC9	Endoplasmic reticulum, Golgi apparatus, Cytosol	√
ZDHHC11	Mitochondria	NA'
ZDHHC12	Nucleoplasm, Intermediate filaments	√
ZDHHC13	Vesicles, Golgi apparatus	√
ZDHHC14	Vesicles	√
ZDHHC15	Nuclear speckles, Cytosol	√
ZDHHC16	Nucleoplasm, Nuclear membrane, Cytosol	NA'
ZDHHC17	Golgi apparatus, Vesicles	√
ZDHHC18	Microtubules	√
ZDHHC19	NA'	NA'
ZDHHC20	Vesicles, Plasma membrane	√
ZDHHC21	Golgi apparatus, Cytosol	√
ZDHHC22	Plasma membrane	NA'
ZDHHC23	Nucleoplasm	NA'
ZDHHC24	Vesicles, Cytosol	√

NA', Not available.
√, detected in the human brain tissue by immunochemistry data of the HPA database.

corresponded to the enrichment analysis results of D-DRG proteins, which only showed that PRDX6 was related to oxidative stress, but not involved in ion channels.

At present, the research on the pathogenesis of diabetes and S-palmitoylation mainly focused on the bidirectional regulation of S-palmitoylation on pancreatic islet function. Under normal physiological conditions, specific G-proteins of H-Ras, Rac1 and Cdc42 were critical S-palmitoylation substrates for islet function and insulin secretion (38). Additionally, those G-proteins were also demonstrated to be S-palmitoylation modified under pathophysiological conditions of glucolipotoxicity, the generation of nitrosative and oxidative stress, and cytokine exposure in the islet-cell (39–42). However, little was known about the mechanism of palmitoylation and DN pain.

In our research, we compared the proteomic data of lumbar DRG of diabetes mice and palmitoylome profiling data of the HUVEC cell lines. Since palmitoylation was a non-specific reaction and thousands of proteins had been proved which could be modified by S-palmitoylation (43), so we convinced that the proteins undergo S-palmitoylation could in other cells types in addition to the HUVEC cells. However, ZDHHCs and palmitic acid were sufficient and necessary conditions for S-palmitoylation of substrates. It was not excluded that other S-palmitoylation substrates in DPN model were not expressed and/or detected in HUVEC cells. The above conclusions did not affect the hypothesis that S-palmitoylation plays an important role in the pathogenesis of DPN. Thus, this study provided a theoretical basis for further biological verification.

In this study, the protein interactions included both functional and physical protein associations, which was based on different kinds of data sources. The interaction score was based on the detailed information of these sources, which would affect the result of each PPI network generated by the STRING tool. The links only indicated the connections between each dot with medium confidence, as we set 4 as the minimum required interaction score. Most of the S-palmitoylations in the human body were catalyzed by PATs of the ZDHHC family. So, potential but weaker connections of ZDHHCs could also exist, in addition to the links visualized in this network. The PPI networks revealed potential interactions among proteins based on prior knowledge, which could potentially explain that ZDHHC6 was not even connected to the cluster of their own gene families.

Palmitoylation substrates were generally paired with PATs, and this correspondence was generally associated with both tissue specificity and subcellular colocalization. To search for the key PATs corresponding to PRDX6 in the nervous system, we analyzed the subcellular localization and tissue specificity of 23 human ZDHHCs. Immunofluorescence results demonstrated that

PRDX6 was mainly localized in the cytoplasm and cell membrane, so we focused on the ZDHHCs localized in the cell membrane or cytoplasm and detected in the nervous system at the translation level (Table 1). To further mine ZDHHCs correlated with PRDX6, we performed the Pearson's correlation analysis for PRDX6 and ZDHHCs by the proteomic data of human normal and cancer tissues (Supplementary Table 7). However, no distinguished PRDX6-ZDHHC connection emerged. Therefore, our analysis could not confirm the specific ZDHHC that catalyzes PRDX6 in D-DRG, and could only initially screen ZDHHC2, ZDHHC5, ZDHHC8, ZDHHC9, ZDHHC15, ZDHHC20, ZDHHC21 and ZDHHC24 as candidates for catalyzing the palmitoylation of PRDX6.

Conclusion

The current work identifies a post-translation regulatory mechanism for DN, PRDX6 breaks the disulfide bond (Cys47-Cys91) and translocates to the cellular membrane, which depends upon the S-palmitoylation of PRDX6 at Cys47. This mechanism causes stable PRDX6-AE3 interactions, and is responsible for the enhanced the $Cl^-/HCO3^-$ currents through AE3. This advanced our knowledge of the association between S-palmitoylation and DN. As such, these outcomes may offer novel insights for alleviating pain in DN.

Data availability statement

Publicly available datasets were analyzed in this study. This data can be found here: https://www.proteinatlas.org/.

Author contributions

YZ: conception and design. YC: survey and collection of data. WW: administrative support. XZ: data analysis and interpretation. All authors manuscript writing and final approval of manuscript.

Conflict of interest

The authors declare that the research was conducted in the absence of any commercial or financial relationships that could be construed as a potential conflict of interest.

Publisher's note

Supplementary material

The Supplementary Material for this article can be found online at: https://www.frontiersin.org/articles/10.3389/fendo.2022.992875/full#supplementary-material

References

1. Abbott CA, Malik RA, Van Ross ER, Kulkarni J, Boulton AJ. Prevalence and characteristics of painful diabetic neuropathy in a large community-based diabetic population in the U.K. *Diabetes Care* (2011) 34:2220–4. doi: 10.2337/dc11-1108

2. Frank T, Nawroth P, Kuner R. Structure-function relationships in peripheral nerve contributions to diabetic peripheral neuropathy. *Pain* (2019) 160 Suppl 1: S29–36. doi: 10.1097/j.pain.0000000000001530

3. Huang F, Wang X, Ostertag EM, Nuwal T, Huang B, Jan YN, et al. TMEM16C facilitates na(+)-activated k+ currents in rat sensory neurons and regulates pain processing. *Nat Neurosci* (2013) 16:1284–90. doi: 10.1038/nn.3468

4. Todorovic SM, Jevtovic-Todorovic V. Targeting of CaV3.2 T-type calcium channels in peripheral sensory neurons for the treatment of painful diabetic neuropathy. *Pflugers Arch* (2014) 466:701–6. doi: 10.1007/s00424-014-1452-z

5. Francois A, Kerckhove N, Meleine M, Alloui A, Barrere C, Gelot A, et al. State-dependent properties of a new T-type calcium channel blocker enhance Ca (V)3.2 selectivity and support analgesic effects. *Pain* (2013) 154:283–93. doi: 10.1016/j.pain.2012.10.023

6. Liu B, Linley JE, Du X, Zhang X, Ooi L, Zhang H, et al. The acute nociceptive signals induced by bradykinin in rat sensory neurons are mediated by inhibition of m-type k+ channels and activation of Ca2+-activated cl- channels. *J Clin Invest* (2010) 120:1240–52. doi: 10.1172/JCI41084

7. Zhang Y, Li F, Fu K, Liu X, Lien IC, Li H. Potential role of s-palmitoylation in cancer stem cells of lung adenocarcinoma. *Front Cell Dev Biol* (2021) 9:734897. doi: 10.3389/fcell.2021.734897

8. Greaves J, Chamberlain LH. Palmitoylation-dependent protein sorting. *J Cell Biol* (2007) 176:249–54. doi: 10.1083/jcb.200610151

9. Linder ME, Deschenes RJ. Palmitoylation: Policing protein stability and traffic. *Nat Rev Mol Cell Biol* (2007) 8:74–84. doi: 10.1038/nrm2084

10. Martin BR. Nonradioactive analysis of dynamic protein palmitoylation. *Curr Protoc Protein Sci* (2013) 73:14 15 1–14 15 9. doi: 10.1002/0471140864.ps1415s73

11. Blanc M, David FPA, van der Goot FG. SwissPalm 2: Protein s-palmitoylation database. *Methods Mol Biol* (2019) 2009:203–14. doi: 10.1007/978-1-4939-9532-5_16

12. Ko PJ, Dixon SJ. Protein palmitoylation and cancer. *EMBO Rep* (2018) 19: e46666. doi: 10.15252/embr.201846666

13. Wei X, Song H, Semenkovich CF. Insulin-regulated protein palmitoylation impacts endothelial cell function. *Arterioscler Thromb Vasc Biol* (2014) 34:346–54. doi: 10.1161/ATVBAHA.113.302848

14. Leal-Julia M, Vilches JJ, Onieva A, Verdes S, Sanchez A, Chillon M, et al. Proteomic quantitative study of dorsal root ganglia and sciatic nerve in type 2 diabetic mice. *Mol Metab* (2022) 55:101408. doi: 10.1016/j.molmet.2021.101408

15. Szklarczyk D, Gable AL, Nastou KC, Lyon D, Kirsch R, Pyysalo S, et al. The STRING database in 2021: Customizable protein-protein networks, and functional characterization of user-uploaded gene/measurement sets. *Nucleic Acids Res* (2021) 49:D605–12. doi: 10.1093/nar/gkaa1074

16. Blum M, Chang HY, Chuguransky S, Grego T, Kandasaamy S, Mitchell A, et al. The InterPro protein families and domains database: 20 years on. *Nucleic Acids Res* (2021) 49:D344–54. doi: 10.1093/nar/gkaa977

17. Lakkaraju AK, Abrami L, Lemmin T, Blaskovic S, Kunz B, Kihara A, et al. Palmitoylated calnexin is a key component of the ribosome-translocon complex. *EMBO J* (2012) 31:1823–35. doi: 10.1038/emboj.2012.15

18. Sorrell SL, Golder ZJ, Johnstone DB, Frankl FEK. Renal peroxiredoxin 6 interacts with anion exchanger 1 and plays a novel role in pH homeostasis. *Kidney Int* (2016) 89:105–12. doi: 10.1038/ki.2015.277

19. Barragan-Iglesias P, Rocha-Gonzalez HI, Pineda-Farias JB, Murbartian J, Godinez-Chaparro B, Reinach PS, et al. Inhibition of peripheral anion exchanger 3 decreases formalin-induced pain. *Eur J Pharmacol* (2014) 738:91–100. doi: 10.1016/j.ejphar.2014.05.029

20. Perez-Rodriguez MJ, Velazquez-Lagunas I, Pluma-Pluma A, Barragan-Iglesias P, Granados-Soto V. Anion exchanger 3 in dorsal root ganglion contributes to nerve injury-induced chronic mechanical allodynia and thermal hyperalgesia. *J Pharm Pharmacol* (2018) 70:374–82. doi: 10.1111/jphp.12868

21. Belkouch M, Dansereau MA, Tetreault P, Biet M, Beaudet N, Dumaine R, et al. Functional up-regulation of Nav1.8 sodium channel in abeta afferent fibers subjected to chronic peripheral inflammation. *J Neuroinflamm* (2014) 11:45. doi: 10.1186/1742-2094-11-45

22. Zhang XY, Wen J, Yang W, Wang C, Gao L, Zheng LH, et al. Gain-of-function mutations in SCN11A cause familial episodic pain. *Am J Hum Genet* (2013) 93:957–66. doi: 10.1016/j.ajhg.2013.09.016

23. Zheng Q, Fang D, Liu M, Cai J, Wan Y, Han JS, et al. Suppression of KCNQ/M (Kv7) potassium channels in dorsal root ganglion neurons contributes to the development of bone cancer pain in a rat model. *Pain* (2013) 154:434–48. doi: 10.1016/j.pain.2012.12.005

24. Yun HM, Park KR, Lee HP, Lee DH, Jo M, Shin DH, et al. PRDX6 promotes lung tumor progression *via* its GPx and iPLA2 activities. *Free Radic Biol Med* (2014) 69:367–76. doi: 10.1016/j.freeradbiomed.2014.02.001

25. Liu GY, Shi JX, Shi SL, Liu F, Rui G, Li X, et al. Nucleophosmin regulates intracellular oxidative stress homeostasis *via* antioxidant PRDX6. *J Cell Biochem* (2017) 118:4697–707. doi: 10.1002/jcb.26135

26. Lo EH. A new penumbra: Transitioning from injury into repair after stroke. *Nat Med* (2008) 14:497–500. doi: 10.1038/nm1735

27. Buonora JE, Mousseau M, Jacobowitz DM, Lazarus RC, Yarnell AM, Olsen CH, et al. Autoimmune profiling reveals peroxiredoxin 6 as a candidate traumatic brain injury biomarker. *J Neurotrauma* (2015) 32:1805–14. doi: 10.1089/neu.2014.3736

28. Yun HM, Jin P, Han JY, Lee MS, Han SB, Oh KW, et al. Acceleration of the development of alzheimer's disease in amyloid beta-infused peroxiredoxin 6 overexpression transgenic mice. *Mol Neurobiol* (2013) 48:941–51. doi: 10.1007/s12035-013-8479-6

29. Fujii T, Fujii J, Taniguchi N. Augmented expression of peroxiredoxin VI in rat lung and kidney after birth implies an antioxidative role. *Eur J Biochem* (2001) 268:218–25. doi: 10.1046/j.1432-1033.2001.01843.x

30. Fisher AB. Peroxiredoxin 6: A bifunctional enzyme with glutathione peroxidase and phospholipase A(2) activities. *Antioxid Redox Signal* (2011) 15:831–44. doi: 10.1089/ars.2010.3412

31. Itoh S, Mizuno K, Aikawa M, Aikawa E. Dimerization of sortilin regulates its trafficking to extracellular vesicles. *J Biol Chem* (2018) 293:4532–44. doi: 10.1074/jbc.RA117.000732

32. Liao J, Zhang Y, Chen X, Zhang J. The roles of peroxiredoxin 6 in brain diseases. *Mol Neurobiol* (2021) 58:4348–64. doi: 10.1007/s12035-021-02427-5

33. Schattauer SS, Land BB, Reichard KL, Abraham AD, Burgeno LM, Kuhar JR, et al. Peroxiredoxin 6 mediates galphai protein-coupled receptor inactivation by cJun kinase. *Nat Commun* (2017) 8:743. doi: 10.1038/s41467-017-00791-2

34. Kwon J, Wang A, Burke DJ, Boudreau HE, Lekstrom KJ, Korzeniowska A, et al. Peroxiredoxin 6 (Prdx6) supports NADPH oxidase1 (Nox1)-based superoxide generation and cell migration. *Free Radic Biol Med* (2016) 96:99–115. doi: 10.1016/j.freeradbiomed.2016.04.009

35. Lee DH, Park JH, Han SB, Yoon DY, Jung YY, Hong JT. Peroxiredoxin 6 overexpression attenuates lipopolysaccharide-induced acute kidney injury. *Oncotarget* (2017) 8:51096–107. doi: 10.18632/oncotarget.17002

36. Shanshan Y, Beibei J, Li T, Minna G, Shipeng L, Li P, et al. Phospholipase A2 of peroxiredoxin 6 plays a critical role in cerebral Ischemia/Reperfusion inflammatory injury. *Front Cell Neurosci* (2017) 11:99. doi: 10.3389/fncel.2017.00099

37. Arevalo JA, Vazquez-Medina JP. The role of peroxiredoxin 6 in cell signaling. *Antioxidants (basel)* (2018) 7(12):172. doi: 10.3390/antiox7120172

38. Kowluru A, Veluthakal R, Rhodes CJ, Kamath V, Syed I, Koch BJ. Protein farnesylation-dependent raf/extracellular signal-related kinase signaling links to cytoskeletal remodeling to facilitate glucose-induced insulin secretion in pancreatic beta-cells. *Diabetes* (2010) 59:967–77. doi: 10.2337/db09-1334

39. Subasinghe W, Syed I, Kowluru A. Phagocyte-like NADPH oxidase promotes cytokine-induced mitochondrial dysfunction in pancreatic beta-cells: Evidence for regulation by Rac1. *Am J Physiol Regul Integr Comp Physiol* (2011) 300:R12–20. doi: 10.1152/ajpregu.00421.2010

40. Syed I, Jayaram B, Subasinghe W, Kowluru A. Tiam1/Rac1 signaling pathway mediates palmitate-induced, ceramide-sensitive generation of superoxides and lipid peroxides and the loss of mitochondrial membrane potential in pancreatic beta-cells. *Biochem Pharmacol* (2010) 80:874–83. doi: 10.1016/j.bcp.2010.05.006

41. Syed I, Kyathanahalli CN, Jayaram B, Govind S, Rhodes CJ, Kowluru RA, et al. Increased phagocyte-like NADPH oxidase and ROS generation in type 2 diabetic ZDF rat and human islets: Role of Rac1-JNK1/2 signaling pathway in mitochondrial dysregulation in the diabetic islet. *Diabetes* (2011) 60:2843–52. doi: 10.2337/db11-0809

42. Mohammed AM, Syeda K, Hadden T, Kowluru A. Upregulation of phagocyte-like NADPH oxidase by cytokines in pancreatic beta-cells: Attenuation of oxidative and nitrosative stress by 2-bromopalmitate. *Biochem Pharmacol* (2013) 85:109–14. doi: 10.1016/j.bcp.2012.09.024

43. Lin H. Protein cysteine palmitoylation in immunity and inflammation. *FEBS J* (2021) 288:7043–59. doi: 10.1111/febs.15728

frontiers | Frontiers in Endocrinology

TYPE Review
PUBLISHED 08 September 2022
DOI 10.3389/fendo.2022.997034

OPEN ACCESS

EDITED BY
Jun Chen,
Qilu Hospital, Shandong University, China

REVIEWED BY
Qi Su,
University of California, San Diego, United States
Qian Wang,
College of Staten Island, United States
Pengfei Zhang,
Institute of Basic Medicine and Cancer (IBMC), (CAS), China

*CORRESPONDENCE
Mingxue Zhou
mingxue78@163.com
Yanbing Gong
gyb_1226@163.com

SPECIALTY SECTION
This article was submitted to Diabetes: Molecular Mechanisms, a section of the journal Frontiers in Endocrinology

RECEIVED 18 July 2022
ACCEPTED 18 August 2022
PUBLISHED 08 September 2022

CITATION
Zhang W, Zhang S, Dong C, Guo S, Jia W, Jiang Y, Wang C, Zhou M and Gong Y (2022) A bibliometric analysis of RNA methylation in diabetes mellitus and its complications from 2002 to 2022.
Front. Endocrinol. 13:997034.
doi: 10.3389/fendo.2022.997034

A bibliometric analysis of RNA methylation in diabetes mellitus and its complications from 2002 to 2022

Wenhua Zhang[1], Shuwen Zhang[1], Chenlu Dong[1], Shuaijie Guo[2,3], Weiyu Jia[1], Yijia Jiang[1], Churan Wang[1], Mingxue Zhou[2,3]* and Yanbing Gong[1]*

[1]Dongzhimen Hospital, Beijing University of Chinese Medicine, Beijing, China, [2]Beijing Hospital of Traditional Chinese Medicine, Capital Medical University, Beijing, China, [3]Cardiovascular Disease Research Department, Beijing Institute of Chinese Medicine, Beijing, China

Background: RNA methylation has emerged as an active research field in diabetes mellitus (DM) and its complications, while few bibliometric analyses have been performed. We aimed to visualize the hotspots and trends using bibliometric analysis to provide a comprehensive and objective overview of the current search state in this field.

Methods: The articles and reviews regarding RNA methylation in DM and its complications were from the Web of Science Core Collection. A retrospective bibliometric analysis and science mapping was performed using the CiteSpace software to plot the knowledge maps and predict the hotspots and trends.

Results: Three hundred seventy-five qualified records were retrieved. The annual publications gradually increased over the past 20 years. These publications mainly came from 66 countries led by Canada and 423 institutions. Leiter and Sievenpiper were the most productive authors, and Jenkins ranked first in the cited authors. *Diabetes Care* was the most co-cited journal. The most common keywords were "Type 2 diabetes", "cardiovascular disease", "diabetes mellitus", and "n 6 methyladenosine". The extracted keywords mainly clustered in "beta-cell function", "type 2 diabetes", "diabetic nephropathy", "aging", and "n6-methyladenosine". N6-methyladenosine (m^6A) in DM and its complications were the developing areas of study.

Conclusion: Studies on RNA methylation, especially m^6A modification, are the current hotspots and the future trends in type 2 diabetes (T2D) and diabetic nephropathy (DN), as well as a frontier field for other complications of DM. Strengthening future cooperation and exchange between countries and institutions is strongly advisable to promote research developments in this field.

KEYWORDS

bibliometric analysis, diabetes mellitus, diabetes complications, N6-methyladenosine (m 6 A), RNA methylation

1 Introduction

DM is a common complicated chronic glycolipid metabolic disorder syndrome characterized by insulin resistance (IR) and insulin deficit (1). DM causes damage to major organs, including kidneys, heart, eyes, nerves, and blood vessels, eventually leading to diabetes complications that seriously threaten the health of individuals (1). According to the 10th edition of the International Diabetes Federation (IDF) Diabetes Atlas, DM has been one of the fast-growing health emergencies of the 21st century and has ranked among the top causes of premature death (2). However, the pathogenesis of DM remains unclear, and it is urgently essential to keep up with the current hotspots to explore the pathogenesis of DM and its complications.

RNA methylation may post-transcriptionally regulate RNA stability, localization, transport, splicing, and translation (3). More than 170 RNA modifications have been identified (4), of which m^{6}A is the most abundant epigenetic modification in eukaryotic RNA. The abundance and effects of m^{6}A on RNA are dynamically regulated by the interplay of methyltransferase, demethylases, and binding proteins. The methyltransferases that perform the modification reaction consist of Methyltransferase Like 3 (METTL3), METTL14, Wilms Tumor 1 Associated Protein (WTAP), etc. Reverse-modified demethylases known as "erasers" include fat mass and obesity-associated protein (FTO), α-ketoglutarate-dependent dioxygenase alkB homolog 5 (ALKBH5), etc. RNA-binding proteins are known as "readers" mainly composed of YTH domain-containing family 1/2/3 (YTHDF1/2/3), and YTH domain-containing protein 1/2 (YTHDC1/2) (5). M^{6}A-mediated post-transcriptional modification is essential in many biological processes such as cell differentiation, stresses, circadian rhythm, cycle regulation, and metabolism (6). Emerging evidence revealed that m^{6}A was involved in many human diseases and provided a potential novel pathogenesis study for the prevention or treatment of various diseases (7), such as cancer, cardiovascular disease (CVD), progeroid syndromes, autoimmune diseases, and metabolic diseases (8–12).

The complicated pathogenesis, as well as the lasting multi-organ damage of DM, made RNA methylation an increasingly interesting topic with a measurable increase in publications. Several studies identified the abnormal m^{6}A levels and key methylesterase of m^{6}A. For example, several studies monitored the decreased m^{6}A in T2D and β-cells (13, 14). Correspondingly, changes in the levels of methylesterase were also monitored, such as METTL3, METTL14, WTAP, FTO, ALKBH5, and YTHDF1 in T2D and its complications (13–15). The abnormal change in m^{6}A and key methylesterase affected cell proliferation, differentiation, apoptosis, and autophagy and led to abnormalities in cell structure and function that participated in the initiation and progression of DM and its complications (16). The current evidence from these studies reported that the upregulated or downregulated levels of m^{6}A were connected with β-cells, renal tubular cells, IR, inflammatory, oxidative stress, lipid levels, obesity, and other unknown mechanisms, which aggravated hyperglycemia and its further damage to other organs (17). Therefore, a systematic review and summary of the topical and major findings of RNA methylation in DM and its complications based on the current literature is urgent and necessary at this stage.

Unlike general systematic reviews, bibliometrics is characterized by mathematical techniques to investigate publication and communication patterns in the distribution of information and to evaluate research trends qualitatively and quantitatively based on bibliographic databases and bibliometrics (18). It not only helps researchers to grasp the hotspots and trends of specific research fields but also helps to quantify the characteristics of the countries, journals, and authors of published articles (19). This analytical method has been widely used in various fields to develop guidelines, understand research hotspots, and evaluate research trends (20). Therefore, this review was conducted using bibliometrics analysis to identify essential evidence in RNA methylation for DM and its complications and to help scholars understand the intellectual backgrounds and the emerging research trends in this field.

2 Materials and methods

2.1 Data sources and search strategy

The Web of Science Core Collection is the largest comprehensive academic information resource covering multiple disciplines (21). To ensure the quality and accessibility of data, all data were downloaded from the Web of Science Core Collection online database with the queries shown in Supplementary Table 1, with no language or region restrictions. The document types were articles or reviews with dates ranging from 1 January 2002 to 28 May 2022.

2.2 Data collection and analysis

Two authors collected the documents from the Web of Science Core Collection according to the set retrieval mode, exported them to a plain text file with full records and cited references, and stored them in download_txt format. Any disagreements were resolved by consensus. All valid data were converted to Microsoft Excel 2019, CiteSpace (5.8. R 3), and GraphPad Prism 9.0, and the review flowchart is shown in Figure 1.

CiteSpace is a Java application for visualizing and analyzing scientific literature trends and patterns (22). It not only helps conduct burst detection, intermediate centrality, and heterogeneous networks and identify and track critical paths and milestone studies during professional development but also

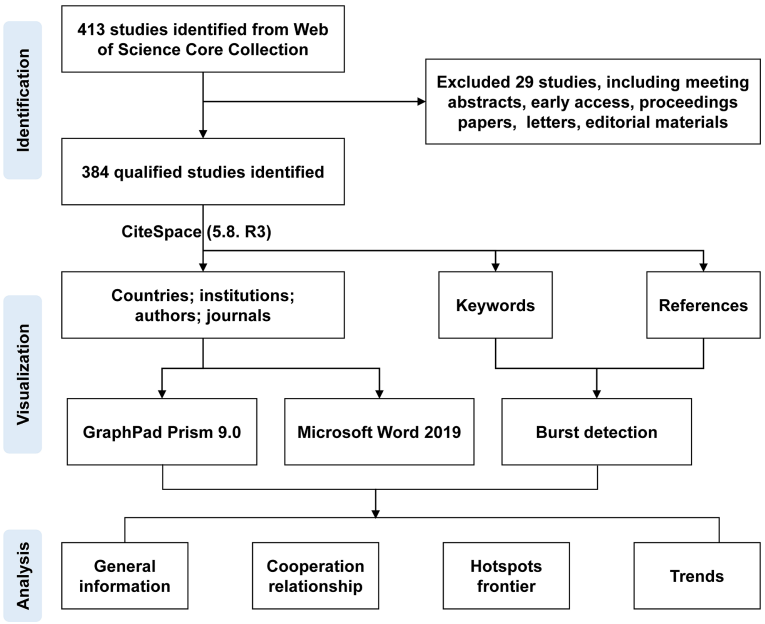

FIGURE 1
Flowchart of the review.

helps detect emerging trends and transient patterns at the research forefront (21). Therefore, this review used the CiteSpace software to conduct a bibliometric analysis of the publications of RNA methylation in DM and its complications, including countries, institutions, authors and cited authors, journals, references and keywords, the bursts of references and keywords, an overlay of journals, and a timeline viewer of keyword clusters.

Microsoft Word 2019 was used to conduct the descriptive statistics on ranks, frequency, attributes, centrality, etc. GraphPad Prism 9.0 was used to analyze and plot the annual publication output. The web tool MapInSeconds (mapinseconds.com) of *Eugene Chen, Darkhorse Analytics* was used to draw the geographical distribution of article publications.

3 Results and analysis

3.1 The trend of publication outputs

A total of 384 documents were collected from the Web of Science Core Collection based on the predefined queries. CiteScape identified no duplications, and 373 qualified records were included in this review. As shown in Figure 2, the research trend was divided into three stages. The first stage with 110 literatures was from 2004 to 2011, when the outputs of literature gradually rose from 6 to 18. There was a slight fluctuation in the second phase, with 13 articles in 2012, 25 articles in 2014, and a drop to 16 articles in 2016. From 2017 was the third stage; annual outputs climbed gradually steadily without any decline, as of 28 May 2022, out of 184 articles. In 2022, only 5 months of publication were counted; it cannot represent the whole annual outputs, but the overall trend in outputs was increasing on RNA methylation in DM and its complications, which suggests that RNA methylation may be a promising direction in this field.

3.2 Analysis of countries/regions distribution

Three hundred seventy-three records were published in 66 countries/regions in the five continents. The deeper color in Figure 3 indicates that the publications were higher in this country, while the gray indicates no articles published. Canada ranked first with the highest number of 245 articles in the field. The USA with 93 articles ranked second, and China with 85 articles ranked third. Both were far ahead of other countries. Annual outputs of the top 10 countries/regions are shown in Figure 4; Canada posted significantly more annual outputs than any other country until 2019, after which Canada and USA decreased, while China overtook other countries to rank first in annual productions.

The collaboration of countries/regions is visualized in Figure 5. Each node with colorful annual rings represents a

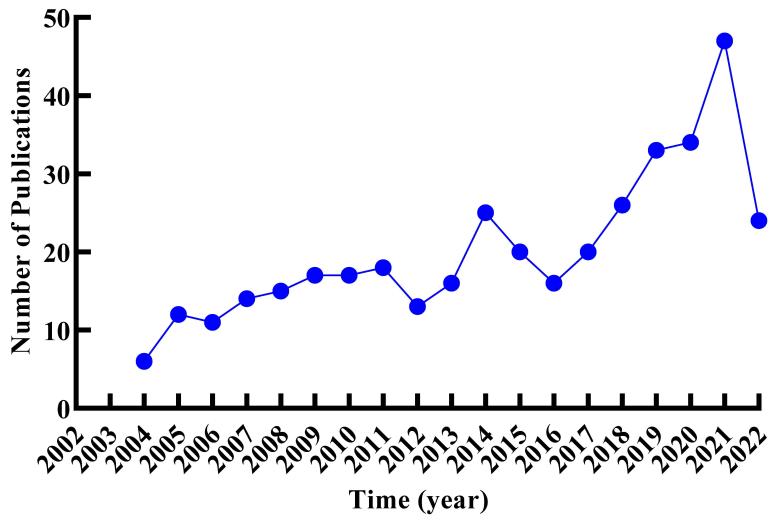

FIGURE 2
Trends of the annual publications related to RNA methylation in DM and its complications.

country, and the size of the node matches the outputs in this country; the color bandwidth corresponds to the outputs for this year, and the wider the ribbon, the higher the number of outputs posted. The results in Figure 5 matched the geographical distribution in Figure 3. The purple color around the nodes represents high centrality. Belgium, Argentina, and Australia were circled in purple, which indicates they have a strong bridge role in this field. The link density between two nodes matches the cooperation strength, and the link color represents the initial cooperation year. Although relatively few articles were issued, Belgium and Argentina had the most cooperative relations with other countries. Among the top countries, Australia had a higher centrality and more cooperation such as Canada, the USA, China, England, Germany, etc.

3.3 Analysis of institutions distribution

A total of 375 qualified articles were published by 423 institutions. As shown in Supplementary Table 2, Univ Toronto (205) and St Michaels Hosp (154) were marked leaders in the publications, followed by McMaster Univ and Univ Saskatchewan. Of the top 10 institutions, seven were in Canada and two were in the USA.

Institutional co-occurrence analysis reflects the collaboration relationship. The map with a network density of 0.0123 comprised 423 nodes and 1368 links. As shown in Figure 6, the Univ Toronto and St Michaels Hosp circled in purple were the two largest nodes, with the highest literature and the strongest centrality, which implied an essential role in this field. The thickness of the line

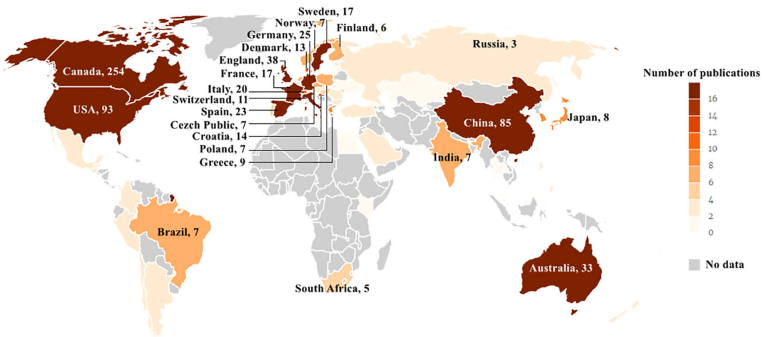

FIGURE 3
Geographical distribution of article publications related to RNA methylation in DM and its complications. The label represents the country and the outputs of the country; the depth of color matched with the number of publications.

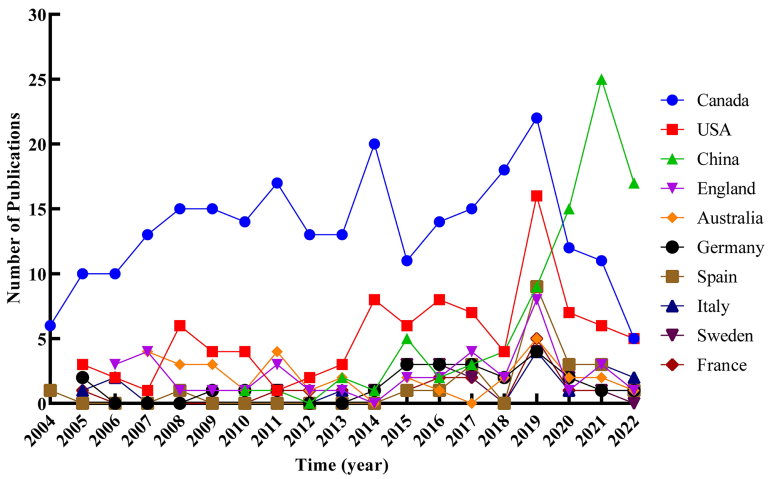

FIGURE 4
Trends of annual publications of the top 10 countries/regions related to RNA methylation in DM and its complications.

between nodes indicates institution collaboration. Most institutions collaborated, for example, McMaster Univ, St Michaels Hosp, Heart and Stroke Fdn Ontario, Tech Univ Dresden, and so on.

To explore the research themes among institutions, log-likelihood tests (LLR) were used to cluster the keywords of the articles published by the institutions by CiteSpace, and the top 10 clusters with different colored areas are shown in Figure 6. "Cluster #0 dpp 4-inhibitors" is the largest cluster, followed by "cluster #1 postprandial glycemia". The top two institutions are clustered in "#3 type 2 diabetes mellitus", which was the focus of the two institutional studies.

3.4 Analysis of authors and cited authors

These publications involved 511 authors, with an average of 1.37 authors per article (Supplementary Table 3). The first eight authors were all from Canada. Leiter was the highest producer with 44 articles; the rest of the authors in this field had more than 10 articles. Jenkins had received 55 citations and was the first cited author, followed by Wolever, Wang, and Sievenpiper.

When author collaborations were analyzed, Figure 7 visualizes the top five author collaboration groups. Leiter, Sievenpiper, Kendall, and others worked together for years and formed the largest collaborative team, of which Leiter is circled

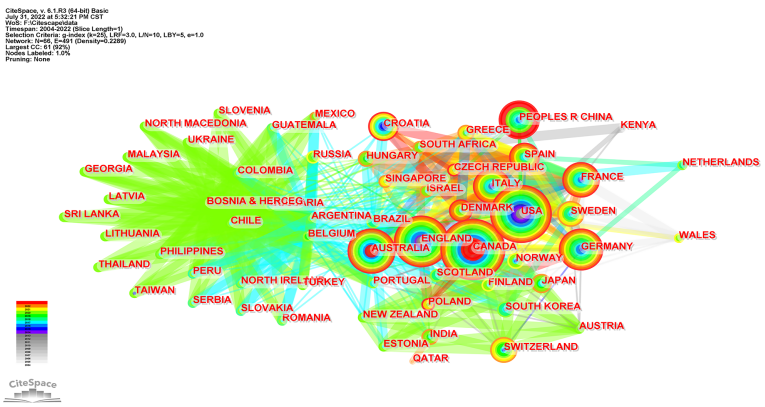

FIGURE 5
Visualization map of countries/regions collaboration analysis related to RNA methylation in DM and its complications. Each node with colorful annual rings represents a country; the color bandwidth corresponds to the outputs of the year; the wider the ribbon, the higher the number of outputs posted and the corresponding node increases. The purple color around the nodes represents high centrality. Link between the two nodes represents the cooperation relationship, and the link color represents the initial cooperation year.

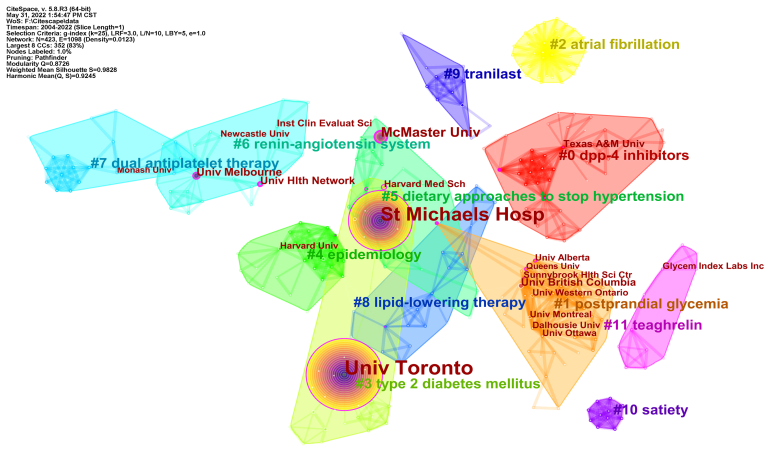

FIGURE 6
Visualization map of institution collaboration analysis related to RNA methylation in DM and its complications. Each node with colorful annual rings represents an institution. Institutions with partnerships make up the different color groups. The text with # represents the keyword clusters of the institutions.

in purple for greater centrality and Wolever with conspicuous red for higher burst. Gilbert, Advani, Kelly, and other authors made up the second collaboration team, of which Kelly is circled red for having publication burst growth in a short time.

3.5 Analysis of cited journals

Co-citation analysis of the journal in the references reveals the authoritative and influential journal in this field. Among the 517 cited journals, eight were cited over 100 times (Table 1). *Diabetes Care* was cited most, while *New England Journal of Medicine* and *Diabetes* followed second. Of the top 10 cited journals, nine were distributed in the Q1 region, with only *PLoS One* belonging to Q2. Among the top 10 journals, the *New England Journal of Medicine* had the highest impact factor (IF) of 91.253, and *Lancet* ranked second with an IF of 79.323.

The dual-map overlay of journals reflects the relationship between the source journals on the left and the target journals on the right, as well as the subjects involved in the journals. As shown in Figure 8, the colorful links represent the relationship between the two journals; there were three main wide citation

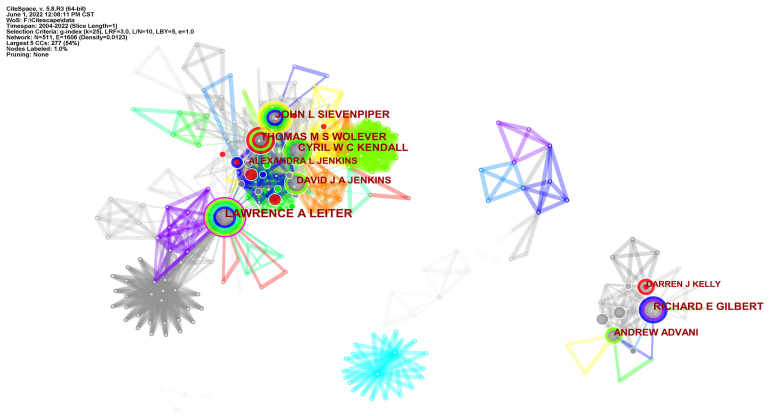

FIGURE 7
Visualization map of the top five author collaboration related to RNA methylation in DM and its complications. Each node with colorful annual rings represents an author. The size of the nodes matches the publications of the author. The nodes circled in purple represent greater centrality; the nodes circled in red represent higher burst. The separate areas made up of nodes and links represent the author collaborative relationships.

TABLE 1 The top 10 co-cited journals related to RNA methylation in DM and its complications.

No.	Co-cited Journal	Citation	Centrality	IF (2020)	JCR
1	*Diabetes Care*	202	0.01	19.112	Q1
2	*New England Journal of Medicine*	168	0.01	91.253	Q1
3	*Diabetes*	154	0.07	9.461	Q1
4	*Lancet*	152	0.03	79.323	Q1
5	*JAMA—Journal of the American Medical Association*	141	0.05	56.274	Q1
6	*Diabetologia*	138	0.01	10.122	Q1
7	*Circulation*	130	0.02	29.69	Q1
8	*Nature*	118	0.07	49.962	Q1
9	*PLoS One*	99	0.03	3.24	Q2
10	*American Journal of Clinical Nutrition*	98	0.04	7.047	Q1

paths, namely two green paths and one green path. The green paths indicated that the journals that involved molecular, biology, genetics and health, nursing, and medicine were always cited by medicine, medical, and clinical journals. The orange paths indicated that the journals that involved molecular, biology, and genetics were cited by molecular, biology, and immunology.

3.6 Analysis of co-cited references and reference burst

When two or more references are cited by several articles, the two references are considered to be a co-citation relationship. Among the 695 cited references, the top eight most frequently co-cited references are shown in Table 2. The reference published by Yang (13) had the highest number of citations, which implied that the research related to this article may be a research hotspot, and five references were cited more than 10 times and were valuable literature in this field.

Reference burst detection helps select the bulged references in a short time from the numerous references and find the most influential cited articles, thus clearly discovering the research frontiers and trends. Figure 9 displays the reference citation burst detection. The reference written by Bhattacharyya (23) had the highest centrality and burst strength and was the bridge between the two related studies, representing the current research hotspot and a turning point. The references published by Committee CDACPGE (2008) and Wang (2014) had the longest burst duration, which suggested a longer active duration of the research. Judged from the last 3 years, the references published by Yang (13), Roundtree (3), and Huang (2018) had a stronger burst, which had become the latest research frontier so far and may continue in the future.

3.7 Analysis of hotspots and frontiers

Keywords represent the research hotspots. We counted the keywords in the literature by CiteSpace and merged the top similar keywords and obtained the top 20 high-frequency keywords in Table 3; “type 2 diabetes”, “cardiovascular disease”, “diabetes mellitus”, “n 6 methyladenosine”, and “expression” had higher frequency. It indicated that they were

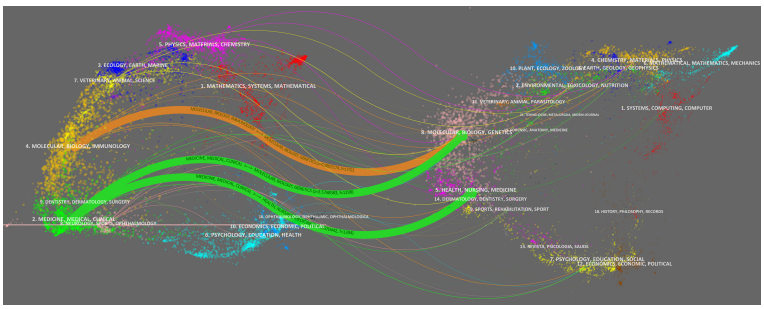

FIGURE 8
The dual-map overlay of journals on RNA methylation in DM and its complications. The left nodes represent the included literature; the right represent the references in the literature. The labels represent the discipline. The link represents the cited path.

TABLE 2 Top eight co-cited references related to RNA methylation in DM and its complications.

No.	Author	Year	Reference	Citation	Centrality
1	Yang Y	2019	Glucose is involved in the dynamic regulation of m^{6}A in patients with type 2 diabetes	16	0.02
2	Roundtree IA	2017	Dynamic RNA modifications in gene expression regulation	15	0
3	Huang HL	2018	Recognition of RNA N-6- methyladenosine by IGF2BP proteins enhances mRNA stability and translation	14	0.19
4	Bhattacharyya OK	2008	Management of cardiovascular disease in patients with diabetes: the 2008 Canadian Diabetes Association guidelines	14	0
5	De Jesus DF	2019	m^{6}A mRNA methylation regulates human beta-cell biology in physiological states and in type 2 diabetes	13	0.01
6	Xie W	2019	METTL3 inhibits hepatic insulin sensitivity *via* N6-methyladenosine modification of Fasn mRNA and promoting fatty acid metabolism	9	0
7	Shi HL	2017	YTHDF3 facilitates translation and decay of N-6-methyladenosine-modified RNA	9	0
8	Lin SB	2016	The m^{6}A Methyltransferase METTL3 promotes translation in human cancer cells	9	0

the popular topics on RNA methylation in DM and its complications.

Keywords bursts were detected to review and predict the phased hotpots and their evolutionary trends of RNA methylation in DM and its complications. As shown in Figure 10, "coronary heart disease", "risk factors", and "mellitus" with stronger bursts of strength emerged earlier and were the topics of early attention. The keywords "mellitus" and "diabetes mellitus", as synonymous terms, had the longest, 7 years of duration burst, followed by "coronary heart disease". Since 2018, the keywords related to RNA methylation have begun to appear and have continued until now. "N 6 methyladenosine" with the strongest burst suggested that it was the hotspot and maybe a turning point with prospective research implications.

Keywords clusters were carried out and presented in a timeline view to observe the basic knowledge structure and the evolution over time of RNA methylation in DM and its complications. A total of 30 clusters were obtained through CiteSpace. The 1–10 clusters were presented in Figure 11. The nodes are chronicled on the horizontal line, which evolved the historical outcomes of the cluster. The clusters' names are listed in order on the right. Cluster "#1 beta-cell function" was the largest cluster and "#2 type 2 diabetes" was the second cluster; "#10 mettl3" was the last one. "#1 beta-cell function" appeared earliest and "#6 stimulated insulin secretion" appeared latest. Cluster "type 2 diabetes", "n6-methyladenosine", "hpv e6/e7", and "mettl3" related studies were available in 2022, while "aging", "stimulated insulin secretion", and "insulin sensitivity" gradually decreased or even disappeared, suggesting a decreased trend in this field. The colored annual node on the horizontal line represents keywords; the position on the line indicates the time of the first literature, and the width of the annual color band matches the amount of literature in this year. It was observed

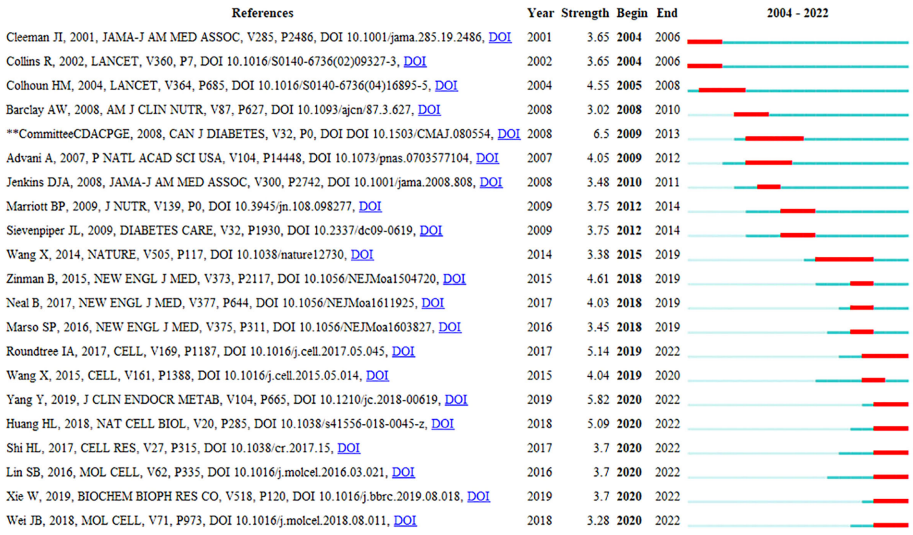

FIGURE 9
Top 21 references with the strongest citation bursts related to RNA methylation in DM and its complications.

10.3389/fendo.2022.997034

TABLE 3 The top 20 keywords related to RNA methylation in DM and its complications.

No.	Keywords	Count	Centrality
1	type 2 diabetes	51	0.21
2	cardiovascular disease	48	0.14
3	diabetes mellitus	38	0.18
4	n 6 methyladenosine	35	0.04
5	expression	33	0.14
6	coronary heart disease	33	0.11
7	disease	29	0.23
8	risk	27	0.3
9	glucose	26	0.13
10	diabetic nephropathy	25	0.11
11	blood pressure	24	0.08
12	insulin resistance	23	0.14
13	mortality	17	0.08
14	messenger RNA	16	0.08
15	association	16	0.07
16	risk factor	16	0.05
17	metaanalysis	15	0.08
18	insulin	14	0.1
19	gene expression	14	0.02
20	RNA	12	0.01

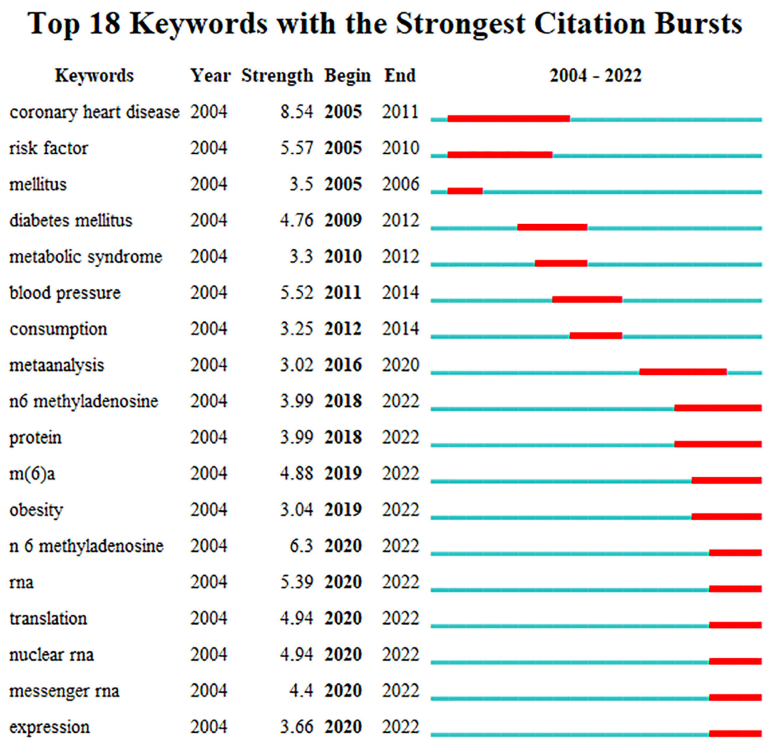

FIGURE 10
Keyword bursts related to RNA methylation in DM and its complications.

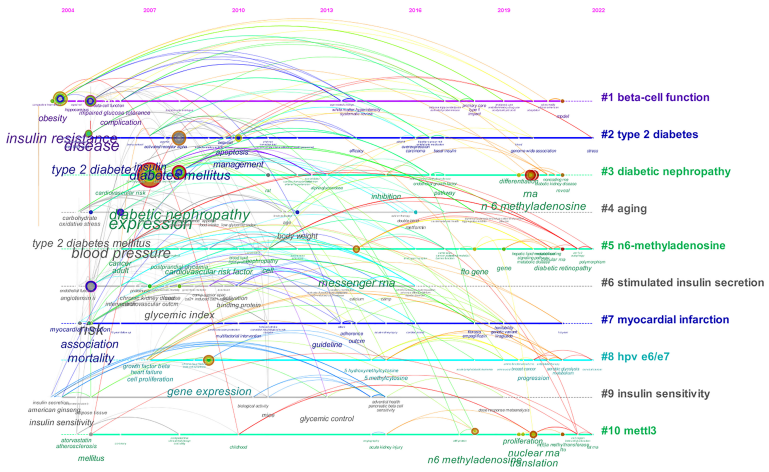

FIGURE 11
CiteSpace visualization timeline view of keywords clustering analysis related to RNA methylation in DM and its complications. The different colored horizontal lines with the label on the right represent the clusters formed by the keywords, the nodes on the horizontal lines represent the keywords, and the position of the nodes on the horizontal lines represents the year in which the literature containing the keywords first appeared, thus forming the timeline of the keywords cluster evolution.

that the nodes of "expression", "diabetic nephropathy", "insulin resistance", "type 2 diabetes", and "diabetes mellitus" were larger, which indicated that there were more published articles on related studies. "Risk", "expression", and "type 2 diabetes" circled in purple had a higher centrality and implied a significant link role in this field. The number of nodes in cluster "diabetic nephropathy", "n6-methyladenosine", and "mettl3" grew in recent years and may be the frontier on RNA methylation in DM and its complications in the future.

4 Discussion

4.1 General information

The output of publications at a particular stage reflects the trends in the research themes. The trends in annual publications showed an overall upward in the number of publications. The period from 2004 to 2011 was a nascent period with few articles published and a waved rise in publications. From 2012 to 2016, the research entered the exploration period. In the last 5 years, the research entered a critical period along with the rapid growth of the literature. It was evident that the research related to RNA methylation in DM and its complication was a hot topic in recent years and had a positive future trend.

Visualization results are based on countries, institutions, and authors in the literature. Canada was the leading country with the highest publications and almost all of the top 10 institutions and authors were from Canada in this field. China has also gradually invested in this field with increasing publications in the last 3 years. However, Canada and China do not have a higher centrality, which implied that the academic cohesion was still insufficient and the bridge role was insignificant. As for the collaboration relationship, there was a collaborative network between countries, but the relationship was relatively loose, and most cooperative institutions and researchers were limited to internal connections, with less international cooperation. This situation may not be conducive to complementary strengths, thus preventing research development. Therefore, it is strongly advisable to import specialized talents or send our countries or institutional personnel to advanced institutions or renowned scholars for targeted training, such as Univ Toronto and St Michaels Hosp. It is necessary to promote international academic exchanges and accelerate research progress in the same field.

To some extent, the frequency of the co-citation reflects the intrinsic scientific value and research backgrounds. The frequency of the co-citation reflects the influence of the author in this field and the centrality reflects the connection with the other authors. Jenkins was the most co-cited author and had higher centrality, indicating a high level of influence in this field and a stronger connection to other authors. Wolever had the higher burst, which indicated that his published reports received a high level of interest over time. The *New England Journal of Medicine*, *Lancet*, and *Nature* were highly specialized journals and influenced the academic directions and the foundations of the field. The dual-map overlay reflects the major studies on RNA methylation in DM and its complications involving various disciplines, including molecular, biology, genetics, etc. Concerning the co-cited references, the most cited article by Yang (13) had a valuable contribution revealing alterations of m^6A and methyltransferase in T2D (13). The article by

Roundtree in 2008 had the highest centrality, reflected the relationship between CVD and DM, and reviewed recommendations for risk factor management in CVD (23).

4.2 Hotspots and frontiers

Keywords articulate the subject of the documents and the timeline viewer reveals the formation process of the cluster. Combined with some similar keywords, the keywords and their clustering showed that DM, T2D, DN, and insulin appeared frequently and had four clusters associated with them. T2D, which accounts for 90% of DM (24), also had a long duration in the timeline map and was the key point of the study. In the complications of DM, DN had the highest frequency and was clustered in #3; DN, as one of the common microvascular complications of DM, is the leading cause of chronic kidney disease (CKD) and end-stage renal disease (ESRD) (25). In addition, "risk factor" and "cardiovascular disease" appeared in the top 20 keywords. Several studies suggested that either hyperglycemia or hypoglycemia was associated with an increased risk of cardiovascular events and mortality, and CVD was the main cause of mortality among DM patients (23, 26). Thus, DM was the main axis of research in terms of frequency or importance. m^6A, expression, RNA, and the clusters "#5 n6-methyladenosine" and "#10 mettl 3" were all involved in the RNA methylation. M^6A was the most studied RNA modification implicated in many fundamental RNA metabolisms such as translation, splicing, stability, and decay (3, 4, 27). METTL3 mediates m^6A methylation of mRNA, which affects the stability of mRNA and its translation into protein (28). M^6A contributed to the development of RNA epigenetics and became a frontier research area.

Burst detection reveals the hotspots, frontiers, and trends. Co-cited references reflect the backgrounds and the baselines. Combining those keywords and keywords clusters, we screened the references related to m^6A in T2D and DN and summarized the current research hotspots and trends in the following aspects; a brief diagram of the current status of research on m^6A and methylesterases in T2D and DN and risk factors for CVD is shown in Figure 12.

4.2.1 Change of m^6A and methylesterase in T2D and DN

Currently, there are guidelines for diagnosing T2D and DN, but specific markers for its pathogenesis are still being explored. Emerging evidence confirmed the change of m^6A in T2D and DN. The levels of m^6A were reduced in the peripheral blood of T2D patients compared with healthy controls. The levels of m^6A were negatively correlated with fasting blood glucose. The upregulated mRNA expression of FTO may be responsible for the reduction of m^6A and was associated with the risk of T2D (14). Another study also reported the decreased level of m^6A in white blood cells of patients with T2D compared with healthy individuals. The study demonstrated that the mRNA expression of the demethylase FTO was upregulated in white blood cells, and high glucose promoted FTO expression, which further induced m^6A to decrease in T2D (13). Additionally, the levels of other m^6A methylesterase were also varied in T2D. The mRNA levels of METTL3, METTL14, and WTAP were increased in the white blood cells of T2D patients compared with

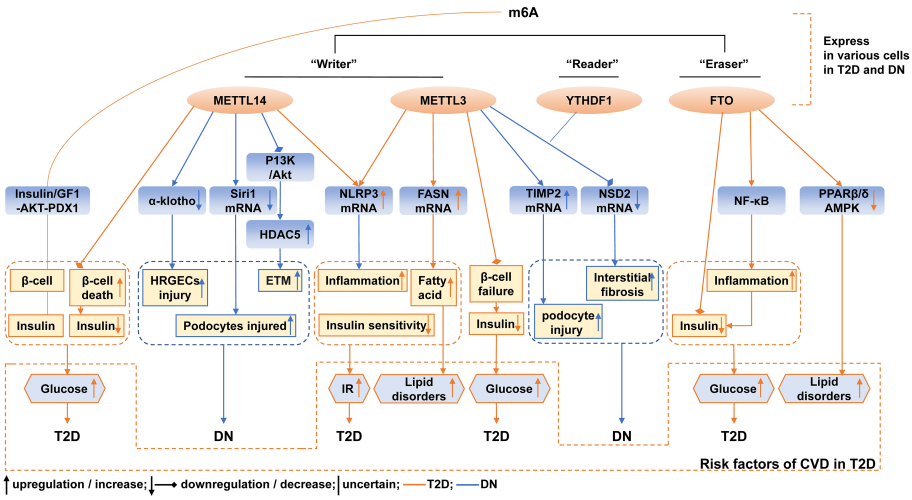

FIGURE 12
Schematic illustration of current mechanism of m^6A and methylesterase in T2D and DN, and CVD risk factors associated with m^6A and methylesterase in T2D. The orange lines represent mechanisms associated with T2D, and the blue lines represent mechanisms associated with DN.

healthy individuals; the high-glucose stimulation promoted the abundance of FTO protein in both patients with T2D and HepG2 cells (13). In the islets, m^6A and m^6A methylesterases were also altered. FTO mRNA expression was lower in T2D islets than in non-diabetic islets (29). METTL3, METTL14, ALKBH5, and YTHDF1 were decreased in the β-cells of T2D patients than in non-diabetic individuals. METTL3 and METTL14 protein levels were also decreased in the whole islets from T2D patients (15). Therefore, alteration of m^6A contents may be a specific biomarker for predicting the risk of T2D and its complications. However, these results should be repeated and validated in a larger population and different experiments. Furthermore, more studies are needed to identify the levels and corresponding causes of m^6A and m^6A methylesterase in T2D and to find their correlation with cellular function. This will help to facilitate the elucidation of the biological significance of m^6A and methylesterase changes in T2D.

The m^6A and m^6A methylesterase levels were also detected in DN. Compared with db/m mice, in the renal tissue of streptozotocin-induced diabetic mice and db/db mice, m^6A modification levels and METTL3 levels were significantly increased (30). In high-glucose-treated mouse mesangial cell lines, the m^6A level was reduced, and the serum level of METTL3 was reduced in patients with DN compared with healthy individuals (31). In HK2, the decreased mRNA expressions of FTO, METTL3, and METTL14 were reported (32). The M^6A level and expression of WTAP were increased in renal tubules but not the glomerulus from patients with DN and HK2 (33). M^6A, METTL3, METTL14, and WTAP were significantly upregulated in the renal cortex of Adriamycin-treated mice than the corresponding controls, and METTL14 was also upregulated in the biopsy samples of patients with DN in comparison to healthy controls (34). In the high-glucose human renal glomerular endothelial cells (HRGECs), METTL14 was significantly increased compared with the normal-glucose HRGECs, and METTL14 was significantly increased in the kidney tissues of DN patients both at the mRNA and protein levels compared with the normal adjacent tissues of renal carcinoma patients (35). FTO expression was significantly reduced in the serum samples of DN patients compared with healthy volunteers (36). Together, these data revealed that the levels of m^6A and m^6A methylesterase varied in DN. However, due to the small number of current studies, more evidence is needed to identify the m^6A and its regulators' change in the kidney, which will facilitate the labeling of specific markers to predict the risk or the progress of DN and thus facilitating the research on pathological or targeted therapies of DN.

4.2.2 Function and mechanism of m^6A and methylesterase in T2D

T2D was characterized by classic β-cell dysfunction and IR (1). The considerable current research focused on trying to determine the pathogenic reason for β-cell dysfunction and IR. Recently, scientists revealed the effect of m^6A methylation on the dysfunction and lower mass of the β-cell, with several proposed mechanisms. The m^6A modification mediated by the methyltransferases METTL3/14 derived functional maturation of neonatal mouse β-cells, and deletion of METTL3/14 resulted in the inability to establish an adequate amount of functional β-cells after birth (37). A study demonstrated that m^6A controlled the insulin/IGF1-Akt-PDX1 pathway, and the ablation of m^6A by targeting METTL3 or METTL14 levels decreased Akt phosphorylation and PDX1 protein levels, resulting in cell-cycle arrest and impaired insulin secretion (15). Another study reported similar results that METTL14 deficiency in β-cell increased cell death, altered cell differentiation, and decreased β-cell mass and insulin secretion (38). The β-cell-specific deletion of METTL3 also induced cell failure and hyperglycemia (39). The mechanism of METTL3/14 regulation of β-cell function was shown to be related to inflammation and oxidative stress (38, 39). Decreased β-cell function can affect insulin secretion and glucose homeostasis. The silencing of FTO expression inhibited insulin secretion by affecting metabolic signaling (29).

In addition, the role of m^6A modification in IR was also explored in many studies. IR was usually defined as impaired glucose uptake by peripheral tissues and overproduction of hepatic glucose (40). A study found that hyperglycemia enhanced FTO expression in the white blood cells of T2D patients, which promoted the mRNA expression of forkhead box O1 (FOXO1), fatty acid synthetase (FASN), glucose-6-phosphatase catalytic subunit (G6PC), and diacylglycerol O-acyltransferase 2 (DGAT2); all four genes played a critical role in glucose and lipid metabolism *via* IR in T2D (13, 41–44). Another evidence supported that METTL3 and m^6A were upregulated in the liver tissues of T2D compared with non-diabetes patients, and the silence of METTL3 expression reduced m^6A methylation and FASN mRNA levels, inhibited fatty acid metabolism thus improving insulin sensitivity, and prevented abnormal lipids and cholesterol metabolism (45). A recent study observed similar results, which reported that the overexpression of METTL3 aggravated high-fat diet (HFD)-induced liver metabolic disorders and IR, the knockout of METTL3 alleviated IR by slowing weight, reducing lipid accumulation (46). METTL3 or METTL14 enhanced the m^6A methylation of NOD-like receptor protein 3 (NLRP3), which led to the As_2O_3-induced hepatic IR (47).

These data not only reflected the vital role of m^6A and methylesterase in the β cell but also suggested that they were simultaneously involved in IR, which ultimately caused abnormalities in glucose. However, the mechanism is complex and multi-targeted, and more research is still needed to discover its downstream target genes that cause alternation in the corresponding pathways and targets. This will help enrich the understanding of the pathogenesis of DM and provide a theoretical basis for m^6A-targeted therapy for DM.

4.2.3 Function and mechanism of m^{6}A and methylesterase in DN

The development of DN is accompanied by many alternations in the structure of multiple renal compartments, and metabolic changes associated with DM lead to glomerular hypertrophy, glomerulosclerosis, tubulointerstitial inflammation, and fibrosis in the kidney (25). Several studies confirmed that m^{6}A and methylesterase were involved in histopathological changes characteristic of DN. For example, the overexpression of METTL14 in HRGECs markedly increased reactive oxygen species (ROS), tumor necrosis factor-alpha (TNF-α), interleukin-6 (IL-6), apoptosis, and suppressed cell proliferation by suppressing the m^{6}A modification of α-klotho, while α-klotho can prevent tubular and glomerular injury and delayed DN (35, 48). However, another study revealed that podocyte-specific METTL14 deletion upregulated Sirt1 expression, thereby alleviating apoptosis and inflammation, regulating autophagy, and delaying the development of proteinuria and glomerulosclerosis (34). Another study reported the overexpression of METTL14 reversed high-glucose-activated phosphatidylinositol-3-kinase/protein kinase B (P13K/Akt) pathway inactivation in HK2 by enhancing phosphatase and tensin homolog (PTEN), followed by the downregulation of histone deacetylase 5 (HDAC5), thus ameliorating DN manifestations such as fibrosis, inflammation, cell death, and albuminuria (32, 49). Overexpression of METTL3 enhanced the stability and expression of nuclear receptor-binding SET domain protein 2 (NSD2) in the high-glucose-induced mouse mesangial cell lines and that NSD2 overexpression attenuated pathological changes in the kidney, including glomerular dilatation, glomerulosclerosis, thylakoid proliferation, and interstitial fibrosis (31). METTL3 was highly expressed in the podocytes of db/db mice and streptozotocin-induced mice compared with db/m mice, and the upregulated expression of METTL3 in podocytes induced by high glucose accounted for the aberrant m^{6}A modification. The METTL3-mediated m6A modification level of TIMP2 mRNA may promote podocyte injury, apoptosis in glomeruli, and kidney inflammation through upregulating the Notch3 and Notch 4 signaling pathways (30). The knockdown of WTAP inhibited pyroptosis and diminished the release of IL-18, IL-1β, caspase-1, and NLRP3 in high-glucose-induced HK-2 cells (33). In clinical applications of regulators targeting RNA modification enzymes, a cell experiment demonstrated the total flavones of Abelmoschus Manihot, the main components of the Huangkui capsule and ameliorated pyroptosis and injury in podocytes under high-glucose conditions by adjusting METTL3-dependent m^{6}A modification and regulating NLRP3-inflammasome activation and PTEN/PK13/Akt signaling (50).

Methylatase-mediated m^{6}A modifications were involved in various renal tissue structural and functional alternations in DN. However, the mechanisms were intricate and complex, covering multiple targets and multiple pathways in various cells. Therefore, future research is necessary to investigate which methylatases are involved in the pathogenesis of DN and determine the exact regulatory and functional mechanisms of these methylatases that participated in the development and progression of DN, and if possible, mechanistic studies on different periods of DN and continuous follow-up may provide a new target for the prevention or treatment of DN.

In this article, more RNA methylation studies focused on T2D and DN, with a small number of studies revealing the role of m^{6}A methylation in other complications of DM. Diabetic retinopathy is the main cause of visual disability and blindness in DM (51). A recent study suggested that alteration of m^{6}A was related to the pathogenesis of diabetic retinopathy such as inflammation, oxidative, and angiogenesis (52). The overexpression of METTL3 alleviated high-glucose-induced retinal pigment epithelium cell division, apoptosis, and pyroptosis, and reduced the levels of IL-1β and IL-18. The overexpression of METTL3 promoted cell proliferation by regulating miR-25-3p/PTEN/Akt signaling (53). However, in another study, the level of m^{6}A RNA modification and METTL3 was increased in diabetic retinal vessels, and the increased METTL3 accelerated pericyte apoptosis and decreased pericyte viability (54). Based on the current research baseline and research background, RNA methylation may be a new hotspot and direction for research on other complications of DM and types of DM.

4.2.4 Risk factors for CVD in DM and its complications

There were few studies of RNA methylation in DM combined with CVD, but in this article, the keywords "cardiovascular disease", "risk factors", "mellitus", and "m^{6}A" appeared both in the burst detection of keywords and references. It is known that T2D is an independent risk factor for CVD; hyperglycemia, IR, dyslipidemia, inflammation, and oxidative stress were also associated with CVD in DM (17, 23). The mechanisms of the above risk factors were all associated with m^{6}A methylation and methylesterase.

Emerging evidence indicated that m^{6}A was closely related to the occurrence and progression of CVD (9, 17). However, whether m^{6}A modification is involved with CVD in DM remained largely incomplete. Diabetic cardiomyopathy (DCM) is defined as impairments of cardiac structure and function caused by the dysregulated glucose and lipid metabolism associated with DM (55, 56). A study demonstrated that in the diabetic heart disease mice model, FTO was downregulated in the heart tissue, and the overexpression of FTO improved the cardiac function by reducing myocardial fibrosis and myocyte hypertrophy in db/db mice (57). METTL14 was significantly downregulated in the heart tissue and serum samples of DCM rats compared to those of normal rats (58). Pyroptosis is programmed cell death and the consequent release of pro-inflammatory mediators such as caspase-1. Several studies suggested that pyroptosis played an important role in the

progression of DCM (59). Enhanced METTL14 inhibited pyroptosis levels in myocardial tissues, including the downregulation of NLRP3, caspase-1, and gasdermin D through downregulating the expression of TINCR lncRNA and NLRP3 (58, 60, 61). The altered cardiac metabolic pathways were also involved in the pathogenesis of DCM (55, 62). A recent study demonstrated that FTO regulates glycolysis in an m^6A-dependent manner and also regulated glucose metabolism by modulating the Akt-GLUT4 axis in the heart failure mouse model, thus regulating the energy supply in the cardiac function and structure (63). Lipotoxicity was also evident in cardiac metabolism. A study demonstrated that FTO not only facilitated adipogenesis and lipid droplet formation but also disordered lipid utilization in skeletal muscles through the inhibition of PPARβ/δ and AMPK pathways; the upregulation of FTO also reduced insulin secretion by the inflammatory NF-κB pathway and led to the development of hyperglycemia and hyperlipidemia (64). Moreover, the other mechanisms of DCM referred to in the Discussion section such as impaired insulin sensitivity, inflammation, and oxidative stress were also closely connected with the progression of DCM (55, 56). However, there were few direct studies that showed a relationship between RNA methylation and other mechanisms of DCM. Therefore, we supposed that methylesterase-mediated m^6A modifications may play a bridge role between the mechanism of DCM and DM. The m^6A methylesterase may be a risk forecast indicator for CVD in DM, but further studies are warranted to systematically assess the role of m^6A modification and the change of m^6A methylesterase in DM combined with CVD.

Apart from the most studied and most abundant m^6A RNA modification, some other types of RNA methylation have been identified, such as N1-methyladenosine (m^1A), 5-methylcytosine (m^5C), N3-methylcytosine (m^3C), N7-methylguanosine (m^7G), 2′-O-methylation, etc., and many studies also revealed their function and mechanism for various diseases (65–70). However, relatively little literature was collected in this paper, although other forms of RNA methylation were retrieved in the Web of Science Core Collection. This may be caused by the fact that other RNA methylation may not have been studied or published yet in DM and its complications, which indicates that we are still at the threshold of this new frontier research that may provide a new research direction in DM and its complications.

5 Strengths and limitations

This study is the first bibliometric analysis to systematically analyze publications related to RNA methylation in diabetes mellitus and its complications in the past 20 years. Unlike traditional systematic reviews, the bibliometric analysis objectively and comprehensively quantifies and evolutionize research hotspots and trends in a field by mathematical techniques. In this review, not only the evidence of hotspots and trends in RNA methylation of DM and its complications were objectively visualized but also the research on the current achievements and prospects was systematically summarized. Moreover, according to the results of the hotspots and frontiers, we provided a detailed review of the change and the mechanisms of m^6A and methylesterase in T2D and DN. We also summarized the mechanism of m^6A and methylesterase in DCM. It is hoped that the comprehensive picture of RNA methylation especially m^6A modification in this review will serve as a baseline and guide for the future development of DM and its complications. Meanwhile, it is hoped that the summary of the current research helps researchers quickly identify the strengths and weaknesses and thus enrich and improve the development of the field.

Inevitably, there were some limitations in this study. Firstly, the restricted database and time make retrieved literature incomplete. Only representative Web of Science Core Collection databases were searched and were limited to the period of 1 January 2002 to 28 May 2022; some updated published literature was not included. Secondly, the diversity of subject terms or the incompleteness of the literature reduced the credibility of atlas mapping. Finally, incomplete extraction of a few isolated keywords by software, articles containing incomplete items excluded by software, or a deficiency in the research itself may also affect the accuracy of the results.

To minimize limitations, we additionally manually retrieved fewer keywords and the updated article and summarized them with the results of the bibliometric analysis to provide scholars with the most recent comprehensive reviews, to quickly get the research backgrounds and keep up with the hotspots and trends in RNA methylation of DM and its complications.

6 Conclusion and perspectives

This reversible RNA methylation added a new dimension to the development of post-transcriptional regulation of gene expression. Convincing evidence suggested that m^6A modification provided novel substantial perspectives on the physiopathology of DM and its complications. In this field, Canada, the USA, and China published the most articles; Univ Toronto and St Michaels Hosp were the leaders in the publication; and professors such as Leiter and Sievenpiper have made outstanding contributions in this field. The literature related to RNA methylation has received the attention of high-level journals and has been widely cited. Especially, m^6A writers, readers, and erasers were the hotspots and trends in T2D and DN, as recent advances highlighted their contribution to the numerous physiological processes of cells and diverse pathological mechanisms of DM and its complications. However, looking toward the future, there are still many significant knowledge gaps to be completed. Firstly, strengthening national and institutional interactions and collaboration is necessary to produce more achievements for the positive upward and rapid expansion of this field. Secondly, the m^6A modification had a difference in organisms

under different conditions, reflecting its complex multi-pathway and multi-target mechanism, and DM also causes multi-organ and tissue damage. Much consolidation evidence is still needed to explore its intricate network mechanisms. Also, other RNA modifications, including m^1A and m^5C, should be further explored. Thirdly, much of the current research has been confined to molecular mechanisms; more attention is urgent, albeit difficult and protracted, and needs to be paid to the clinical applications targeting m^6A, such as proposing non-invasive clinical specific biomarkers of the mechanisms or progression of DM, especially predictive markers of risk for its complications DN and CVD. Meanwhile, research on small-molecule modulators targeting m^6A for DM and its complications is necessary to fill the gaps in current clinical applications.

Author contributions

YG, MZ, and WZ conceived the work. WZ wrote the manuscript. YG and MZ discussed and edited the manuscript. SZ, CD, and SG collected and analyzed the data. WJ, YJ, and CW checked the results. All authors contributed to the article and approved the submitted version.

Funding

This work was supported by the National Administration of Traditional Chinese Medicine Young Qi Huang Scholars support project (National Traditional Chinese Medicine Human Education Development [2020] No. 7).

Acknowledgments

The authors thank Dongzhimen Hospital, Beijing University of Chinese Medicine, and Beijing Hospital of Traditional Chinese Medicine, for their support of this work and the reviewers for allowing us to improve the manuscript.

Conflict of interest

The authors declare that the research was conducted in the absence of any commercial or financial relationships that could be construed as a potential conflict of interest.

Publisher's note

Supplementary material

The Supplementary Material for this article can be found online at: https://www.frontiersin.org/articles/10.3389/fendo.2022.997034/full#supplementary-material

References

1. American Diabetes association. diagnosis and classification of diabetes mellitus. *Diabetes Care* (2013) 36 Suppl 1(Suppl 1):S67–74. doi: 10.2337/dc13-S067

2. Sun H, Saeedi P, Karuranga S, Pinkepank M, Ogurtsova K, Duncan BB, et al. IDF diabetes atlas: Global, regional and country-level diabetes prevalence estimates for 2021 and projections for 2045. *Diabetes Res Clin Pract* (2022) 183:109119. doi: 10.1016/j.diabres.2021.109119

3. Roundtree IA, Evans ME, Pan T, He C. Dynamic RNA modifications in gene expression regulation. *Cell* (2017) 169(7):1187–200. doi: 10.1016/j.cell.2017.05.045

4. Frye M, Harada BT, Behm M, He C. RNA Modifications modulate gene expression during development. *Science* (2018) 361(6409):1346–9. doi: 10.1126/science.aau1646

5. Yang Y, Hsu PJ, Chen YS, Yang YG. Dynamic transcriptomic M^6A decoration: Writers, erasers, readers and functions in RNA metabolism. *Cell Res* (2018) 28(6):616–24. doi: 10.1038/s41422-018-0040-8

6. Zhao BS, Roundtree IA, He C. Post-transcriptional gene regulation by mRNA modifications. *Nat Rev Mol Cell Biol* (2017) 18(1):31–42. doi: 10.1038/nrm.2016.132

7. He PC, He C. M^6A RNA methylation: From mechanisms to therapeutic potential. *EMBO J* (2021) 40(3):e105977. doi: 10.15252/embj.2020105977

8. He L, Li H, Wu A, Peng Y, Shu G, Yin G. Functions of N^6-methyladenosine and its role in cancer. *Mol Cancer* (2019) 18(1):176. doi: 10.1186/s12943-019-1109-9

9. Wu S, Zhang S, Wu X, Zhou X. M^6A RNA methylation in cardiovascular diseases. *Mol Ther* (2020) 28:2111–9. doi: 10.1016/j.ymthe.2020.08.010

10. Li Y, Wang J, Huang C, Shen M, Zhan H, Xu K. RNA N^6-methyladenosine: A promising molecular target in metabolic diseases. *Cell Biosci* (2020) 10(10):19. doi: 10.1186/s13578-020-00385-4

11. Wu Z, Shi Y, Lu M, Song M, Yu Z, Wang J, et al. METTL3 counteracts premature aging *Via* M^6A-dependent stabilization of mis12 mRNA. *Nucleic Acids Res* (2020) 48(19):11083–96. doi: 10.1093/nar/gkaa816

12. Wang Y, Li L, Li J, Zhao B, Huang G, Li X, et al. The emerging role of M^6A modification in regulating the immune system and autoimmune diseases. *Front Cell Dev Biol* (2021) 9:755691. doi: 10.3389/fcell.2021.755691

13. Yang Y, Shen F, Huang W, Qin S, Huang JT, Sergi C, et al. Glucose is involved in the dynamic regulation of M^6A in patients with type 2 diabetes. *J Clin Endocrinol Metab* (2019) 104(3):665–73. doi: 10.1210/jc.2018-00619

14. Shen F, Huang W, Huang JT, Xiong J, Yang Y, Wu K, et al. Decreased N^6-methyladenosine in peripheral blood RNA from diabetic patients is associated with FTO expression rather than ALKBH5. *J Clin Endocrinol Metab* (2015) 100(1):E148–54. doi: 10.1210/jc.2014-1893

15. De Jesus DF, Zhang Z, Kahraman S, Brown NK, Chen MJ, Hu J, et al. M^6A mRNA methylation regulates human β-cell biology in physiological states and in type 2 diabetes. *Nat Metab* (2019) 1(8):765–74. doi: 10.1038/s42255-019-0089-9

16. Geng X, Li Z, Yang Y. Emerging role of epitranscriptomics in diabetes mellitus and its complications. *Front Endocrinol (Lausanne)* (2022) 13:907060. doi: 10.3389/fendo.2022.907060

17. Zhang B, Jiang H, Dong Z, Sun A, Ge J. The critical roles of M^6A modification in metabolic abnormality and cardiovascular diseases. *Genes Dis* (2020) 8(6):746–58. doi: 10.1016/j.gendis.2020.07.011

18. Smith DR. Bibliometrics, dermatology and contact dermatitis. *Contact Dermatitis* (2008) 59(3):133–6. doi: 10.1111/j.1600-0536.2008.01405.x

19. Ma CQ, Su H, Li HJ. Global research trends on prostate diseases and erectile dysfunction: A bibliometric and visualized study. *Front Oncol* (2021) 10:627891. doi: 10.3389/fonc.2020.627891

20. Guler AT, Waaijer CJ, Palmblad M. Scientific workflows for bibliometrics. *Scientometrics* (2016) 107:385–98. doi: 10.1007/s11192-016-1885-6

21. Lv J, Li Y, Shi S, Liu S, Xu X, Wu H, et al. Frontier and hotspot evolution in cardiorenal syndrome: A bibliometric analysis from 2003 to 2022. *Curr Probl Cardiol* (2022), 101238. [Online ahead of print] doi: 10.1016/j.cpcardiol.2022

22. Chen CM. Citespace II: Detecting and visualizing emerging trends and transient patterns in scientific literature. *J Am Soc Inf Sci Technol* (2006) 57(3):359–77. doi: 10.1002/asi.20317

23. Bhattacharyya OK, Shah BR, Booth GL. Management of cardiovascular disease in patients with diabetes: The 2008 Canadian diabetes association guidelines. *CMAJ* (2008) 179(9):920–6. doi: 10.1503/cmaj.080554

24. Stumvoll M, Goldstein BJ, van Haeften TW. Type 2 diabetes: Principles of pathogenesis and therapy. *Lancet* (2005) 365(9467):1333–46. doi: 10.1016/s0140-6736(05)61032-x

25. Alicic RZ, Rooney MT, Tuttle KR. Diabetic kidney disease: Challenges, progress, and possibilities. *Clin J Am Soc Nephrol* (2017) 12(12):2032–45. doi: 10.2215/CJN.11491116

26. Stephanie AA, Pablo A, Belinda C, Philip EC, Bastiaan E de G, Brian MF. Hypoglycaemia, cardiovascular disease, and mortality in diabetes: Epidemiology, pathogenesis, and management. *Lancet Diabetes Endocrinol* (2019) 7(5):385–96. doi: 10.1016/S2213-8587(18)30315-2

27. Liu N, Dai Q, Zheng G, He C, Parisien M, Pan T. N^6-Methyladenosine-Dependent RNA structural switches regulate RNA-protein interactions. *Nature* (2015) 518(7540):560–4. doi: 10.1038/nature14234

28. Shi H, Wei J, He C. Where, when, and how: Context-dependent functions of RNA methylation writers, readers, and erasers. *Mol Cell* (2019) 74(4):640–50. doi: 10.1016/j.molcel.2019.04.025

29. Taneera J, Prasad RB, Dhaiban S, Mohammed AK, Haataja L, Arvan P, et al. Silencing of the FTO gene inhibits insulin secretion: An in vitro study using grinch cells. *Mol Cell Endocrinol* (2018) 472(472):10–7. doi: 10.1016/j.mce.2018.06.003

30. Jiang L, Liu X, Hu X, Gao L, Zeng H, Wang X, et al. METTL3-mediated M^6A modification of TIMP2 mRNA promotes podocyte injury in diabetic nephropathy. *Mol Ther* (2022) 30(4):1721–40. doi: 10.1016/j.ymthe.2022.01.002

31. Tang W, Zhao Y, Zhang H, Peng Y, Rui Z. METTL3 enhances NSD2 mRNA stability to reduce renal impairment and interstitial fibrosis in mice with diabetic nephropathy. *BMC Nephrol* (2022) 23(1):124. doi: 10.1186/s12882-022-02753-3

32. Xu ZX, Jia KQ, Wang H, Gao F, Zhao S, Li F, et al. METTL14-regulated PI3k/Akt signaling pathway *via* PTEN affects HDAC5-mediated epithelial-mesenchymal transition of renal tubular cells in diabetic kidney disease. *Cell Death Dis* (2021) 12(1):32. doi: 10.1038/s41419-020-03312-0

33. Lan J, Xu B, Shi X, Pan Q, Qing T. WTAP-mediated N^6-methyladenosine modification of NLRP3 mRNA in kidney injury of diabetic nephropathy. *Cell Mol Biol Lett* (2022) 27(1):51. doi: 10.1186/s11658-022-00350-8

34. Lu Z, Liu H, Song N, Liang Y, Zhu J, Chen J, et al. METTL14 aggravates podocyte injury and glomerulopathy progression through N^6-Methyladenosine-Dependent downregulating of Sirt1. *Cell Death Dis* (2021) 12(10):881. doi: 10.1038/s41419-021-04156-y

35. Li M, Deng L, Xu G. METTL14 promotes glomerular endothelial cell injury and diabetic nephropathy *via* M^6A modification of α-klotho. *Mol Med* (2021) 27(1):106. doi: 10.1186/s10020-021-00365-5

36. Sun Q, Geng H, Zhao M, Li Y, Chen X, Sha Q, et al. FTO-mediated M^6A modification of SOCS1 mRNA promotes the progression of diabetic kidney disease. *Clin Transl Med* (2022) 12(6):e942. doi: 10.1002/ctm2.942

37. Wang Y, Sun J, Lin Z, Zhang W, Wang S, Wang W, et al. M^6A mRNA methylation controls functional maturation in neonatal murine β-cells. *Diabetes* (2020) 69(8):1708–22. doi: 10.2337/db19-0906

38. Liu J, Luo G, Sun J, Men L, Ye H, He C, et al. METTL14 is essential for β-cell survival and insulin secretion. *Biochim Biophys Acta Mol Basis Dis* (2019) 1865(9):2138–48. doi: 10.1016/j.bbadis.2019.04.011

39. Li XZ, Jiang YZ, Sun X, Wu Y, Chen Z. METTL3 is required for maintaining β-cell function. *Metabolism* (2021) 116:154702. doi: 10.1016/j.metabol.2021.154702

40. DeFronzo RA. Pathogenesis of type 2 diabetes mellitus. *Med Clin North Am* (2004) 88(4):787–835. doi: 10.1016/j.mcna.2004.04.013

41. Li Y, Ma Z, Jiang S, Hu W, Li T, Di S, et al. A global perspective on FOXO1 in lipid metabolism and lipid-related diseases. *Prog Lipid Res* (2017) 66:42–9. doi: 10.1016/j.plipres.2017.04.002

42. Menendez JA, Vazquez-Martin A, Ortega FJ, Fernandez-Real JM. Fatty acid synthase: Association with insulin resistance, type 2 diabetes, and cancer. *Clin Chem* (2009) 55(3):425–38. doi: 10.1373/clinchem.2008.115352

43. Jornayvaz FR, Birkenfeld AL, Jurczak MJ, Kanda S, Guigni BA, Jiang DC, et al. Hepatic insulin resistance in mice with hepatic overexpression of diacylglycerol acyltransferase 2. *Proc Natl Acad Sci U.S.A.* (2011) 108(14):5748–52. doi: 10.1073/pnas.1103451108

44. Farah BL, Landau DJ, Sinha RA, Brooks ED, Wu Y, Fung SYS, et al. Induction of autophagy improves hepatic lipid metabolism in glucose-6-Phosphatase deficiency. *J Hepatol* (2016) 64(2):370–9. doi: 10.1016/j.jhep.2015.10.008

45. Xie W, Ma LL, Xu YQ, Wang BH, Li SM. METTL3 inhibits hepatic insulin sensitivity *Via* N^6-methyladenosine modification of FASN mRNA and promoting fatty acid metabolism. *Biochem Biophys Res Commun* (2019) 518(1):120–6. doi: 10.1016/j.bbrc.2019.08.018

46. Li YH, Zhang QY, Cui GS, Zhao F, Tian X, Sun BF, et al. M^6A regulates liver metabolic disorders and hepatogenous diabetes. *Genomics Proteomics Bioinf* (2020) 18(4):371–83. doi: 10.1016/j.gpb.2020.06.003

47. Qiu T, Wu C, Yao X, Han Q, Wang N, Yuan W, et al. As3mt facilitates NLRP3 inflammasome activation by M6A modification during arsenic-induced hepatic insulin resistance. *Cell Biol Toxicol* (2022), 1–7. [Online ahead of print] doi: 10.1007/s10565-022-09703-7

48. Wang Q, Ren D, Li Y, Xu G. Klotho attenuates diabetic nephropathy in db/db mice and ameliorates high glucose-induced injury of human renal glomerular endothelial cells. *Cell Cycle* (2019) 18(6-7):696–707. doi: 10.1080/15384101.2019.1580495

49. Hadden MJ, Advani A. Histone deacetylase inhibitors and diabetic kidney disease. *Int J Mol Sci* (2018) 19(9):2630. doi: 10.3390/ijms19092630

50. Liu BH, Tu Y, Ni GX, Yan J, Yue L, Li ZL, et al. Total flavones of abelmoschus manihot ameliorates podocyte pyroptosis and injury in high glucose conditions by targeting METTL3-dependent M^6A modification-mediated NLRP3-inflammasome activation and PTEN/PI3k/Akt signaling. *Front Pharmacol* (2021) 12:667644. doi: 10.3389/fphar.2021.667644

51. Yau JW, Rogers SL, Kawasaki R, Lamoureux EL, Kowalski JW, Bek T, et al. Global prevalence and major risk factors of diabetic retinopathy. *Diabetes Care* (2012) 35(3):556–64. doi: 10.2337/dc11-1909

52. Kumari N, Karmakar A, Ahamad Khan MM, Ganesan SK. The potential role of M^6A RNA methylation in diabetic retinopathy. *Exp Eye Res* (2021) 208:108616. doi: 10.1016/j.exer.2021.108616

53. Zha X, Xi X, Fan X, Ma M, Zhang Y, Yang Y. Overexpression of METTL3 attenuates high-glucose induced RPE cell pyroptosis by regulating mir-25-3p/PTEN/Akt signaling cascade through DGCR8. *Aging (Albany NY)* (2020) 12(9):8137–50. doi: 10.18632/aging.103130

54. Suo L, Liu C, Zhang QY, Yao MD, Ma Y, Yao J, et al. Mettl3-mediated N^6-methyladenosine modification governs pericyte dysfunction during diabetes-induced retinal vascular complication. *Theranostics* (2022) 12(1):277–89. doi: 10.7150/thno.63441

55. Ritchie RH, Abel ED. Basic mechanisms of diabetic heart disease. *Circ Res* (2020) 126(11):1501–25. doi: 10.1161/CIRCRESAHA.120.315913

56. Tan Y, Zhang Z, Zheng C, Wintergerst KA, Keller BB, Cai L. Mechanisms of diabetic cardiomyopathy and potential therapeutic strategies: Preclinical and clinical evidence. *Nat Rev Cardiol* (2020) 17(9):585–607. doi: 10.1038/s41569-020-0339-2

57. Ju W, Liu K, Ouyang S, Liu Z, He F, Wu J. Changes in N^6-methyladenosine modification modulate diabetic cardiomyopathy by reducing myocardial fibrosis and myocyte hypertrophy. *Front Cell Dev Biol* (2021) 9:702579. doi: 10.3389/fcell.2021.702579

58. Meng L, Lin H, Huang X, Weng J, Peng F, Wu S. METTL14 suppresses pyroptosis and diabetic cardiomyopathy by downregulating TINCR LncRNA. *Cell Death Dis* (2022) 13(1):38. doi: 10.1038/s41419-021-04484-z

59. Xu Y, Fang H, Xu Q, Xu C, Yang L, Huang C. LncRNA GAS5 inhibits NLRP3 inflammasome activation-mediated pyroptosis in diabetic cardiomyopathy by targeting mir-34b-3p/AHR. *Cell Cycle* (2020) 19(22):3054–65. doi: 10.1080/15384101.2020.1831245

60. Broz P. Immunology: Caspase target drives pyroptosis. *Nature* (2015) 526(7575):642–3. doi: 10.1038/nature15632

61. Liu X, Zhang Z, Ruan J, Pan Y, Magupalli VG, Wu H, et al. Inflammasome-activated gasdermin d causes pyroptosis by forming membrane pores. *Nature* (2016) 535(7610):153–8. doi: 10.1038/nature18629

62. Jia G, Hill MA, Sowers JR. Diabetic cardiomyopathy: An update of mechanisms contributing to this clinical entity. *Circ Res* (2018) 122(4):624–38. doi: 10.1161/CIRCRESAHA.117.311586

63. Zhang BJ, Jiang H, Wu J, Cai Y, Dong Z, Zhao Y, et al. M^6A demethylase FTO attenuates cardiac dysfunction by regulating glucose uptake and glycolysis in mice with pressure overload-induced heart failure. *Signal Transduct Target Ther* (2021) 6(1):377. doi: 10.1038/s41392-021-00699-w

64. Yang Z, Yu GL, Zhu X, Peng TH, Lv YC. Critical roles of FTO-mediated mRNA M^6A demethylation in regulating adipogenesis and lipid metabolism: Implications in lipid metabolic disorders. *Genes Dis* (2022) 9(1):51–61. doi: 10.1016/j.gendis.2021.01.005

65. Zhou Y, Kong Y, Fan W, Tao T, Xiao Q, Li N, et al. Principles of RNA methylation and their implications for biology and medicine. *BioMed Pharmacother* (2020) 131:110731. doi: 10.1016/j.biopha.2020.110731

66. Ayadi L, Galvanin A, Pichot F, Marchand V, Motorin Y. RNA ribose methylation (2'-O-Methylation): Occurrence, biosynthesis and biological functions. *Biochim Biophys Acta Gene Regul Mech* (2019) 1862(3):253–69. doi: 10.1016/j.bbagrm.2018.11.009

67. Trixl L, Lusser A. The dynamic RNA modification 5-methylcytosine and its emerging role as an epitranscriptomic mark. *Wiley Interdiscip Rev RNA* (2019) 10 (1):e1510. doi: 10.1002/wrna.1510

68. Xu Y, Zhang M, Zhang Q, Yu X, Sun Z, He Y, et al. Role of main RNA methylation in hepatocellular carcinoma: N^6-methyladenosine, 5-methylcytosine, and N^1-methyladenosine. *Front Cell Dev Biol* (2021) 9:767668. doi: 10.3389/fcell.2021.767668

69. Song B, Tang Y, Chen K, Wei Z, Rong R, Lu Z, et al. m7GHub: Deciphering the location, regulation and pathogenesis of internal mrna N^7-methylguanosine (M^7G) sites in human. *Bioinformatics* (2020) 36(11):3528–36. doi: 10.1093/bioinformatics/btaa178

70. Fu Y, Dominissini D, Rechavi G, He C. Gene expression regulation mediated through reversible M^6A RNA methylation. *Nat Rev Genet* (2014) 15 (5):293–306. doi: 10.1038/nrg3724

frontiers | Frontiers in Endocrinology

TYPE Original Research
PUBLISHED 21 September 2022
DOI 10.3389/fendo.2022.967822

OPEN ACCESS

EDITED BY
Wenxiang Hu,
Guangzhou Laboratory, China

REVIEWED BY
Heng Wan,
Southern Medical University, China
Elettra Mancuso,
University of Magna Graecia, Italy

*CORRESPONDENCE
Liguo Chen
tchenly@jnu.edu.cn
Xiaoshan Zhao
zhaoxs0609@163.com
Ya Xiao
xiaoya0527@126.com

†These authors have contributed equally to this work

SPECIALTY SECTION
This article was submitted to Diabetes: Molecular Mechanisms, a section of the journal Frontiers in Endocrinology

RECEIVED 13 June 2022
ACCEPTED 01 September 2022
PUBLISHED 21 September 2022

CITATION
Bai Z, Xie T, Liu T, Chen Z, Yu L, Zhang C, Luo J, Chen L, Zhao X and Xiao Y (2022) An integrated RNA sequencing and network pharmacology approach reveals the molecular mechanism of dapagliflozin in the treatment of diabetic nephropathy. *Front. Endocrinol.* 13:967822. doi: 10.3389/fendo.2022.967822

An integrated RNA sequencing and network pharmacology approach reveals the molecular mechanism of dapagliflozin in the treatment of diabetic nephropathy

Zhenyu Bai[1†], Ting Xie[1†], Tianhao Liu[2†], Zedong Chen[1], Linde Yu[3,4], Chao Zhang[1], Jincheng Luo[1], Liguo Chen[1*], Xiaoshan Zhao[5*] and Ya Xiao[1*]

[1]School of Traditional Chinese Medicine, Jinan University, Guangzhou, China, [2]Department of Gastroenterology, Affiliated Hospital of Jiangnan University, Wuxi School of Medicine, Jiangnan University, Wuxi, China, [3]GuangDong Province Engineering Technology Research Institute of Traditional Chinese Medicine (TCM), Guangzhou, China, [4]Emergency Department, GuangDong Second Traditional Chinese Medicine Hospital, Guangzhou, China, [5]School of Traditional Chinese Medicine, Southern Medical University, Guangzhou, China

Dapagliflozin, an inhibitor of sodium-glucose cotransporter 2 (SGLT2), is a new type of oral hypoglycemic drugs which can promote glucose excretion in the kidney. Studies have shown that dapagliflozin has renoprotective effect in the treatment of type 2 diabetes. However, the underlying mechanism remains unclear. Here, we combined integrated RNA sequencing and network pharmacology approach to investigate the molecular mechanism of dapagliflozin for diabetic nephropathy (DN). Dapagliflozin significantly relieved glucose intolerance, urinary albumin/creatinine ratio (UACR) and renal pathological injuries of db/db mice. The LncRNA and mRNA expression in kidney tissues from control group (CR), db/db group (DN) and dapagliflozin group (DG) were assessed by RNA sequencing. We identified 7 LncRNAs and 64 mRNAs common differentially expressed in CR vs DN and DN vs DG, which were used to construct co-expression network to reveal significantly correlated expression patterns in DN. In addition, network pharmacology was used to predict the therapeutic targets of dapagliflozin and we constructed component-target-pathway network according to the results of RNA sequencing and network pharmacology. We found that SMAD9, PPARG, CD36, CYP4A12A, CYP4A12B, CASP3, H2-DMB2, MAPK1, MAPK3, C3 and IL-10 might be the pivotal targets of dapagliflozin for treating DN and these genes were mainly enriched in pathways including TGF-β signaling pathway, PPAR signaling pathway, Chemokine signaling pathway, etc. Our results have important implication and provide novel insights into the protective mechanism of dapagliflozin for treating DN.

KEYWORDS

diabetic nephropathy, dapagliflozin, RNA sequencing, network pharmacology, sodium-glucose cotransporter 2

Introduction

Diabetes has become a significant public health issue in recent years and is estimated to affect nearly 700 million people worldwide by 2045 (1). Diabetic nephropathy (DN), a major complication of diabetes, can lead to end-stage kidney disease (ESKD) and mainly manifest as hypertrophy, mesangial expansion and thickened basement membrane (2). Persistent hyperglycemia causes renal inflammation, apoptosis and oxidative stress, which may be closely related with DN progression (3). Recently, sodium-glucose transport protein 2 (SGLT2) inhibitors have been developed for the treatment of hyperglycemia (4, 5). Dapagliflozin, a selective inhibitor of SGLT2, can lower blood glucose *via* blocking glucose reabsorption in the renal proximal tubule and stimulating urinary glucose excretion without increasing insulin release (6). Several large clinical trials have been performed to investigate the effect of SGLT2 inhibitors on renal outcomes. In the clinical trial, dapagliflozin significantly reduced renal events (7). Therefore, dapagliflozin can act as a new pharmacologic option for overcoming DN progression in patients with diabetes. Interestingly, dapagliflozin also exerts renoprotective effect and prevents the progression to ESKD regardless of the presence or absence of diabetes (8), indicating that dapagliflozin protect the kidney *via* pleiotropic effects beyond glycemic control. Previous studies have showed that SGLT2 inhibitors can induce tubulo-glomerular feedback, reduce glomerular hyperfiltration and simulate antioxidant and anti-inflammatory signaling pathway (9, 10). However, little is known about the underlying molecular mechanism of dapagliflozin in the treatment of DN.

RNA sequencing (RNA-SEQ) is one of the most advanced techniques to explore the mechanism of various diseases (11, 12). Based on the advantages of high sensitivity and resolution, whole transcriptome sequencing can reveal crucial roles of coding and non-coding RNAs and provide new insights into gene expression changes. Long non-coding RNA (LncRNA) are regulatory RNAs over 200 nucleotides (nt) which does not encode proteins. LncRNA is localized in the nucleus or cytoplasm, and some LncRNA structures are similar to mRNA with polyA tail. Some LncRNAs have conserved secondary structures that can interact with proteins, DNA and RNA and regulate multiple biological processes (13). With the development of RNA-SEQ technology, increasing numbers of LncRNAs have been identified. Studies showed that LncRNA MALAT1 promotes renal fibrosis and injury in DN *in vivo* and vitro (14, 15). Li et al. reported that LncRNATug1/PGC1a has renoprotective effect *via* regulating mitochondrial remodeling and urea cycle metabolites in diabetic mice (16). LncRNA Erbb4-IR was reported to promote renal fibrosis *via* inhibiting miR-29b in DN (17). Although emerging studies showed LncRNAs involved in DN pathogenesis, the functional roles of LncRNAs are largely unknown. Particularly, the regulatory mechanism of LncRNAs and the whole transcriptome in DN treated by dapagliflozin has not been studied.

Network pharmacology has attracted more and more attention. It constructs the connections between components, diseases and signaling pathways and offers a practical approach to elucidate the pharmacological mechanisms of agents (18). It is a powerful tool for establishing a "component-gene-disease" network. Therefore, combining RNA sequencing technologies and network pharmacology is a good strategy to study the mechanisms of dapagliflozin for DN.

Thus, we conducted a comprehensive study to investigated the mechanism of renoprotective effect of dapagliflozin on diabetic mice. First, RNA sequencing was carried out to identify differentially expressed LncRNAs and mRNAs in db/m mice, db/db mice and db/db mice treated with dapagliflozin. Then, co-expression network of differentially expressed LncRNAs/mRNAs was established. Finally, combining with network pharmacology and bioinformatics analysis, component- target-pathway network was constructed to identify the key genes targeted by dapagliflozin.

Materials and methods

Animal model and treatments

C57BL/KsJ leptin receptor-deficient (db/db) and db/m male mice were provided by the Model Animal Research Institute of Nanjing University. The animals were 4-6 weeks old. Six db/m mice comprised control group (CR). Twelve db/db mice were randomly divided into two groups: the db/db group (DN, n=6) and db/db+ Dapagliflozin group (DG, n=6). Mice in DG group were fed 50mg/Kg dapagliflozin-supplemented diet, while mice in CR and DN group were fed control diet. Dapagliflozin was from AstraZeneca Pharmaceuticals LP. After twelve-week dietary intervention, the mice were anaesthetized with sodium pentobarbital (60 mg/kg iP). Body weight was recorded once a week and oral glucose tolerance test was conducted once four weeks. Blood was collected from orbital venous and kidney tissues were collected for further study. Blood glucose was measured by blood glucose metre (Roche Diabetes Care GmbH, UK). The experiment was approved by the Animal Experiment Ethics Committee of Jinan University.

Serum and urine biochemistry assays

Serum creatinine levels and blood urea nitrogen (BUN) were assessed using the Quanti Chrom Creatinine Assay Kit

(BioAssay Systems, USA). Urinary albumin was measured using the mouse urinary albumin ELISA kit (Bethyl Laboratories, USA). Urinary albumin/creatinine ratio (UACR) was calculated as urinary albumin/creatinine ratio.

Oral glucose tolerance test

The test was measured at fourth week, eighth week and twelfth week. First, the mice were fasted for 6 hours and received glucose solution with 2.0 g/kg by gavage. Finally, the blood glucose level was tested at 0, 30, 60, 90, and 120 minutes.

Histopathology

The kidneys were harvested and fixed in 4% paraformaldehyde for 1-2h. Then, the samples were dehydrated, immersed in xylene and embedded in paraffin. The samples were cut into 5 μm thick sections and used for hematoxylin-eosin (HE), Periodic acid-Schiff (PAS) and Masson staining. All sections were observed by a microscope (Olympus, Tokyo, Japan) and assessed by Image-Pro Plus 6.0 software (Media Cybernetics, Bethesda, MD).

Total RNA extraction, library construction and sequencing

Total RNA was extracted from renal tissues in three groups (n = 3 for each) by TRIzol (Invitrogen) reagent. RNA purity and RNA integrity were assessed by Agilent 2200 TapeStation (Agilent Technologies, USA). Ribosomal RNA was eliminated using Ribo-Zero™ kit (Epicentre, Madison, WI, USA) and fragmented to approximately 200bp. Subsequently, the purified RNAs were used to synthesis first strand and second strand cDNA according to instructions of NEBNext® Ultra™ RNA Library Prep Kit for Illumina (NEB, USA). The purified library products were assessed by Agilent 2200 TapeStation and Qubit®2.0(Life Technologies, USA). The libraries were paired-end sequenced at Guangzhou RiboBio Co., Ltd. (Guangzhou, China) using IlluminaHiSeq 3000 platform.

Identification of new LncRNA

After removing low-quality reads, the clean data was assembled using the StringTie based on the reads mapped to the reference genome. Gffcompare program was used to annotate the transcripts. Putative protein-coding RNAs were filtered out using a minimum length and exon number threshold. Transcripts with lengths between 200 nt and 300 nt could be selected as LncRNA candidates, which were submitted to further screening by CPC/CNCI/Pfam to distinguish the protein-coding genes from the noncoding genes.

Differentially expressed mRNA and LncRNA Genes (DEGs and DELncRNAs)

Paired-end reads were aligned to the mouse reference genome mm10 with HISAT2. HTSeq v0. 6.0 was used to count the reads numbers mapped to each gene. RPKM was used to evaluate the sample expression level (expected number of Reads PerKilobase of transcript sequence per Million base pairs sequenced). An adjusted P-value threshold of <0.05 and $|\log2(\text{fold change})| > 1$ was utilized to identify differentially expressed genes.

Co-expression network of differentially expressed LncRNAs/mRNAs

To investigate the relationships between LncRNAs and mRNAs, we constructed a LncRNA/mRNA transcripts co-expression network. A given threshold (absolute Pearson correlation coefficients no less than 0.7 and p-values less than 0.05) was used to filter the results. The co-expression network was illustrated by Cytoscape software.

GO terms and KEGG pathway enrichment analysis

Differentially expressed mRNAs were utilized for Gene ontology (GO) functional enrichment and Kyoto Encyclopedia of Genes and Genomes (KEGG) pathway analyses by the KOBAS3.0 software. A P-value < 0.05 was determined to be significant in the enrichment analysis of the gene sets.

Network pharmacological analysis of therapeutic pathways and targets of dapagliflozin in the treatment of DN

Firstly, the bioactive component and potential pharmacological targets of dapagliflozin were obtained by CHEMBL, STITCH, Drugbank, Pubchem and PubMed. Secondly, we got the pathogenic targets of DN through searching for the keyword “diabetic nephropathy” in GeneCards, Online Mendelian Inheritance in Man and PharmGkb databases. Thirdly, we intersected the above two sets to obtain potential targets of dapagliflozin in DN by the Venny2.1 online tool. Fourthly, a protein-protein interaction (PPI) network was constructed by STRING online database based on the obtained target genes. The top 20 target genes were selected to perform KEGG and GO enrichment analysis.

Construction of component- target-pathway network

A component- target- pathway network was constructed to obtain the key targets and pathway of dapagliflozin in DN by Cytoscape3.8.2 based on the data of KEGG enrichment analysis of RNA sequencing and network pharmacology.

Quantitative real-time PCR

Total RNA was extracted from the kidneys using TRIzol kit (Invitrogen, Carlsbad, CA). An Invitrogen (Carlsbad, CA) kit was used to perform reverse transcription. Real-time quantitative RT-PCR was conducted by the Bio–Rad 96FX circulation system (Bio-Rad, USA) with SYBR Green Master Mix. The relative expression levels of genes were calculated by the 2-ΔΔCq method. The primers for genes for qRT-PCR were listed in Table S1.

Western blotting

Proteins were extracted from renal tissues using RIPA method. A BCA protein detection kit was used to measure protein concentrations. After subjecting to SDS-PAGE, proteins were transferred to nitrocellulose membranes. Then, membranes were incubated with primary antibodies overnight as follows: anti-IL-10 (1:1000,ab189392), anti-PPAR gamma (1:1000, ab272718), anti-CD36 (1:1000, ab252923), anti-Caspase-3 (1:2000, ab184787), anti-MAPK1 (1:2000, ab32081), anti-MAPK3 (1:1000, ab32537), anti-C3 (1:3000, ab97462), anti-SMAD9 (1:1000, ab80255), anti-GAPDH (1:500, ab8245). Membranes were incubated with the HRP-conjugated secondary antibodies. Gel-pro analyser software was used to analysis the images.

Statistical analysis

GraphPad Prism 7 software was used for statistical analysis. The data were expressed as the mean ± SE. Comparisons of multiple groups were performed by one-way ANOVA. Student's t-test was used to determine significant differences between two independent groups. $P<0.05$ was considered statistically significant.

Results

Dapagliflozin ameliorated renal injury in DN mouse model

Body weight, 24-hour urinary protein, UACR, BUN, serum creatinine, fasting blood glucose (FBG) and glucose tolerance were used to assess the effect of dapagliflozin in DN mouse model. Mice in DN group and dapagliflozin group had markedly increased body weight compared with that in CR group (Figure 1A). Db/db mice had significantly high FBG, 24-hour urinary albumin, BUN, serum creatinine, UACR and obvious glucose intolerance. The dapagliflozin group showed markedly reduced FBG, serum creatinine, UACR and improved glucose intolerance comparing to db/db mice models (Figures 1B–G). Dapagliflozin tended to decrease 24-hour urinary albumin, but this effect failed to reach statistical significance.

As to pathological changes, HE staining showed that db/db mice had glomerular enlargement and glomerular capillary loops dilatation. PAS and Masson staining revealed that db/db mice had mesangial matrix, mesangial expansion, thickened basement membrane and increased renal fibrosis. Treatment with dapagliflozin alleviated these pathological injuries (Figures 1H). Quantitative analysis also showed statistically significant differences in pathology (Figures 1I). Taken together, dapagliflozin can improve glucose intolerance, UACR and kidney injuries.

Identification of differentially expressed LncRNAs in DN

The bioinformatics analysis was divided into two independent comparisons:CR vs DN and DN vs DG. Volcano plots and heat map provided an overview of LncRNAs differential expressed in the two comparisons (Figures 2A–D). Venn diagrams revealed that there were 172 differentially expressed LncRNAs in CR vs DN, of which 100 were up-regulated and 72 were down-regulated (Figures 2E–G). There were 40 differentially expressed LncRNAs in DN vs DG, among which 29 were up-regulated and 11 were down-regulated (Figures 2E–G). As shown in Table 1, 7 common differentially expressed LncRNAs (NR_015554.2, XR_382492.3, XR_382493.3, XR_382494.3, XR_388840.1, XR_873495.2 and XR_876705.2) were found in the two comparisons, and dapagliflozin could reverse the expression changes of 7 LncRNAs. The top 10 upregulated and downregulated LncRNAs in CR vs DN and DN vs DG respectively was listed in Tables S2 and S3.

Identification of differentially expressed mRNAs in DN

We analyzed the differentially expressed mRNAs between groups. Volcano plots and heat map offered an overview of mRNAs differential expressed in CR vs DN and DN vs DG (Figures 3A–D). Compared with CR group, 1459 mRNAs were markedly expressed in the DN group (797 upregulated and 662 downregulated). Compared with DN group, 228 mRNAs were

10.3389/fendo.2022.967822

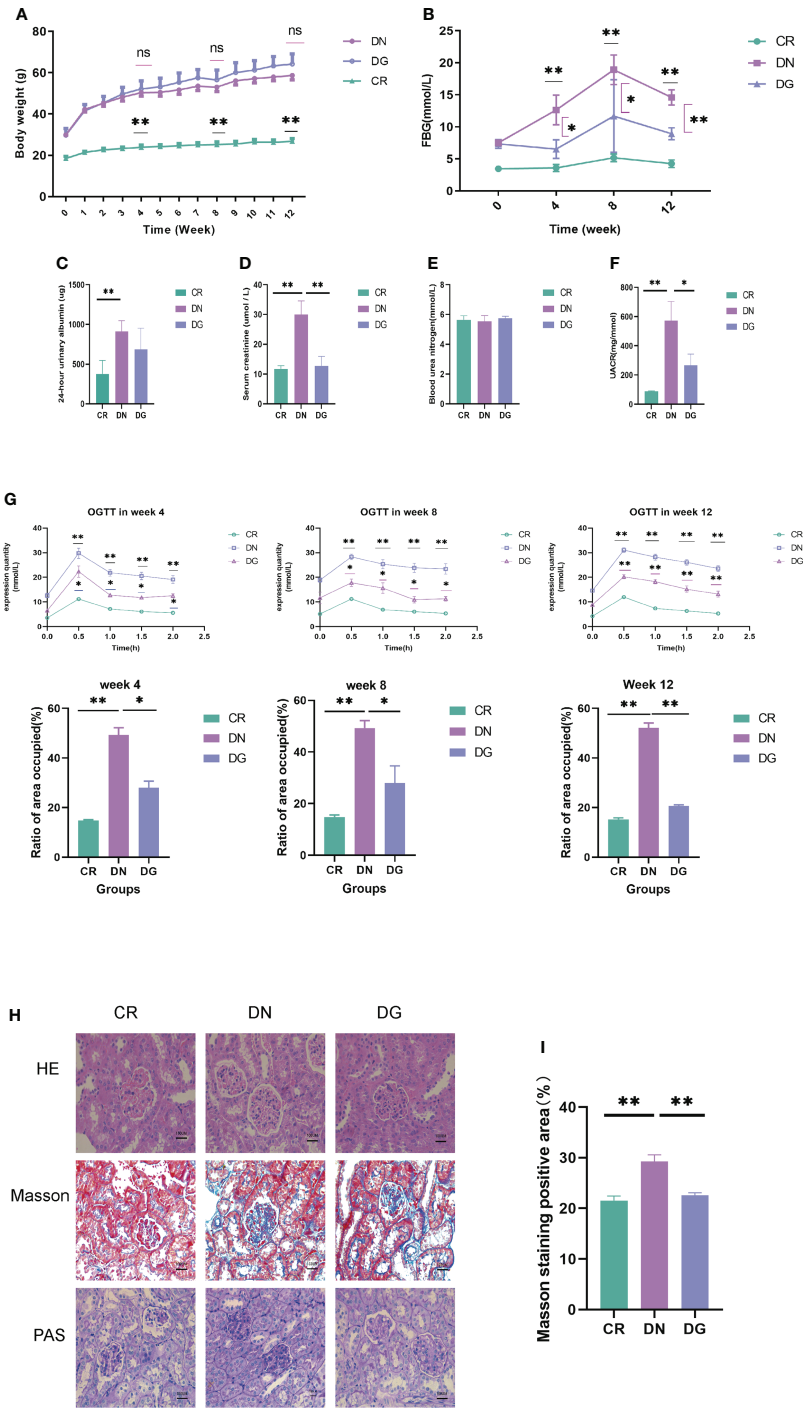

FIGURE 1
Dapagliflozin improved kidney injury in db/db mice. **(A)** The body weights recorded every week (n=6). **(B)** Quantitative analysis of fasting blood glucose (FBG) (n=6). **(C)** Quantitative analysis of 24-hour urinary albuamin (n=4-5). **(D)** Quantitative analysis of serum creatinine (SCR) (n=5). **(E)** Quantitative analysis of blood urea nitrogen (BUN) (n=5). **(F)** Quantitative analysis of urinary albumin/creatinine ratio (UACR) (n=4). **(G)** The levels of OGTT and AUC at week4, week8 and week12 (n=6). **(H-I)** The pathologic changes in kidneys *via* HE, PAS and Masson staining. Data are presented as the mean ± SE. *P < 0.05; **P < 0.001. AUC, Area under the curve; CR, control group; DN, diabetic nephropathy group; DG, dapagliflozin group; OGTT, Oral glucose tolerance test. ns, no significant.

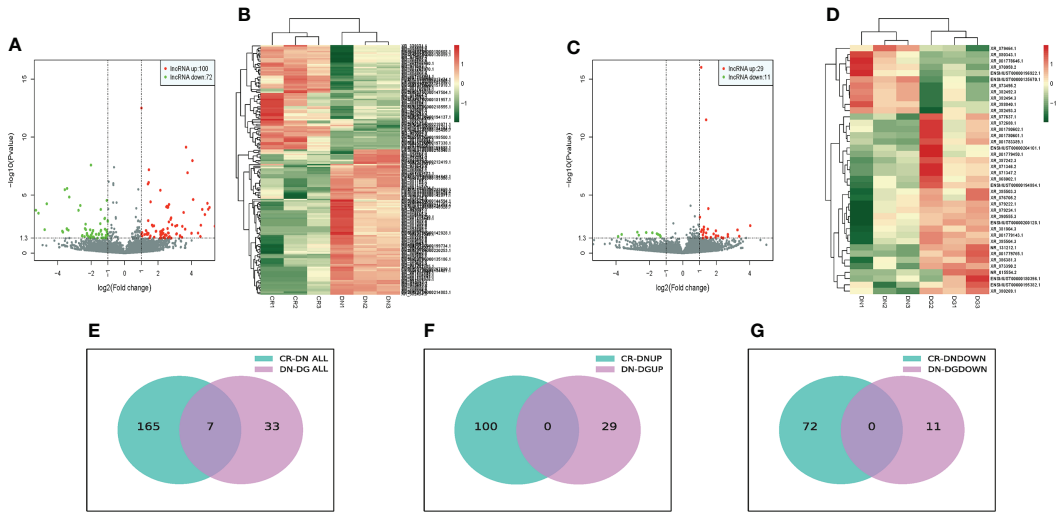

FIGURE 2
Differentially expressed LncRNAs in DN (n=3). **(A, B)** Volcano plots **(A)** and heatmaps **(B)** for comparison between CR and DN. **(C, D)** Volcano plots**(C)** and heatmaps **(D)** for comparison between DN and DG. **(E)** Overlap of the differentially expressed LncRNAs in the comparisons between CR vs DN and DN vs DG. **(F)** Upregulated differentially expressed LncRNAs in the comparisons between CR vs DN and DN vs DG. **(G)** Downregulated differentially expressed LncRNAs in the comparisons between CR vs DN and DN vs DG. CR, control group; DN, diabetic nephropathy group; DG, dapagliflozin group.

significantly expressed in the DG group (152 upregulated and 76 downregulated) (Figures 3E–G). As shown in Venn diagrams, 64 common differentially expressed mRNAs were found in CR vs DN and DN vs DG. The top 10 upregulated and downregulated mRNAs in CR vs DN and DN vs DG respectively was listed in Tables S4 and S5.

The co-expression network of LncRNA-mRNA

We constructed heatmaps to show the expression patterns of LncRNAs and mRNAs in CR, DN and DG groups (Figures 4A, B). Thus, we build a co-expression network using the common differentially expressed LncRNAs and mRNAs in the three groups. We found that 7 differentially expressed LncRNAs were co-expressed with the 63 differentially expressed mRNAs and may have targeted these genes (Figure 4C).

Functional enrichment analysis of the differentially expressed mRNAs and LncRNAs

Potential target genes of 7 common differentially expressed LncRNAs (DELncRNAS) in the two comparisons were predicted bioinformatically. GO analysis revealed that these genes were enriched mainly in pathways such as glycerophospholipid

TABLE 1 The differentially expressed LncRNAs in the three groups.

Gene ID	Gene symbol	Log2 (fold change)		P-Value	
		CR-DN	DN-DG	CR-DN	DN-DG
NR_015554.2	AI506816	-5.535820015	4.037966831	1.10E-06	0.004185984
XR_382492.3	2010203P06Rik	2.788783699	-1.375859426	0.000886101	0.027335057
XR_382493.3	2010203P06Rik	2.654227803	-1.546562094	0.001974919	0.02068988
XR_382494.3	2010203P06Rik	3.538211533	-1.32722677	0.000306679	0.035530862
XR_873495.2	2010203P06Rik	2.755958903	-1.368824543	0.00120733	0.028809256
XR_388840.1	Gm35001	2.637250895	-2.18855647	0.018245622	0.016443863
XR_876705.2	Gm22146	-1.909626787	1.677984089	0.03972669	0.043126027

CR, Control group; DN, diabetic nephropathy group; DG, Dapagliflozin group.

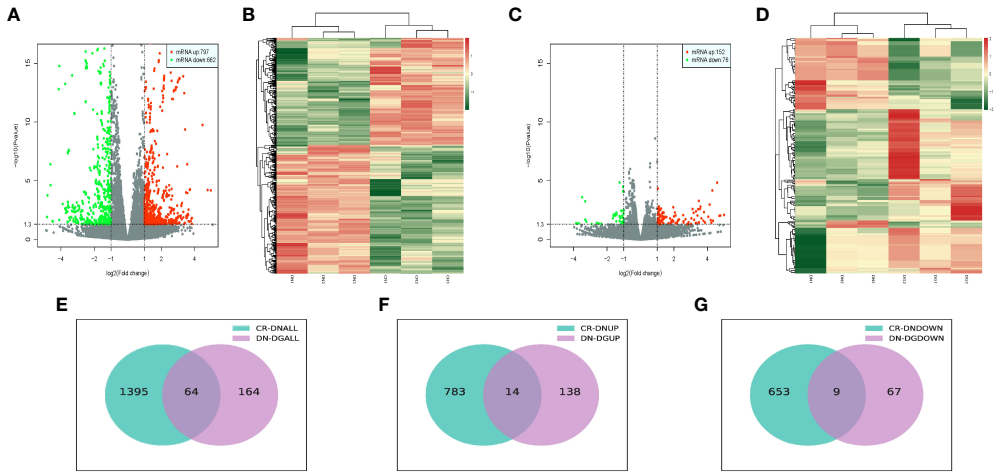

FIGURE 3
Differentially expressed mRNAs in DN (n=3). **(A, B)** Volcano plots **(A)** and heatmaps **(B)** for comparison between CR and DN. **(C, D)** Volcano plots **(C)** and heatmaps **(D)** for comparison between DN and DG. **(E)** Overlap of the differentially expressed mRNAs in the comparisons between CR vs DN and DN vs DG. **(F)** Upregulated differentially expressed mRNAs in the comparisons between CR vs DN and DN vs DG. **(G)** Downregulated differentially expressed mRNAs in the comparisons between CR vs DN and DN vs DG. CR, control group; DN, diabetic nephropathy group; DG, dapagliflozin group.

metabolic process, telomere maintenance, exonuclease activity, etc (Figure 5A). Then, we annotated these DELncRNA-target mRNA genes by KEGG pathway analysis. The results revealed that the genes were evidently enriched in non–homologous end–joining, glutamatergic synapse, sphingolipid signaling pathway (Figure 5B).

Meanwhile, we performed GO and KEGG analysis to annotate the 63 common differentially expressed mRNAs in the two comparisons. GO analysis revealed that these genes were enriched mainly in positive regulation of membrane invagination, regulation of phagocytosis, positive regulation of lipid storage (Figure 5C). KEGG pathway analysis showed that the genes were evidently enriched in PPAR signaling pathway, phagosome, fatty acid degradation, arachidonic acid metabolism, complement and coagulation cascades, etc (Figure 5D).

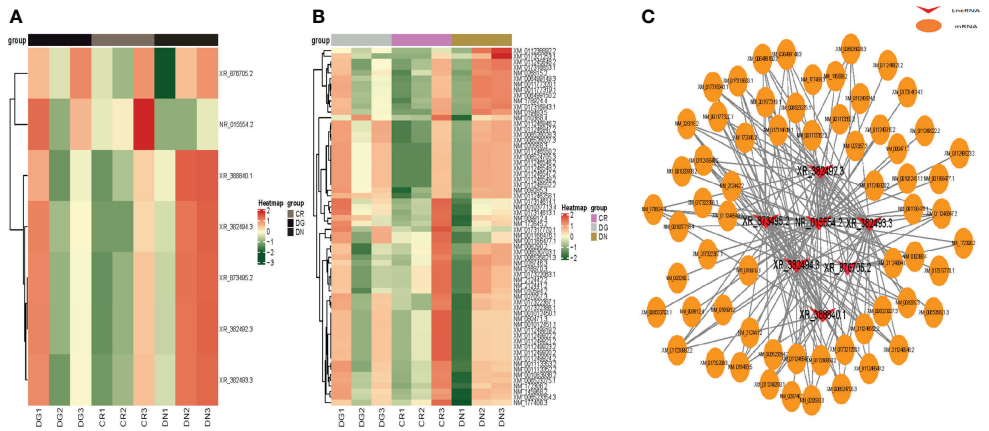

FIGURE 4
Co-expression network of LncRNA-mRNA. **(A, B)** Heatmap showing clustering analysis of differentially expressed LncRNAs **(A)** and mRNAs **(B)** in CR, DN and DG. **(C)** LncRNA-mRNA co-expression network in 7 LncRNAs and 63 mRNAs. CR, control group; DN, diabetic nephropathy group; DG, dapagliflozin group.

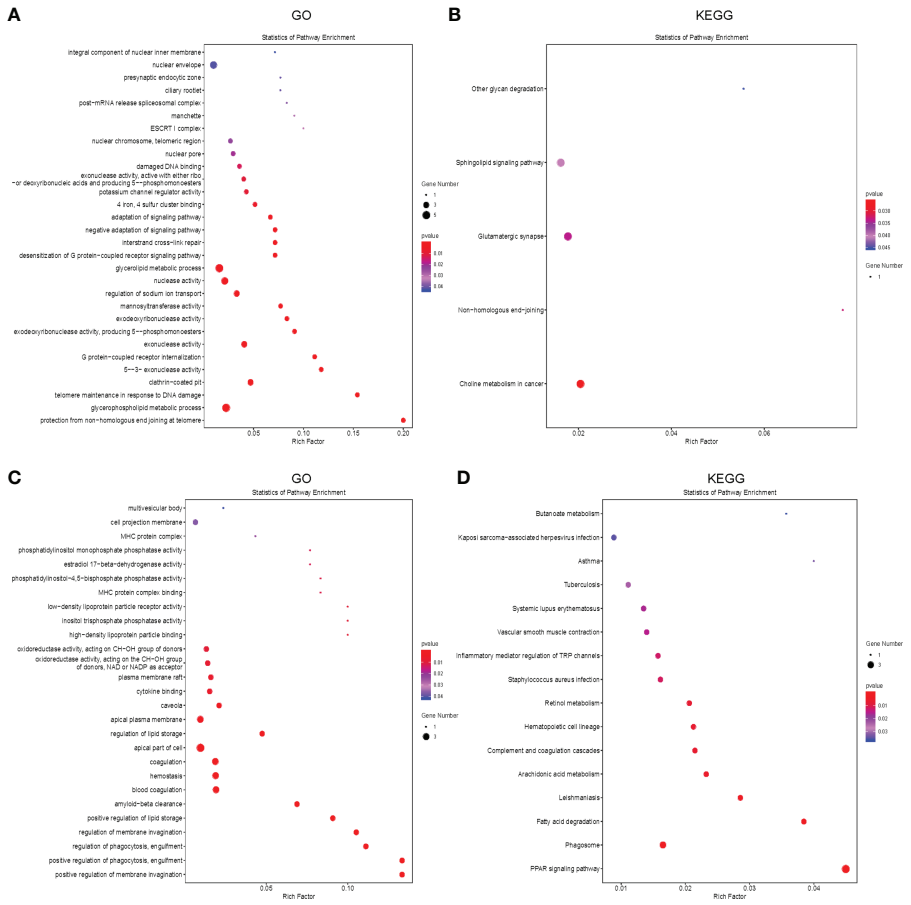

FIGURE 5
Functional enrichment analysis of the differentially expressed mRNAs and LncRNAs. **(A, B)** The bubble plot showing GO analysis **(A)** and KEGG analysis **(B)** for differentially expressed LncRNAs in CR, DN and DG. **(C, D)** The Bubble plot showing GO analysis **(C)** and KEGG analysis **(D)** for differentially expressed mRNAs in CR, DN and DG, CR, control group; DN, diabetic nephropathy group; DG, dapagliflozin group.

Identification of candidate targets of dapagliflozin in the treatment of DN by network pharmacology

Veen diagram showed that 255 genes candidate targets of dapagliflozin were searched out from the drug database (Figure 6A) and 3555 candidate genes of DN were collected from disease databases (Figure 6B). After intersection, a total of 110 overlapping genes were identified (Figure 6C). To estimate the role of the therapeutic target genes, the 110 overlapping genes were used to construct PPI network and were sorted in descending order by degree with the topology parameters of PPI network (Figure 6D). The top 20 core genes were submitted to perform GO and KEGG enrichment analysis, which revealed that these genes were enriched mainly in MAPK signaling, PPAR signaling pathway and PI3k-Akt signaling pathway, etc (Figures 6E, F).

Component- target-pathway network construction

To more accurately identify the mechanisms of dapagliflozin for DN, we performed KEGG enrichment analysis using the 63 mRNAs involved in LncRNA-mRNA co-expression network and the 20 core genes identified by network pharmacology. Pathways that the above two sets of genes are commonly involved in are considered to play important roles. The commonly involved pathways are including TGF-beta signaling pathway, Tuberculosis, Chagas disease (American trypanosomiasis), Leishmaniasis, Pertussis, Viral carcinogenesis, Herpes simplex infection, Staphylococcus aureus infection, Legionellosis, Chemokine signaling pathway, PPAR signaling pathway, Vascular smooth muscle contraction, Toxoplasmosis, Influenza A,Viral myocarditis and Signaling pathways regulating pluripotency of stem cells. Then, we used Cytoscape3.8.2 to

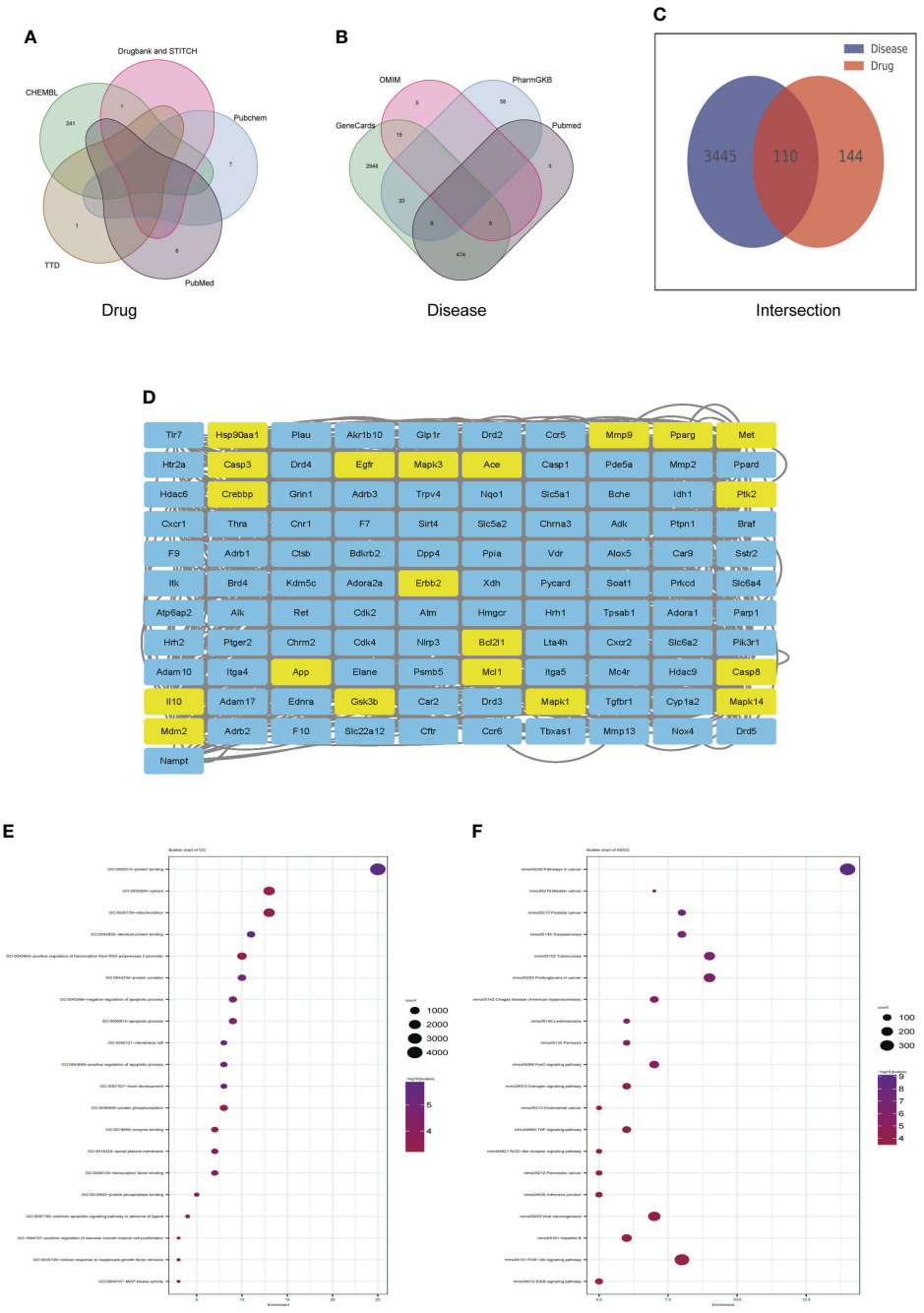

FIGURE 6
Identification of candidate targets of Dapagliflozin in the treatment of DN by network pharmacology. **(A)** The Veen diagram showing candidate targets of dapagliflozin from the drug database. **(B)** The Veen diagram showing candidate targets of DN from disease databases. **(C)** Overlap of the differentially expressed genes between candidate targets of dapagliflozin and DN. **(D)** PPI network of the 110 overlapping genes between candidate targets of dapagliflozin and DN. The top 20 core genes were highlighted in yellow. **(E, F)** GO **(E)** and KEGG **(F)** enrichment analysis of the top 20 core genes. DN, diabetic nephropathy.

construct component-target-pathway network based on the data of KEGG enrichment analysis of RNA Sequencing and Network Pharmacology (Figure 7). We found that CD36, SMAD9, H2-DMB2, CYP4A12a, CYP4A12b, Ccr1, C3, MAPK1, MAPK3, CASP3, PPARG, IL10 might be the key targets for dapagliflozin in treating DN and these genes were evidently enriched in pathways including PPAR signaling pathway, Chemokine signaling pathway, TGF-β signaling pathway, etc.

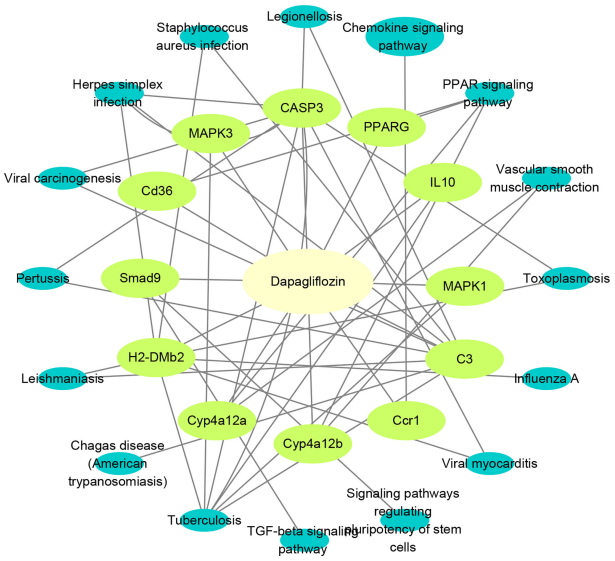

FIGURE 7
Construction of component-target-pathway network. Light yellow represents dapagliflozin, light green represents potential targets and dark blue represents gene-related signaling pathways.

Validation of key LncRNAs and genes by qRT-PCR and western blotting

To verify the RNA sequencing and network pharmacology results, seven LncRNAs and twelve mRNAs were performed by qRT-PCR in the kidneys from the three groups. We found that XR_382492.4, XR_873495.3, XR-388840.1 and XR_382493.3 were markedly upregulated and NR-015554.2, XR_382494.3 and XR-876705.2 were significantly downregulated in DN group compared with CR group. Dapagliflozin can reverse the expression changes of XR_382492.4, XR_873495.3, XR-388840.1, NR-015554.2, XR-382493.3 and XR-876705.2 (Figure 8). Dapagliflozin tended to increase the expression of XR_382494.3, but this effect failed to reach statistical significance.

Meanwhile, mRNA expression of SMAD9, CASP3, H2-DMB2, MAPK1, MAPK3 and C3 were upregulated and

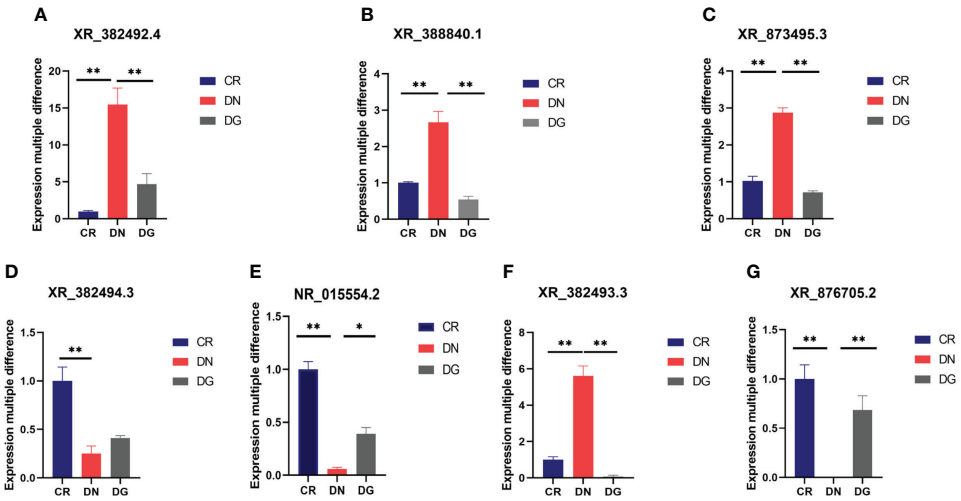

FIGURE 8
(A–G) Validation of key LncRNAs by qRT-PCR (n=6). Data are presented as the mean ± SE. *P < 0.05; **P < 0.001. CR, control group; DN, diabetic nephropathy group; DG, dapagliflozin group.

CYP4A12A, CYP4A12B, CD36, PPARG, and IL-10 were downregulated in DN group compared with CR group. Dapagliflozin can reverse the expression changes of all these genes (Figure 9). CCR1 was decreased in DN group compared with CR group and dapagliflozin tended to increase the expression of CCR1 but it failed to achieve the statistical level. As shown in Figure 10, protein expression of SMAD9, CASP3, MAPK1, MAPK3 and C3 were markedly increased and PPARG, CD36, and IL-10 were significantly decreased in DN group compared with CR group. Dapagliflozin can reverse the expression changes of all these proteins. The results indicated that SMAD9, CASP3, H2-DMB2, MAPK1, MAPK3, C3, CYP4A12A, CYP4A12B, CD36, PPARG, and IL-10 maybe potential targets of Dapagliflozin in DN.

Discussion

DN is the main cause of ESKD worldwide (19). Identifying novel molecular mechanisms and targets underlying DN progression will be beneficial for developing novel therapeutic approaches (20). Dapagliflozin has been shown to have protective effect in cardiomyopathy and kidney disease, especially against complications associated with diabetes (21, 22). Clinical evidence has confirmed that the renoprotective effect of dapagliflozin goes beyond glucosuric effect, which are not fully elucidated. In addition, dapagliflozin can not only improve glycemic control, but also reduce body weight and lower blood pressure. We proposed that dapagliflozin may protect against DN through other unknown effects. Previous studies suggested that dapagliflozin improved albuminuria and tubulointerstitial fibrosis in DN *via* suppressing SGK1 and reversing the T-cell imbalance (23). A new report indicated that dapagliflozin exerts protective effects on DN by reducing cellular senescence and inhibiting oxidative stress (24). However, these studies mainly focused on specific molecular signaling pathways, no studies explored the whole transcriptome changes of dapagliflozin in DN mice. Here, we used RNA sequencing and network pharmacology to systematically disclose the mechanisms of dapagliflozin in the treatment of DN.

Emerging studies have investigated the role of LncRNAs in DN (25–27). However, this is the first study exploring LncRNAs of dapagliflozin in treating DN. We identified 172 differentially expressed LncRNAs in CR vs DN and 40 differentially expressed LncRNAs in DN vs DG. 7 common differentially expressed LncRNAs (NR_015554.2, XR_382492.3, XR_382493.3, XR_382494.3, XR_388840.1, XR_873495.2 and XR_876705.2) were found in the two comparisons, and results of qRT-PCR

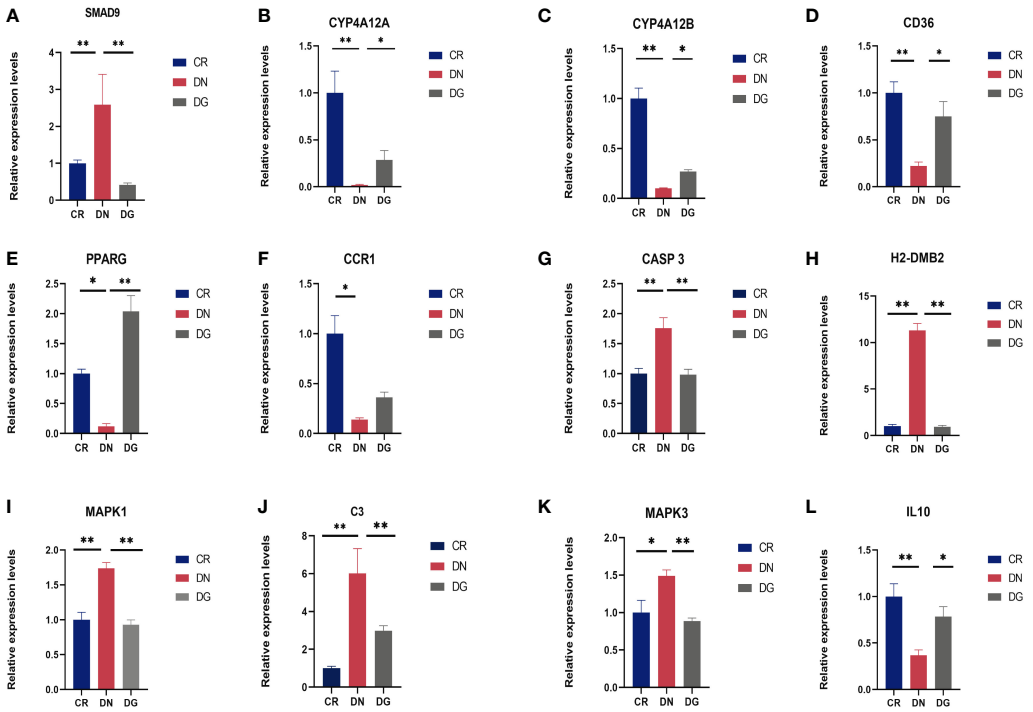

FIGURE 9
(A-L) Validation of key targets by qRT-PCR (n=6). Data are presented as the mean ± SE. *P < 0.05; **P < 0.001. CR, control group; DN, diabetic nephropathy group; DG, dapagliflozin group.

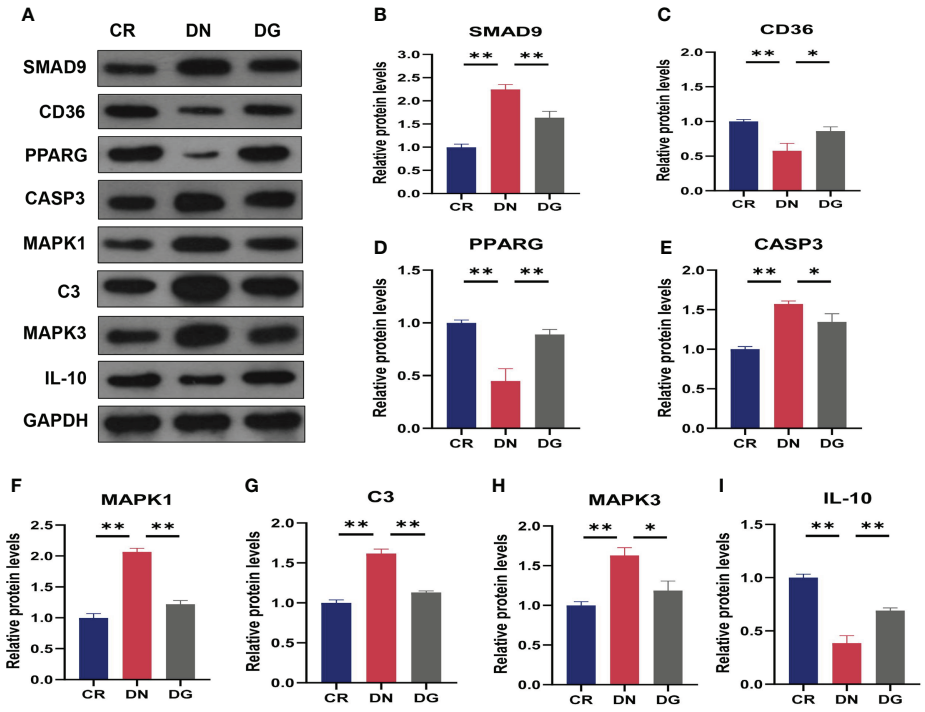

FIGURE 10
Validation of key targets by western blotting (n=3). **(A)** The protein expression of key targets was detected by western blotting. **(B–I)** Densitometry analysis of western blotting. Data are presented as the mean ± SE. *P < 0.05; **P < 0.001. CR, control group; DN, diabetic nephropathy group; DG, dapagliflozin group.

revealed that dapagliflozin can reverse the expression changes of XR_382492.4, XR_873495.3, XR-388840.1, NR-015554.2, XR-382493.3 and XR-876705.2. Of these novel LncRNAs, only NR_015554.2 (LncRNA AI506816) has been reported, which was related with multiparity (28), whereas the current state of evidence for other LncRNAs has so far been unknown. Meanwhile, our data revealed that 63 mRNAs were common differentially expressed in CR vs DN and DN vs DG. Then, we constructed a lncRNA-mRNA co-expression network, which is a powerful tool to predict the function of LncRNA. The co-expression network identified 7 lncRNAs and 63 mRNAs involving in the core co-expression network. These genes were related to PPAR signaling pathway, phagosome, fatty acid degradation, arachidonic acid metabolism, complement and coagulation cascades. A recent study showed that dapagliflozin can enhanced fatty acid metabolism in DN mice (29). Dapagliflozin was demonstrated to ameliorate DN by promoting Crry and inhibiting complement over-activation in diabetic model (30). These reports supported our results.

Furthermore, in order to find the hub genes involved in the protective effect of dapagliflozin in the treatment of DN, we used network pharmacology for predicting the therapeutic targets of dapagliflozin and performed integrated analysis based on the data of RNA sequencing and network pharmacology. We found 110 differentially expressed overlapping genes between candidate targets of dapagliflozin and DN and the top 20 core genes were obtained by PPI network. We further construct component-target-pathway network and collected 11 hub genes including SMAD9, CYP4A12a, CYP4A12b, CD36, PPARG, CASP3, H2-DMB2, MAPK1, C3, MAPK3, IL10, which were mainly enriched in TGF-β signaling pathway, PPAR signaling pathway and chemokine signaling pathway. TGF-β family signaling plays a vital role in the regulation of cell growth, differentiation, and development, especially in fibrosis in many organ systems (31). SMADs are key intracellular transducers which transduces signals from TGF-β family members. SMAD9, also known as SMAD8, was reported to be involved in diabetic renal tubulointerstitial fibrosis (32). A recent study revealed that SMAD9 was highly expressed in the blood of diabetes patients and in streptozotocin-induced rat retinas, which indicated that SMAD9 was closely related with diabetic retinopathy (33). SMAD9 was also reported to be expressed in human kidneys (34). Similarly, our results revealed that SMAD9 was increased in DN mice and dapagliflozin can downregulate the expression of SMAD9, indicating that SMAD9 may be a potential target of dapagliflozin for DN. Peroxisome proliferators-activated receptors (PPARs), a group of nuclear proteins that including

PPAR-alpha, PPAR-beta/delta and PPAR-gamma, have been implicated in the regulation of gene transcription and metabolic processes (35). Studies have demonstrated that members of the cytochrome P-450 4 (CYP4) family have the PPAR response element and can be regulated by PPAR-alpha (36). CYP4 proteins can convert arachidonic acid (AA) to 20-hydroxyeicosatetraenoic acids (20-HETE), which can either reduce albuminuria or cause injury by promoting podocyte apoptosis or tubular hypertrophy (37, 38). In the present study, CYP4A12a and CYP4A12b were found to be decreased in the DN mice and dapagliflozin can increase the expression of the two genes. We speculated that the downregulation of CYP4A12a and CYP4A12b cause reduced synthesis of 20-HETE, leading to impaired kidney function. A previous study indicated that the mRNA levels of CYP4A12a and CYP4A12b are decreased in renal cortex tissues from db/db mice, which is consistent with our results (39). PPAR-gamma (PPARG) plays a critical role in adipogenesis and insulin sensitivity and PPARG polymorphism contributes to the development of DN in diabetic patients (40). Thiazolidinedione (TZD), a high-affinity synthetic ligand for PPARG, has been demonstrated to improve insulin resistance, reduce proteinuria and ameliorate renal function in diabetic nephropathy (41). In addition, studies reported that Pparg null-mice present increased glucosuria, albuminuria, decreased creatinine clearance and mesangial expansion (42).Our data also showed that PPARG was significantly downregulated in the DN mice and dapagliflozin can upregulate the expression of PPARG. Scavenger receptor CD36, also known as fatty acid translocase (FAT), is a surface glycoprotein. It can function in many processes including fatty acid metabolism, apoptosis, angiogenesis, phagocytosis and inflammation and act as a transcriptional regulator of PPARG (43). It has been reported that CD36 can be a plausible prognostic marker for DN (44). Currently, the regulatory effect of CD36 on insulin resistance is still controversial. Studies suggested that overexpression of CD36 can promotes the development of metabolic syndrome and insulin resistance (45), while CD36-deficient patients presented impaired glucose metabolism, insulin resistance and hyperlipidemia (46). Loss of CD36 deficiency can lead to hepatic insulin resistance and impair hepatic insulin signaling in mice fed a low-fat diet (47). A recent study showed that CD36 was highly expressed in renal tubules in mice fed a high-fat diet (48). However, according to our findings, db/db mice presented downregulated expression level of CD36 and dapagliflozin can reverse the expression changes. We speculated the expression levels of CD36 may be affected by different nutritional status, which partly explains CD36 plays a contradictory role in glucose metabolism. The above results indicated that dapagliflozin exerts protective effects on DN through PPAR signaling pathway involving PPARG, CYP4A12a, CYP4A12b and CD36, which have not been previously reported. Significantly, the genes identified by the lncRNA-mRNA co-expression network were also enriched in PPAR signaling pathway, which regulates metabolic homeostasis, lipid, glucose and energy metabolism. Thiazolidinedione, act as PPARG agonist, was limited used in patients with diabetes due to its effect of increasing sodium reabsorption, leading to fluid retention and edema (49). Thus, considering the effect of sodium excreting and activating PPARG, patients with DN may benefit more from combination of dapagliflozin and thiazolidinedione than a single therapy, which was supported by previous studies (50).

In addition, we found that MAPK1, MAPK3, C3, CASP3 and H2-DMB2 were increased in db/db mice, whereas IL-10 were decreased in db/db mice and dapagliflozin can reverse the expression of these genes. Previous studies concluded that dapagliflozin protected against DN and reduced urinary albumin excretion *via* reducing the expression of MAPK signaling pathways (51, 52). Immune inflammation plays a pivotal role in the pathogenesis of DN. Complement C3 was proved to be negatively related to the glomerular filtration rate in patients with DN and could be immune-related biomarkers of DN (53). It has been reported that dapagliflozin can attenuate complement over-activation and upregulate the anti-inflammatory cytokine IL-10 in diabetic mice (30, 54), which consisted with our results again. Recent studies showed that CASP3 was upregulated in diabetic rats and diabetic human kidney tubuli (55, 56). However, there are lack of evidence about relationships between CASP3 and dapagliflozin. H2-DMB2, playing a key role in antigen presentation by MHC class II molecules, has not been studied in DN.

Notably, in order to verify whether these hub genes play the same role in human, we searched human gene-disease databases including DisGeNET, GeneCardSuite and OMIM to screen the genes related with DN. We found that PPARG, CD36, MAPK1, MAPK3, CASP3, C3 and IL10 were related with DN, while the evidence of SMAD9, CYP4A12a, CYP4A12b and H2-DMB2 in DN was absent. Therefore, these results may provide us with new possible mechanisms mediating the pathogenesis of DN and also offer us new potential targets of dapagliflozin for DN.

Although we systematically elucidated the underlying molecular mechanisms of dapagliflozin in the treatment of DN, there were still several limitations in our study. First, the sample size in each group submitted for RNA sequencing was limited. Second, detailed interactions of the co-expressed lncRNAs and mRNAs are needed in future studies. Third, the functions of the hub genes obtained by RNA sequencing and network pharmacology need to be further verified *in vivo* and *in vitro*.

In conclusion, we combined RNA sequencing and network pharmacology to explore the potential mechanisms of dapagliflozin in DN. Our study demonstrated that dapagliflozin might treat DN through regulating TGF-β signaling pathway, PPAR signaling pathway and chemokine signaling pathway by targeting 11 hub genes (SMAD9, PPARG, CD36, CYP4A12A, CYP4A12B,CASP3, H2-DMB2, MAPK1, MAPK3, C3, IL-10). Our research provides new insights into the protective mechanism of dapagliflozin for DN.

Data availability statement

The data presented in the study are deposited in the Sequence Read Archive (SRA) repository, accession numbers SRR19792050, SRR19792049, SRR19792048, SRR19792047, SRR19792046, SRR19792045, SRR19792044, SRR19792043 and SRR19792042.

Ethics statement

The animal study was reviewed and approved by The Animal Experiment Ethics Committee of Jinan University.

Author contributions

YX, XZ, and LC conceived and designed the study; ZB, TX, and TL conducted the experiments and obtained the data; ZC, LY, CZ, and JL analyzed and collated the data; YX and ZB drafted and written the final version of the manuscript. ZB, TX, and TL contributed equally to this work. All authors approved the final version of the manuscript.

Funding

This work was supported by the National Natural Science Foundation of China (no.82074307, no.82174148), the Natural Science Foundation of Guangdong Province, China (no.2018030310451) and Wuxi Municipal Health Commission Scientific Research Fund Youth Project (Q202106).

Conflict of interest

The authors declare that the research was conducted in the absence of any commercial or financial relationships that could be construed as a potential conflict of interest.

Publisher's note

Supplementary material

The Supplementary Material for this article can be found online at: https://www.frontiersin.org/articles/10.3389/fendo.2022.967822/full#supplementary-material

References

1. Saeedi P, Petersohn I, Salpea P, Malanda B, Karuranga S, Unwin N, et al. Global and regional diabetes prevalence estimates for 2019 and projections for 2030 and 2045: Results from the international diabetes federation diabetes atlas, 9(th) edition. *Diabetes Res Clin Pract* (2019) 157:107843. doi: 10.1016/j.diabres.2019.107843

2. Cole JB, Florez JC. Genetics of diabetes mellitus and diabetes complications. *Nat Rev Nephrol* (2020) 16(7):377–90. doi: 10.1038/s41581-020-0278-5

3. Donate-Correa J, Luis-Rodríguez D, Martín-Núñez E, Tagua VG, Hernández-Carballo C, Ferri C, et al. Inflammatory targets in diabetic nephropathy. *J Clin Med* (2020) 9(2):458. doi: 10.3390/jcm9020458

4. Mottl AK, Alicic R, Argyropoulos C, Brosius FC, Mauer M, Molitch M, et al. KDOQI US commentary on the KDIGO 2020 clinical practice guideline for diabetes management in CKD. *Am J Kidney Dis* (2022) 79(4):457–79. doi: 10.1053/j.ajkd.2021.09.010

5. Wright AK, Carr MJ, Kontopantelis E, Leelarathna L, Thabit H, Emsley R, et al. Primary prevention of cardiovascular and heart failure events with SGLT2 inhibitors, GLP-1 receptor agonists, and their combination in type 2 diabetes. *Diabetes Care* (2022) 45(4):909–18. doi: 10.2337/dc21-1113

6. Provenzano M, Pelle MC, Zaffina I, Tassone B, Pujia R, Ricchio M, et al. Sodium-glucose Co-transporter-2 inhibitors and nephroprotection in diabetic patients: More than a challenge. *Front Med (Lausanne).* (2021) 8:654557. doi: 10.3389/fmed.2021.654557

7. Wiviott SD, Raz I, Bonaca MP, Mosenzon O, Kato ET, Cahn A, et al. Dapagliflozin and cardiovascular outcomes in type 2 diabetes. *N Engl J Med* (2019) 380(4):347–57. doi: 10.1056/NEJMoa1812389

8. Heerspink HJL, Stefánsson BV, Correa-Rotter R, Chertow GM, Greene T, Hou FF, et al. Dapagliflozin in patients with chronic kidney disease. *N Engl J Med* (2020) 383(15):1436–46. doi: 10.1056/NEJMoa2024816

9. Fioretto P, Zambon A, Rossato M, Busetto L, Vettor R. SGLT2 inhibitors and the diabetic kidney. *Diabetes Care* (2016) 39 Suppl 2:S165–71. doi: 10.2337/dcS15-3006

10. Sawaf H, Thomas G, Taliercio JJ, Nakhoul G, Vachharajani TJ, Mehdi A. Therapeutic advances in diabetic nephropathy. *J Clin Med* (2022) 11(2):378. doi: 10.3390/jcm11020378

11. Scherer F, Kurtz DM, Diehn M, Alizadeh AA. High-throughput sequencing for noninvasive disease detection in hematologic malignancies. *Blood* (2017) 130 (4):440–52. doi: 10.1182/blood-2017-03-735639

12. Rao DA, Arazi A, Wofsy D, Diamond B. Design and application of single-cell RNA sequencing to study kidney immune cells in lupus nephritis. *Nat Rev Nephrol* (2020) 16(4):238–50. doi: 10.1038/s41581-019-0232-6

13. Mattick JS. Non-coding RNAs: the architects of eukaryotic complexity. *EMBO Rep* (2001) 2(11):986–91. doi: 10.1093/embo-reports/kve230

14. Huang H, Zhang G, Ge Z. lncRNA MALAT1 promotes renal fibrosis in diabetic nephropathy by targeting the miR-2355-3p/IL6ST axis. *Front Pharmacol* (2021) 12:647650. doi: 10.3389/fphar.2021.647650

15. Zhang J, Jiang T, Liang X, Shu S, Xiang X, Zhang W, et al. lncRNA MALAT1 mediated high glucose-induced HK-2 cell epithelial-to-mesenchymal transition and injury. *J Physiol Biochem* (2019) 75(4):443–52. doi: 10.1007/s13105-019-00688-2

16. Li L, Long J, Mise K, Galvan DL, Overbeek PA, Tan L, et al. PGC1α is required for the renoprotective effect of lncRNA Tug1 *in vivo* and links Tug1 with urea cycle metabolites. *Cell Rep* (2021) 36(6):109510. doi: 10.1016/j.celrep.2021.109510

17. Sun SF, Tang PMK, Feng M, Xiao J, Huang XR, Li P, et al. Novel lncRNA Erbb4-IR promotes diabetic kidney injury in db/db mice by targeting miR-29b. *Diabetes* (2018) 67(4):731–44. doi: 10.2337/db17-0816

18. Nogales C, Mamdouh ZM, List M, Kiel C, Casas AI, Schmidt H. Network pharmacology: Curing causal mechanisms instead of treating symptoms. *Trends Pharmacol Sci* (2022) 43(2):136–50. doi: 10.1016/j.tips.2021.11.004

19. Samsu N. Diabetic nephropathy: Challenges in pathogenesis, diagnosis, and treatment. *BioMed Res Int* (2021) 2021:1497449. doi: 10.1155/2021/1497449

20. Dhillon S. Dapagliflozin: A review in type 2 diabetes. *Drugs* (2019) 79 (10):1135–46. doi: 10.1007/s40265-019-01148-3

21. Arow M, Waldman M, Yadin D, Nudelman V, Shainberg A, Abraham NG, et al. Sodium-glucose cotransporter 2 inhibitor dapagliflozin attenuates diabetic cardiomyopathy. *Cardiovasc Diabetol* (2020) 19(1):7. doi: 10.1186/s12933-019-0980-4

22. Nicholson MK, Ghazal Asswad R, Wilding JP. Dapagliflozin for the treatment of type 2 diabetes mellitus - an update. *Expert Opin Pharmacother* (2021) 22(17):2303–10. doi: 10.1080/14656566.2021.1953471

23. Wang D, Zhang Z, Si Z, Yang Y, Li S, Xue Y. Dapagliflozin reverses the imbalance of T helper 17 and T regulatory cells by inhibiting SGK1 in a mouse model of diabetic kidney disease. *FEBS Open Bio* (2021) 11(5):1395–405. doi: 10.1002/2211-5463.13147

24. Kim MN, Moon JH, Cho YM. Sodium-glucose cotransporter-2 inhibition reduces cellular senescence in the diabetic kidney by promoting ketone body-induced NRF2 activation. *Diabetes Obes Metab* (2021) 23(11):2561–71. doi: 10.1111/dom.14503

25. Wen L, Zhang Z, Peng R, Zhang L, Liu H, Peng H, et al. Whole transcriptome analysis of diabetic nephropathy in the db/db mouse model of type 2 diabetes. *J Cell Biochem* (2019) 120(10):17520–33. doi: 10.1002/jcb.29016

26. Jing J, Song L, Zuo D, Li W, Sun Y, Ma X, et al. Transcriptome expression profiles associated with diabetic nephropathy development. *Mol Cell Biochem* (2022) 477(7):1931–46. doi: 10.1007/s11010-022-04420-5

27. Yang H, Zhang Z, Peng R, Zhang L, Liu H, Wang X, et al. RNA-Seq analysis reveals critical transcriptome changes caused by sodium butyrate in DN mouse models. *Biosci Rep* (2021) 41(4):BSR20203005. doi: 10.1042/bsr20203005

28. Liu JL, Zuo RJ, Peng Y, Fu YS. The impact of multiparity on uterine gene expression and decidualization in mice. *Reprod Sci* (2016) 23(5):687–94. doi: 10.1177/1933719115612131

29. Zou M, Chen Y, Zheng Z, Sheng S, Jia Y, Wang X, et al. High-salt attenuates the efficacy of dapagliflozin in tubular protection by impairing fatty acid metabolism in diabetic kidney disease. *Front Pharmacol* (2021) 12:741087. doi: 10.3389/fphar.2021.741087

30. Chang DY, Li XQ, Chen M, Zhao MH. Dapagliflozin ameliorates diabetic kidney disease *via* upregulating crry and alleviating complement over-activation in db/db mice. *Front Pharmacol* (2021) 12:729334. doi: 10.3389/fphar.2021.729334

31. Chung JY, Chan MK, Li JS, Chan AS, Tang PC, Leung KT, et al. TGF-β signaling: From tissue fibrosis to tumor microenvironment. *Int J Mol Sci* (2021) 22 (14):7575. doi: 10.3390/ijms22147575

32. Xiao Y, Jiang X, Peng C, Zhang Y, Xiao Y, Liang D, et al. BMP-7/Smads-induced inhibitor of differentiation 2 (Id2) upregulation and Id2/Twist interaction was involved in attenuating diabetic renal tubulointerstitial fibrosis. *Int J Biochem Cell Biol* (2019) 116:105613. doi: 10.1016/j.biocel.2019.105613

33. Dong L, Zhang Z, Liu X, Wang Q, Hong Y, Li X, et al. RNA Sequencing reveals BMP4 as a basis for the dual-target treatment of diabetic retinopathy. *J Mol Med (Berl).* (2021) 99(2):225–40. doi: 10.1007/s00109-020-01995-8

34. Fagerberg L, Hallström BM, Oksvold P, Kampf C, Djureinovic D, Odeberg J, et al. Analysis of the human tissue-specific expression by genome-wide integration of transcriptomics and antibody-based proteomics. *Mol Cell Proteomics.* (2014) 13 (2):397–406. doi: 10.1074/mcp.M113.035600

35. Sanjay, Sharma A, Lee HJ. Role of phytoconstituents as PPAR agonists: Implications for neurodegenerative disorders. *Biomedicines* (2021) 9(12):1914. doi: 10.3390/biomedicines9121914

36. Hardwick JP, Osei-Hyiaman D, Wiland H, Abdelmegeed MA, Song BJ. PPAR/RXR regulation of fatty acid metabolism and fatty acid omega-hydroxylase (CYP4) isozymes: Implications for prevention of lipotoxicity in fatty liver disease. *PPAR Res* (2009) 2009:952734. doi: 10.1155/2009/952734

37. Gangadhariah MH, Luther JM, Garcia V, Paueksakon P, Zhang MZ, Hayward SW, et al. Hypertension is a major contributor to 20-hydroxyeicosatetraenoic acid-mediated kidney injury in diabetic nephropathy. *J Am Soc Nephrol* (2015) 26(3):597–610. doi: 10.1681/asn.2013090980

38. Eid AA, Gorin Y, Fagg BM, Maalouf R, Barnes JL, Block K, et al. Mechanisms of podocyte injury in diabetes: role of cytochrome P450 and NADPH oxidases. *Diabetes* (2009) 58(5):1201–11. doi: 10.2337/db08-1536

39. Wang M, Yao D, Wang S, Yan Q, Lu W. Long non-coding RNA ENSMUST00000147869 protects mesangial cells from proliferation and fibrosis induced by diabetic nephropathy. *Endocrine* (2016) 54(1):81–92. doi: 10.1007/s12020-016-0950-5

40. Liu L, Zheng T, Wang F, Wang N, Song Y, Li M, et al. Pro12Ala polymorphism in the PPARG gene contributes to the development of diabetic nephropathy in Chinese type 2 diabetic patients. *Diabetes Care* (2010) 33(1):144–9. doi: 10.2337/dc09-1258

41. Yang J, Zhou Y, Guan Y. PPARγ as a therapeutic target in diabetic nephropathy and other renal diseases. *Curr Opin Nephrol Hypertens* (2012) 21 (1):97–105. doi: 10.1097/MNH.0b013e32834de526

42. Toffoli B, Gilardi F, Winkler C, Soderberg M, Kowalczuk L, Arsenijevic Y, et al. Nephropathy in pparg-null mice highlights PPARγ systemic activities in metabolism and in the immune system. *PloS One* (2017) 12(2):e0171474. doi: 10.1371/journal.pone.0171474

43. Maréchal L, Laviolette M, Rodrigue-Way A, Sow B, Brochu M, Caron V, et al. The CD36-PPARγ pathway in metabolic disorders. *Int J Mol Sci* (2018) 19 (5):1529. doi: 10.3390/ijms19051529

44. Shiju TM, Mohan V, Balasubramanyam M, Viswanathan P. Soluble CD36 in plasma and urine: A plausible prognostic marker for diabetic nephropathy. *J Diabetes Complications.* (2015) 29(3):400–6. doi: 10.1016/j.jdiacomp.2014.12.012

45. Wilson CG, Tran JL, Erion DM, Vera NB, Febbraio M, Weiss EJ. Hepatocyte-specific disruption of CD36 attenuates fatty liver and improves insulin sensitivity in HFD-fed mice. *Endocrinology* (2016) 157(2):570–85. doi: 10.1210/en.2015-1866

46. Yamashita S, Hirano K, Kuwasako T, Janabi M, Toyama Y, Ishigami M, et al. Physiological and pathological roles of a multi-ligand receptor CD36 in atherogenesis; insights from CD36-deficient patients. *Mol Cell Biochem* (2007) 299 (1-2):19–22. doi: 10.1007/s11010-005-9031-4

47. Yang P, Zeng H, Tan W, Luo X, Zheng E, Zhao L, et al. Loss of CD36 impairs hepatic insulin signaling by enhancing the interaction of PTP1B with IR. *FASEB J* (2020) 34(4):5658–72. doi: 10.1096/fj.201902777RR

48. Huang CC, Chou CA, Chen WY, Yang JL, Lee WC, Chen JB, et al. Empagliflozin ameliorates free fatty acid induced-lipotoxicity in renal proximal tubular cells *via* the PPARγ/CD36 pathway in obese mice. *Int J Mol Sci* (2021) 22 (22):12408. doi: 10.3390/ijms222212408

49. Nissen SE, Wolski K. Effect of rosiglitazone on the risk of myocardial infarction and death from cardiovascular causes. *N Engl J Med* (2007) 356 (24):2457–71. doi: 10.1056/NEJMoa072761

50. Han E, Shin E, Kim G, Lee JY, Lee YH, Lee BW, et al. Combining SGLT2 inhibition with a thiazolidinedione additively attenuate the very early phase of diabetic nephropathy progression in type 2 diabetes mellitus. *Front Endocrinol (Lausanne)* (2018) 9:412. doi: 10.3389/fendo.2018.00412

51. Chen G, Wang H, Zhang W, Zhou J. Dapagliflozin reduces urinary albumin excretion by downregulating the expression of cAMP, MAPK, and cGMP-PKG signaling pathways associated genes. *Genet Test Mol Biomark* (2021) 25(10):627–37. doi: 10.1089/gtmb.2021.0086

52. Song Y, Guo F, Liu Y, Huang F, Fan X, Zhao L, et al. Identification of circular RNAs and functional competing endogenous RNA networks in human proximal tubular epithelial cells treated with sodium-glucose cotransporter 2 inhibitor dapagliflozin in diabetic kidney disease. *Bioengineered* (2022) 13 (2):3911–29. doi: 10.1080/21655979.2022.2031391

53. Wang Y, Zhao M, Zhang Y. Identification of fibronectin 1 (FN1) and complement component 3 (C3) as immune infiltration-related biomarkers for diabetic nephropathy using integrated bioinformatic analysis. *Bioengineered* (2021) 12(1):5386–401. doi: 10.1080/21655979.2021.1960766

54. Liu L, Luo H, Liang Y, Tang J, Shu Y. Dapagliflozin ameliorates STZ-induced cardiac hypertrophy in type 2 diabetic rats by inhibiting the calpain-1 expression and nuclear transfer of NF-κB. *Comput Math Methods Med* (2022) 2022:3293054. doi: 10.1155/2022/3293054

55. Zhang Q, Xiao X, Zheng J, Li M, Yu M, Ping F, et al. Shenqi jiangtang granule ameliorates kidney function by inhibiting apoptosis in a diabetic rat model. *Evid. Based Complement Alternat Med* (2019) 2019:3240618. doi: 10.1155/2019/3240618

56. Das RR, Rahman MA, Al-Araby SQ, Islam MS, Rashid MM, Babteen NA, et al. The antioxidative role of natural compounds from a green coconut mesocarp undeniably contributes to control diabetic complications as evidenced by the associated genes and biochemical indexes. *Oxid Med Cell Longev* (2021) 2021:9711176. doi: 10.1155/2021/9711176

frontiers | Frontiers in Endocrinology

TYPE Original Research
PUBLISHED 26 September 2022
DOI 10.3389/fendo.2022.1004564

OPEN ACCESS

EDITED BY
Chunjie Jiang,
University of Pennsylvania,
United States

REVIEWED BY
Baochen Fang,
North Dakota State University,
United States
Jinyang Cai,
Virginia Commonwealth University,
United States
Xiangxiang Hu,
University of North Carolina at Chapel Hill, United States

*CORRESPONDENCE
Oksana Maksymchuk
o.v.maksymchuk@imbg.org.ua;
mksusha@gmail.com

†These authors have contributed equally to this work and share first authorship

SPECIALTY SECTION
This article was submitted to Diabetes: Molecular Mechanisms, a section of the journal Frontiers in Endocrinology

RECEIVED 27 July 2022
ACCEPTED 30 August 2022
PUBLISHED 26 September 2022

CITATION
Maksymchuk O, Shysh A and Stroy D (2022) Treatment with omega-3 PUFAs does not increase the risk of CYP2E1-dependent oxidative stress and diabetic liver pathology. *Front. Endocrinol.* 13:1004564. doi: 10.3389/fendo.2022.1004564

Treatment with omega-3 PUFAs does not increase the risk of CYP2E1-dependent oxidative stress and diabetic liver pathology

Oksana Maksymchuk[1*†], Angela Shysh[2†] and Dmytro Stroy[2]

[1]Department of Molecular Oncogenetics, Institute of Molecular Biology and Genetics, National Academy of Sciences of Ukraine, Kyiv, Ukraine, [2]Department of General and Molecular Pathophysiology, Bogomoletz Institute of Physiology, National Academy of Sciences of Ukraine, Kyiv, Ukraine

An increase in CYP2E1 expression is a key factor in the development of diabetic oxidative liver damage. Long-term treatment with omega-3 PUFAs, which are CYP2E1 substrates, may affect CYP2E1 expression in the liver. In this work, we performed Western blot analysis, biochemical methods, and microscopic ultrastructural studies of the liver in a streptozotocin-induced rat model of type 1 diabetes to investigate whether long-term treatment with omega-3 PUFAs could induce CYP2E1-dependent oxidative stress and diabetic liver pathology. Significant hyperglycemia and lack of natural weight gain were observed in the diabetic rats compared to non-diabetic controls. A 2.5-fold increase in CYP2E1 expression (protein content and activity) was also observed in the diabetic rats. In addition, signs of oxidative stress were found in the liver of the diabetic rats. A significant increase in transaminases and GGT level in blood serum was also observed, which could indicate marked destruction of liver tissue. Diabetic dyslipidemia (increased triacylglycerol levels and decreased HDL-C levels) was found. Treatment of the diabetic animals with an omega-3-enriched pharmaceutical composition of PUFAs had no effect on CYP2E1 levels but contributed to a two-fold decrease in enzyme activity. The intensity of lipid peroxidation also remained close to the diabetic group. However, at the same time, antioxidant protection was provided by induction of antioxidant enzyme activity. Examination of the liver ultrastructure revealed no characteristic signs of diabetic pathology. However, omega-3 PUFAs did not normalize blood glucose levels and serum lipid profile. Thus, long-term treatment of diabetic rats with omega-3 PUFAs does not increase the risk of CYP2E1-dependent oxidative stress and development of liver pathology but prevents some diabetic ultrastructural damage to hepatocytes.

KEYWORDS

omega-3 PUFAs, CYP2E1, oxidative stress, diabetes, liver

10.3389/fendo.2022.1004564

Introduction

Diabetes mellitus is one of the most common endocrine diseases in people of all ages around the world. Today, the problem of widespread prevalence of this disease among young people is particularly relevant. Diabetes mellitus is the cause of development and progression of pathology of systems and organs, including liver. In patients with type 2 diabetes mellitus, severe liver disease is often the cause of death (1). Unlike type 2 diabetes, type 1 diabetic liver disease develops slowly and is often asymptomatic. At the same time, an increase in liver-specific enzymes (gamma-glutamyl transferase (GGT), alanine aminotransferase (ALT), aspartate aminotransferase (AST)) is detected in the blood serum of patients, which may indicate the onset of liver pathology (2). The development of liver pathology in type 1 diabetics has been demonstrated in animal models, particularly in our recent work, which showed a sharp increase in liver-specific enzymes in blood serum, significant ultrastructural disturbances, and evidence of oxidative stress in the liver (3).

It is well known that oxidative stress is one of the main mechanisms for the development of diabetes mellitus. It has been shown that cytochrome P450 2E1 (CYP2E1) is the main source of reactive oxygen species (ROS) formation in the liver and that an increase in the expression of this enzyme is one of the key factors for the development of oxidative stress in the liver (4). It was found that oxidative stress mediated by the ROS generated by CYP2E1 damages hepatocytes by peroxidation of cellular macromolecules, namely, lipid peroxidation, protein carbonylation, and oxidative damage to DNA. This leads to an increase in apoptotic processes in hepatocytes and liver fibrosis. CYP2E1-dependent oxidative processes can lead to inhibition of lipid excretion processes and their accumulation in liver cells, as well as the development of fatty dystrophy (4). In addition, increased levels of circulating ketone bodies and acetone (substrates of CYP2E1) in the blood may cause an increase in CYP2E1 in the diabetic liver, leading to the development of insulin resistance. Insulin resistance, in turn, contributes to the maintenance of high levels of CYP2E1 and the progression of oxidative damage in hepatocytes (5). Insulin resistance also causes increased gluconeogenesis (6), and CYP2E1 plays a leading role in these processes. This contributes to an increase in glucose levels in liver cells and the development of hyperglycogenosis. In addition, ROS causes an increase in the expression of cytokines and stimulates inflammatory processes in the liver (7). Through the oxidation of fatty acids, CYP2E1 is also involved in *de novo* lipogenesis in fatty liver, whereby an interaction between CYP2E1 and PPARα-mediated fatty acid homeostasis has been demonstrated (8). The leading role of CYP2E1 in enhancing apoptotic processes and the development of liver fibrosis has been demonstrated (9). The demonstrated relationship between oxidative stress and the development of diabetic pathology provides a scientific basis for investigating the potential of using various natural compounds with antioxidant properties for the prevention and treatment of diabetic disease.

The antioxidant properties of omega-3 polyunsaturated fatty acids (PUFAs) have been demonstrated in animal disease models and in patients with cardiopathology and visceral organ pathology (10, 11). It should be noted that these compounds are substrates for CYP2E1 and may contribute to the accumulation of this protein in cells, which may increase the risk of oxidative stress. This should be considered when taking these compounds long-term, especially in diseases associated with high expression of CYP2E1, such as diabetic liver (4). In this work, we investigated the effect of long-term consumption of omega-3-enriched pharmaceutical composition of PUFAs on the level of CYP2E1 expression as a key factor in the initiation and development of liver pathology in diabetes mellitus. Prooxidant and antioxidant processes were also investigated, and the effect of omega-3 PUFAs on the ultrastructure of hepatocytes during the development of experimental diabetes was examined.

Materials and methods

Animal care and streptozotocin-induced diabetic rat model

Male Wistar rats (2 months old) were maintained in animal cages with free access to food and water on a 12/12-h light/dark cycle and room temperature. All animals were fed a standard diet. The non-diabetic control group included intact rats. Type 1 diabetes was induced by a single intraperitoneal injection of streptozotocin (STZ) at a dose of 50 mg/kg b.w.

The studies were conducted on three groups of animals: six non-diabetic control rats, six STZ-diabetic rats, and six STZ-diabetic rats treated with the pharmaceutical drug EPADOL (0.1 ml/100 g b.w. per day) purchased from Kyiv Vitamin Factory. EPADOL is the omega-3-enriched pharmaceutical composition of PUFAs. EPADOL contains ethyl esters of omega-3 PUFAs: 300 mg eicosapentaenoic acid (EPA) and 200 mg docosahexaenoic acid (DHA) per 1 ml. Thus, each animal received approximately 30 mg EPA and 20 mg DHA esters per 100 g b.w. per day.

STZ-diabetic rats were administered EPADOL by oral gavage once daily in the morning starting on the third day after STZ injection and for a period of 4 weeks. Blood glucose levels of all rats were checked three times: before injection of STZ, on the third day after injection (start of the experiment), and on the 28th day of the experiment (end of the experiment). A blood glucose level greater than 14 mmol/l on the third day after STZ injection was considered to indicate diabetes. Blood serum glucose levels were determined with an automated biochemical analyzer (Prestige 24i, Tokyo Boeki, Japan). The rats were decapitated under sodium pentobarbital anesthesia (60

mg/kg b.w.) at the end of the experiment. All manipulations of laboratory animals were performed in accordance with the European Convention for the Protection of Vertebrate Animals used for Experimental and other Scientific Purposes (Strasbourg, 1986). The protocol was approved by the Local Committee on Bioethics (registration number: 0114U007233).

Western blot analysis and protein measurement

Preparation of liver samples for Western blot analysis and measurement of CYP2E1 protein levels were performed as previously described (12). CYP2E1 was identified using anti-CYP2E1 antibodies produced in Rabbit (Sigma-Aldrich, USA). The beta-actin (loading control) were visualized by mouse anti-beta-actin antibodies (Sigma-Aldrich, USA). Western blot analysis was carried out according to the manufacturer's instruction for the use of antibodies. The treatment of membranes with secondary antibodies (Sigma-Aldrich, USA) was followed by chemiluminescence detection according to manufacturers' instructions. Western blots were visualized and calculated using the ChemiDoc XRS+ system with Image Lab software (Bio-Rad, USA). Relative protein levels were calculated by comparing CYP2E1 levels with beta-actin levels and expressed as relative units.

Measurement of monooxygenase activity of CYP2E1 in liver microsomes

Liver microsomes were obtained, and the p-nitrophenol (PNP) hydroxylase activity of CYP2E1 in microsomes was determined as previously described (3). Liver microsomes were obtained by ultracentrifugation at 100,000g for 60 min at 4°C. After ultracentrifugation, the microsomal pellet was suspended in storage buffer containing 100 mM Tris–HCl, pH 6.8, and 20% glycerol and aliquots were frozen at -70°C until needed. The reaction mixture for the measurement of the activity of CYP2E1 had the composition 1.0 mg of microsomal protein, 200 mM PNP (Sigma-Aldrich, USA) in 0.1 M potassium phosphate buffer (pH 6.8), and 1.0 mM ascorbic acid. The mixture was preincubated for 5 min at 37°C, and reaction was carried out with 1 mM NADPH (Sigma-Aldrich, USA) for 2 min at 37°C. The p-nitrocatechol (PNC) formed from PNP was detected by spectrophotometric measurement with absorbance of 546 nm. CYP2E1 activity values were expressed as nmol of p-nitrocatechol per minute per milligram of microsomal protein.

Oxidative stress markers

Levels of lipid peroxidation (LPO), catalase, and superoxide dismutase (SOD) in liver tissue were determined as previously described (12). The level of LPO was determined in liver homogenates by assessing the level of malondialdehyde (MDA) as the main product of the reaction between thiobarbituric acid and lipid peroxides. Catalase activity was measured by hydrogen peroxide (H_2O_2) degradation. The reaction mixture consisted of 0.25% tissue homogenate, and 0.03% H_2O_2 (Sigma-Aldrich, USA) was incubated at 37°C for 10 min. The residual H_2O_2 was determined by adding ammonium molybdate and measured spectrophotometrically at 410 nm. SOD was assayed using nicotinamide adenine dinucleotide and phenazine methosulfate reagents for the reduction of nitro blue tetrazolium salt into blue-colored formazan measured spectrophotometrically at 560 nm.

The MDA values were expressed as mkmol per milligram of protein. The values of enzyme activities were expressed as U/mg protein (one unit of catalase activity means the amount of enzyme degrading 1 mkmol H_2O_2 per minute, one unit of SOD activity – the amount of enzyme oxidizing 1 nmol NADH per minute).

Electron microscopic studies of rat livers

Preparation of liver tissues for microscopic studies of the ultrastructure of the liver was performed as previously described (3). For electron microscopic examination, 40–60-nm-thick ultrathin sections were contrasted with 1% uranyl acetate and lead citrate solution according to the method of Reynolds. The studies were performed using an electron microscope JEM 100CX (JEOL, Japan).

Measurement of serum transaminases, gamma-glutamyl transferase levels, and lipid profile

The levels of activity of ALT, AST, and GGT in blood serum are useful biomarkers for liver pathology. A lipid profile is a test that measures the amount of total cholesterol, triacylglycerol (TAG), low-density lipoprotein cholesterol (LDL-C), and high-density lipoprotein cholesterol (HDL-C) in blood serum. Blood serum was obtained as previously described (3). The levels of activity of the enzymes and a lipid profile in blood serum were measured using an automated biochemical analyzer (Tokyo Boeki Prestige 24i, Japan, and HTI Biochem FC-200, USA).

Statistical analysis

Statistical analysis was performed using Status software (http://status-please.herokuapp.com). Data were tested for normal distribution with Shapiro–Wilk test. Dispersion equality was tested using Levine test. Tukey-HSD test was

used for multiple comparisons. Differences in means between groups were tested using one-way ANOVA and t-test. Statistically significant results were considered at $p < 0.05$. Results are presented as mean ± standard deviation (SD).

Results

Blood glucose levels and body weight of animals

All animals had physiological body weight values at the beginning of the experiment. At the end of the experiment, body weight values increased in the control group (27% compared to the time of the start of the experiment, $p = 0.002$), whereas the values remained unchanged in the diabetic group (Table 1).

Before the start of the experiment, the blood glucose levels of all intact animals were within the physiological range (approximately 8 mmol/l). In the diabetic group, a significant increase in blood glucose levels (three-fold compared to the intact control group, $p = 0.001$) was observed on the third day after injection of STZ. At the end of the experiment, glucose levels were four times higher than in the intact control ($p = 0.001$) (Table 1).

Treatment with omega-3 PUFAs did not decrease glucose levels in the diabetic rats. These levels remained elevated by more than 3.5-fold compared with non-diabetic controls ($p = 0.001$) (Table 1). No changes in body weight were observed in the diabetic rats administered with omega-3 PUFAs during the experiment (Table 1).

CYP2E1 activity and protein levels in the liver

A 2.5-fold increase in CYP2E1 protein level was observed in the liver of STZ-diabetic rats compared to the non-diabetic control ($p = 0.030$) (Figure 1). It was also found that an increase in the enzyme level resulted in a more than two-fold increase in its monooxygenase activity ($p = 0.001$) (Figure 2).

It was found that administration of omega-3 PUFAs to diabetic rats did not result in a significant change in CYP2E1 levels compared to the STZ-diabetic group ($p = 0.388$) (Figure 1). At the same time, CYP2E1 activity was significantly decreased (two-fold) compared to the diabetic group ($p = 0.001$) and approached the levels of the non-diabetic control group ($p = 0.192$) (Figure 2).

Oxidative stress markers in the liver of STZ-induced diabetic rats

Previously, it was shown that an increase in CYP2E1 expression can lead to the development of oxidative stress in cells (4). We found the signs of this stress in the liver of experimental diabetic animals. A 1.9-fold increase in malondialdehyde levels (*diabetic vs. control*, $p = 0.008$) was observed, which may indicate an intensification of lipid peroxidation processes. At the same time, a depletion of the antioxidant system was observed. Specifically, catalase and SOD activities were decreased 2.8-fold and 1.8-fold, respectively, in the livers of diabetic animals compared to non-diabetic controls, but for SOD there were no statistically significant data (catalase, $p = 0.015$; SOD, $p = 0.312$) (Figure 3).

It was found that treatment with omega-3 PUFAs did not decrease peroxide processes, which remained close to the diabetic group. At the same time, the levels of catalase and SOD activity increased by 2.4-fold and 8-fold, respectively, compared to the diabetic group, but for catalase there were no statistically significant data (catalase, $p = 0.062$; SOD, $p = 0.001$). Catalase activity remained at the control level, and the SOD activity was 4.5-fold higher than in the non-diabetic control group ($p = 0.001$). Thus, no signs of oxidative stress were detected in the livers of diabetic rats consuming omega-3 PUFAs (Figure 3).

Electron microscopic studies of the livers of experimental animals

In our recent study, the structural characteristics of the livers of intact as well as STZ-diabetic male Wistar rats were described. No signs of liver pathology were detected in the liver samples of the intact rats (3). At the same time, we found significant ultrastructural changes (structural and functional damage to organelles, especially mitochondria, as well as signs of

TABLE 1 Body weight and glucose levels in the blood of the experimental animals.

Animals	Body weight, g		Blood glucose levels, mmol/L	
	Start of experiment	End of experiment	Start of experiment	End of experiment
Non-diabetic rats	172.0 ± 17.175	218.0 ± 14.404*	8.08 ± 0.228	8.14 ± 0.329
STZ-diabetic rats	162.14 ± 11.495	162.86 ± 24.640	25.91 ± 3.765 ◆	31.91 ± 2.042 ◆
STZ-diabetic rats administered with omega 3 PUFAs	178.83 ± 9.806	181.17 ± 18.280	22.97 ± 1.663 ◆	29.02 ± 2.941 ◆

Values are means ± SD, n = 6 rats in each group. *p ≤ 0.01 compared to the start of the experiment (Student's t-test), ◆p ≤ 0.001 compared to the nondiabetic group (one-way ANOVA).

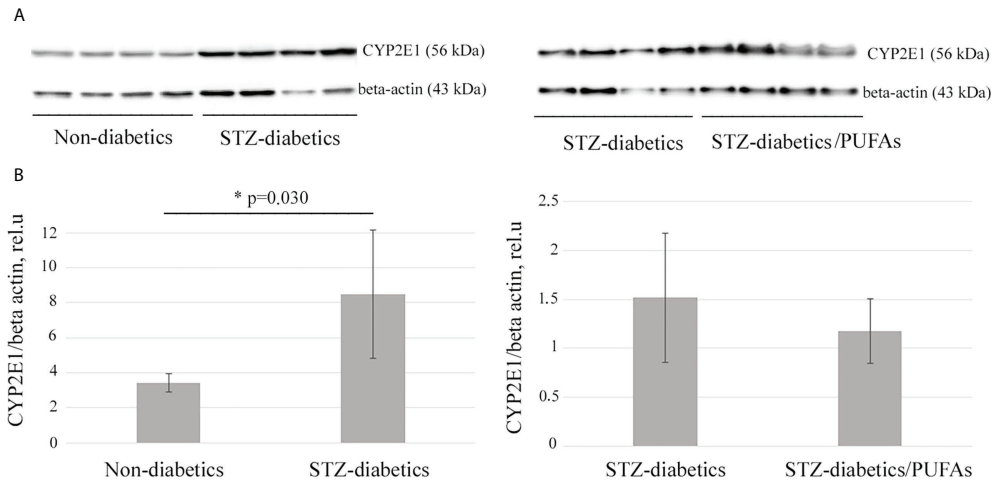

FIGURE 1
CYP2E1 protein levels in the liver of experimental rats. **(A)** Western blot analysis of total liver lysates probed with specific anti-CYP2E1 antibodies. Beta-actin is a loading control. **(B)** Quantification of Western blotting results. *p-values < 0.05 were considered statistically significant (Student's t-test). Means ± SD (n = 4 in each group).

disturbances in metabolic processes, including fat dystrophy) in the livers of the diabetic animals (3).

In this work, we investigated the ultrastructural features of liver tissue from diabetic rats treated with omega-3 PUFAs. We found a marked granularity of the endoplasmic reticulum, which may indicate an increase in protein synthesis in hepatocytes (Figures 4A, B). Different forms of mitochondria were detected: most of the organelles showed signs of normal adult functional forms with vesicular cristae (Figure 4A), some of the organelles showed signs of young forms with an electron-dense matrix without clearly defined cristae (Figure 4E), and some of the mitochondria showed apoptotic changes (Figure 4C) and destructive changes (Figure 4D). The presence of different forms of mitochondria with a predominance of functionally active mitochondria may indicate optimal energy production in cells. The formation of a large number of nuclear pores of considerable size (Figures 4C–E) was found, probably indicating the activation of the processes of transport of informational and protein molecules across the nuclear membrane. This may also be evidenced by the location of mitochondria in the perinuclear region (Figures 4C, D). A considerable number of glycogen granules were found, some of which are collected in rosettes (Figure 4F).

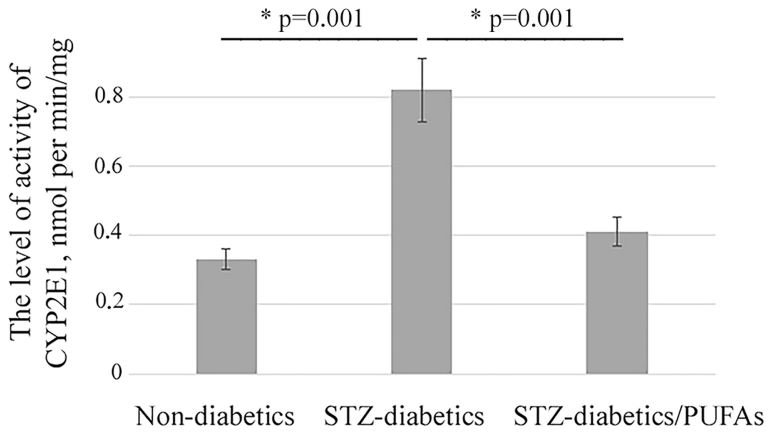

FIGURE 2
p-Nitrophenol hydroxylase activity of CYP2E1 in microsomes from liver of experimental animals; *p-values < 0.05 were considered statistically significant (one-way ANOVA). Means ± SD (n = 4-6 in each group).

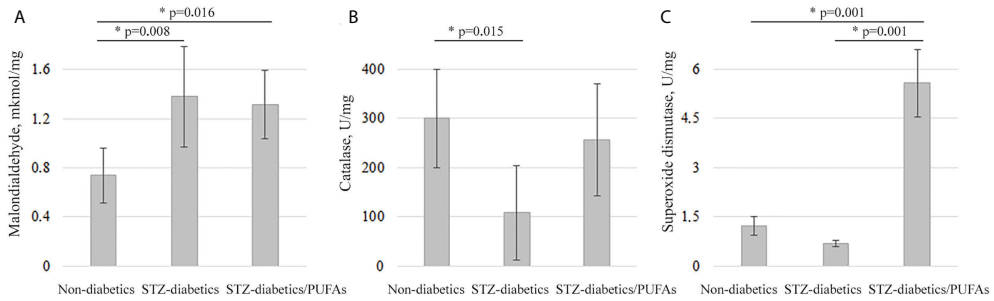

FIGURE 3
Oxidative stress markers in the liver tissues of the experimental animals. **(A)** Malondialdehyde levels, **(B)** catalase activity, **(C)** superoxide dismutase activity. *p-values < 0.05 were considered statistically significant (one-way ANOVA). Means ± SD (n = 6 in each group).

Thus, in the present work, we have shown that treatment with omega-3 PUFAs prevents damage to the ultrastructure of the liver of diabetic rats, namely, structural and functional damage to organelles, especially mitochondria and the nucleus, which we had previously demonstrated in liver samples from diabetic rats (3). Biosynthetic processes and the processes of transport of molecules across the nuclear membrane were significantly enhanced. There were also signs of normal function of the mitochondrial apparatus. It should be noted that no lipid granules were found in the samples studied, which may indicate the prevention of the development of lipid dystrophy, which often occurs in diabetic liver. However, there were signs of impaired carbohydrate metabolism in the liver samples (Figure 4).

Serum markers of a liver destruction STZ-induced diabetic rat model

The signs of liver pathology were found in the blood serum of the diabetic rats. We discovered increased activity of transaminases: ALT (by 3.8-fold), AST (by 1.7-fold), and GGT (by more than 5-fold) compared to control (ALT, p = 0.001; AST, p = 0.001; GGT, p = 0.001) (Figure 5).

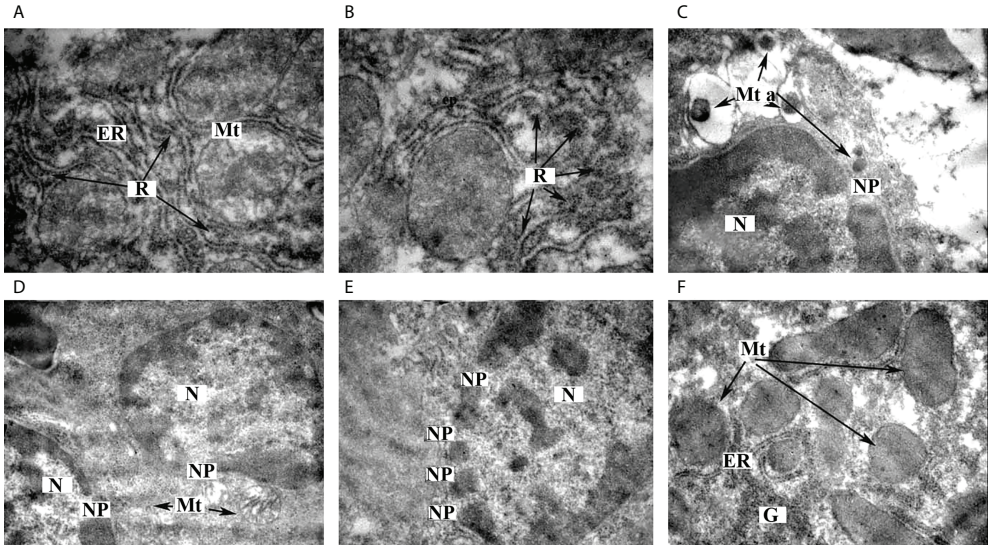

FIGURE 4
Ultrastructural features of hepatocytes from STZ-diabetic rats administered with omega-3 PUFAs. **(A)** Ultrastructure of endoplasmic reticulum, ×12,000. **(B)** Localization of ribosomes on the ER membrane, ×12,000. **(C)** Ultrastructure of apoptotic mitochondria, ×6,400. **(D)** Ultrastructure of nucleus, ×6,400. **(E)** Transport of informational and protein molecules between the nucleus and cytoplasm of hepatocyte, ×8,000. **(F)** Glycogen granules in hepatocytes, ×8,000. *ER*—endoplasmic reticulum, *G*—glycogen granules, *Mt*—mitochondria, *Mt a*—apoptotic mitochondria, *N*—nucleus, *NP*—nuclear pores, *R*—ribosomes.

It was found that the levels of ALT, AST, and GGT activity in the blood serum of the diabetic animals administered with omega-3 PUFAs were significantly lower (approximately by 2-fold) than in the diabetic group (ALT, $p = 0.001$; AST, $p = 0.001$; GGT, $p = 0.001$). Thus, AST approached control values, while ALT and GGT remained elevated compared to the non-diabetic control group (ALT, $p = 0.011$; AST, $p = 0.060$; GGT, $p = 0.001$) (Figure 5).

Serum lipid profile of STZ-induced diabetic rats

The lipid profile abnormality (dyslipidemia) is a common symptom of diabetes, as well as a risk factor for non-alcoholic fatty liver disease (13, 14). Some signs of dyslipidemia were found in the blood serum of the diabetic rats. We discovered increased levels of the triacylglycerol (68%) and decreased level of the high-density lipoprotein cholesterol (39%) compared to non-diabetic control (TAG, $p = 0.013$; HDL-C, $p = 0.001$). The levels of total cholesterol and low-density lipoprotein cholesterol approached control values (cholesterol, $p = 0.200$; LDL-C, $p = 0.179$) (Table 2).

It was found that the cholesterol, TAG, LDL-C, and HDL-C levels in the blood serum of the diabetic animals administered with omega-3 PUFAs did not change compared to the diabetic group (cholesterol, $p = 0.436$; TAG, $p = 0.287$; LDL-C, $p = 0.795$; and HDL-C, $p = 0.900$). Thus, the treatment with omega-3 PUFAs did not contribute to the normalization of the lipid profile (*diabetics/PUFAs vs. non-diabetic control*, cholesterol, $p = 0.842$; TAG, $p = 0.001$; LDL-C, $p = 0.444$; HDL-C, $p = 0.001$) (Table 2).

Discussion

Due to their antioxidant, anti-inflammatory, antiapoptotic, and other beneficial properties, omega-3-enriched pharmaceutical compositions of PUFAs are widely used for the prevention of the pathologies of the cardiovascular and endocrine systems, especially in diabetes mellitus (11). It should be noted that the systemic metabolism of PUFAs entering the body from the outside occurs mainly in the liver (15). Enzymes of the cytochrome P450 superfamily, especially CYP2E1, play the main role in the metabolism of omega PUFAs (16). Omega-3 PUFAs, as substrates, can increase the expression level of CYP2E1 in cells. We have recently shown that a diet enriched with omega-3 PUFAs leads to an increase in CYP2E1 levels in the liver of young healthy animals (12). It has also been shown that an increase in CYP2E1 expression can lead to oxidative stress, oxidative ultrastructural damage, and the development of pathology (4). Therefore, the question arises whether long-term treatment with CYP2E1 substrates may increase the risk of developing CYP2E1-dependent oxidative stress in some diseases (including diabetes) whose pathogenesis is closely associated with increased expression of CYP2E1. Our work aimed to address this question.

In our experiment, we detected an increase in the level and activity of CYP2E1 in the liver of diabetic rats. Several factors could lead to this, including a decrease in the inhibitory effect of insulin on gene transcription, substrate stabilization of CYP2E1 molecules by acetone and ketone bodies, and intensification of gluconeogenesis with active participation of CYP2E1 (17). Such increased expression of CYP2E1 could cause the development of oxidative stress, the signs of which were found in diabetic liver in the present study. In our previous work, we found that CYP2E1-dependent oxidative stress caused ultrastructural damage in the liver tissue of diabetic animals, which was accompanied by a significant increase in liver damage biomarkers in serum (12). In the present work, liver tissue destruction was also evidenced by an increase in serum markers of liver pathology. Our previous ultrastructural studies have found signs of fatty liver in diabetic rats (12). It is known that defects in insulin action, increased concentrations of free fatty acids, and non-infectious inflammation lead to the disturbed regulation of lipoprotein

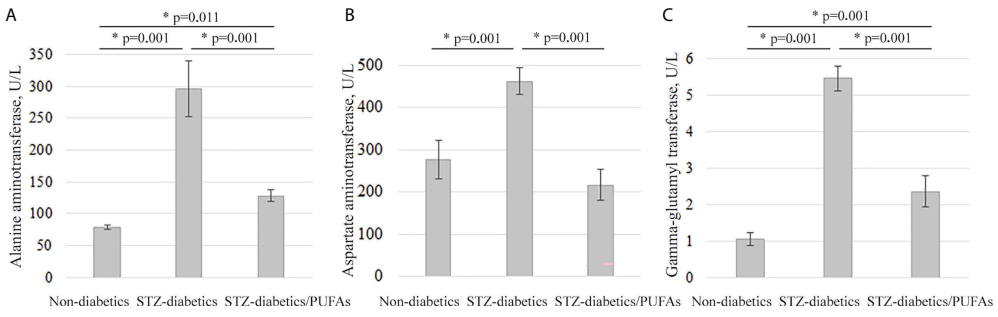

FIGURE 5
Serum markers of liver destruction in the experimental animals. **(A)** Alanine aminotransferase levels, **(B)** aspartate aminotransferase levels, and **(C)** gamma-glutamyl transferase levels. *p-values < 0.05 were considered statistically significant (one-way ANOVA). Means ± SD (n = 6 in each group).

10.3389/fendo.2022.1004564

TABLE 2 Serum lipid profile of experimental animals.

Animals	Total cholesterol, mmol/L	Triacylglycerol, mmol/L	High-density lipoprotein cholesterol, mmol/L	Low-density lipoprotein cholesterol, mmol/L
Non-diabetic rats	1.09 ± 0.304	0.57 ± 0.029	0.46 ± 0.085	0.74 ± 0.288
STZ-diabetic rats	0.80 ± 0.240	0.95 ± 0.238 *	0.28 ± 0.008 *	0.49 ± 0.218
STZ-diabetic rats administered with omega 3 PUFAs	1.00 ± 0,266	1.14 ± 0.259 *	0.28 ± 0.021 *	0.58 ± 0.149

Values are means ± SD, n = 6 rats in each group. *p ≤ 0.01 compared to the non-diabetic group (one-way ANOVA).

metabolism in the liver, resulting in an abnormal serum lipid profile in diabetics (14). It was shown that dyslipidemia is a risk factor for non-alcoholic fatty liver disease (15). It was found that CYP2E1-mediated mechanisms may be involved in such processes (7, 8). We have identified signs of dyslipidemia, namely, an increase in TAG level and a decrease in HDL-C level. A similar lipid profile abnormality was found in patients with type 1 diabetes (18).

We investigated the level of CYP2E1 expression (as a key factor in the development of pathology) in the liver of diabetic rats treated with omega-3 PUFAs. We found no changes in the level of the enzyme but noted a significant decrease in its activity compared to the non-treated diabetic group. Such maintenance of a high CYP2E1 content may be associated with a high level of substrates that stabilize the enzyme molecule and protect it from rapid degradation. At the same time, a high level of CYP2E1 substrates may cause the effect of substrate inhibition (19), which we observed when studying the p-nitrophenol hydroxylase activity of the enzyme *in vitro*. The increased expression of CYP2E1 may be the reason for the high peroxide processes we observed in the liver of diabetic rats treated with omega-3 PUFAs. It was shown that increased CYP2E1 expression and CYP2E1-dependent oxidative processes can lead to the development of fatty dystrophy (4). In our recent studies, we observed signs of lipid metabolism disorders in the liver of diabetic rats (3). In the present work, administration of omega-3 PUFAs led to some activation of antioxidant enzymes, which could prevent oxidative damage to the liver. The ability of omega-3 PUFAs to activate antioxidant resources has also been demonstrated by other authors (11). It was shown that omega-3 fatty acid treatment may have beneficial effects in regulating hepatic lipid metabolism (20). Indeed, we found no signs of fatty liver. However, the serum lipid profile did not normalize. Dyslipidemia is due to insulin dysregulation and hyperglycemia (14), and omega-3 PUFAs do not affect these processes.

Thus, consumption of omega-3 PUFAs was shown to prevent oxidative damage to liver tissue in diabetic rats. This contributed to the maintenance of the processes of biosynthesis, energy metabolism, and lipid metabolism in liver cells. The absence of significant structural and functional disorders of the liver of diabetic rats treated with omega-3 PUFAs can be demonstrated by the data of microscopic ultrastructural analysis and biochemical analysis of the level of serum markers of liver pathology.

It should be noted that significant accumulations of glycogen in liver cells and hyperglycemia were also detected in the present work. These data may indicate inhibition of the processes of glucose entry into the liver and stimulation of gluconeogenesis in the cells, with an increase in CYP2E1 levels playing a leading role in the activation of this process. Thus, it was found that treatment with omega-3 PUFAs did not normalize carbohydrate metabolism in the liver of diabetic rats.

Conclusion

We detected a significant increase in CYP2E1 expression (protein content and activity) and found evidence of oxidative stress, which may have been induced by a high CYP2E1 concentration in the liver of diabetic rats. The significant increase in blood serum transaminases detected could indicate marked destruction of liver tissue. All these signs could indicate the development of diabetic pathology in the liver of the experimental animals. Significant hyperglycemia and diabetic dyslipidemia (increased triacylglycerol levels and decreased HDL-C levels) were found. Lack of natural weight gain in the rats was also noted.

Treatment of the diabetic animals with an omega-3-enriched pharmaceutical composition of PUFAs had no effect on CYP2E1 levels, which remained at the diabetic levels, but contributed to a decrease in enzyme activity. The high level of CYP2E1 could be the reason for the high level of peroxide processes. However, due to the induction of antioxidant activity, treatment with omega-3 PUFAs may prevent oxidative damage to the liver. Examination of the ultrastructure of liver tissues and cells revealed no signs of diabetic pathology, with the exception of hyperglycogenosis. The markedly increased accumulation of glycogen granules in the hepatocytes, as well as the significant hyperglycemia, might indicate that the omega-3 PUFAs have no effect on

carbohydrate metabolism. We also found no signs of fatty liver disease. However, the serum lipid profile did not normalize.

Thus, the results obtained might indicate that long-term treatment of diabetic animals with omega-3 PUFAs does not increase the risk of CYP2E1-dependent oxidative stress and the development of liver pathology but rather prevents some diabetic ultrastructural damage to hepatocytes.

Data availability statement

The original contributions presented in the study are included in the article/Supplementary Material. Further inquiries can be directed to the corresponding author.

Ethics statement

The animal study was reviewed and approved by The Local Committee on Bioethics (registration number: 0114U007233), Bogomoletz Institute of Physiology, National Academy of Sciences of Ukraine, Kyiv, Ukraine.

Author contributions

OM and AS contributed equally to this work and share first authorship. OM and AS made substantial contributions to the conception and design, as well as acquisition and analysis of data, and participated in data analysis and critical review of the manuscript for important intellectual content. OM performed Western blot analysis and CYP2E1 activity measurements. AS examined markers of oxidative stress. DS conducted statistical analysis. The first draft of the manuscript was written by OM. All authors contributed to the revision of the manuscript and read and approved the submitted version.

Funding

The authors declare that this study received funding from the National Research Foundation of Ukraine under the project "*Support* for *Research of Leading and Young Scientists*" (No. 20220.02/0332). The funder was not involved in the study design, collection, analysis, interpretation of data, the writing of this article, or the decision to submit it for publication.

Acknowledgments

The authors thank Dr. Katherine Rozova (Bogomoletz Institute of Physiology, National Academy of Sciences of Ukraine) for valuable help with microscopic studies. The authors thank Academic Proofreading (https://www.academicproofreading.uk/) for their significant contribution to the English language editing of the manuscript.

Conflict of interest

The authors declare that the research was conducted in the absence of any commercial or financial relationships that could be construed as a potential conflict of interest.

Publisher's note

All claims expressed in this article are solely those of the authors and do not necessarily represent those of their affiliated organizations, or those of the publisher, the editors and the reviewers. Any product that may be evaluated in this article, or claim that may be made by its manufacturer, is not guaranteed or endorsed by the publisher.

References

1. Ahmadieh H, Azar ST. Liver disease and diabetes: Association, pathophysiology, and management. *Diabetes Res Clin Pract* (2014) 104:53–62. doi: 10.1016/j.diabres.2014.01.003

2. van Beek JH, de Moor MH, de Geus EJ, Lubke GH, Vink JM, Willemsen G, et al. The genetic architecture of liver enzyme levels: GGT, ALT and AST. *Behav Genet* (2013) 43:329–39. doi: 10.1007/s10519-013-9593-y

3. Maksymchuk O, Shysh A, Rosohatska I, Chashchyn M. Quercetin prevents type 1 diabetic liver damage through inhibition of CYP2E1. *Pharmacol Rep* (2017) 69:1386–92. doi: 10.1016/j.pharep.2017.05.020

4. Harjumäki R, Pridgeon CS, Ingelman-Sundberg M. CYP2E1 in alcoholic and non-alcoholic liver injury. roles of ROS, reactive intermediates and lipid overload. *Int J Mol Sci* (2021) 22:8221. doi: 10.3390/ijms22158221

5. Bessone F, Razori MV, Roma MG. Molecular pathways of nonalcoholic fatty liver disease development and progression. *Cell Mol Life Sci* (2019) 76:99–128. doi: 10.1007/s00018-018-2947-0

6. Schattenberg JM, Czaja MJ. Regulation of the effects of CYP2E1-induced oxidative stress by JNK signaling. *Redox Biol* (2014) 3:7–15. doi: 10.1016/j.redox.2014.09.004

7. Ganji SH, Kashyap ML, Kamanna VS. Niacin inhibits fat accumulation, oxidative stress, and inflammatory cytokine IL-8 in cultured hepatocytes: Impact on non-alcoholic fatty liver disease. *Metabolism* (2015) 64:982–90. doi: 10.1016/j.metabol.2015.05.002

8. Wan YY, Cai Y, Li J, Yuan Q, French B, Gonzalez FJ, et al. Regulation of peroxisome proliferator activated receptor alpha-mediated pathways in alcohol fed cytochrome P450 2E1 deficient mice. *Hepatol Res* (2001) 19:117–30. doi: 10.1016/S1386-6346(00)00089-9

9. Bansal S, Liu CP, Sepuri NB, Anandatheerthavarada HK, Selvaraj V, Hoek J, et al. Mitochondria-targeted cytochrome P450 2E1 induces oxidative damage and augments alcohol-mediated oxidative stress. *J Biol Chem* (2010) 285:24609–19. doi: 10.1074/jbc.M110.121822

10. Fazelian S, Moradi F, Agah S, Hoseini A, Heydari H, Morvaridzadeh M, et al. Effect of omega-3 fatty acids supplementation on cardio-metabolic and oxidative stress parameters in patients with chronic kidney disease: a systematic review and meta-analysis. *BMC Nephrol* (2021) 22:160. doi: 10.1186/s12882-021-02351-9

11. Oppedisano F, Macrì R, Gliozzi M, Musolino V, Carresi C, Maiuolo J, et al. The anti-inflammatory and antioxidant properties of n-3 PUFAs: Their role in cardiovascular protection. *Biomedicines* (2020) 8:306. doi: 10.3390/biomedicines8090306

12. Maksymchuk O, Shysh A, Chashchyn M, Moibenko O. Dietary omega-3 polyunsaturated fatty acids alter fatty acid composition of lipids and CYP2E1 expression in rat liver tissue. *Int J Vitam Nutr Res* (2015) 85:322–8. doi: 10.1024/0300-9831/a000296

13. Peng K, Mo Z, Tian G. Serum lipid abnormalities and nonalcoholic fatty liver disease in adult males. *Am J Med Sci* (2017) 353:236–41. doi: 10.1016/j.amjms.2017.01.002

14. Tomkin GH, Owens D. Diabetes and dyslipidemia: characterizing lipoprotein metabolism. *Diabetes Metab Syndr Obes* (2017) 10:333–43. doi: 10.2147/DMSO.S115855

15. Alves-Bezerra M, Cohen DE. Triglyceride metabolism in the liver. *Compr Physiol* (2017) 8:1–8. doi: 10.1002/cphy.c170012

16. Arnold C, Konkel A, Fischer R, Schunck WH. Cytochrome P450-dependent metabolism of omega-6 and omega-3 long-chain polyunsaturated fatty acids. *Pharmacol Rep* (2010) 62:536–47. doi: 10.1016/S1734-1140(10)70311-X

17. Dey A, Kumar SM. Cytochrome P450 2E1 and hyperglycemia-induced liver injury. *Cell Biol Toxicol* (2011) 27:285–310. doi: 10.1007/s10565-011-9188-4

18. Vergès B. Lipid disorders in type 1 diabetes. *Diabetes Metab* (2009) 35:353–60. doi: 10.1016/j.diabet.2009.04.004

19. Collom SL, Laddusaw RM, Burch AM, Kuzmic P, Perry MDJr, Miller GP. CYP2E1 substrate inhibition. mechanistic interpretation through an effector site for monocyclic compounds. *J Biol Chem* (2008) 283:3487–96. doi: 10.1074/jbc.M707630200

20. Scorletti E, Byrne CD. Omega-3 fatty acids, hepatic lipid metabolism, and nonalcoholic fatty liver disease. *Annu Rev Nutr* (2013) 33:231–48. doi: 10.1146/annurev-nutr-071812-161230

frontiers | Frontiers in Endocrinology

TYPE Review
PUBLISHED 21 October 2022
DOI 10.3389/fendo.2022.1027686

OPEN ACCESS

EDITED BY
Jean Buteau,
University of Alberta, Canada

REVIEWED BY
Wan Zhuo,
Fourth Military Medical University, China
Mahmoud Gabr,
Mansoura University, Egypt

*CORRESPONDENCE
Jun Chen
junchen001@outlook.com
Li Chen
chenli3@email.sdu.edu.cn

SPECIALTY SECTION
This article was submitted to Diabetes: Molecular Mechanisms, a section of the journal Frontiers in Endocrinology

RECEIVED 25 August 2022
ACCEPTED 07 October 2022
PUBLISHED 21 October 2022

CITATION
Yang M, Chen J and Chen L (2022) The roles of mesenchymal stem cell-derived exosomes in diabetes mellitus and its related complications. *Front. Endocrinol.* 13:1027686. doi: 10.3389/fendo.2022.1027686

The roles of mesenchymal stem cell-derived exosomes in diabetes mellitus and its related complications

Mengmeng Yang[1], Jun Chen[1,2,3,4]* and Li Chen[1,2,3,4]*

[1]Department of Endocrinology, Qilu Hospital, Shandong University, Jinan, China, [2]Institute of Endocrine and Metabolic Diseases of Shandong University, Jinan, China, [3]Key Laboratory of Endocrine and Metabolic Diseases, Shandong Province Medicine & Health, Jinan, China, [4]Jinan Clinical Research Center for Endocrine and Metabolic Diseases, Jinan, China

Diabetes mellitus is a type of metabolic disease characterized by hyperglycemia, primarily caused by defects in insulin secretion, insulin action, or both. Long-term chronic hyperglycemia can lead to diabetes-related complications, causing damage, dysfunction, and failure of different organs. However, traditional insulin and oral drug therapy can only treat the symptoms but not delay the progressive failure of pancreatic beta cells or prevent the emergence of diabetic complications. Mesenchymal stem cells have received extensive attention due to their strong immunoregulatory functions and regeneration effects. Mesenchymal stem cell-derived exosomes (MSC-Exos) have been proposed as a novel treatment for diabetic patients as they have demonstrated superior efficiency to mesenchymal stem cells. This review summarizes the therapeutic effects, mechanisms, challenges, and future prospects of MSC-Exos in treating diabetes mellitus and its related complications. This review supports the potential use of MSC-Exos in future regenerative medicine to overcome the current difficulties in clinical treatment, particularly in treating diabetes.

KEYWORDS

diabetes mellitus, complications, mesenchymal stem cells, exosomes, β-cell

Abbreviations: DM, Diabetes mellitus; T1DM, Type 1 diabetes mellitus; T2DM, Type 2 diabetes mellitus; β-cells, Beta cells; MSCs, Mesenchymal stem cells; MSC-Exos, Mesenchymal stem cell-derived exosomes; BMMSCs, Bone marrow MSCs; AMSCs, Adipose MSCs; UCBMSCs, Umbilical blood MSCs; PTMSCs, Perinatal tissues mesenchymal stem cells; HucMSCs, Human umbilical cord MSCs; MVBs, Multivesicular bodies; AMSC-Exos, Adipose-derived mesenchymal stem cell-derived exosomes; MenMSC-Exos, Menstrual blood mesenchymal stem cell-derived exosomes; BMMSC-Exos, Bone marrow mesenchymal stem cell-derived exosomes; VEGF, Vascular endothelial growth factor; WJMSC-Exos, Wharton's jelly mesenchymal stem cell-derived exosomes; IMSC-Exos, Islet MSC-like cells-derived exosomes; GLUT4, Glucose transporter 4; STZ, Streptozotocin; HucMSC-Exos, Human umbilical cord mesenchymal stem cell-derived exosomes; UCBMSC-Exos, Umbilical cord blood mesenchymal stem cell-derived exosomes; DKD, Diabetic kidney disease; SCr, Serum creatinine; BUN, Blood urea nitrogen; UALB, Urine albumin; MiRNAs, MicroRNAs; DFU, Diabetic foot ulcer; NO, Nitric oxide; HG, High glucose; SMCs, Smooth muscle cells; EMVs, Exosome mimetic vesicles.

1 Introduction

Diabetes mellitus is (DM) a metabolic disease characterized by hyperglycemia. It is primarily divided into Type 1 diabetes mellitus (T1DM), which occurs due to absolute deficiency in insulin secretion caused by autoimmune destruction of pancreatic beta cells (β-cells). Additionally, Type 2 diabetes mellitus (T2DM) is caused by insulin resistance or islets β-cells dysfunction (1, 2). Diabetes has become the ninth leading cause of mortality, with the total number of people with diabetes quadrupled in the past three decades (3). More than 440 million people are currently affected by the diabetes epidemic, with approximately 1 in 10 adults having diabetes, with T2DM accounting for 90% (3). Long-term chronic hyperglycemia can lead to diabetes-related complications, causing damage, dysfunction, and failure of multiple organs and tissues, such as the eyes, kidneys, nerves, heart, blood vessels, etc. Most patients with T2DM have at least one of these complications, with cardiovascular complications being the most common cause of mortality (3). Meanwhile, T1DM is closely associated with various microvascular and macrovascular complications (4). The rising prevalence and serious complications have made diabetes a huge challenge that significantly jeopardizes public health.

Insulin injection and oral hypoglycemic medications are the traditional treatments for diabetes. However, these treatments cannot slow down the progressive failure of pancreatic β-cells and prevent the emergence of diabetic complications. Recently, researchers have focused on mesenchymal stem cells (MSCs) therapy as a potential treatment option for diabetic patients. MSCs are the heterogeneous subset of stromal stem cells that can be isolated from various tissues, including the umbilical cord, amniotic fluid, menstrual blood, bone marrow, adipose tissue, and others. MSCs exhibit self-renewal and the potential for multi-lineage differentiation, including mesodermal lineages, such as adipocytes, osteocytes, chondrocytes, etc. (5, 6). MSCs have emerged as the most promising source of cells for transplantation in recent years due to their immunomodulatory (7), paracrine (8), and trans-differentiation regulatory functions (9). Emerging studies have reported that MSCs are crucial in treating diabetes and its related complications (10–12). However, there are limitations in MSCs cell therapy, namely organ residence (13), limited utilization (14), thrombogenesis (15), low survival rate *in vivo* (16), and tumorigenicity potential (17, 18). Accumulating evidence indicates that MSCs exert their therapeutic effects mainly through the paracrine mechanisms, prompting extensive studies on mesenchymal stem cell-conditioned medium (8, 19, 20). Mesenchymal stem cell-derived exosomes (MSC-Exos) have been proven to be equally effective as MSCs in treating diabetes and related complications (21–23). In some studies, MSC-Exos have demonstrated a superior therapeutic and regenerative effect in treating T1DM compared with the parental cells (24). Furthermore, it is easier to maintain exosomes than MSCs, in addition to being a safer option due to the fewer membrane-bound proteins and lack of direct tumorigenicity (25). The ability of cell-free exosome therapy to circumvent the aforementioned shortcomings of MSCs transplantation combined with its excellent therapeutic effects and safety makes it a new strategy for the treatment of diabetes and diabetic complications. This review summarizes the biological characteristics of exosomes and their applications in the treatment of diabetes and its related complications. This review also elucidates the potential underlying mechanisms and we discuss the challenges related to their applications.

2 Properties of MSCs

MSCs are a class of pluripotent stem cells belonging to the mesoderm, which have all the common characteristics of stem cells, namely self-renewal and multidirectional differentiation ability. MSCs can differentiate into osteogenic, chondrogenic, and adipogenic lineages. Studies have proven that MSCs play important roles in many diseases including diabetes and related complications.

The most prevalent types of MSCs are mainly derived from bone marrow, adipose tissue, and perinatal tissues (human umbilical cord, umbilical blood, amniotic membrane, placenta, etc.). The biological properties of MSCs from various tissue origins vary. Both bone marrow MSCs (BMMSCs) and adipose MSCs (AMSCs) have trilineage differentiation potential. However, BMMSCs exhibit enhanced osteogenic and chondrogenic differentiation, whereas AMSCs are typically more likely to exhibit an adipogenic differentiation (26). Interestingly, umbilical blood MSCs (UCBMSCs) and placenta MSCs can differentiate into only two lineages (27). Even though there are conflicting results regarding the differentiation potential of perinatal tissues MSCs (PTMSCs), Marianna et al. confirmed that UCBMSCs have a lower adipogenic potential (28). In addition to the differentiation potential, the surface markers of MSCs are different. Compared to BMMSCs and AMSCs, human umbilical cord MSCs (HucMSCs) have higher levels of CD10, CD49d, CD54, CD200, and PDL2 expression, but lower levels of CD119, IFNγR1, and CD183 expression (29, 30). Coagulation factor III or tissue factor (TF)/CD142 levels were increased in AMSCs and PTMSCs compared to the BMMSCs (31, 32). Furthermore, the immunomodulatory properties of MSCs also differ. *In vitro* experiments showed that HucMSCs had a stronger inhibitory effect on T cell proliferation than placenta MSCs, followed by AMSCs and BMMSCs (33). However, according to other studies, BMMSCs exhibit more significant T cell suppressive capacity with increased expression of PDL1, IL10, and TGFβ1 (27, 34). Compared to BMMSCs and AMSCs, PTMSCs had the lowest expression of HLA antigens (HLA-DMA, HLA-DPB1, and HLA-DR) and immune-related genes (JAG1, TLR4, TLR3, NOTCH2, and NOTCH3), as well as reduced amounts of IL1α, IL6, and IL8 in the secretory group and increased IDO, IL1β, LIF and TNFβ2 (33, 35).

Studies have reported that MSCs act through their paracrine function and that MSCs are able to secrete a large number of RNAs, lipids, as well as a variety of soluble factors packaged in extracellular vesicles.

3 Biological characteristics of exosomes

Exosomes are a kind of extracellular vesicles with lipid bilayer membranes, which are cup-shaped structures under the microscope, ranging from 30-150 nm in diameter. Exosomes are formed in a process that involves double invagination of the plasma membrane and the formation of multivesicular bodies (MVBs). The plasma membrane is invaginated into a cup-like structure, thus forming early-sorting endosomes, which further mature into late-sorting endosomes with the involvement of the trans-Golgi network and endoplasmic reticulum (36–38). Meanwhile, intraluminal vesicles accumulate in late-sorting endosomes, converting them into MVBs. MVBs can be degraded by autophagosomes or lysosomes, or they can fuse with the plasma membrane to release intraluminal vesicles in the form of exosomes (29). Exosomes are taken up by recipient cells and participate in intercellular communication in three ways: receptor-ligand interaction, direct membrane fusion, and endocytosis/phagocytosis (39).

The nanoscale of exosomes allows them to be readily absorbed, cross the blood-brain barrier, and avoid being degraded by endosomes and lysosomal. While the lipid bilayer membrane structure can protect the cargo from degradation in the physical environment and provide long-term release effects to increase biological activity. Exosomes contain various molecular components, including DNA, RNA, lipids, and proteins derived from their parent cells, and are capable of performing important biological functions. In normal physiological processes, exosomes are able to participate in cell proliferation, immune regulation, neural communication, reproduction and development, and homeostasis. However, in pathological conditions, exosomes may interfere with immune responses, participate in the pathogenesis of tumors and neurodegenerative diseases, and even bring about pathogenic infections (39).

4 The roles of mesenchymal stem cell-derived exosomes in diabetes and its associated complications

4.1 Mesenchymal stem cell-derived exosomes and type 1 diabetes mellitus

T1DM is an autoimmune disease characterized by β-cells dysfunction and death, absolute insulin deficiency, and elevated blood glucose levels caused by autoreactive immune cells (40, 41). Therefore, inhibiting islet inflammation in T1DM and keeping a balance between auto-reactive effector T cells and regulatory T cells *in vivo* help to alleviate the injury and apoptosis of β-cells. Exosomes have been proven to have a robust immunomodulatory effect. Studies have reported that adipose-derived mesenchymal stem cell-derived exosomes (AMSC-Exos) exhibit immunomodulatory effects on T cells. The exosomes can also improve hyperglycemia symptoms in T1DM mice while increasing the number of regulatory T cells without affecting the proliferation index of lymphocytes (42). As the disease progresses, the number of pancreatic islets gradually decreases in T1DM patients due to inflammatory cells infiltrating the pancreatic islets and causing immune destruction of β-cells (43). Menstrual blood mesenchymal stem cell-derived exosomes (MenMSC-Exos) promote islet regeneration *via* the pancreas and duodenal homeobox one pathway, improve β-cells mass, and enhance insulin secretion in T1DM rats (44). Additionally, MSC-Exos have shown better therapeutic and regenerative effects than MSCs alone. Within four weeks of treatment with bone marrow mesenchymal stem cell-derived exosomes (BMMSC-Exos), T1DM rats showed a significant reduction in blood glucose levels and increased plasma insulin levels. Additionally, histopathology examination also revealed that the islets cells were regenerated, the number and size of Langerhans islets increased, while fibrosis and inflammation were reduced. However, the above indices were only slightly improved when the rats were treated with BMMSCs rather than BMMSC-Exos (45).

Islet transplantation is a prominent treatment for patients with T1DM. However, its application is limited by the shortage of organ donors and the loss of islets during the pre-transplant culture period and post-transplantation (46). Therefore, improving islet survival and function and preventing islet cell apoptosis are the key factors in islet transplantation. Vascular endothelial growth factor (VEGF), a pro-survival and anti-apoptotic factor that maintains islet mass, is expressed in islets but attenuated in isolated islets. Reduced expression of VEGF is associated with islet dysfunction and cell death. VEGF also facilitates the revascularization of transplanted islets, which is essential for long-term graft survival (47, 48). Exosomes from Wharton's jelly mesenchymal stem cell (WJMSC-Exos) increase the expression of VEGF in co-cultured islets.

Furthermore, WJMSC-Exos can downregulate apoptotic genes such as BAD and BAX while upregulating the anti-apoptotic gene, BCL-2, and pro-survival gene, PI3K. PI3K can accelerate cell survival by activating Akt and inhibiting BAD and BAX (49), enhancing islet cell viability and reducing apoptosis. Proinflammatory cytokines trigger the expression of apoptosis and hypoxia-related genes, including iNOS, Fas, Caspase-3, and miR-375, causing immune rejection, and resulting in the destruction and dysfunction of transplanted islets. BMMSC-Exos can deliver siFAS and anti-miR-375, reduce immune

activity and inhibit early apoptosis of transplanted islets (50). In the future, exosome therapy may eventually enable T1DM patients to reduce or eliminate insulin usage.

In addition to being utilized to treat T1DM, MSC-Exos may also be involved in its pathogenesis. According to *in vitro* research, islet MSC-like cells-derived exosomes (iMSC-Exos) are highly immunostimulatory. These exosomes may also contain specific antigens that stimulate autoreactive B cells, which in turn activate autoreactive T and B cells in prodromal diabetic NOD mice (a spontaneous disease model for T1DM) by binding to TLR. Additionally, the induction of auto-reactive Th1 cells was correlated with serum iMSC-Exos levels, with greater iMSC-Exos levels being linked to a rise in reactive Th1 cells. Therefore, iMSC-Exos may function as autoimmune triggers in NOD mice by acting as autoantigen carriers with strong adjuvant activity (51).

4.2 Mesenchymal stem cell-derived exosomes and type 2 diabetes mellitus and insulin resistance

T2DM, which accounts for 90% of patients with diabetes, is primarily caused by peripheral insulin resistance, pancreatic β-cells mass loss, and β-cells dysfunction (52). Glucose transporter 4 (GLUT4) is the major glucose transporter in adipose and skeletal muscle tissues and is strongly associated with peripheral insulin resistance in T2DM. GLUT4 translocation disorders and decreased expression reduce glucose uptake in skeletal muscle and adipose tissue, aggravating insulin resistance (53). In the T2DM rat model established by a high-fat diet and streptozotocin (STZ), human umbilical cord mesenchymal stem cell-derived exosomes (HucMSC-Exos) significantly ameliorated hyperglycemia in T2DM rats, restored insulin receptor substrate1 and the phosphorylation of protein kinase B (tyrosine site), and promoted the expression and membrane translocation of GLUT4 in skeletal muscle. Furthermore, HucMSC-Exos increased glycogen storage *in vivo* to maintain glucose homeostasis and inhibit STZ-induced β-cells apoptosis by restoring insulin secretion in T2DM rats (54). It was also reported that Langerhans islet induced atrophy and structural disorder in T2DM rats. A treatment using HucMSC-Exos restored islet structure, reduced the homeostatic model assessment of insulin resistance, and enhanced insulin sensitivity by promoting glucose uptake *via* GLUT1-4 in T2DM rats (55).

In conclusion, HucMSC-Exos can alleviate β-cells destruction and reverse peripheral insulin resistance. Hyperglycemia in diabetic patients encourages β-cells oxygen consumption, leading to β-cells hypoxia and a decline of PDX1 and MAFA, resulting in β-cells apoptosis and dysfunction (56, 57). HucMSC-Exos was shown to alleviate β-cells apoptosis under hypoxia by relieving hypoxia-induced endoplasmic reticulum stress and inhibiting p38 MAPK signaling in β-cells, which is mediated by the abundant miR-21 in HucMSC-Exos (58). Promoting islet regeneration and increasing insulin production is vital to restore T2DM. Umbilical cord blood mesenchymal stem cell-derived exosomes (UCBMSC-Exos) increased the proliferation of proliferative cells in Langerhans islets in STZ-induced diabetic mice, promoting pancreatic regeneration and improved insulin production by regulating the Extl3-Reg-cyclinD1 pathway (59). In summary, MSC-Exos can alleviate insulin resistance in insulin-sensitive tissues, such as the liver, muscle, and fat, and restore the function of β-cells.

4.3 Mesenchymal stem cell-derived exosomes and diabetic kidney disease

Diabetic kidney disease (DKD) is one of the severe microvascular complications of diabetes and a leading cause of end-stage renal disease worldwide (60). DKD pathogenesis involves various functional and structural changes, including hemodynamic changes, oxidative stress, mesangial cell expansion, and the development of glomerulosclerosis and fibrosis (61). The main clinical feature of DKD is persistent albuminuria, which can further develop into a decrease in glomerular filtration rate and renal tubular and interstitial lesions (62). Under diabetic conditions, almost all renal resident cells of DKD exhibit autophagy disorder (63). Exosomes from various tissues have been applied to treat DKD. BMMSC-Exos was reported to facilitate DKD by upregulating the autophagy function inhibited by the mTOR signaling pathway. Multiple injections of BMMSC-Exos significantly improved renal function in DKD mice, as observed in the significant decrease in serum creatinine (SCr), blood urea nitrogen (BUN), and urine albumin (UALB) levels. The injections also decreased the mesangial dilatation and improved renal fibrosis (64).

Exosomes contain abundant microRNAs (miRNAs), which play essential roles in immunoregulation, regulation of cell function, and homing mechanisms. miR-125a carried by AMSC-Exos mediated the protective effect of exosomes on DKD rats by inhibiting the HDAC1/ET1 axis (65). Meanwhile, miR-let-7a transported by BMMSC-Exos inhibited USP22 in the kidney tissue of DKD rats, leading to the decrease of SCr, BUN, triglycerides, and total cholesterol. Such action resulted in renal cells apoptosis and oxidative stress inhibition, and downregulation of N-cadherin and vimentin expression (66). In addition, BMMSC-Exos mediated its ameliorating effect on DKD rats by inhibiting the JAK2/STAT3 pathway (67).

Podocytes are terminally differentiated visceral epithelial cells that are an independent component of the glomerular filtration membrane, essential for maintaining glomerular filtration barrier function (68). Human urine stem cells-derived exosomes inhibited high glucose-induced VEGFA

expression in podocytes by transporting miR-16-5p, promoting podocyte proliferation, and preventing apoptosis (69). In addition, miR-215-5p carried by AMSC-Exos attenuated high glucose-induced migration and injury in the mouse glomerular podocyte. It inhibited the expression of downstream ZEB2, alleviating podocyte injury and epithelial-mesenchymal transdifferentiation (70). BMMSC-Exos was also reported to inhibit STZ-induced apoptosis and degeneration of renal tubular epithelial cells in diabetic rats (71). Studies have shown that HucMSC-Exos carried abundant miR-146a-5p, which promotes M2 macrophage polarization by targeting the TRAF6-STAT1 signaling pathway to suppress renal inflammation and restore renal function (72). These findings suggest the possible role of miRNAs in mediating the amelioration of renal resident cells in the DKD model treated with various exosomes from various sources.

Urinary exosomes can be served as markers of DKD. In a study by Zubiri et al., it was found that the expression of regucalcin protein in renal tissue was reduced in diabetic kidneys, and this significant change can be reflected in urinary exosomes. Therefore, urinary exosomal regucalcin protein assay can be utilized for early diagnosis and progression monitoring of DKD (73). However, it is unclear whether urinary exosomes originate from urinary MSCs or from kidney-resident cells. For example, WT1 protein levels in urinary exosomes of patients with DKD increase with declining renal function, while WTI protein is also a marker and transcription factor for podocytes. Therefore, WT1 protein is likely to be derived from exosomes of podocytes rather than MSC-Exos (74).

4.4 Mesenchymal stem cell-derived exosomes and diabetic foot ulcer

Diabetic foot ulcer (DFU) is one of the leading causes of lower extremity amputation, which can be life-threatening in severe cases. About 6.3% of diabetic patients worldwide may develop diabetic foot diseases (75), with 17% and 5% requiring minor and major amputations, respectively, after one year (76). Diabetic neuropathy and peripheral vascular disease are the leading causes of DFU (77). The pathogenesis of DFU is multifactorial, with neuropathy, ischemia, and infection being the three main factors that are possibly combined with other factors such as diabetic skeletal disease, trauma, foot biomechanics, and weight bearing. Chronic wound healing in DFU is a complex dynamic physiological process that can be divided into four stages: hemostasis, inflammation, proliferation, and remodeling. Angiogenesis is critical in determining diabetic wound healing outcomes (78).

Multiple findings have indicated that BMMSC-Exos can enhance the proliferation and migration of fibroblasts, promoting diabetic wound healing (22, 79). Evangelos et al. found that BMMSC-Exos activated AKT, ERK 1/2, and STAT3 and induced the expression of many trophic factors (e.g., HGF, IL-6, IGF1, NGF, and SDF1) (22). In addition, Bi et al. reported that the therapeutic effect of exosomes on DFU models was mediated by the lncRNA H19 carried by BMMSC-Exos, which inhibited miR-152-3p and increased PTEN expression (79). Similarly, AMSC-Exos were found to improve the conditions of DFU models. It was reported that AMSC-Exos negatively regulated the expression of MMP1 and MMP3 in WS1, promoting collagen synthesis and wound healing. The treatment also inhibited cicatrix formation (80). Studies have also reported the role of lincRNA and miRNA in AMSCs-Exos in wound healing. A study demonstrated wound healing in diabetic mice promoted by induction of MIRI-128-3P/SIRT1-mediated autophagy with the overexpression of mmu_circ_0000250-modified AMSC-Exos (81). AMSC-Exos overexpressing linc00511 was also reported to accelerate angiogenesis and encourage healing of DFU through the inhibition of PAQR3-induced degradation of Twist1 ubiquitin (82). In one study, miR-21-5p mimics were loaded into AMSC-Exos by electroporation. The engineered AMSC-Exos promoted keratinocyte proliferation and migration *via* Wnt/β-catenin signaling *in vitro* and accelerated diabetic wound healing by increasing re-epithelialization, collagen remodeling, angiogenesis, and vascular maturation (83). Additionally, HucMSC-Exos can modulate endothelial cell function by reducing oxidative stress and inflammatory responses, promoting angiogenesis, and ultimately accelerating diabetic wound healing (84). Another study revealed that MenMSC-Exos facilitated wound healing primarily by promoting angiogenesis, enhancing re-epithelialization and wound closure rate, and altering the ratio of collagen type I/III (85). MSC-Exos participate in regulating the whole process of wound healing, treating diabetic foot ulcers. However, further research is required to determine the optimal way to incorporate exosomes in clinical applications.

4.5 The applications of mesenchymal stem cell-derived exosomes in other diabetic complications

MSC-Exos have also been applied in treating other diabetic complications, such as diabetic retinopathy, diabetic erectile dysfunction, diabetic osteoporosis, cognitive impairment, diabetic cardiomyopathy, and peripheral neuropathy, summarized in Table 1. The studies have demonstrated the role of MSC-Exos in ameliorating diabetic conditions and related complications.

4.5.1 Mesenchymal stem cell-derived exosomes and diabetic retinopathy

Diabetic retinopathy (DR) is a severe and long-term vision-impairing disease. DR is characterized by complications such as

microaneurysms, exudates, hemorrhages, retinal neovascularization, and retinal edema. Because DR is considered a microvascular disease, various anti-VEGF approaches have been used clinically to prevent diabetic retinal neurovascular disease, including retinal neovascularization, vitreous hemorrhage, etc. However, anti-VEGF drugs cannot treat vision loss due to retinal ischemia and degeneration. Anti-VEGF drugs are also ineffective for treating early DR, although their effectiveness for advanced DR has been proven. A recent finding suggests that anti-VEGF may also impair neuronal survival and function (101).

Studies have shown that cell therapy using MSCs confers a specific protective effect on DR due to the immunomodulatory properties of MSCs (102, 103). However, due to ethical and safety issues related to MSCs transplantation, such as proliferative vitreoretinopathy, vitreous opacity, and vision loss (104), the treatment of DR with MSCs is still controversial. The therapeutic efficacy of MSCs is mainly attributable to paracrine-generated exosomes, whereby MSC-Exos have been shown to exert beneficial effects in ocular disease models (105–107). In recent years, researchers have reported that MSC-Exos could also significantly improve DR. Li et al. used real-time imaging methods such as fundus fluorescein angiography and optical coherence tomography to observe the fundus of rats. Combined with hematoxylin-eosin staining, it was observed that HucMSC-Exos could alleviate diabetes-induced retinal neuronal degeneration and inhibit microvascular disease. HucMSC-Exos also significantly reduced the loss of neuronal cells and retinal vascular damage in diabetic rats (108). A study revealed that HucMSC-Exos could transfer BDNF to retinal neurons and activate the BDNF-TrkB pathway to enhance high glucose (HG)-stimulated neuronal cell viability and inhibit its apoptosis (109). Another study reported that HucMSC-Exos transported miR-17-3p and ameliorated retinal inflammation and oxidative damage in DR mice by targeting STAT1 (110). Previous research has also revealed that BMMSC-Exos could inhibit oxidative stress, enhance angiogenesis, and induce an inflammatory reaction in the retinal cells of DR mice. The action is carried out by transporting miR-486-3p and miR-133b-3p through downregulation of the TLR4/NF-κB pathway and FBN1, respectively, resulting in inhibition of retinal cell

TABLE 1 The role of mesenchymal stem cell-derived exosomes in other diabetic complications.

Diabetic complications	Exosomes sources	Mechanism of action	Effect	Ref
Diabetic retinopathy	HucMSCs	Alleviates retinal neuronal degeneration Inhibits microvascular disease Reduces the loss of neuronal cells and retinal vascular damage	Alleviates the disease progression	(86)
	HucMSCs	Activates the BDNF-TrkB pathway	Enhances neuronal cell viability and inhibit its apoptosis	(87)
	HucMSCs	Transports miR-17-3p and targets STAT1	Ameliorates retinal inflammation and oxidative damage	(88)
	BMMSCs	Down-regulates TLR4/NF-κB pathway and FBN1	Inhibits the oxidative stress, angiogenesis enhancement and inflammatory reaction Reduces retinal cell apoptosis	(89, 90)
	BMMSCs	Interacts with the miR-34a-5p/XBP1 signaling pathway	Inhibits human retinal microvascular endothelial cells endothelial-mesenchymal transition (EndMT) and capillaries angiogenesis	(91)
Erectile dysfunction	AMSCs	Restores the expression of cGMP by transporting corin enhances the expressions of nNOS, ANP and BNP	Improves the impaired neurovascular function Inhibits the expression of inflammatory factors	(92)
	AMSCs	Transfers pro-angiogenic microRNA and anti-fibrotic microRNA	Shows angiogenic properties and induces endothelial cell proliferation Reduces cavernous fibrosis and restores erectile function	(93)
	BMMSCs	Inhibits programmed cell death 4(PDCD4)	Promotes CCSMCs proliferation, and Inhibits CCSMCs apoptosis	(94)
Diabetic osteoporosis	BMMSCs	Transfers miR-140-3p Inhibits plexinB1/RhoA/ROCK signaling pathway	Promotes osteogenesis	(95)
	AMSCs	Suppresses the activation of NLRP3 inflammasome	Inhibits the production and secretion of pro-inflammatory cytokines and the bone resorption of osteoclasts	(96)
Cognitive impairment	BMMSCs	Suppresses oxidative stress and increased synaptic density Inhibits the proliferation of microglia in the brain Restores abnormal ultrastructure of neurons, astrocytes and blood vessels	Alleviates the disease progression	(97)
Diabetic cardiomyopathy	BMMSCs	Inhibits TGF-β1/Smad2 signaling pathway	Ameliorates DM-induced myocardial injury and fibrosis	(98)
Peripheral neuropathy	BMMSCs	Transfers miR-146a inhibits TLR4/NF-κB pathway	Increases the number of intraepidermal nerve fibers, myelin sheath thickness, and axonal diameter of the sciatic nerve Suppresses pro-inflammatory gene expression	(99, 100)

apoptosis (111, 112). In addition, Song et al. reported that BMMSC-Exos carrying the lncRNA SNHG7 could inhibit HG-stimulated human retinal microvascular endothelial cells endothelial-mesenchymal transition and capillaries angiogenesis by interacting with the miR-34a-5p/XBP1 signaling pathway (113).

4.5.2 Mesenchymal stem cell-derived exosomes and erectile dysfunction

Erectile dysfunction is one of the major complications of diabetes, occurring in about 50% of men with diabetes within ten years of diagnosis (114). Various factors contribute to diabetic erectile dysfunction (DED), including hyperglycemia, hypertension, hyperlipidemia, insulin resistance, androgen deficiency, and vascular and neuronal abnormalities (115, 116). Mechanisms that mediate DED mainly include increased advanced glycation end products, impaired neuronal nitric oxide synthase (nNOS) synthesis, elevated levels of oxygen free radicals, and decreased levels of cyclic guanosine monophosphate (cGMP)-dependent kinase-1 and Nitric oxide (NO). Endothelial dysfunction is the primary pathophysiology of DED, which is characterized by the disability of the endothelium to generate vasodilatory messengers and maintain vasodilation and vascular homeostasis (117, 118). Growing evidence suggests that DED is a vascular disease (119).

AMSCs have attracted considerable attention as a practical cell transplantation resource for treating DED. Previous studies have demonstrated that the NO-cGMP pathway plays a vital role in maintaining normal erectile function since the loss of cGMP leads to DED (120). AMSC-Exos restored the expression of cGMP by transporting corin and enhanced the expressions of nNOS, ANP, and BNP. This action improved the impaired neurovascular function of DM rats and inhibited the expression of inflammatory factors, reversing the DED conditions caused by DM (121). Dai et al. demonstrated the angiogenic properties of AMSC-Exos, and their roles in inducing endothelial cells proliferation *in vitro*, reducing cavernous fibrosis, and restoring erectile function in diabetic rats. The study also reported the miRNA sequencing of AMSC-Exos, revealing the presence of pro-angiogenic (miR-126, miR-130a, and miR-132) microRNA and anti-fibrotic microRNA (miR-let7b and miR-let7c), which might have mediated the role of AMSC-Exos in improving the DED conditions (122). Part of the pathophysiology of DED involves a contraction-relaxation imbalance of smooth muscle cells (SMCs). Cavernous SMCs (CCSMCs) have been reported to modulate a phenotypic transition from a contractile to a proliferative state under hyperglycemic conditions, which may play an essential role in the pathogenesis of DED (123). Li et al. reported that BMMSC-Exos could transport miR-21-5p to inhibit programmed cell death 4 (PDCD4), promote CCSMCs proliferation, and inhibit CCSMCs apoptosis, improving DED in the DM rat model (124).

4.5.3 Mesenchymal stem cell-derived exosomes and diabetic osteoporosis

Growing evidence suggests a strong interaction between glucose levels and changes in bone metabolism. Impaired bone healing is considered a significant complication associated with DM. T2DM also causes changes in bone metabolism, impairs bone quality, and results in decreased bone strength, increased fracture risk, and impaired bone healing (125, 126). It was reported that the duration of fracture healing in DM patients is prolonged by 87% (127). BMMSCs are considered to be a promising source of engineered tissue cells that not only exhibit osteogenic differentiation properties but can also stimulate osteogenesis required for bone regeneration (128). Several studies have shown that exosomes mediate the role of MSCs in promoting osteogenesis and potentially regulating bone metabolism (129, 130). Furthermore, MSCs-Exos are more stable than MSCs for therapeutic intervention in specific physiological environments (131).

Studies have revealed that BMMSC-Exos also mediate the effect of BMMSCs in promoting osteogenesis, offering excellent potential in regulating bone metabolism. Wang et al. reported that both BMMSC-Exos of normal rats and BMMSC-Exos of diabetic rats could promote osteoblastogenesis and mineralization in BMMSCs of normal and DM rats, respectively. Additionally, Normal-BMMSC-Exos have demonstrated a more significant osteogenic effect on osteoblastogenesis than DM-BMMSC-Exos. Further studies found that BMMSC-Exos transfer miR-140-3p and miR-140-3p and promote osteogenesis by inhibiting the plexinB1/RhoA/ROCK signaling pathway (132). Inflammation is one of the leading causes of diabetic osteoporosis. Cheng et al. found that AMSC-Exos could inhibit the production and secretion of proinflammatory cytokines (e.g., IL-18 and IL-1β) in osteoclasts and inhibit the bone resorption by osteoclasts through the inactivation of NLRP3 inflammasome (133, 134). Studies have also revealed that AMSC-Exos overexpressing miR-146a exhibits a more substantial inhibitory effect than normal AMSC-Exo, whereas miR-146a-Exo inhibits the activation of the inflammasome by inhibiting HG-related osteoclast inflammatory response, improving diabetic osteoporosis *in vivo*.

4.5.4 Mesenchymal stem cell-derived exosomes and cognitive impairment

Diabetes-related cognitive impairment is a global challenge, with epidemiological studies reporting that the incidence of dementia in diabetic patients is two to three times higher than in nondiabetic patients. Multiple mechanisms are thought to contribute to diabetes-related dementia, including abnormal glucose metabolism (e.g., hyperglycemia and hypoglycemia), abnormal insulin action (e.g., insulin deficiency and insulin resistance), vascular abnormalities, and oxidative stress in the central nervous system (86, 135). The damage to hippocampal neurons and astrocytes is considered the most critical problem of

cognitive impairment caused by diabetes. Mineko Fujimiya et al. reported that BMMSC-Exos could improve learning and memory impairment in diabetic mice. It was also reported that BMMSC-Exos do not increase the number of neurons but suppress oxidative stress and increase synaptic density while inhibiting the proliferation of microglia in the brain from restoring the abnormal ultrastructure of neurons, astrocytes, and blood vessels (87).

4.5.5 Mesenchymal stem cell-derived exosomes and diabetic cardiomyopathy

Cardiovascular disease is the leading cause of death in diabetic patients, including diabetic cardiomyopathy. The main characteristics of diabetic cardiomyopathy include myocardial fibrosis, chronic inflammation, and cardiac structure and function changes caused by chronic hyperglycemia in the absence of myocardial ischemia and hypertensive heart disease (88, 89). Lin et al. demonstrated that BMMSC-Exos could ameliorate DM-induced myocardial injury and fibrosis by inhibiting the TGF-β1/Smad2 signaling pathway (90).

4.5.6 Mesenchymal stem cell-derived exosomes and peripheral neuropathy

Diabetic peripheral neuropathy (DPN) is one of the common chronic complications of diabetes (91). By 2030, around 50 million people worldwide will suffer from DPN (92). Therefore, there is an urgent need to develop effective therapies designed to improve DPN. Liu et al. reported that BMMSC-Exos significantly reduced thermal and mechanical stimulation thresholds and increased nerve conduction velocity in DPN mice. Histopathological analysis revealed that BMMSC-Exos significantly increased the density of FITC-dextran-perfused vessels and increased the number of intraepidermal nerve fibers, myelin sheath thickness, and axonal diameter of the sciatic nerve. BMMSC-Exos could also attenuate neurovascular dysfunction and facilitate functional recovery in DPN mice by inhibiting TLR4/NF-κB pathway and suppressing proinflammatory gene expression. Notably, studies have shown that BMMSC-Exos overexpressing miR-146a amplifies the therapeutic effect in DPN compared to normal exosomes (93, 94).

5 Mesenchymal stem cell-derived exosomes for drug delivery

The therapeutic roles of MSC-Exos in diabetes and related complications were summarized above. More and more studies demonstrated that MSC-Exos can be applied as carriers for drugs in addition to miRNAs, proteins, and other cargoes. The lipid bilayer membrane structure of MSC-Exos can protect the integrity and the biological activity of drugs, and the membrane modification of MSC-Exos can achieve targeted drug delivery. Additionally, the low immunogenicity, low tumorigenicity, and high biocompatibility of MSC-Exos guarantee the safety of treatment. Exosomes have been explored to load different drugs to treat various diseases. For instance, Wang et al. loaded miR-34a into BMMSC-Exos to treat glioma (136). Other researchers load chemotherapy drugs such as adriamycin and paclitaxel into MSC-Exos for the treatment of tumor diseases with reduced drug side effects (137, 138). In diabetes treatment, miR-21-5p mimics were loaded into AMSC-Exos for diabetic wound healing (83). In the future, it is intended to investigate MSC-Exos' potential to carry more potent drugs for the treatment of diabetes and related complications.

6 Which component in exosomes mediates the therapeutic effects?

Various cellular components, including RNAs (e.g., mRNAs, miRNAs, lincRNAs, etc.), DNAs, proteins, and lipids, are contained in exosomes (139) (Figure 1, left panel). However, nearly all current research has suggested that proteins and RNAs mediate the process of exosomes, whereas DNAs and lipids have received relatively little attention. MiRNAs are particularly prevalent in the research on several types of exosomal RNAs. Many studies have performed deep miRNA sequencing on MSC-Exos from various sources, or MSC-Exos that have been pretreated and genetically modified, to explore the roles of different miRNAs in different MSC-Exos for the treatment of other diseases (101, 102, 140). MiRNAs transported by exosomes serve critical roles in modulating the processes for treating diabetes and related complications. However, according to Toh et al., the concentration of pre-miRNAs in exosomes is inadequate to trigger biological reactions. Additionally, miRNAs are only biologically active when they bind to RNA-induced silencing complexes, yet exosomes typically lack the full RNA-induced silencing complexes.

Meanwhile, biological processes can be triggered by the concentration of proteins in exosomes at therapeutic doses, exhibiting ATP generation by a glycolytic enzyme, which suggests that proteins might be the primary driver of MSC-Exos therapeutic activity (103). With the development of proteomics technology, scientists can now identify the composition of proteins in exosomes and further analyze their functions. Numerous studies have identified the proteins in MSC-Exos from various sources. The proteomics of BMMSC-Exos, AMSC-Exos, and HucMSC-Exos was systematically and comprehensively researched, leading to the discovery of 431, 457, and 771 proteins, respectively. Bioinformatics analysis of the shared and unique proteins of the three exosomes revealed that HucMSC-Exos have remarkable tissue damage healing capacity.

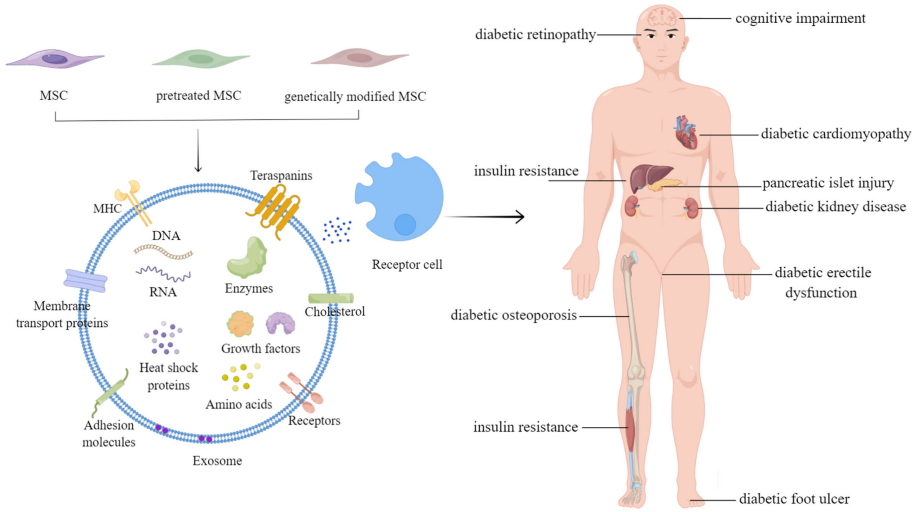

FIGURE 1
The applications of mesenchymal stem cell-derived exosomes in diabetes mellitus and related complications.

Additionally, the study suggested the regeneration ability of BMMSC-Exos and the role of AMSC-Exos in immune regulation (104). Proteomics has been used to research the functions of exosomes in various disorders, including heart attacks, pulmonary fibrosis, and Alzheimer's disease (105–107). Despite the application of proteomics, it is important to determine which protein is crucial in the pathogenesis of a disease.

In conclusion, the prevailing theory holds that exosomes play a critical role in controlling intercellular communication *via* proteins and miRNAs. There is a need for a comprehensive investigation of the mechanism of exosomes in treating diabetes and its related complications. Similarly, the roles of DNAs and lipids in exosomes cannot be disregarded.

7 How do we improve the therapeutic effects of exosomes?

As mentioned earlier, exosomes from various tissues have various therapeutic effects on diabetes and related complications. However, the paracrine action of MSCs may be easily affected in a physicochemical environment due to the potential replicative senescence and reduced stability during the passage process, which reduces their therapeutic efficiency. Therefore, it is vital to identify the correct approach to enhance the therapeutic effect of exosomes. Researchers have found that MSC-Exos could deliver a superior therapeutic effect when subjected to specific pretreatments or genetic modifications. In addition, biomaterials can be used to encapsulate exosomes to strengthen their controlled-release effect and broaden their therapeutic effects (Table 2).

Previous studies have shown that the pretreatment of MSCs with physical, chemical, and biological factors effectively enhances the biological activity of MSC-Exos and improves their repair efficacy in tissue engineering and regenerative medicine (108). For example, exosomes extracted from IL-1β-pretreated MSCs exhibited a higher IL-10 and TGF-β than exosomes extracted from untreated MSCs (109). In addition, hypoxia pretreatment increases angiogenesis and neuroprotection, improves MSCs proliferation and migration, and enhances MSCs engraftment efficiency compared to MSCs under normal culture conditions (110). Compared with normoxic exosomes, 215 miRNAs were upregulated, and 369 were downregulated in hypoxic AMSC-Exos. The upregulated miR-21-3p/miR-126-5p/miR-31-5p and the downregulated miR-99b/miR-146-a could activate the relevant signaling pathways, promoting fibroblast proliferation and migration (111). Deferoxamine has been shown to induce hypoxic effects. Studies have reported that both HypAMSC-Exos and deferoxamine-pretreated BMMSC-Exos could accelerate diabetic wound healing by regulating PI3K/AKT signaling pathway (111, 112). The activation of the PI3K/Akt/eNOS pathway is a key process in stimulating angiogenesis, enhancing human umbilical vein endothelial cells viability, and promoting capillary formation (113). NO produced by eNOS is a vasoactive substance secreted by the vascular endothelial system, which plays a vital role in maintaining vascular homeostasis (114). The activation of PI3K/Akt leads to phosphorylation of eNOS, resulting in NO production. Conversely, inhibition of the PI3K/Akt pathway results in reduced eNOS phosphorylation and inhibition of NO production, which is associated with endothelial cell dysfunction (115). Additionally, exosomes of

TABLE 2 The different exosome engineering strategies.

Diabetic complications	Exosomes sources	Pretreatment/Genetic modification/Biomaterials	Ref
Diabetic foot ulcer	AMSCs	Overexpressed mmu_circ_0000250	(81)
	AMSCs	Overexpressed linc00511	(82)
	AMSCs	Loaded miR-21-5p mimics	(83)
	AMSCs	Hypoxia pretreated	(111)
	BMMSCs	Deferoxamine pretreated	(112)
	BMMSCs	Atorvastatin pretreated	(116)
	BMMSCs	Pioglitazone pretreated	(117)
	BMMSCs	Melatonin pretreated	(120)
	HucMSCs	Lipopolysaccharide pretreated	(121)
	AMSCs	Overexpressed Nrf2	(122)
	HucMSCs	Nanohydrogel	(125)
	AMSCs	Hydrogel	(123)
	Synovium MSCs	Chitosan/overexpressed miR-126-3p	(127)
	Gingival mesenchymal stem cells	Chitosan/silk hydrogel	(128)
Diabetic osteoporosis	AMSCs	Overexpressed miR-146a	(141)
Peripheral neuropathy	BMMSCs	Overexpressed miR-146a	(100)

BMMSCs pretreated with atorvastatin and pioglitazone can activate the PI3K/AKT/eNOS pathway, enhance the biological function of human umbilical vein endothelial cells, and promote neovascularization (116, 117). Macrophage polarization plays an important role in diabetic wound healing. M1 macrophages produce proinflammatory cytokines such as IL-1β and TNF-α, which may lead to organ dysfunction. Meanwhile, M2 macrophages are related to the production and secretion of anti-inflammatory cytokines, associated with reduced inflammatory response (118). An increase in the M2 phenotype and a decrease in the M1 phenotype contribute to diabetic wound repair (119). In addition, both melatonin-pretreated BMMSC-Exos and lipopolysaccharide-pretreated HucMSC-Exos can enhance the polarization of macrophages toward the M2 phenotype, thereby inhibiting the inflammatory response and promoting diabetic wound healing (120, 121). Studies have also reported that AMSC-Exos overexpressing Nrf2 could alleviate the progression of DFU in diabetic patients by preventing endothelial progenitor cell senescence and inhibiting ROS and inflammatory cytokine expression. Such actions result in reduced inflammation, improved angiogenesis, and rapid wound healing (122).

Exosomes are typically injected to treat diabetic foot wound healing, but infection and other factors could aggravate even a tiny wound. However, achieving good treatment outcomes is challenging because exosomes are quickly cleared and easily inactivated *in vitro*. Therefore, researchers have designed various biomaterials to encapsulate and protect exosomes, improving their effectiveness and maintaining the moisture level in damaged tissues (123, 124).

Mei et al. demonstrated that the exosomes encapsulated in hydrogel could effectively promote skin cell proliferation, migration, and angiogenesis and accelerate the healing of diabetic wounds compared with the non-encapsulated exosome (123, 125, 126). A novel nanohydrogel (NH) composed of polyvinyl alcohol (PVA) and alginate (Alg) was combined with HucMSC-Exos to form an Exo@H complex. This complex could activate the ERK1/2 signaling pathway and elevate SMA, CD31, SR-B1, and VEGF expression in diabetic wound, mediating diabetic wound healing (125). An injectable, self-healing, and antibacterial polypeptide-based FHE hydrogel encapsulating AMSC-Exos has been demonstrated to accelerate granulation tissue formation, re-epithelialization, and collagen remodeling at the wound site. Compared with the FHE hydrogel group, the pure exosomes group, and the control group, the skin appendages were more abundant, and the scar tissue was reduced in the FHE@exo hydrogel group (123). Zhang et al. used chitosan to encapsulate exosomes derived from synovial mesenchymal stem cells overexpressing miR-126-3p (SMSC-126-Exos). They found that SMSC-126-Exos could significantly activate PI3K/AKT and MAPK/ERK pathways compared with pure SMSC-Exos.

Moreover, the controlled release of SMSC-126-Exos significantly increased re-epithelialization and collagen deposition at the wound site, activating and promoting neovascular maturation (127). In addition, a chitosan/silk hydrogel sponge biomaterial has also been used as a support for exosomes derived from gingival MSCs. The exosome-hydrogel complexes could promote the re-epithelialization, deposition, and remodeling of the extracellular matrix. These complexes also promote angiogenesis and neuronal ingrowth, accelerating cutaneous wound healing in STZ-induced diabetic rats (128).

Unfortunately, there are no universal pretreatments of MSCs that can be beneficial for the therapy of different diabetic

complications. Researchers should further investigate the mechanisms of exosomes in ameliorating diseases and explore the potential alternatives to modify the current methods.

8 Challenges and prospects

Diabetes and its complications can be treated effectively using MSC-Exos, as described in the preceding sections. However, it is necessary to resolve several issues before incorporating MSC-Exos in treating diabetes.

One key challenge in treating diabetes with MSC-Exos is the effect of residing tissues on MSC-Exos. According to previous studies, when exosomes were infused through the tail vein, only a few remained in the liver and spleen for 24 or 48 h (129, 130), probably because the liver and spleen are rich in blood. Therefore, it is crucial to explore the mechanisms of how MSC-Exos homing targets tissues and how it plays a long-term therapeutic role. It is interesting to know whether damaged target tissues secrete chemokines and cytokines that guide exosome homing *in vivo*. Several studies have revealed that MSCs can release various mediators, including immunosuppressive molecules, growth factors, exosomes, chemokines, complement components, and multiple metabolites, to regulate the inflammatory balance and microenvironment of damaged tissues when exposed to inflammatory environments (131). Exosomes may be dynamic depending on the state of the residing tissue, such as immunomodulation, tissue damage repair, or regeneration. It would be ideal for MSC-Exos to encourage angiogenesis when treating DFU but block it when treating DR. The finding suggests investigating why the same type of MSC-Exos can have opposing effects in various injured tissues.

Additionally, the controlled-release MSC-Exos technology applications in diabetes only apply to diabetic foot ulcers. There is a need to optimize the targeting and sustained-release technology of MSC-Exos *in vivo* to treat diabetic complications like the pancreatic injury, DKD and others. This optimization will prevent MSC-Exos from being destroyed by the physicochemical environment *in vivo* and help them play a long-term effect.

Secondly, MSC-Exos have been showing significant heterogeneity. MSC-Exos derived from different tissues have unique characteristics. Exosomes from different tissues have different proteomic characteristics, which can be used as a guide when choosing which exosomes to use for disease treatment (104, 132). Furthermore, exosomes from various tissue sources may have different therapeutic effects on the same disease. The use of MSCs from the same tissue source can rarely ensure the standardization of MSC-Exos content and their therapeutic effects on diseases because of the varied culture conditions, such as medium, cell production, and dimensions of the culture environment (two-dimensional or three-dimensional). Additionally, different exosome extraction methods can also cause heterogeneity in its contents. Therefore, when carrying out MSC-Exos therapy, it is important to consider an approach that can maximize the effectiveness of exosome therapy, i.e., ensuring the consistency in exosome isolation methods and the sources of exosomes, etc.

Finally, further clinical investigations are required to verify the therapeutic effect of MSC-Exos on diabetes and its associated complications. There have already been some clinical trials using MSC-Exos to treat these diseases (available online: http://www.clinicaltrials.gov/) (Table 3). In one of the clinical trials using UCBMSC-EV in chronic kidney disease, it was demonstrated that administration of UCBMSC-EV was safe and the treatment improved the inflammatory immune response and overall renal function in patients with grade III-IV CKD, as evidenced by significant improvements in eGFR, Scr, Bun and UACR, increases in plasma TGF-β1 and IL-10, and decreases in TNF-α plasma levels in these patients (133). Therefore, it is critical to conduct additional fundamental research and clinical trials. These studies will result in the discovery of novel treatments for diabetes and its related complications.

In addition to treating diseases, exosomes can be employed as natural drug carriers to deliver drugs, such as siRNAs, shRNAs, and other molecules. Modification of exosomes can enhance the therapeutic effect and targeting ability. For example, miR-21-5p mimics were electroporated into AMSC-Exos, exploiting the natural availability and biocompatibility of exosomes as extracellular miRNA transport particles to promote diabetic cutaneous wound healing (83). Exosomes carrying diverse therapeutic drugs may perform crucial therapeutic functions in the future.

Numerous nanovesicles can be generated by cell extrusion or polymer nanoparticles coated with cell membranes. These nanovesicles are called exosome mimetic vesicles (EMVs). While exosomes produced by cells are limited, EMVs are abundant. EMVs are comparable to exosomes in size, structure, and components and can also participate in cell-to-cell communication (134). Proteomic analysis of EMVs and exosomes derived from HucMSCs revealed that they share about 80% of the same protein while also containing unique proteins. EMVs and exosomes derived from HucMSCs have tissue repair ability, promoting wound healing and angiogenesis in mice (135). Future research must determine whether different MSC-derived EMVs have the same therapeutic effect as exosomes and whether they can be applied to diabetes and associated complications and other diseases.

Conclusion

Diabetes is a chronic condition that severely threatens global public health. This review outlines the roles and mechanisms of

TABLE 3 Clinical trial of MSC-Exos in the treatment of diabetes and related complications.

Disease	Intervention	Follow up	Location	State	ClinicalTrials.gov Identifier
Diabetes Mellitus Type 1	UCBMSC- microvesicles	3 months	Sahel Teaching Hospital Sahel, Cairo, Egypt, 11522	Unkown	NCT02138331
Foot, Diabetic	Personalized Nutritional Intervention and MSC-Exos	1/2/3 months	Hospital Universitario Reina Sofia de Córdoba Córdoba, Andalucía, Spain, 14004	Not yet recruiting	NCT05243368
Macular Holes	MSC-Exos	24 weeks	Tianjin Medical University Hospital Tianjin, China	Active, not recruiting	NCT03437759
Chronic Kidney Disease	UCBMSC- extracellular vesicles	1 year	Sahel Teaching Hospital Sahel, Cairo, Egypt, 11522	Concluded	(133)

MSC-Exos in treating diabetes and its related complications (Figure 1). MSC-Exos have shown promising results in treating diabetes and may develop into a successful strategy for treating diabetes and complications in the future.

Author contributions

LC and JC designed and supervised the study. MY performed and drafted the manuscript. All authors contributed to the article and approved the submitted version.

Funding

This work was supported by the National Natural Science Foundation of China (82070800; LC) and Shandong Excellent Young Scientists Fund Program (Overseas, 2022HWYQ-027; JC).

Conflict of interest

The authors declare that the research was conducted in the absence of any commercial or financial relationships that could be construed as a potential conflict of interest.

Publisher's note

References

1. Diagnosis and classification of diabetes mellitus. *Diabetes Care* (2013), 36(Suppl 1): S67–74. doi: 10.2337/dc13-S067

2. Schmidt A. Highlighting diabetes mellitus: The epidemic continues. *Arterioscler Thromb Vasc Biol* (2018) 38(1):e1–8. doi: 10.1161/ATVBAHA.117.310221

3. Zheng Y, Ley SH, Hu FB. Global aetiology and epidemiology of type 2 diabetes mellitus and its complications. *Nat Rev Endocrinol* (2018) 14(2):88–98. doi: 10.1038/nrendo.2017.151

4. Bhattarai S, Godsland LF, Misra S, Johnston DG, Oliver N. Metabolic health and vascular complications in type 1 diabetes. *J Diabetes Complicat* (2019) 33 (9):634–40. doi: 10.1016/j.jdiacomp.2019.05.026

5. Uccelli A, Moretta L, Pistoia V. Mesenchymal stem cells in health and disease. *Nat Rev Immunol* (2008) 8(9):726–36. doi: 10.1038/nri2395

6. Ding D, Shyu W, Lin S. Mesenchymal stem cells. *Cell Transplant* (2011) 20 (1):5–14. doi: 10.3727/096368910X

7. Castro-Manrreza M, Montesinos J. Immunoregulation by mesenchymal stem cells: biological aspects and clinical applications. *J Immunol Res* (2015) 2015:394917. doi: 10.1155/2015/394917

8. Yu B, Zhang X, Li X. Exosomes derived from mesenchymal stem cells. *Int J Mol Sci* (2014) 15(3):4142–57. doi: 10.3390/ijms15034142

9. Rosset P, Deschaseaux F, Layrolle P. Cell therapy for bone repair. *Orthop Traumatol Surg Res* (2014) 100(1 Suppl):S107–12. doi: 10.1016/j.otsr.2013.11.010

10. Pixley JS. Mesenchymal stem cells to treat type 1 diabetes. *Biochim Biophys Acta Mol Basis Dis* (2020) 1866(4):165315. doi: 10.1016/j.bbadis.2018.10.033

11. Xiang E, Han B, Zhang Q, Rao W, Wang ZF, Chang C, et al. Human umbilical cord-derived mesenchymal stem cells prevent the progression of early diabetic nephropathy through inhibiting inflammation and fibrosis. *Stem Cell Res Ther* (2020) 11(1):336. doi: 10.1186/s13287-020-01852-y

12. Qi Y, Ma J, Li S, Liu W. Applicability of adipose-derived mesenchymal stem cells in treatment of patients with type 2 diabetes. *Stem Cell Res Ther* (2019) 10 (1):274. doi: 10.1186/s13287-019-1362-2

13. Nagaishi K, Ataka K, Echizen E, Arimura Y, Fujimiya M. Mesenchymal stem cell therapy ameliorates diabetic hepatocyte damage in mice by inhibiting infiltration of bone marrow-derived cells. *Hepatology* (2014) 59(5):1816–29. doi: 10.1002/hep.26975

14. Osugi M, Katagiri W, Yoshimi R, Lnukai T, Hibi H, Ueda M. Conditioned media from mesenchymal stem cells enhanced bone regeneration in rat calvarial bone defects. *Tissue Eng Part A* (2012) 18(13-14):1479–89. doi: 10.1089/ten.tea.2011.0325

15. Tatsumi K, Ohashi K, Matsubara K, Kohori A, Ohno T, Kakidchi H, et al. Tissue factor triggers procoagulation in transplanted mesenchymal stem cells

leading to thromboembolism. *Biochem Biophys Res Commun* (2013) 431(2):203–9. doi: 10.1016/j.bbrc.2012.12.134

16. Zimmermann CE, Gierloff M, Hedderich J, Acil Y, Wiltfang J, Terheyden H. Survival of transplanted rat bone marrow-derived osteogenic stem cells *in vivo*. *Tissue Eng Part A* (2011) 17(7-8):1147–56. doi: 10.1089/ten.tea.2009.0577

17. Barkholt L, Flory E, Jekerle V, Lucas-Samuel S, Ahnert L, Bisset L, et al. Risk of tumorigenicity in mesenchymal stromal cell-based therapies–bridging scientific observations and regulatory viewpoints. *Cytotherapy* (2013) 15(7):753–9. doi: 10.1016/j.jcyt.2013.03.005

18. Zhu W, Xu W, Jiang R, Qian H, Chen M, Hu J, et al. Mesenchymal stem cells derived from bone marrow favor tumor cell growth *in vivo*. *Exp Mol Pathol* (2006) 80(3):267–74. doi: 10.1016/j.yexmp.2005.07.004

19. Zhao X, Zhan Y, Sun X, Xing Y, Wang X, Yang Q. Immunomodulation of MSCs and MSC-derived extracellular vesicles in osteoarthritis. *Front Bioeng Biotechnol* (2020) 8:575057. doi: 10.3389/fbioe.2020.575057

20. Guillamat-Prats R. The role of MSC in wound healing, scarring and regeneration. *Cells* (2021) 10(7): 1729. doi: 10.3390/cells10071729

21. Mathew B, Ravindran S, Liu X, Torres L, Chennakesavalu M, Huang CC, et al. Mesenchymal stem cell-derived extracellular vesicles and retinal ischemia-reperfusion. *Biomaterials* (2019) 197:146–60. doi: 10.1016/j.biomaterials.2019.01.016

22. Shabbir A, Cox A, Rodriguez-Menocal L, Salgado M, Badivas EV. Mesenchymal stem cell exosomes induce proliferation and migration of normal and chronic wound fibroblasts, and enhance angiogenesis *in vitro*. *Stem Cells Dev* (2015) 24(14):1635–47. doi: 10.1089/scd.2014.0316

23. Nakano M, Kubota K, Kobayashi E, Chikenji TS, Saito Y, Konari N, et al. Bone marrow-derived mesenchymal stem cells improve cognitive impairment in an alzheimer's disease model by increasing the expression of microRNA-146a in hippocampus. *Sci Rep* (2020) 10(1):10772. doi: 10.1038/s41598-020-67460-1

24. Keshtkar S, Kaviani M, Sarvestani FS, Ghahremani MH, Aghdaei MH, AI-Abdullah IH, et al. Exosomes derived from human mesenchymal stem cells preserve mouse islet survival and insulin secretion function. *EXCLI J* (2020) 19:1064–80. doi: 10.17179/excli2020-2451

25. Keshtkar S, Azarpira N, Ghahremani MH. Mesenchymal stem cell-derived extracellular vesicles: novel frontiers in regenerative medicine. *Stem Cell Res Ther* (2018) 9(1):63. doi: 10.1186/s13287-018-0791-7

26. Mohamed-Ahmed S, Fristad I, Lie SA, Suliman S, Mustafa K, Vindenes H, et al. Adipose-derived and bone marrow mesenchymal stem cells: a donor-matched comparison. *Stem Cell Res Ther* (2018) 9(1):168. doi: 10.1186/s13287-018-0914-1

27. Heo JS, Choi Y, Kim HS, Kim HO. Comparison of molecular profiles of human mesenchymal stem cells derived from bone marrow, umbilical cord blood, placenta and adipose tissue. *Int J Mol Med* (2016) 37(1):115–25. doi: 10.3892/ijmm.2015.2413

28. Karagianni M, Brinkmann I, Kinzebach S, Grassl M, Weiss C, Bugert P, et al. A comparative analysis of the adipogenic potential in human mesenchymal stromal cells from cord blood and other sources. *Cytotherapy* (2013) 15(1):76–88. doi: 10.1016/j.jcyt.2012.11.001

29. Amable PR, Teixeira MVT, Carias RBV, Granjeiro JM, Borojevic R. Protein synthesis and secretion in human mesenchymal cells derived from bone marrow, adipose tissue and wharton's jelly. *Stem Cell Res Ther* (2014) 5(2):53. doi: 10.1186/scrt442

30. Donders R, Bogie JFJ, Ravanidis S, Gervois P, Vanheusden M, Maree R, et al. Human wharton's jelly-derived stem cells display a distinct immunomodulatory and proregenerative transcriptional signature compared to bone marrow-derived stem cells. *Stem Cells Dev* (2018) 27(2):65–84. doi: 10.1089/scd.2017.0029

31. Christy BA, Herzig MC, Montgomery RK, Delavan C, Bynum JA, Reddoch KM, et al. Procoagulant activity of human mesenchymal stem cells. *J Trauma Acute Care Surg* (2017) 83(1 Suppl 1):S164–9. doi: 10.1097/TA.0000000000001485

32. Shiratsuki S, Terai S, Murata Y, Takami T, Yamamoto N, Fujisawa K, et al. Enhanced survival of mice infused with bone marrow-derived as compared with adipose-derived mesenchymal stem cells. *Hepatol Res* (2015) 45(13):1353–9. doi: 10.1111/hepr.12507

33. Li X, Bai J, Ji X, Li R, Yuan Y, Wang Y. Comprehensive characterization of four different populations of human mesenchymal stem cells as regards their immune properties, proliferation and differentiation. *Int J Mol Med* (2014) 34 (3):695–704. doi: 10.3892/ijmm.2014.1821

34. Petrenko Y, Vackova I, Kekulova K, Chudickova, M, Koci Z, Turnovcova K, et al. A comparative analysis of multipotent mesenchymal stromal cells derived from different sources, with a focus on neuroregenerative potential. *Sci Rep* (2020) 10(1):4290. doi: 10.1038/s41598-020-61167-z

35. Jin HJ, Bae YK, Kim M, Kwon SJ, Jeon HB, Choi SJ, et al. Comparative analysis of human mesenchymal stem cells from bone marrow, adipose tissue, and umbilical cord blood as sources of cell therapy. *Int J Mol Sci* (2013) 14(9):17986–8001. doi: 10.3390/ijms140917986

36. Kalluri R. The biology and function of exosomes in cancer. *J Clin Invest* (2016) 126(4):1208–15. doi: 10.1172/JCI81135

37. Mathieu M, Martin-Jaular L, Lavieu G, Thery C. Specificities of secretion and uptake of exosomes and other extracellular vesicles for cell-to-cell communication. *Nat Cell Biol* (2019) 21(1):9–17. doi: 10.1038/s41556-018-0250-9

38. Hessvik NP, Llorente A. Current knowledge on exosome biogenesis and release. *Cell Mol Life Sci* (2018) 75(2):193–208. doi: 10.1007/s00018-017-2595-9

39. He C, Zheng S, Luo Y, Wang B. Exosome theranostics: Biology and translational medicine. *Theranostics* (2018) 8(1):237–55. doi: 10.7150/thno.21945

40. Wang Z, Xie Z, Lu Q, Chang C, Zhou Z. Beyond genetics: What causes type 1 diabetes. *Clin Rev Allergy Immunol* (2017) 52(2):273–86. doi: 10.1007/s12016-016-8592-1

41. Pang H, Luo S, Huang G, Xia Y, Xie Z, Zhou Z. Advances in knowledge of candidate genes acting at the beta-cell level in the pathogenesis of T1DM. *Front Endocrinol (Lausanne)* (2020) 11:119. doi: 10.3389/fendo.2020.00119

42. Nojehdehi S, Soudi S, Hesampour A, Rasouli S, Soleimani M, Hashemi SM. Immunomodulatory effects of mesenchymal stem cell-derived exosomes on experimental type-1 autoimmune diabetes. *J Cell Biochem* (2018) 119(11):9433–43. doi: 10.1002/jcb.27260

43. Ilonen J, Lempainen J, Veijola R. The heterogeneous pathogenesis of type 1 diabetes mellitus. *Nat Rev Endocrinol* (2019) 15(11):635–50. doi: 10.1038/s41574-019-0254-y

44. Mahdipour E, Salmasi Z, Sabeti N. Potential of stem cell-derived exosomes to regenerate beta islets through pdx-1 dependent mechanism in a rat model of type 1 diabetes. *J Cell Physiol* (2019) 234(11):20310–21. doi: 10.1002/jcp.28631

45. Sabry D, Marzouk S, Zakaria R, Ibrahim HA, Samir M. The effect of exosomes derived from mesenchymal stem cells in the treatment of induced type 1 diabetes mellitus in rats. *Biotechnol Lett* (2020) 42(8):1597–610. doi: 10.1007/s10529-020-02908-y

46. Danobeitia JS, Fernandez LA. Clinical islet transplantation: recent advances in the field. *Clin Transpl* (2012), 193–200.

47. Cross SE, Richards SK, Clark A, Benest AV, Bates DO, Mathieson PW, et al. Vascular endothelial growth factor as a survival factor for human islets: effect of immunosuppressive drugs. *Diabetologia* (2007) 50(7):1423–32. doi: 10.1007/s00125-007-0670-8

48. Miao G, Ostrowski RP, Mace J, Hough J, Hopper A, Peverini R, et al. Dynamic production of hypoxia-inducible factor-1alpha in early transplanted islets. *Am J Transplant* (2006) 6(11):2636–43. doi: 10.1111/j.1600-6143.2006.01541.x

49. Downward J. PI 3-kinase, akt and cell survival. *Semin Cell Dev Biol* (2004) 15 (2):177–82. doi: 10.1016/j.semcdb.2004.01.002

50. Wen D, Peng Y, Liu D, Weizmann Y, Mahato RI. Mesenchymal stem cell and derived exosome as small RNA carrier and immunomodulator to improve islet transplantation. *J Control Rel* (2016) 238:166–75. doi: 10.1016/j.jconrel.2016.07.044

51. Rahman MJ, Regn D, Bashratyan R, Dai YD. Exosomes released by islet-derived mesenchymal stem cells trigger autoimmune responses in NOD mice. *Diabetes* (2014) 63(3):1008–20. doi: 10.2337/db13-0859

52. Nyenwe EA, Jerkins TW, Umpierrez GE, Kitabchi AE. Management of type 2 diabetes: evolving strategies for the treatment of patients with type 2 diabetes. *Metabolism* (2011) 60(1):1–23. doi: 10.1016/j.metabol.2010.09.010

53. Alam F, Islam MA, Khalil MI, Gan SH. Metabolic control of type 2 diabetes by targeting the GLUT4 glucose transporter: Intervention approaches. *Curr Pharm Des* (2016) 22(20):3034–49. doi: 10.2174/1381612822666160307145801

54. Sun Y, Shi H, Yin S, Ji C, Zhang X, Zhang B, et al. Human mesenchymal stem cell derived exosomes alleviate type 2 diabetes mellitus by reversing peripheral insulin resistance and relieving beta-cell destruction. *ACS Nano* (2018) 12(8):7613–28. doi: 10.1021/acsnano.7b07643

55. Yap SK, Tan KL, Rahaman NYA, Hamid NFS, Ooi DU, Tor YS, et al. Human umbilical cord mesenchymal stem cell-derived small extracellular vesicles ameliorated insulin resistance in type 2 diabetes mellitus rats. *Pharmaceutics* (2022) 14(3): 649. doi: 10.3390/pharmaceutics14030649

56. Dionne KE, Colton CK, Yarmush ML. Effect of hypoxia on insulin secretion by isolated rat and canine islets of langerhans. *Diabetes* (1993) 42(1):12–21. doi: 10.2337/diab.42.1.12

57. Sato Y, Inoue M, Yoshizawa T, Yamagata K. Moderate hypoxia induces beta-cell dysfunction with HIF-1-independent gene expression changes. *PloS One* (2014) 9(12):e114868. doi: 10.1371/journal.pone.0114868

58. Chen J, Chen J, Cheng Y, Fu Y, Zhao H, Tang M, et al. Mesenchymal stem cell-derived exosomes protect beta cells against hypoxia-induced apoptosis via miR-21 by alleviating ER stress and inhibiting p38 MAPK phosphorylation. *Stem Cell Res Ther* (2020) 11(1):97. doi: 10.1186/s13287-020-01610-0

59. Sharma R, Kumari M, Mishra S, Chaudhary Dk, Kumar A, Avni B, et al. Exosomes secreted by umbilical cord blood-derived mesenchymal stem cell attenuate diabetes in mice. *J Diabetes Res 2021* (2021), 2021, 9534574. doi: 10.1155/2021/9534574

60. Martinez-Castelao A, Navarro-Gonzalez JF, Gorriz JL, Alvaro FD. The concept and the epidemiology of diabetic nephropathy have changed in recent years. *J Clin Med* (2015) 4(6):1207–16. doi: 10.3390/jcm4061207

61. Forbes JM, Coughlan MT, Cooper ME. Oxidative stress as a major culprit in kidney disease in diabetes. *Diabetes* (2008) 57(6):1446–54. doi: 10.2337/db08-0057.

62. Abbate M, Zoja C, Remuzzi G. How does proteinuria cause progressive renal damage? *J Am Soc Nephrol* (2006) 17(11):2974–84. doi: 10.1681/ASN.2006040377

63. Yang D, Livingston MJ, Liu Z, Dong G, Zhang M, Chen JK, et al. Autophagy in diabetic kidney disease: regulation, pathological role and therapeutic potential. *Cell Mol Life Sci* (2018) 75(4):669–88. doi: 10.1007/s00018-017-2639-1

64. Ebrahim N, Ahmed IA, Hussien N, Dessouky AA, Farid AS, Elshazly AM, et al. Mesenchymal stem cell-derived exosomes ameliorated diabetic nephropathy by autophagy induction through the mTOR signaling pathway. *Cells* (2018) 7(12): 226. doi: 10.3390/cells7120226

65. Hao Y, Miao J, Liu W, Cai K, Huang X, Peng L, et al. Mesenchymal stem cell-derived exosomes carry MicroRNA-125a to protect against diabetic nephropathy by targeting histone deacetylase 1 and downregulating endothelin-1. *Diabetes Metab Syndr Obes* (2021) 14:1405–18. doi: 10.2147/DMSO.S286191

66. Mao R, Shen J, Hu X. BMSCs-derived exosomal microRNA-let-7a plays a protective role in diabetic nephropathy via inhibition of USP22 expression. *Life Sci* (2021) 268:118937. doi: 10.1016/j.lfs.2020.118937

67. Wang S, Bao L, Fu W, Deng L, Ran J. Protective effect of exosomes derived from bone marrow mesenchymal stem cells on rats with diabetic nephropathy and its possible mechanism. *Am J Transl Res* (2021) 13(6):6423–30.

68. Zhou LL, Hou FF, Wang GB, Yang F, Xie D, Wang YP, et al. Accumulation of advanced oxidation protein products induces podocyte apoptosis and deletion through NADPH-dependent mechanisms. *Kidney Int* (2009) 76(11):1148–60. doi: 10.1038/ki.2009.322

69. Duan YR, Chen BP, Chen F, Yang SX, Zhu CY, Ma YL, et al. Exosomal microRNA-16-5p from human urine-derived stem cells ameliorates diabetic nephropathy through protection of podocyte. *J Cell Mol Med* (2021) 25 (23):10798–813. doi: 10.1111/jcmm.14558

70. Jin J, Wang Y, Zhao L, Zou W, Tan M, He Q. Exosomal miRNA-215-5p derived from adipose-derived stem cells attenuates epithelial-mesenchymal transition of podocytes by inhibiting ZEB2. *BioMed Res Int 2020* (2020), 2020: 2685305. doi: 10.1155/2020/2685305

71. Nagaishi K, Mizue Y, Chikenji T, Otani M, Nakano M, Konari N, et al. Mesenchymal stem cell therapy ameliorates diabetic nephropathy via the paracrine effect of renal trophic factors including exosomes. *Sci Rep* (2016); 6: 34842. doi: 10.1038/srep34842

72. Zhang Y, Le X, Zheng S, Zhang K, He J, Liu M, et al. MicroRNA-146a-5p-modified human umbilical cord mesenchymal stem cells enhance protection against diabetic nephropathy in rats through facilitating M2 macrophage polarization. *Stem Cell Res Ther* (2022) 13(1):171. doi: 10.1186/s13287-022-02855-7

73. Zubiri I, Posada-Ayala M, Benito-Martin A, Maroto A, Martin-Lorenzo M, Cannata-Ortiz P, et al. Kidney tissue proteomics reveals regucalcin downregulation in response to diabetic nephropathy with reflection in urinary exosomes. *Transl Res* (2015) 166(5):474–484.e4. doi: 10.1016/j.trsl.2015.05.007

74. Kalani A, Mohan A, Godbole MM, Bhatia E, Gupta A, Sharma RK, et al. Wilm's tumor-1 protein levels in urinary exosomes from diabetic patients with or without proteinuria. *PloS One* (2013) 8(3):e60177. doi: 10.1371/journal.pone.0060177

75. Zhang P, Lu J, Jing Y, Tang S, Zhu D, Bi Y. Global epidemiology of diabetic foot ulceration: a systematic review and meta-analysis (dagger). *Ann Med* (2017) 49 (2):106–16. doi: 10.1080/07853890.2016.1231932

76. Prompers L, Schaper N, Apelqvist J, Edmonds M, Jude E, Mauricio D, et al. Prediction of outcome in individuals with diabetic foot ulcers: focus on the differences between individuals with and without peripheral arterial disease. the EURODIALE study. *Diabetologia* (2008) 51(5):747–55. doi: 10.1007/s00125-008-0940-0

77. Sinwar PD. The diabetic foot management - recent advance. *Int J Surg* (2015) 15:27–30. doi: 10.1016/j.ijsu.2015.01.023

78. Martin P. Wound healing–aiming for perfect skin regeneration. *Science* (1997) 276(5309):75–81. doi: 10.1126/science.276.5309.75

79. Li B, Luan S, Chen J, Zhou Y, Wang T, Li Z, et al. The MSC-derived exosomal lncRNA H19 promotes wound healing in diabetic foot ulcers by upregulating PTEN via MicroRNA-152-3p. *Mol Ther Nucleic Acids* (2020) 19:814–26. doi: 10.1016/j.omtn.2019.11.034

80. Zhao B, Zhang X, Zhang Y, Lu Y, Zhang W, Lu S, et al. Human exosomes accelerate cutaneous wound healing by promoting collagen synthesis in a diabetic mouse model. *Stem Cells Dev* (2021) 30(18):922–33. doi: 10.1089/scd.2021.0100

81. Shi R, Jin Y, Hu W, Lian W, Cao C, Han S, et al. Exosomes derived from mmu_circ_0000250-modified adipose-derived mesenchymal stem cells promote wound healing in diabetic mice by inducing miR-128-3p/SIRT1-mediated autophagy. *Am J Physiol Cell Physiol* (2020) 318(5):C848–56. doi: 10.1152/ajpcell.00041.2020

82. Qiu J, Shu C, Li X, Ye C, Zhang WC. Exosomes from linc00511-overexpressing ADSCs accelerates angiogenesis in diabetic foot ulcers healing by suppressing PAQR3-induced Twist1 degradation. *Diabetes Res Clin Pract* (2021) 180:109032. doi: 10.1016/j.diabres.2021.109032

83. Lv Q, Deng J, Chen Y, Wang Y, Liu B, Liu J. Engineered human adipose stem-Cell-Derived exosomes loaded with miR-21-5p to promote diabetic cutaneous wound healing. *Mol Pharm* (2020) 17(5):1723–33. doi: 10.1021/acs.molpharmaceut.0c00177

84. Yan C, Xv Y, Lin Z, Endo Y, Xue H, Hu Y, et al. Human umbilical cord mesenchymal stem cell-derived exosomes accelerate diabetic wound healing via ameliorating oxidative stress and promoting angiogenesis. *Front Bioeng Biotechnol* (2022) 10:829868. doi: 10.3389/fbioe.2022.829868

85. Dalirfardouei R, Jamialahmadi K, Jafarian AH, Mahdipour E. Promising effects of exosomes isolated from menstrual blood-derived mesenchymal stem cell on wound-healing process in diabetic mouse model. *J Tissue Eng Regener Med* (2019) 13(4):555–68. doi: 10.1002/term.2799

86. Fu Y, Gao X, He GH, Chen S, Gu ZH, Zhang YL, et al. Protective effects of umbilical cord mesenchymal stem cell exosomes in a diabetic rat model through live retinal imaging. *Int J Ophthalmol* (2021) 14(12):1828–33. doi: 10.18240/ijo.2021.12.04

87. Gao X, He GH, Zhang XT, Chen S. Protective effect of human umbilical cord mesenchymal stem cell-derived exosomes on rat retinal neurons in hyperglycemia through the brain-derived neurotrophic factor/TrkB pathway. *Int J Ophthalmol* (2021) 14(11):1683–9. doi: 10.18240/ijo.2021.11.06

88. Li W, Jin LY, Cui YB, Xie N. Human umbilical cord mesenchymal stem cells-derived exosomal microRNA-17-3p ameliorates inflammatory reaction and antioxidant injury of mice with diabetic retinopathy via targeting STAT1. *Int Immunopharmacol* (2021) 90:107010. doi: 10.1016/j.intimp.2020.107010

89. Li W, Jin L, Cui Y, Nie A, Xie N, Liang G. Bone marrow mesenchymal stem cells-induced exosomal microRNA-486-3p protects against diabetic retinopathy through TLR4/NF-kappaB axis repression. *J Endocrinol Invest* (2021) 44(6):1193–207. doi: 10.1007/s40618-020-01405-3

90. Liang G, Qin Z, Luo Y, Yin J, Shi Z, Wei R, et al. Exosomal microRNA-133b-3p from bone marrow mesenchymal stem cells inhibits angiogenesis and oxidative stress via FBN1 repression in diabetic retinopathy. *Gene Ther* (2022). doi: 10.1038/s41434-021-00310-5

91. Cao X, Xue LD, Di Y, Li T, Tian YJ, Song Y. MSC-derived exosomal lncRNA SNHG7 suppresses endothelial-mesenchymal transition and tube formation in diabetic retinopathy via miR-34a-5p/XBP1 axis. *Life Sci* (2021) 272:119232. doi: 10.1016/j.lfs.2021.119232

92. Wang J, Mi Y, Wu S, You X, Huang Y, Zhu J, et al. Exosomes from adipose-derived stem cells protect against high glucose-induced erectile dysfunction by delivery of corin in a streptozotocin-induced diabetic rat model. *Regener Ther* (2020) 14:227–33. doi: 10.1016/j.reth.2020.03.002

93. Zhu LL, Huang X, Yu W, Chen H, Chen Y, Dai YT. Transplantation of adipose tissue-derived stem cell-derived exosomes ameliorates erectile function in diabetic rats. *Andrologia* (2018) 50(2). doi: 10.1111/and.12871

94. Huo W, Li Y, Zhang Y, Li H. Mesenchymal stem cells-derived exosomal microRNA-21-5p downregulates PDCD4 and ameliorates erectile dysfunction in a rat model of diabetes mellitus. *FASEB J* (2020) 34(10):13345–60. doi: 10.1096/fj.202000102RR

95. Wang N, Liu X, Tang Z, Wei X, Dong H, Liu Y, et al. Increased BMSC exosomal miR-140-3p alleviates bone degradation and promotes bone restoration by targeting Plxnb1 in diabetic rats. *J Nanobiotechnol* (2022) 20(1):97. doi: 10.1186/s12951-022-01267-2

96. Zhang L, Wang Q, Su H, Cheng J. Exosomes from adipose derived mesenchymal stem cells alleviate diabetic osteoporosis in rats through suppressing NLRP3 inflammasome activation in osteoclasts. *J Biosci Bioeng* (2021) 131(6):671–8. doi: 10.1016/j.jbiosc.2021.02.007

97. Nakano M, Nagaishi K, Konari N, Saito Y, Chikenji T, Mizue Y, et al. Bone marrow-derived mesenchymal stem cells improve diabetes-induced cognitive impairment by exosome transfer into damaged neurons and astrocytes. *Sci Rep* (2016) 6:24805. doi: 10.1038/srep24805

98. Lin Y, Zhang F, Lian XF, Peng WQ, Yin CY. Mesenchymal stem cell-derived exosomes improve diabetes mellitus-induced myocardial injury and fibrosis via inhibition of TGF-beta1/Smad2 signaling pathway. *Cell Mol Biol (Noisy-le-grand)* (2019) 65(7):123–6. doi: 10.14715/cmb/2019.65.7.21

99. Fan B, Li C, Szalad A, Wang L, Pan W, Zhang R, et al. Mesenchymal stromal cell-derived exosomes ameliorate peripheral neuropathy in a mouse model of diabetes. *Diabetologia* (2020) 63(2):431–43. doi: 10.1007/s00125-019-05043-0

100. Fan B, Chopp M, Zhang ZG, Liu XS. Treatment of diabetic peripheral neuropathy with engineered mesenchymal stromal cell-derived exosomes enriched

with microRNA-146a provide amplified therapeutic efficacy. *Exp Neurol* (2021) 341:113694. doi: 10.1016/j.expneurol.2021.113694

101. Cao JY, Wang B, Tang TT, Wen Y, Li ZL, Feng ST, et al. Exosomal miR-125b-5p deriving from mesenchymal stem cells promotes tubular repair by suppression of p53 in ischemic acute kidney injury. *Theranostics* (2021) 11 (11):5248–66. doi: 10.7150/thno.54550

102. Casado-Diaz A, Quesada-Gomez JM, Dorado G. Extracellular vesicles derived from mesenchymal stem cells (MSC) in regenerative medicine: Applications in skin wound healing. *Front Bioeng Biotechnol* (2020) 8:146. doi: 10.3389/fbioe.2020.00146

103. Toh WS, Lai RC, Zhang B, Lim SK. MSC exosome works through a protein-based mechanism of action. *Biochem Soc Trans* (2018) 46(4):843–53. doi: 10.1042/BST20180079

104. Wang ZG, He ZY, Liang S, Yang Q, Cheng P, Chen AM. Comprehensive proteomic analysis of exosomes derived from human bone marrow, adipose tissue, and umbilical cord mesenchymal stem cells. *Stem Cell Res Ther* (2020) 11(1):511. doi: 10.1186/s13287-020-02032-8

105. Kore RA, Wang X, Ding Z, Griffin R, Tackett AJ, Mehta JL. MSC exosome-mediated cardioprotection in ischemic mouse heart comparative proteomics of infarct and peri-infarct areas. *Mol Cell Biochem* (2021) 476(4):1691–704. doi: 10.1007/s11010-020-04029-6

106. Mansouri N, Willis GR, Fernandez-Gonzalez A, Reis M, Nassiri S, Mitsialis SA, et al. Mesenchymal stromal cell exosomes prevent and revert experimental pulmonary fibrosis through modulation of monocyte phenotypes. *JCI Insight* (2019) 4(21). doi: 10.1172/jci.insight.128060

107. Reza-Zaldivar EE, Hernandez-Sapiens MA, Minjarez B, Gutierrez-Mercado YK, Marquez- Aguirre AL, Canales-Aguirre AA. Potential effects of MSC-derived exosomes in neuroplasticity in alzheimer's disease. *Front Cell Neurosci* (2018) 12:317. doi: 10.3389/fncel.2018.00317

108. Hu C, Li L. Preconditioning influences mesenchymal stem cell properties *in vitro* and *in vivo*. *J Cell Mol Med* (2018) 22(3):1428–42. doi: 10.1111/jcmm.13492

109. Mokarizadeh A, Delirezh N, Morshedi A, Mosayebi G, Farshid AA, Maidani K. Microvesicles derived from mesenchymal stem cells: potent organelles for induction of tolerogenic signaling. *Immunol Lett* (2012) 147(1-2):47–54. doi: 10.1016/j.imlet.2012.06.001

110. Ferrer RA, Wobus M, List C, Wehner R, Schonfeldt C, Brocard B, et al. Mesenchymal stromal cells from patients with myelodyplastic syndrome display distinct functional alterations that are modulated by lenalidomide. *Haematologica* (2013) 98(11):1677–85. doi: 10.3324/haematol.2013.083972

111. Wang J, Wu H, Peng Y, Zhao Y, Qin Y, Zhang Y, et al. Hypoxia adipose stem cell-derived exosomes promote high-quality healing of diabetic wound involves activation of PI3K/Akt pathways. *J Nanobiotechnol* (2021) 19(1):202. doi: 10.1186/s12951-021-00942-0

112. Ding J, Wang X, Chen B, Zhang J, Xu J. Exosomes derived from human bone marrow mesenchymal stem cells stimulated by deferoxamine accelerate cutaneous wound healing by promoting angiogenesis. *BioMed Res Int* (2019) 2019:9742765. doi: 10.1155/2019/9742765

113. Chen J, Huang Y, Hu X, Bian X, Nian S. Gastrodin prevents homocysteine-induced human umbilical vein endothelial cells injury via PI3K/Akt/eNOS and Nrf2/ARE pathway. *J Cell Mol Med* (2021) 25(1):345–57. doi: 10.1111/jcmm.16073

114. Lu YA, Jiang Y, Yang HW, Hwang J, Jeon YJ, Ryu B. Diphlorethohydroxycarmalol isolated from ishige okamurae exerts vasodilatory effects via calcium signaling and PI3K/Akt/eNOS pathway. *Int J Mol Sci* (2021) 22 (4). doi: 10.3390/ijms22041610

115. Qu K, Cha H, Ru Y, Que H, Xing M. Buxuhuayu decoction accelerates angiogenesis by activating the PI3K-Akt-eNOS signalling pathway in a streptozotocin-induced diabetic ulcer rat model. *J Ethnopharmacol* (2021) 273:113824. doi: 10.1016/j.jep.2021.113824

116. Yu M, Liu W, Li J, Lu J, Lu H, Jia W, et al. Exosomes derived from atorvastatin-pretreated MSC accelerate diabetic wound repair by enhancing angiogenesis via AKT/eNOS pathway. *Stem Cell Res Ther* (2020) 11(1):350. doi: 10.1186/s13287-020-01824-2

117. Hu Y, Tao R, Chen L, Xiong Y, Xue H, Hu L, et al. Exosomes derived from pioglitazone-pretreated MSCs accelerate diabetic wound healing through enhancing angiogenesis. *J Nanobiotechnol* (2021) 19(1):150. doi: 10.1186/s12951-021-00894-5

118. Gordon S, Martinez FO. Alternative activation of macrophages: mechanism and functions. *Immunity* (2010) 32(5):593–604. doi: 10.1016/j.immuni.2010.05.007

119. Liu F, Qiu H, Xue M, Zhang S, Zhang X, Xu J, et al. MSC-secreted TGF-beta regulates lipopolysaccharide-stimulated macrophage M2-like polarization via the Akt/FoxO1 pathway. *Stem Cell Res Ther* (2019) 10(1):345. doi: 10.1186/s13287-019-1447-y

120. Liu W, Yu M, Xie D, Wang L, Ye C, Zhu Q, et al. Melatonin-stimulated MSC-derived exosomes improve diabetic wound healing through regulating macrophage M1 and M2 polarization by targeting the PTEN/AKT pathway. *Stem Cell Res Ther* (2020) 11(1):259. doi: 10.1186/s13287-020-01756-x

121. Ti D, Hao H, Tong C, Liu J, Dong L, Zheng J, et al. LPS-preconditioned mesenchymal stromal cells modify macrophage polarization for resolution of chronic inflammation via exosome-shuttled let-7b. *J Transl Med* (2015) 13:308. doi: 10.1186/s12967-015-0642-6

122. Li X, Xie X, Lian W, Shi R, Han S, Zhang H, et al. Exosomes from adipose-derived stem cells overexpressing Nrf2 accelerate cutaneous wound healing by promoting vascularization in a diabetic foot ulcer rat model. *Exp Mol Med* (2018) 50(4):1–14. doi: 10.1038/s12276-018-0058-5

123. Wang C, Wang M, Xu T, Zhang X, Lin C, Gao W, et al. Engineering bioactive self-healing antibacterial exosomes hydrogel for promoting chronic diabetic wound healing and complete skin regeneration. *Theranostics* (2019) 9 (1):65–76. doi: 10.7150/thno.29766

124. Pankongadisak P, Suwantong O. Enhanced properties of injectable chitosan-based thermogelling hydrogels by silk fibroin and longan seed extract for bone tissue engineering. *Int J Biol Macromol* (2019) 138:412–24. doi: 10.1016/j.ijbiomac.2019.07.100

125. Zhang Y, Zhang P, Gao X, Chang L, Chen Z, Mei X. Preparation of exosomes encapsulated nanohydrogel for accelerating wound healing of diabetic rats by promoting angiogenesis. *Mater Sci Eng C Mater Biol Appl* (2021) 120:111671. doi: 10.1016/j.msec.2020.111671

126. Yang J, Chen Z, Pan D, Li H, Shen J. Umbilical cord-derived mesenchymal stem cell-derived exosomes combined pluronic F127 hydrogel promote chronic diabetic wound healing and complete skin regeneration. *Int J Nanomed* (2020) 15:5911–26. doi: 10.2147/IJN.S249129

127. Tao SC, Guo SC, Li M, Ke QF, Guo YP, Zhang CQ. Chitosan wound dressings incorporating exosomes derived from MicroRNA-126-Overexpressing synovium mesenchymal stem cells provide sustained release of exosomes and heal full-thickness skin defects in a diabetic rat model. *Stem Cells Transl Med* (2017) 6 (3):736–47. doi: 10.5966/sctm.2016-0275

128. Shi Q, Qian Z, Liu D, Sun J, Wang X, Liu H, et al. GMSC-derived exosomes combined with a Chitosan/Silk hydrogel sponge accelerates wound healing in a diabetic rat skin defect model. *Front Physiol* (2017) 8:904. doi: 10.3389/fphys.2017.00904

129. Grange C, Tapparo M, Bruno S, Chatterjee D, Quesenberry PJ, Tetta C, et al. Biodistribution of mesenchymal stem cell-derived extracellular vesicles in a model of acute kidney injury monitored by optical imaging. *Int J Mol Med* (2014) 33(5):1055–63. doi: 10.3892/ijmm.2014.1663

130. Abello J, Nguyen TDT, Marasini R, Aryal S, Weiss ML. Biodistribution of gadolinium- and near infrared-labeled human umbilical cord mesenchymal stromal cell-derived exosomes in tumor bearing mice. *Theranostics* (2019) 9 (8):2325–45. doi: 10.7150/thno.30030

131. Shi Y, Wang Y, Li Q, Liu K, Hou J, Shao C, et al. Immunoregulatory mechanisms of mesenchymal stem and stromal cells in inflammatory diseases. *Nat Rev Nephrol* (2018) 14(8):493–507. doi: 10.1038/s41581-018-0023-5

132. Liu B, Qian G, Cao W, Li CH, Pan SH, Wang L, et al. Proteomics analyses reveal functional differences between exosomes of mesenchymal stem cells derived from the umbilical cord and those derived from the adipose tissue. *Cell J* (2021) 23 (1):75–84. doi: 10.22074/cellj.2021.6969

133. Nassar W, Sabry EI-Ansary M, Mostafa D, Fayad MA, Kotb T, E, et al. Umbilical cord mesenchymal stem cells derived extracellular vesicles can safely ameliorate the progression of chronic kidney diseases. *Biomater Res* (2016) 20:21. doi: 10.1186/s40824-016-0068-0

134. Oh K, Kim SR, Kim DK, Seo MW, Lee C, Lee HM, et al. *In vivo* differentiation of therapeutic insulin-producing cells from bone marrow cells via extracellular vesicle-mimetic nanovesicles. *ACS Nano* (2015) 9(12):11718–27. doi: 10.1021/acsnano.5b02997

135. Zhang Z, Mi T, Jin L, Li M, Hao C, Huang Z, et al. Comprehensive proteomic analysis of exosome mimetic vesicles and exosomes derived from human umbilical cord mesenchymal stem cells. *Stem Cell Res Ther* (2022) 13 (1):312. doi: 10.1186/s13287-022-03008-6

136. Wang B, Wu ZH, Lou PY, Chai C, Han SY, Ning JF, et al. Human bone marrow-derived mesenchymal stem cell-secreted exosomes overexpressing microRNA-34a ameliorate glioblastoma development via down-regulating MYCN. *Cell Oncol (Dordr)* (2019) 42(6):783–99. doi: 10.1007/s13402-019-00461-z

137. Gomari H, Forouzandeh Moghadam M, Soleimani M. Targeted cancer therapy using engineered exosome as a natural drug delivery vehicle. *Onco Targets Ther* (2018) 11:5753–62. doi: 10.2147/OTT.S173110

138. Melzer C, Rehn V, Yang Y, Bahre H, Ohe JCD, Hass R. Taxol-loaded MSC-derived exosomes provide a therapeutic vehicle to target metastatic breast cancer and other carcinoma cells. *Cancers (Basel)* (2019) 11(6), 798. doi: 10.3390/cancers11060798.

139. Simpson RJ, Kalra H, Mathivanan S. ExoCarta as a resource for exosomal research. *J Extracell Vesicles* (2012) 1, 1. doi: 10.3402/jev.v1i0.18374.

140. Zhao J, Li X, Hu J, Chen F, Qiao S, Sun X, et al. Mesenchymal stromal cell-derived exosomes attenuate myocardial ischaemia-reperfusion injury through miR-182-regulated macrophage polarization. *Cardiovasc Res* (2019) 115(7):1205–16. doi: 10.1093/cvr/cvz040

141. Zhang L, Wang Q, Su H, Cheng J. Exosomes from adipose tissues derived mesenchymal stem cells overexpressing MicroRNA-146a alleviate diabetic osteoporosis in rats. *Cell Mol Bioeng* (2022) 15(1):87–97. doi: 10.1007/s12195-021-00699-4

frontiers | Frontiers in Endocrinology

TYPE Original Research
PUBLISHED 14 November 2022
DOI 10.3389/fendo.2022.991803

OPEN ACCESS

EDITED BY
Jian Ma,
Harbin Medical University, China

REVIEWED BY
Sunbin Deng,
Harvard Medical School, United States
Chen Li,
Free University of Berlin, Germany

*CORRESPONDENCE
Junxia Yan
20457456@qq.com
Wenxu Hong
szbloodcenter@hotmail.com

†These authors have contributed equally to this work

SPECIALTY SECTION
This article was submitted to Diabetes: Molecular Mechanisms, a section of the journal Frontiers in Endocrinology

RECEIVED 12 July 2022
ACCEPTED 25 October 2022
PUBLISHED 14 November 2022

CITATION
Li Y, Gong C, Xu Y, Liang X, Chen X, Hong W and Yan J (2022) Genetic regulation of *THBS1* methylation in diabetic retinopathy.
Front. Endocrinol. 13:991803.
doi: 10.3389/fendo.2022.991803

Genetic regulation of *THBS1* methylation in diabetic retinopathy

Yaqi Li[1,2†], Chunmei Gong[2†], Yuanfei Xu[2], Xiongshun Liang[3], Xiaoping Chen[4], Wenxu Hong[3*] and Junxia Yan[1,5*]

[1]Department of Epidemiology and Health Statistics, XiangYa School of Public Health, Central South University, Changsha, Hunan, China, [2]Animal Laboratory, Shenzhen Center for Chronic Disease Control, Shenzhen, China, [3]Central Laboratory, Shenzhen Center for Chronic Disease Control, Shenzhen, China, [4]Institute of Clinical Pharmacology, Central South University, Changsha, China, [5]Hunan Provincial Key Laboratory of Clinical Epidemiology, XiangYa School of Public Health, Central South University, Changsha, Hunan, China

Background: Diabetic retinopathy (DR) is a common and serious microvascular complication of diabetes mellitus (DM), but its pathological mechanism, especially the formation mechanism of new blood vessels remains unclear. Thrombospondin-1 (*THBS1*) is a potent endogenous inhibitor of angiogenesis and it was found over expressed in DR in our previous study. Our study aimed to determine whether overexpression of *THBS1* is associated with its promoter methylation level, and whether methylation of *THBS1* is regulated by genetic variants in DR.

Methods: Patients diagnosed with DR and DM patients without retinal problems were included in the case-control study. DNA methylation detection of *THBS1* by bisulfite sequencing and genotyping of specific SNPs by MassARRAY analysis were performed in the patients recruited from 2019-2020. Real time quantitative PCR was performed to obtain mRNA expression of *THBS1* in the patients recruited from August to October 2022. The differentially methylated CpG loci of *THBS1* were identified by logistic regression, and associations between 13 SNPs and methylation levels of CpG loci were tested by methylation quantitative trait loci (meQTLs) analysis. Mediation analysis was applied to determine whether CpG loci were intermediate factors between meQTLs and DR.

Results: 150 patients diagnosed with DR and 150 DM patients without retinal complications were enrolled in the first recruitment, seven DR patients and seven DM patients were enrolled in the second recruitment. The patients with DR showed promoter hypomethylation of *THBS1* (P value = 0.002), and six out of thirty-nine CpG sites within two CpG islands (CGIs) showed hypomethylation(P value < 0.05). *THBS1* mRNA expression in peripheral blood was significantly higher in DR patients than in DM patients. Five out of thirteen cis-meQTLs were identified to be associated with CpG sites: rs13329154, rs34973764 and rs5812091 were associated with cis-meQTLs of CpG-4 (P value=0.0145, 0.0095, 0.0158), rs11070177 and rs1847663 were associated with cis-meQTLs of CpG-2 and CpG-3 respectively (P

value=0.0201, 0.0275). CpG-4 methylation significantly mediated the effect of the polymorphism rs34973764 on DR (B=0.0535, Boot 95%CI: 0.004~0.1336).

Conclusion: *THBS1* overexpression is related to *THBS1* hypomethylation in patients with DR. DNA methylation may be genetically controlled in DR.

KEYWORDS

meQTL, DNA methylation, *THBS1*, diabetic retinopathy, genetic regulation

Introduction

Diabetic retinopathy (DR) is a common and serious microvascular complication of diabetes mellitus (DM), and has long been regarded as one of the major public health problems in the world (1, 2). An up-to-date evaluation report showed that one in five patients with DM worldwide had DR, and the number of adults with DR worldwide was estimated to rise from 103.12 million in 2020 to 160.5 million in 2045 (3). Clinically, DR not only leads to visual impairment and blindness, but also signifies an enhanced risk of cardiovascular disease, atherosclerosis and diabetic peripheral neuropathy (4–7). Glycemic control is routinely recommended to prevent the complications of DM. However, multiple basic studies have found that retinopathy induced by long-term exposure to hyperglycemia persists after glycemic control (8). Despite advances in the treatment with anti-angiogenic drugs (9), patients with DR might still experience adverse effects on their quality of life and financial circumstances. Accordingly, in order to reduce the prevalence of vision impairment and blindness caused by DR, it is imperative to discover more specific and sensitive biomarkers and explore its detailed etiology.

Early clinical characteristics of DR, such as microaneurysms and intraretinal microvascular abnormalities, are caused by changes in the cellular composition of the capillary wall (10). With the occurrence of capillary blockage and retinal ischemia in DR, neovascularization arises on the retina, resulting in proliferative DR (11). However, the pathological mechanism of DR, especially the formation mechanism of new blood vessels remains unclear. Thrombospondin-1 (*THBS1*) is a commonly matrix-cellular glycoprotein that plays a significant role in retinal vascular homeostasis (12, 13). Importantly, *THBS1* is a potent endogenous inhibitor of angiogenesis. *THBS1* was found to inhibit endothelial cell migration and proliferation and stimulate apoptosis by regulating vascular endothelial growth factor activity (14). *THBS1* may be involved in the development and progression of DR (15). Overexpression of *THBS1* impairs retinal vascular development and neointima formation in mice (16). In addition, deficiency of *THBS1* expression in retinal endothelial cells resulted in the accelerated proliferation and increased angiogenesis (16, 17). Moreover, we analyzed two gene expression datasets of DR patients (GSE94019 and GSE60436) (18, 19), which were downloaded from the Gene Expression Omnibus (GEO) (20), and found that the expression of *THBS1* was significantly up-regulated in the fibrovascular membrane of DR compared to normal retinal tissue in both datasets (adjusted P value = 3.58×10^{-3}; 3.56×10^{-8}) (data not published). Thus, we hypothesized that *THBS1* is a critical molecular in the development of DR, but the detailed mechanism underlying *THBS1* over-expression in DR is still unknown.

DNA methylation is a critical epigenetic alteration with the potential to illuminate the differential expression of *THBS1* in DR. DNA methylation status is closely correlated with gene expression (21). For example, hypermethylation of gene promoter regions can decreases DNA accessibility and inhibit transcription factors from binding, causing gene inactivation (i.e., inhibition of gene expression). Furthermore, since Maghbooli et al. first found higher global DNA methylation level in patients with DR (22), subsequent studies have confirmed that DNA methylation of some genes was indeed different in patients with DR (23–25). DNA methylation is therefore a critical factor related to gene expression, and cannot be ignored in the development of DR. According to our previous analysis of two datasets, differential expression of anti-angiogenic factor-*THBS1* was identified in patients with DR. However, whether *THBS1* methylation is involved in DR remains unknown. Moreover, the association between genetic variation and DNA methylation in humans has been extensively studied, and methylation quantitative trait loci (meQTL) may exert a regulatory effect on methylation at related cytosine-phosphate-guanine (CpG) sites (including cis and trans effect) (26–28). Particularly, meQTL pairs formed by SNPs and CpG loci tend to be enriched for functionally relevant features, such as gene expression, metabolic functions and clinical manifestations (29). Therefore, identifying the genetic regulation of DNA methylation can help us figure out the mechanisms by which genetic variation influences complex phenotypes. In light of these findings, exploring whether methylation of *THBS1* gene is genetically regulated may provide insight into the role of *THBS1* in DR and shed new light on the molecular networks and biological mechanisms of DR.

Our study aimed to determine whether overexpression of *THBS1* is associated with its promoter methylation level, and whether methylation of *THBS1* is regulated by genetic variants in DR.

Methods and materials

Study population

Patients diagnosed with DR and DM patients without retinal complications were recruited in the case-control study from communities in Shenzhen City, Guangdong Province, China. The patients recruited from 2019 to 2020 were for the study of *THBS1* methylation detection and specific SNPs genotyping, and the patients recruited from August to September 2022 were for *THBS1* mRNA testing. Patients in the case group were adult males or females with a history of T2DM, impaired vision, and previously diagnosed with DR by Fluorescence fundus angiography or optical coherence tomography. Patients in the control group were previously diagnosed with T2DM {according to the Chinese Guidelines for the Prevention and Treatment of Type 2 Diabetes [2017 Edition (30)]} without retinopathy. The case and control subjects were matched for age, sex, and duration of disease. Patients with diabetic foot, diabetic nephropathy, macular edema, history of other eye diseases or eye surgery, malignant tumors, severe liver and kidney dysfunction, mental illness, and alcohol or drug abuse were excluded. This study was approved by the Ethics Committee of Shenzhen Center for Chronic Disease Control. Written informed consent was signed by all participants.

Questionnaire survey

Questionnaire survey was conducted among the patients recruited from 2019 to 2020 for demographic information (gender and age), anthropometric data [height, weight and body mass index (BMI)], diabetic duration, history of hypertension and information on lifestyle (smoking and drinking frequency) of patients enrolled. BMI = weight/height^2 (kg/m^2). Hypertension was defined as systolic blood pressure (SBP) ≥140 mmHg and/or diastolic blood pressure (DBP) ≥ 90 mmHg, or a prior history of hypertension or use of antihypertensive medications. Smokers are defined as those who smoke one or more cigarettes a day for more than one year. Drinkers were defined as those who consumed more than 50 ml alcohol per week on average and drank for more than six months. The collected questionnaire data was sorted out by using EPIDATA software and recorded by two people.

Blood sample collection and DNA Extraction

5 ml fasting peripheral blood of all participants were collected by vacuum collection tubes after fasting for 12 hours. The blood samples of the first recruited patients were centrifuged, divided and stored in a refrigerator at -80℃. DNA was extracted from their peripheral blood by Blood Genomic DNA Extraction Kit (Omega, American). The blood samples of the secondly recruited patients were centrifuged, divided and used for subsequent mRNA level testing.

Biochemical index detection

Glycosylated hemoglobin (HbA1c), fasting blood glucose (FPG), urea (UREA), creatinine (Cr), triglycerides (TG), total cholesterol (TC), low-density lipoprotein cholesterol (LDL-C) and high-density lipoprotein cholesterol (HDL-C) were tested among the patients recruited from 2019-2020 with Beckman-LX20 automatic biochemical analyzer.

THBS1 methylation detection

The detailed information on CpG islands and CpG sites of *THBS1* gene is provided in Table S1. Bisulfite conversion of DNA was performed by EZ DNA methylation-Gold ™ Kit (ZYMO, CA, USA). The modified DNA was amplified by multiple PCR (HotStart Taq polymerase, TaKaRa, Dalian, China). Primers with Index sequences were used to introduce specific tag sequences to the end of target and region by PCR amplification (Herculase® II Fusion DNA Polymerase, Agilent Technologies, CA, USA). The information on Primer sequences of *THBS1* is provided in Table S2. The PCR products were electrophoresed with 2% agarose gel and purified with TIANGEN Gel Extraction kit (TIANGEN, Beijing, China). Finally, data on *THBS1* methylation was obtained using Illumina Hiseq or Nova SEQ platform for high-throughput sequencing.

Genotyping of specific SNPs

Genomic DNA extracted from peripheral blood was analyzed by mass spectrometry using MassARRAY (Agena Bioscience), and then genotyping of those thirteen SNPs was performed. GTEx portal (https://www.gtexportal.org/home/index.html) was used to search for expression quantitative trait Loci (eQTL) of *THBS1* gene, and thirteen eQTLs existing both in whole blood and fibroblasts were selected as SNPs to be detected. Detailed information on SNPs is listed in Table 1.

TABLE 1 Detailed information about SNPs.

SNP	Chromosome	Location(GRCh38.p13)	Gene	Region	Alleles
rs11070177	15	39250064	C15orf54	2KB Upstream Variant	C>T
rs13329154	15	39252947	C15orf54	Non Coding Transcript Variant	C>T
rs143182940	15	39309678-39309680	–		delCTT
rs156657	15	39249331	C15orf54	2KB Upstream Variant	C>T
rs1847663	15	39253913	C15orf54	Non Coding Transcript Variant	A>G
rs201057385	15	39336247-39336252	–		delAAG
rs202208752	15	39321928-39321932	–		delGATAT
rs34401261	15	39248232-39248235	–		delTTC/dupTTC
rs34973764	15	39279332-39279333	–		insC/insG
rs36015436	15	39266666-39266668	–		delTA/dupTA
rs5812091	15	39304767	–		dupC
rs5812094	15	39313990-39313994	–		dupTGAC
rs71745389	15	39339794-39339798	–		delGAGA/dupGAGA

The genotyping process was completed by Shanghai Tianhao Biotechnology Company. The quality evaluation of a SNP included minor allele frequency (MAF>5%), call rate(>95%).

mRNA extraction, cDNA synthesis and real time Quantitative PCR

Peripheral blood samples were treated with Red Blood Cell Lysis Buffer (Beyotime Biotechnology, Shanghai) and total RNA was extracted from cells using the Trizol method (TRIzol, Reagent life, USA). cDNA was synthesized from 1μg of total RNA using PrimeScriptTM RT reagent Kit with gDNA Eraser (Perfect real time) (TAKARA, Japan). The concentration and purity of RNA were determined by spectrophotometry (NanoVue Plus, GE healthcare UK limited, the United Kingdom). *THBS1* mRNA expression was measured by real time quantitative PCR(RT-PCR) with TB Green® Premix Ex Taq™ II (TAKARA, Japan). The optimal number of PCR cycles and the mixing ratio of primers were determined according to the instruction of TB green reagent (Code No. RR820A). PCR products were quantified using TB Green. Beta-actin (ACTB) was used as an endogenous control to normalize expression levels. The ranges of linear amplification for the target gene and for the ACTB genes were studied. Data were normalized relative to the expression level of ACTB for each sample. Primers used for RT-PCR were human *THBS1*-1, 5'-TTGTCTTTGGAACCACACCA-3'(sense) and 5'-TGGACAGCTCATCACAGGAG-3' (antisense); and ACTB 5'-GATGAGATTGGCATGGCTTT-3' (Sense) and 5'-CACCTTCACCGGTCAGTTT -3' (antisense). The expression levels of mRNA were represented as $2^{-\Delta\Delta CT}$.

Statistic analysis

In terms of basic characteristics, continuous variables with normal distribution were presented as mean ± standard deviation, and independent two-sample t-tests were used to compare differences between the case and control group. Continuous variables without normal distribution were presented as medians (percentile 25, percentile 75), Wilcoxon rank sum test was performed to identify differences between groups. Categorical variables were presented using percentages and chi-square tests were used to compare differences between groups. All those tests were conducted two-tailed in IBM SPSS 25 software, and P<0.05 was considered significant.

The differentially methylated CpG loci of *THBS1* were identified using univariate logistic regression in SPSS software. Associations between each SNP and methylation levels of differentially methylated CpG loci were tested to identify meQTLs using linear regression in the software PLINK (31). The independent variable was the genotype of the SNP, and the additive model was adopted. Given that we had previously tried to keep the distribution of most critical confounding factors-age, gender and diabetic duration to be the same between the case group and the control group, so we did not adjust for other factors. Cis-meQTL was defined as being less than 500kb upstream or downstream of CpG sites from the associated CpG loci, otherwise as trans-meQTLs. To examine the independence of these meQTLs, linkage disequilibrium (LD) analysis was performed by Haploview 4.2 programme (32). r^2 was obtained as a measure of LD based on our study population. To explore the relationship between meQTLs and DR, binary logistic regressions were performed in dominant, recessive and additive models in SPSS software. HbA1c and TC were adjusted in three models. P<0.05 was considered significant.

To determine whether methylation at CpG loci was an intermediate factor between genetic variation and DR, we performed a mediation analysis by using macro PROCESS (v3.4 by Andrew F. Hayes) in SPSS. Model 4 was used for our analysis, which represented a simple mediation model (the type occurring when only one variable regulated the effect of a cause

on an outcome) (33). 5000 bias-corrected Bootstrap sample was used for the significance test. It is sufficient to support a claim of mediation effect when the 95% bootstrap confidence intervals of the indirect effect (as quantified with ab) does not include zero (34). We can determine whether there is an intermediate effect of methylation, by calculating whether the indirect effect of genetic variation on disease is significant.

Results

Characteristics of the participants

From 2019 to 2020, 150 patients diagnosed with DR and 150 DM patients without retinal complications were enrolled in our study. Their clinical characteristics are summarized in Table 2. Since we matched the age, sex and duration of disease between the case group and the control group, the mean age of both groups was about 56 years, 55% were female, and the median duration of disease was 8 and 9 years, respectively. As illustrated in the table, BMI and the proportion of hypertension patients were comparable between the case and control groups. HbA1c, FPG, UREA, TC, LDL-C in the case group were significantly higher than those in the control group (P value<0.05).

From August to September 2022, seven DR patients and seven DM patients without retinal complications were enrolled in our study. Since we had matched age and gender of the participants in the case group and control group, the average ages of the case group and the control group are 60.14 ± 8.17 and 59.86 ± 7.51, with four females in each group.

Methylation analysis

There are two CpG islands (CGIs) in *THBS1* gene, which contains 23 and 16 CpG sites respectively, and five CpG sites of CGI-2 are in the gene body of *THBS1* (Figure 1). Methylation levels of 39 CpG loci on *THBS1* gene were tested in all subjects (Table S1). The patients with DR showed a lower methylation level of *THBS1* than the patients with DM (P value = 0.002) (Table S1). To be specific, the methylation levels of six CpG loci in the patients with DR were significantly different from those with DM, and all the 6 CpG loci in the patients with DR showed hypomethylation (P value<0.05) (Table 3). All these six sites are located in the promoter region of *THBS1*, CpG-5 locates downstream of the transcription start site (TSS), and other sites locates upstream of the TSS. The box plots of methylation levels of *THBS1* and six CpG loci in the two groups are shown in Figure 2.

Identification of *THBS1* meQTL

The meQTL association analyses between 6 differentially methylated CpG sites and 13 SNPS were performed by the software PLINK, and the results are shown in Table S3. Five SNPs were associated with three differentially methylated CpG loci, all of which were cis-meQTLs upstream of the associated CpG loci. Box plots of methylation level plotted against genotypes for five meQTLs are shown in Figure 3. rs13329154(C>T), rs34973764(insC), rs5812091(dupC) were cis-meQTLs of CpG-4 (P value=0.0145, 0.0095, 0.0158; distance between SNPs and associated CpG site: 319kb, 297kb, 269kb respectively). Variations in these SNPs were

TABLE 2 Clinical characteristics of subjects.

	Cases(n=150)	Controls(n=150)	P value
Age,years	56.63 ± 9.29	56.69 ± 9.07	0.955
Female,n(%)	55(36.7)	55(36.7)	1
BMI,kg/m^2	24.61 ± 3.04	24.86 ± 3.11	0.502
Diabetic duration,years	8.00(4.00,13.00)	9.00(4.50,12,5)	0.593
Hypertension,n(%)	73(48.7)	79(42.7)	0.564
Smoking,n(%)	40(26.7)	35(23.3)	0.594
Drinking,n(%)	52(34.7)	45(30.0)	0.459
HbA1c,%	7.10(6.13,8.50)	6.60(5.80,7.30)	0.002
FPG,mmol/L	8.35(6.70,10.80)	6.90(5.85,8.65)	<0.001
UREA,mmol/L	5.30(4.43,6.55)	4.90(4.20,5.90)	0.021
Cr,umol/L	71.80(57.10,85.10)	72.30(58.65,88.10)	0.542
TG,mmol/L	1.58(1.13,2.25)	1.54(1.03,2.30)	0.489
TC,mmol/L	5.33 ± 1.34	4.95 ± 1.17	0.008
LDL-C,mmol/L	3.62 ± 0.92	3.33 ± 0.87	0.009
HDL-C,mmol/L	1.28 ± 0.29	1.24 ± 0.27	0.226

HbA1c, Glycosylated hemoglobin; FPG, fasting blood glucose; UREA, urea; Cr, creatinine; TG, triglycerides; TC, total cholesterol; LDL-C, low density lipoprotein cholesterol; HDL-C, high-density lipoprotein cholesterol.

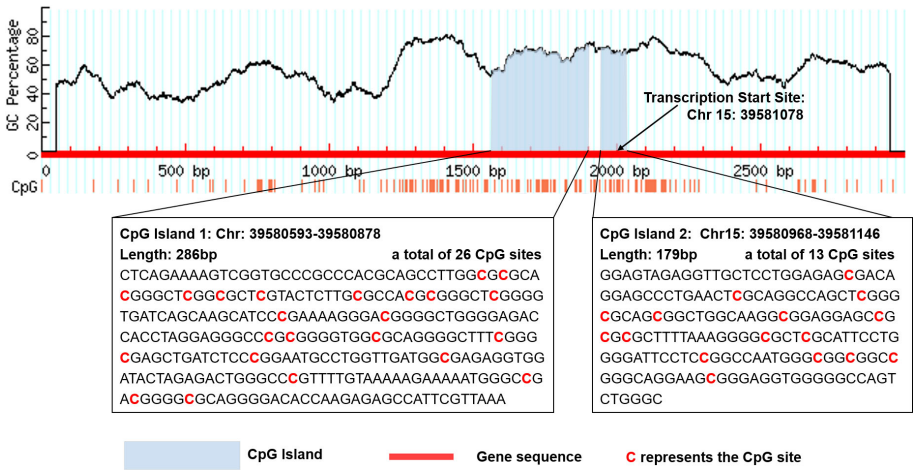

FIGURE 1
Location of the two CpG islands in THBS1 gene.

TABLE 3 Methylation analysis of *THBS1*.

	Chromosome 15 position(hg38)	Distance to TSS*	Menthylation Level, %		OR (95%CI)	P-value
			Cases	Controls		
CpG-1	39580843	-235	1.5140 ± 1.0131	1.8454 ± 1.1113	0.733 (0.581-0.926)	0.009
CpG-2	39580809	-269	1.6157 ± 1.0592	1.9062 ± 1.4094	0.823 (0.678-0.999)	0.049
CpG-3	39580741	-337	2.3637 ± 1.2478	2.6636 ± 1.3417	0.834 (0.697-0.999)	0.048
CpG-4	39580731	-347	1.5805 ± 1.0157	1.8695 ± 1.3641	0.812 (0.663-0.993)	0.042
CpG-5	39581083	5	1.0382 ± 0.6342	1.1875 ± 0.6098	0.678 (0.468-0.982)	0.040
CpG-6	39581002	-76	5.2338 ± 0.9362	5.6450 ± 1.1914	0.687 (0.545-0.866)	0.002
THBS1	39581078-39599466	–	1.8701 ± 0.2300	1.9704 ± 0.2923	0.191 (0.069-0.532)	0.002

*The distance of the site to the transcription start site on the reference genome, with a minus sign indicating that the site is upstream of the transcription start site.

associated with reduced methylation level. In addition, rs11070177 (C>T) and rs1847663(A>G) were cis-meQTLs of CpG-2 and CpG-3 (P value=0.0201, 0.0275; distance between SNPs and associated CpG site: 323kb, 319kb), and methylation levels of CpG-2 and CpG-3 increased with the number of allelic mutations. LD analysis between these five meQTLs showed a low degree of LD (r^2<30%) (Figure 4). Association analysis between these five meQTLs and DR showed that none of these meQTLs were associated with DR in dominant, recessive and additive models (Table S4).

Mediation effect

The indirect mediation routes of five meQTLs on DR through methylation of three CpG loci are shown in Table 4. In the five established mediation models, CpG-4 methylation significantly mediated the effect of the polymorphism rs34973764 on DR (B=0.0535, Boot 95%CI: 0.004~0.1336) (Table 4). Analysis of indirect effects showed that the variant allele of rs34973764 predicted hypomethylation levels at CpG-4 (a=-0.272, p value=0.009), and the incidence of DR increased with hypomethylation level at CpG-4 (b=-0.197, p value=0.0596) (Figure 5). Although the total and direct effect of rs34973764 on DR were not significant (total effect: c=-0.006, p value=0.973; direct effect: c'=-.0575, p value=0.7464), the indirect effect showed significant. Therefore, rs34973764 may act as a risk SNP for DR through CpG-4.

THBS1 mRNA expression

THBS1 mRNA expression in peripheral blood was significantly higher in DR patients than in DM patients ($2^{-\Delta\Delta CT}$ median (percentile 25, 75): 3.67(1.41-8.03) vs. 1.00(0.53-1.33), p value=0.025). Comparison of *THBS1* mRNA expression levels in the two groups is shown in Figure S1.

10.3389/fendo.2022.991803

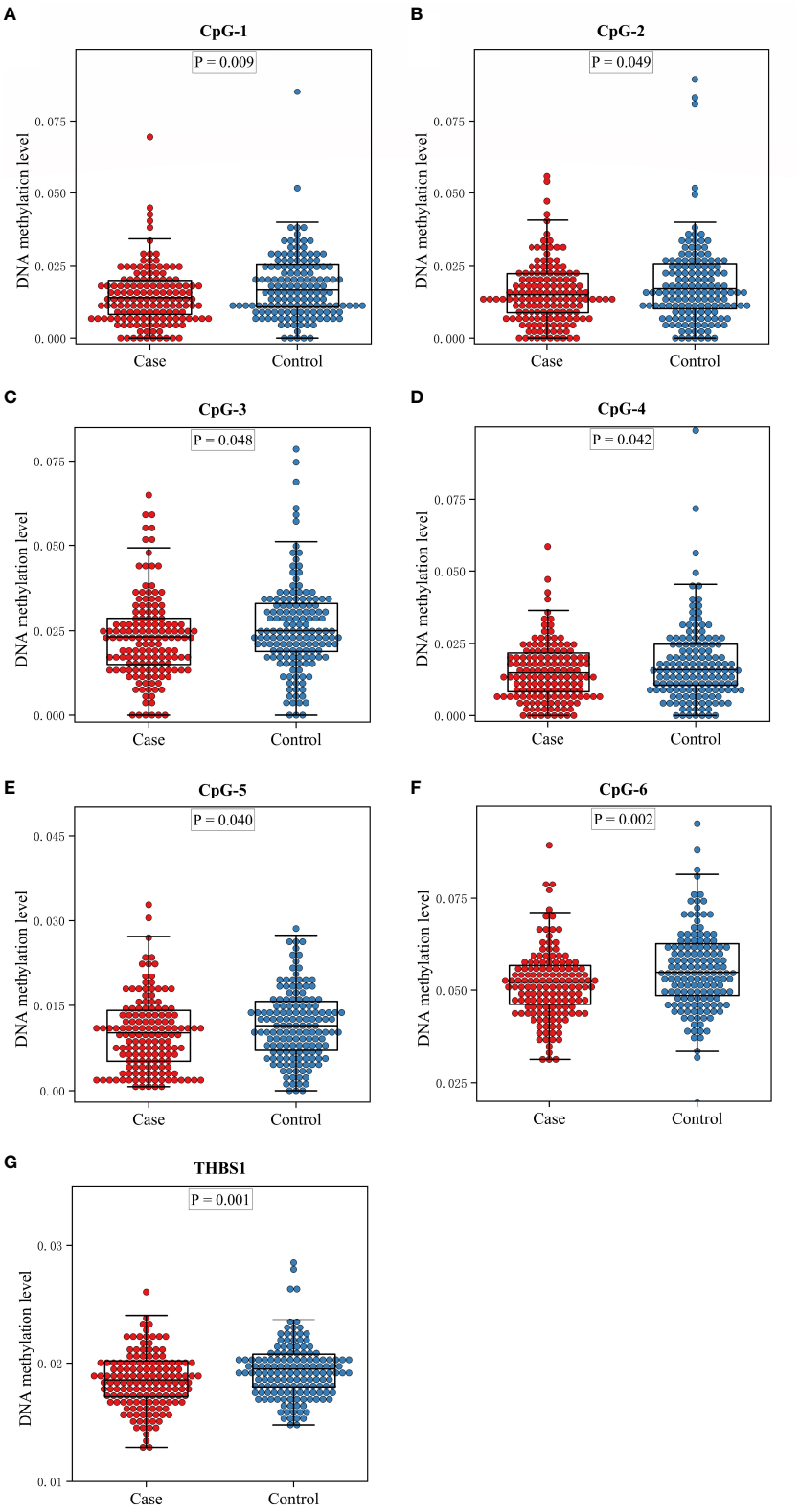

FIGURE 2
The box plots of methylation levels of *THBS1* in the case and control groups. **(A–F)** Methylation levels of six CpG loci with significant difference in the case and control group. **(G)** Methylation levels of THBS1 in the case and control group.

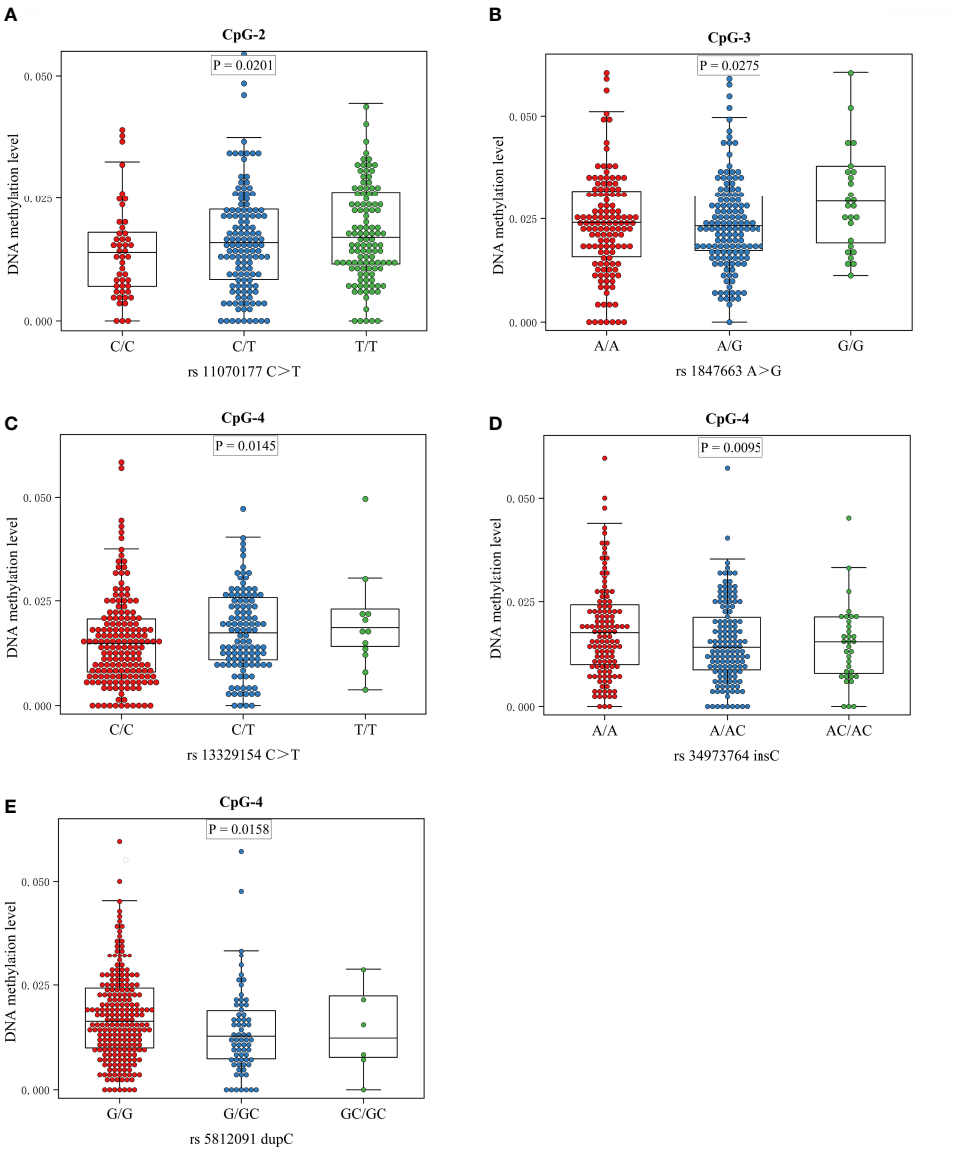

FIGURE 3
Boxplots showing methylation level plotted against genotypes for five meQTLs: Center lines show the medians; box limits indicate the 25th and 75th percentiles; whiskers extend to the 5th and 95th percentiles. **(A)** The association between genotype at rs11070177 and methylation level at CpG-2; **(B)** the association between genotype at rs1847663 and methylation level at CpG-3; **(C–E)** the association between genotypes at rs13329154, rs34973764, rs5812091 and methylation level at CpG-4.

Discussion

In our study, the patients with DR showed significant hypomethylation of *THBS1* compared to those with T2DM, and 6 out of 39 CpG sites showed hypomethylation. Moreover, 5 out of 13 SNPs were identified to be associated with three differentially methylated CpG loci of *THBS1*. CpG-4 methylation mediated the effect of rs34973764 on DR in the mediation analysis, providing data evidence that *THBS1* methylation may be regulated by genetic variation in DR.

THBS1 is an endogenous molecule functioning as anti-angiogenesis and has been proven to regulate ocular vascular homeostasis (35). Numerous studies revealed the critical role of *THBS1* in the onset and progression of DR, especially in its neovascularization and vascular abnormalities. In the differential expression analysis performed prior to this study, results showed that the mRNA expression of *THBS1* in the fibrovascular membrane of DR patients was significantly up-regulated in both datasets (GSE94019 and GSE60436) (18, 19). This result has been confirmed in other studies. Bian et al. found that patients with DR

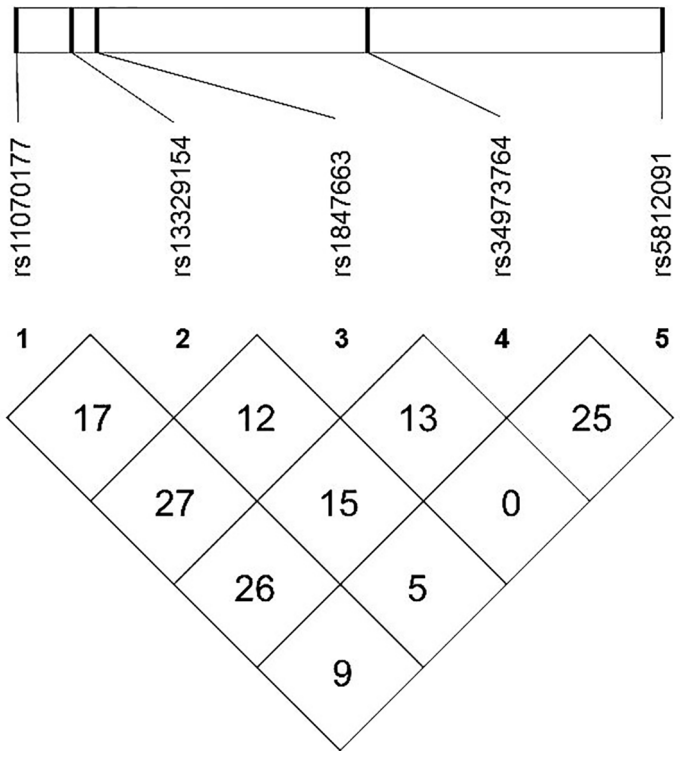

FIGURE 4
Linkage disequilibrium (LD) map among five meQTLs: LD r^2(%) based on our study population are shown in the boxes.

exhibited significantly elevated serum THBS1 compared to patients with T2DM, patients with proliferative DR in particular showed the highest *THBS1* (36). Wang et al. observed high expression of *THBS1* in the retina of DR rats (37). Wu et al. identified that mice with *THBS1* over-expressing in the lens showed attenuated retinal vascular development and impaired neovascularization (16). Hence, the expression of THBS1 is highly associated with the formation of new blood vessels, which may have a significant impact on the development of DR.

It is widely accepted that the expression of genes is affected by genetic regulation or epigenetic modification, which is adjustable and susceptible to environmental factors. So, it is imperative to figure out the association between the expression and epigenetic modification of *THBS1* in DR. Given that DNA methylation is an important epigenetic modification that has been studied the most, our study focused on how DNA methylation affects expression in DR. In our research, the methylation level of *THBS1* was significantly lower in the patients with DR compared to with DM. Besides, methylation levels of six CpG sites of *THBS1* showed a significant difference between those two groups, and all of these sites showed decreased DNA methylation in cases with DR. Then we examined *THBS1* mRNA expression levels in another recruited patients, and the results showed that the mRNA expression level of *THBS1* in peripheral blood was significantly higher in DR patients than in DM patients. In addition, patients with DR are typically poor in glycemic control, as supported by our data. Studies confirmed that hyperglycemia can result in irreversible alterations in the activity of DNA methyltransferases and hydroxymethylase (38). Moreover, *THBS1* expression was significantly increased in the high-glucose environment in keratinocytes and diabetic rat model, which was induced through DNA hypomethylation (39). Thus, we speculate that high glucose may have an impact on the *THBS1* methylation *via* enzyme activity, resulting in alterations of *THBS1* expression in DR. Since the existing research is restricted, additional research is necessary to clarify the mechanism of methylation and expression

TABLE 4 The results of mediation analysis.

Indirect effect						B	BootSE	Boot 95%CI
rs11070177	→	CpG-2	→	DR		-0.0488	0.0328	-0.1254~0.0003
rs1847663	→	CpG-3	→	DR		-0.0438	0.0322	-0.1180~0.0092
rs13329154	→	CpG-4	→	DR		-0.0547	0.0433	-0.1586~0.004
rs34973764*	→	CpG-4	→	DR		0.0535	0.0349	0.0004~0.1336
rs5812091	→	CpG-4	→	DR		0.0635	0.0453	-0.0047~0.1727

*Bootstrap 95% confidence interval of the indirect effect does not include zero.

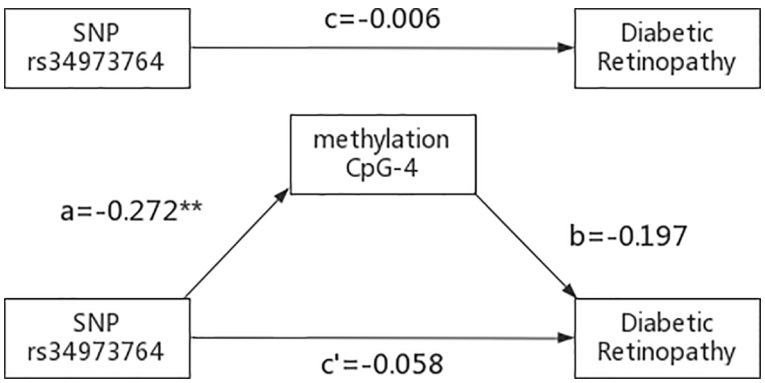

FIGURE 5
Results of the mediation analysis: Indirect effect of rs34973764 on diabetic retinopathy through methylation of CpG-4 and total effect (regression coefficients). **p ≤.001.

of *THBS1* in DR.DNA methylation has been previously described to have a genetic basis, and numerous studies have investigated the relationship between DNA methylation and genetic variation throughout the genome to identify meQTLs (40). In our meQTL analysis, there were five cis-CpG-SNPs associations identified, including three *THBS1* methylation loci and five SNPs. The rare allele of rs13329154, rs34973764, rs5812091 exhibited significantly decreased levels of CpG-4 methylation, while the rare allele of rs11070177 and rs1847663 exhibited significantly increased levels of CpG-2 and CpG-3 methylation respectively. Rs13329154, rs11070177 and rs1847663 are located in the noncoding region of C15orf54 gene, while rs34973764, rs5812091 have not been characterized. C15orf54 gene has not been well understood, and up-regulated expression of C15orf54 was first found to be associated with the risk of gastric cancer in a recent bioinformatics analysis (41). In addition, there is no association between these five meQTLs and DR in dominant, recessive and additive models in our research, and these five meQTLs have not been reported to be associated to any phenotypes or diseases in prior studies. Hence, more research is needed to determine how C15orf54 gene polymorphism affects *THBS1* methylation in DR.

meQTLs are highly enriched in GWAS signals (42), implying that meQTLs are associated with an elevated risk of disease. Studies have shown that meQTLs may exert an influence on disease risk *via* altering DNA methylation (40). In the mediation study, CpG-4 methylation mediated the effect of rs34973764 on DR, which may be supporting evidence for genetic regulation of DNA methylation in DR. Although the total effect of rs34973764 on DR was not significant, rs34973764 had a significant indirect effect on the DR *via* the mediator of CpG-4 methylation. One possible explanation is that rs34973764 functions in DR *via* two or more additional mediation pathways, and those additional pathways operate oppositely from the CpG-4 methylation pathway. However, the function of rs34973764 and its impact on CPG-4 are not yet fully understood, so the underlying molecular processes of meQTLs are unknown. The most common explanation for the cis-meQTL effect is that SNPs at protein binding sites affect the function of sequence-specific binding proteins, such as transcription factors, and thus change the methylation pattern of adjacent CpGs (40). Future research combining SNPs, DNA methylation, and gene expression are needed to better understand the pathology of DR.

There are several limitations in our study. Firstly, DR is classified as either proliferative or non-proliferative (11), but in our study, we did not divide patients into those two categories. Therefore, we could not obtain dynamic changes in *THBS1* methylation level as the disease progressed. Secondly, the SNPs we detected were not from genome-wide SNPs, but eQTLs related to *THBS1*, which represented only a small fraction of meQTLs of *THBS1*. Thirdly, the sample size was relatively insufficient, especially in the detection of *THBS1* mRNA expression levels, hence case-control and cohort studies with larger sample size are needed to confirm these findings.

In conclusion, *THBS1* overexpression is related to *THBS1* hypomethylation in patients with DR. DNA methylation may be genetically controlled in DR.

Data availability statement

The original contributions presented in the study are included in the article/Supplementary Material. Further inquiries can be directed to the corresponding authors.

Ethics statement

The studies involving human participants were reviewed and approved by the Ethics Committee of Shenzhen Center for Chronic Disease Control. The patients/participants provided their written informed consent to participate in this study.

Author contributions

YL and CG contributed equally to this work. CG and WH contributed to the design of the work. YL contributed to manuscript written and statistical analyses. Data acquisition and analysis were carried out by YX and XL. JY and CG reviewed the paper. All authors contributed to the article and approved the submitted version.

Funding

This work was supported by the Sanming Project of Medicine of Shenzhen (SZSM201811057), National Natural Science of Guang dong province (2019A1515010358) and Guangdong Medical Research Fund Project (2017196).

Acknowledgments

We thank all participants for providing samples and those involved in the sample collection.

Conflict of interest

The authors declare that the research was conducted in the absence of any commercial or financial relationships that could be construed as a potential conflict of interest.

Publisher's note

Supplementary material

The Supplementary Material for this article can be found online at: https://www.frontiersin.org/articles/10.3389/fendo.2022.991803/full#supplementary-material

References

1. Hashemi H, Rezvan F, Pakzad R, Ansaripour A, Heydarian S, Yekta A, et al. Global and regional prevalence of diabetic retinopathy; a comprehensive systematic review and meta-analysis. *Semin Ophthalmol* (2021) 157:1–16. doi: 10.1080/08820538.2021.1962920

2. Cheung N, Mitchell P, Wong TY. Diabetic retinopathy. *Lancet (London England)* (2010) 376:124–36. doi: 10.1016/S0140-6736(09)62124-3

3. Teo ZL, Tham YC, Yu M, Chee ML, Rim TH, Cheung N, et al. Global prevalence of diabetic retinopathy and projection of burden through 2045: Systematic review and meta-analysis. *Ophthalmology* (2021) 128:1580–91. doi: 10.1016/j.ophtha.2021.04.027

4. Shoeibi N, Bonakdaran S. Is there any correlation between diabetic retinopathy and risk of cardiovascular disease? *Curr Diabetes Rev* (2017) 13:81–6. doi: 10.2174/1573399812666151012115355

5. Gao L, Zhao W, Yang JK, Qin MZ. Proliferative diabetic retinopathy in patients with type 2 diabetes correlates with the presence of atherosclerosis cardiovascular disease. *Diabetol Metab Syndr* (2021) 13:48. doi: 10.1186/s13098-021-00666-z

6. Rasheed R, Pillai GS, Kumar H, Shajan AT, Radhakrishnan N, Ravindran GC. Relationship between diabetic retinopathy and diabetic peripheral neuropathy - neurodegenerative and microvascular changes. *Indian J Ophthalmol* (2021) 69:3370–5. doi: 10.4103/ijo.IJO_1279_21

7. Ellis TP, Choudhury RH, Kaul K, Chopra M, Kohner EM, Tarr JM, et al. Diabetic retinopathy and atherosclerosis: is there a link? *Curr Diabetes Rev* (2013) 9:146–60. doi: 10.2174/1573399811309020006

8. Zhang L, Chen B, Tang L. Metabolic memory: mechanisms and implications for diabetic retinopathy. *Diabetes Res Clin Pract* (2012) 96:286–93. doi: 10.1016/j.diabres.2011.12.006

9. Wang W, Lo ACY. Diabetic retinopathy: Pathophysiology and treatments. *Int J Mol Sci* (2018) 19:1–14. doi: 10.3390/ijms19061816

10. Lechner J, O'Leary OE, Stitt AW. The pathology associated with diabetic retinopathy. *Vision Res* (2017) 139:7–14. doi: 10.1016/j.visres.2017.04.003

11. Kollias AN, Ulbig MW. Diabetic retinopathy: Early diagnosis and effective treatment. *Deutsches Arzteblatt Int* (2010) 107:75–83. doi: 10.3238/arztebl.2010.0075

12. Hiscott P, Paraoan L, Choudhary A, Ordonez JL, Al-Khaier A, Armstrong DJ. Thrombospondin 1, thrombospondin 2 and the eye. *Prog Retinal Eye Res* (2006) 25:1–18. doi: 10.1016/j.preteyeres.2005.05.001

13. Sims JN, Lawler J. Thrombospondin-1-Based antiangiogenic therapy. *J Ocular Pharmacol Ther* (2015) 31:366–70. doi: 10.1089/jop.2015.0018

14. Huang T, Sun L, Yuan X, Qiu H. Thrombospondin-1 is a multifaceted player in tumor progression. *Oncotarget* (2017) 8:84546–58. doi: 10.18632/oncotarget.19165

15. Wang S, Gottlieb JL, Sorenson CM, Sheibani N. Modulation of thrombospondin 1 and pigment epithelium-derived factor levels in vitreous fluid of patients with diabetes. *Arch Ophthalmol* (2009) 127:507–13. doi: 10.1001/archophthalmol.2009.53

16. Wu ZF, Wang SJ, Sorenson CM, Sheibani N. Attenuation of retinal vascular development and neovascularization in transgenic mice over-expressing thrombospondin-1 in the lens. *Dev Dynamics* (2006) 235:1908–20. doi: 10.1002/dvdy.20837

17. Wang Y, Wang S, Sheibani N. Enhanced proangiogenic signaling in thrombospondin-1-deficient retinal endothelial cells. *Microvascular Res* (2006) 71:143–51. doi: 10.1016/j.mvr.2006.02.004

18. Ishikawa K, Yoshida S, Kobayashi Y, Zhou Y, Nakama T, Nakao S, et al. Microarray analysis of gene expression in fibrovascular membranes excised from patients with proliferative diabetic retinopathy. *Invest Ophthalmol Visual Sci* (2015) 56:932–46. doi: 10.1167/iovs.14-15589

19. Lam JD, Oh DJ, Wong LL, Amarnani D, Park-Windhol C, Sanchez AV, et al. Identification of RUNX1 as a mediator of aberrant retinal angiogenesis. *Diabetes* (2017) 66:1950–6. doi: 10.2337/db16-1035

20. Wang Z, Monteiro CD, Jagodnik KM, Fernandez NF, Gundersen GW, Rouillard AD, et al. Extraction and analysis of signatures from the gene expression omnibus by the crowd. *Nat Commun* (2016) 7:1–11. doi: 10.1038/ncomms12846

21. Bansal A, Pinney SE. DNA Methylation and its role in the pathogenesis of diabetes. *Pediatr Diabetes* (2017) 18:167–77. doi: 10.1111/pedi.12521

22. Maghbooli Z, Hossein-nezhad A, Larijani B, Amini M, Keshtkar A. Global DNA methylation as a possible biomarker for diabetic retinopathy. *Diabetes/metabolism Res Rev* (2015) 31:183–9. doi: 10.1002/dmrr.2584

23. Kowluru RA, Santos JM, Mishra M. Epigenetic modifications and diabetic retinopathy. *BioMed Res Int* (2013) 2013:635284. doi: 10.1155/2013/635284

24. Wu J, Liu LL, Cao M, Hu A, Hu D, Luo Y, et al. DNA Methylation plays important roles in retinal development and diseases. *Exp Eye Res* (2021) 211:108733. doi: 10.1016/j.exer.2021.108733

25. Kumari N, Karmakar A, Ganesan SK. Targeting epigenetic modifications as a potential therapeutic option for diabetic retinopathy. *J Cell Physiol* (2020) 235:1933–47. doi: 10.1002/jcp.29180

26. Zhi D, Aslibekyan S, Irvin MR, Claas SA, Borecki IB, Ordovas JM, et al. SNPs located at CpG sites modulate genome-epigenome interaction. *Epigenetics* (2013) 8:802–6. doi: 10.4161/epi.25501

27. Hellman A, Chess A. Extensive sequence-influenced DNA methylation polymorphism in the human genome. *Epigenet Chromatin* (2010) 3:11. doi: 10.1186/1756-8935-3-11

28. Smith AK, Kilaru V, Kocak M, Almli LM, Mercer KB, Ressler KJ, et al. Methylation quantitative trait loci (meQTLs) are consistently detected across ancestry, developmental stage, and tissue type. *BMC Genomics* (2014) 15:1–11. doi: 10.1186/1471-2164-15-145

29. Hawe JS, Wilson R, Schmid KT, Zhou L, Lakshmanan LN, Lehne BC, et al. Genetic variation influencing DNA methylation provides insights into molecular mechanisms regulating genomic function. *Nat Genet* (2022) 54:18–+. doi: 10.1038/s41588-021-00969-x

30. Chinese Medical Association Diabetic Society. Guidelines for the prevention and control of type 2 diabetes in China (2017 edition). *Chin J Pract Internal Med* (2018) 38:292–344. doi: 10.19538/j.nk2018040108

31. Purcell S, Neale B, Todd-Brown K, Thomas L, Ferreira MA, Bender D, et al. PLINK: a tool set for whole-genome association and population-based linkage analyses. *Am J Hum Genet* (2007) 81:559–75. doi: 10.1086/519795

32. Barrett JC, Fry B, Maller J, Daly MJ. Haploview: analysis and visualization of LD and haplotype maps. *Bioinformatics* (2005) 21:263–5. doi: 10.1093/bioinformatics/bth457

33. Preacher KJ, Hayes AF. SPSS And SAS procedures for estimating indirect effects in simple mediation models. *Behav Res Methods Instruments Comput* (2004) 36:717–31. doi: 10.3758/bf03206553

34. Hayes AF, Rockwood NJ. Regression-based statistical mediation and moderation analysis in clinical research: Observations, recommendations, and implementation. *Behav Res Ther* (2017) 98:39–57. doi: 10.1016/j.brat.2016.11.001

35. Farnoodian M, Sorenson CM, Sheibani N. Negative regulators of angiogenesis, ocular vascular homeostasis, and pathogenesis and treatment of exudative AMD. *J Ophthalmic Vision Res* (2018) 13:470–86. doi: 10.4103/jovr.jovr_67_18

36. Bian Z, Sun Q, Wang J, Hu Y, Qie H, Zhao X, et al. Clinical value of thrombospondin-1 in patients with type 2 diabetic retinopathy. *Department Endocrinol* (2017) 25:703–6. doi: 10.3969/j.issn.1006-6187.2017.08.006

37. Wang J, Zhang X, Zhang H. Expression of thrombospondin-1 in STZ-induced diabetic retinopathy in rats. *J Mol Cell Biol* (2006) 39:431–7. doi: 10.3321/j.issn:1673-520X.2006.05.006

38. Mishra M, Kowluru RA. The role of DNA methylation in the metabolic memory phenomenon associated with the continued progression of diabetic retinopathy. *Invest Ophthalmol Visual Sci* (2016) 57:5748–57. doi: 10.1167/iovs.16-19759

39. Lan CC, Huang SM, Wu CS, Wu CH, Chen GS. High-glucose environment increased thrombospondin-1 expression in keratinocytes *via* DNA hypomethylation. *Trans Res* (2016) 169:91–101 e1-3. doi: 10.1016/j.trsl.2015.11.002

40. Villicana S, Bell JT. Genetic impacts on DNA methylation: research findings and future perspectives. *Genome Biol* (2021) 22:1–35. doi: 10.1186/s13059-021-02347-6

41. Liu M, Li J, Huang Z, Li Y. Gastric cancer risk-scoring system based on analysis of a competing endogenous RNA network. *Transl Cancer Res* (2020) 9:3889–902. doi: 10.21037/tcr-19-2977

42. Shi JX, Marconett CN, Duan JB, Hyland PL, Li P, Wang ZM, et al. Characterizing the genetic basis of methylome diversity in histologically normal human lung tissue. *Nat Commun* (2014) 5:1–11. doi: 10.1038/ncomms4365

frontiers | Frontiers in Endocrinology

TYPE Original Research
PUBLISHED 04 January 2023
DOI 10.3389/fendo.2022.1077514

OPEN ACCESS

EDITED BY
Jian Ma,
Harbin Medical University, China

REVIEWED BY
Chen Li,
Free University of Berlin, Germany
Fabio Nicoli,
Northumbria Healthcare NHS Foundation Trust, United Kingdom
Bowen Xing,
Children's Hospital of Philadelphia, United States

*CORRESPONDENCE
Yixin Zhang
zhangyixin6688@163.com
Peiru Min
aru_ren@msn.com

†These authors have contributed equally to this work and share first authorship

SPECIALTY SECTION
This article was submitted to Diabetes: Molecular Mechanisms, a section of the journal Frontiers in Endocrinology

RECEIVED 23 October 2022
ACCEPTED 13 December 2022
PUBLISHED 04 January 2023

CITATION
Li M, Ma H, Zhang S, Peng Y, Ding L, Zhang Y and Min P (2023) Potential therapeutic effect of NK1R antagonist in diabetic non-healing wound and depression.
Front. Endocrinol. 13:1077514.
doi: 10.3389/fendo.2022.1077514

Potential therapeutic effect of NK1R antagonist in diabetic non-healing wound and depression

Mingyu Li[1†], Hao Ma[1†], Shunuo Zhang[1], Yuan Peng[1], Liang Ding[2], Yixin Zhang[1*] and Peiru Min[1*]

[1]Department of Plastic and Reconstructive Surgery, Shanghai Ninth People's Hospital affiliated to Shanghai Jiao Tong University School of Medicine, Shanghai, China, [2]State Key Laboratory for Chemistry and Molecular Engineering of Medical Resources, School of Chemistry and Pharmaceutical Sciences, Guangxi Normal University, Guilin, China

Diabetes is a global disease with huge impacts on patients due to its complications, among which non-healing wounds and depression are common and challenging. The neurokinin 1 receptor (NK1R) inhibitor, aprepitant has been broadly applied for an antidepressant effect in depressive patients. Recent literature has indicated a therapeutic effect of downregulation in NK1R to diabetes-related fracture, cardiomyopathy, gastroparesis, and ocular surface disorders. In this study, differential expression genes in diabetes and depression were analyzed based on several RNA sequencing datasets from the GEO database to confirm NK1R in the overlapping set. Interaction network and gene set enrichment analysis were subsequently conducted. As a result, NK1R-related genes took part in angiogenesis, epithelial-mesenchymal transition (EMT), collagen deposition, and inflammation in diabetes and depression. *In vivo*, the downregulation of NK1R was proved to promote vascular proliferation and enhance diabetic wound healing, which provides a potential therapeutic target for the management of diabetic non-healing wounds and depression.

KEYWORDS

NK1R, aprepitant, T1DM, depression, wound healing

Introduction

Diabetes mellitus (DM) is a worldwide health problem associated with severe complications that influence both the patient's quality of life and survival (1). As one of the major categories, Type 1 DM (T1DM) exhibits hyperglycemia, significant microvascular injury and a chronic inflammatory response thus resulting in peripheral

nerve damage and impaired wound healing, especially at sacrococcygeal region and extremities (2, 3). Moreover, patients with T1DM tend to develop psychiatric morbidity (4). It has been stated that more than thirty percent of patients with T1DM may be suffered from depression (5). Although the exact mechanism remains unclear, treatment with insulin cannot simply manage the aforementioned conundrums simultaneously.

Recent studies have demonstrated the key role of neurogenic inflammation (NI) caused by the secretion of the proinflammatory neuropeptides from peripheral neurons in diabetes and depression (6, 7). As the specific receptor of neuropeptide Substance P (SP), the neurokinin-1 receptor (NK1R) is found expressed on neurons, epithelial cells, fibroblasts, and immune cells, thus mediating NI and contributes to inflammatory diseases and psychosomatic disorders (8). Aprepitant, the NK1R antagonist which originally developed for the blockage of the SP-NK1R pathway, has been broadly proved effective and beneficial for varies of depressions by both fundamental researches and clinical trials (9–13). On the other hand, NK1R antagonist demonstrated potential therapeutic effects for diabetic fractures, gastroparesis, and ocular surface diseases (14–16).

Therapeutic targets of diabetes have been widely studied. However, potential effects of aprepitant in diabetic non-healing wound were still lack of investigation. In this study, we hypothesized that NK1R played a vital role through inflammation in the development of T1DM-related non-healing wounds and depression. Moreover, inhibition of NK1R activation and subsequent pro-inflammatory initiation would possess a therapeutic effect in diabetic non-healing wound. The GSE37450 and GSE198597 dataset were used to explore the potential therapeutic effect of aprepitant for T1DM-related non-healing wounds and depression, respectively.

Materials and methods

Data acquisition and processing

The RNA sequencing data of T1DM and depression were downloaded from the Gene Expression Omnibus (GEO) database (https://www.ncbi.nlm.nih.gov/geo/). GSE37450 was used to analyze T1DM gene expression and GSE198597 was used to analyze depression gene expression.

Differential expression analysis

After log2 transformation, we used R (version 4.1.2) to calculate the differential expression of spleen leukocytes between normal and NOD mice in GSE37450. We performed lmFit and eBays functions in the limma package for multiple linear regression and statistical tests to obtain the significance of each differential expressed gene. The same methods were applied to GSE198597 for differential expression of the hypothalamus between normal and depressed C57BL/6N mice.

Enrichment analysis

We performed Gene set enrichment analysis (GSEA) using the GSEA software (GSEA version: 4.2.3) from Broad Institute (https://www.gsea-msigdb.org/gsea/index.jsp). We downloaded Gene Ontology gene sets containing BP, CC, and MF subsets as well as hallmark gene sets in the Molecular Signatures Database (MSigDB). The minimum number of the gene set was 5, and the maximum number of the gene set was 5000. After a thousand resampling, we obtained the related pathways and molecular mechanisms in MSigDB.

Correlation and interaction analysis

Protein interaction data were derived from the STRING database (https://string-db.org). The interaction network was depicted in Cytoscape (version 3.4.1). Then, Pearson correlation analysis by the corr. test function of the psych package was performed for the NK1R-related genes in overlapped gene sets. In addition, the heatmaps of overlapped genes in each disease were obtained from a complex heatmap package.

Animals

C57BL/6 mice (male, 6 weeks old) were supplied by ShengChang Biotech (Shanghai, China). All animal experiments were approved by the Animal Experimentation Ethics Committee of the School of Medicine, Shanghai Jiao Tong University. C57BL/6 mice were accommodated in a controlled habitat and provided with water and rodent food for 1 week to be familiarized with their habitat.

Diabetes induction

After a week of adaptive feeding, C57BL/6 mice were singly intraperitoneally injected with streptozotocin (STZ, 150mg/kg, Sigma-Aldrich, S0130) in a freshly prepared citrate buffer (0.1 M, pH 4.5). In the next 5 days, the blood glucose was measured by a blood glucose monitor (Supplementary Materials, Table S1). The mice that showed blood glucose concentrations above 16.7 mM were considered diabetic and used for further experimentation.

Full-thickness wound model in diabetic mice

After diabetes induction, a total of 24 diabetic mice were anesthetized by intraperitoneal injection of 10% chloral hydrate (3.5 mL per 1 kg body weight). Before wound fabrication, the dorsal side of the mice was shaved, depilated, and disinfected. Then, an oval wound (about 6 mm in diameter) was created on the dorsum of the mouse. The NK-1R antagonist aprepitant (Med Chem Express, CAS No. 170729-80-3, 15uL/wound) was injected around the wounds immediately. The 24 mice were randomly divided into 4 groups: 0uM (PBS, control) group; 200uM-aprepitant group; 500uM-aprepitant group and 1000uM-aprepitant group. Treatments were performed every day until Day 15. Digital photographs were taken at day 0, 5, 10, and 15. A circular marker (6mm in diameter) was placed around the wound to standardize the measurements. ImageJ software was used to calculate the wound area of each photographic image. Besides, body weight was also established at day 0, 5, 10, and 15.

Histological analysis

After 15 days, all remaining mice were sacrificed, and the surrounding tissues of wounds were obtained for histological analysis. The wounds were fixed with 4% paraformaldehyde for tissue fixation. After being dehydrated with a series of graded ethanol, the tissues were embedded in paraffin and cut into 5-μm-thick longitudinal section. Then, the sections were stained with hematoxylin and eosin (H&E) and Masson's trichrome stain. The image was taken by a microscope (Nikon, Japan).

Immunohistochemistry analysis

The expression of CD31 in wounds was examined using an anti-CD31 antibody (Abcam, ab28364) by a standard immunohistochemistry protocol. Dewaxed sections were incubated with primary anti-CD31 antibody (Abcam, ab28364) at a dilution of 1:300 for 1 h at room temperature and then incubated with goat anti-mouse immunoglobulin (HRP, Abcam, ab6789) secondary antibody for 30 min at room temperature. The image was taken by a microscope (Nikon, Japan).

Quantitative RT-PCR analysis

After 15 days, all remaining mice were sacrificed, and the surrounding tissues of wounds were obtained for qRT-PCR. Wound skin tissues were stored in liquid nitrogen and total RNA was extracted using TRIzol reagent (Invitrogen, USA) according to the manufacturer's protocol. Then, 1 μg of total RNA was reverse transcribed into cDNA using the FastKing cDNA synthesis kit (Tiangen Biotech, China). qRT-PCR was performed with TB Green Premix (Takara, Japan). The mRNA expression levels of GAD1, ALDH1B1, FOXP2 were detected. PCR primers were designed based on sequences from the corresponding genes (Supplementary Materials, Table S2). All data were normalized using GAPDH as the internal control by the Δ-CT method.

Western blotting

Total proteins were extracted using RIPA lysis buffer containing phosphatase and protease inhibitors (Beyotime Biotechnology, China). The concentration of total protein was detected with a BCA Protein Assay kit (Beyotime Biotechnology, China). Equal amounts (20 μg) of protein were separated using 4–20% SDS-PAGE gels. The proteins were then transferred to nitrocellulose membranes (0.45μm; Millipore, USA). The membranes were blocked with 5% non-fat milk for 1 h at room temperature and incubated with primary antibodies (Supplementary Materials, Table S3) overnight at 4°C. After washing, the membranes were incubated with goat anti-rabbit secondary antibodies (Table S2). Finally, the membranes were visualized using the Odyssey CLx Infrared Imaging System (LI-COR Biosciences, Lincoln,Nebraska, USA). GAPDH and β-actin protein intensities were used as internal controls.

Statistical analysis

Data analysis was performed using GraphPad Prism (9.0.0, America). Continuous variables are presented as the mean (± standard deviation, SD). One-way analysis of variance (ANOVA) was performed to compare the means of multiple groups, and if significant, a *post hoc* Tukey's test was used to explore the pairwise differences between groups. P-values< 0.05 were considered statistically significant.

Results

1 NK1R was both up-regulated in T1DM and depression

By differential expression analysis of GSE37450, NK1R was found up-regulated in T1DM. Among all of the differentially expressed genes, NK1R belonged to the top-ranking sets. In hallmark gene sets, we found that differentially expressed genes in T1DM were significantly correlated with epithelial-

mesenchymal transition (EMT), inflammatory response, myogenesis, apical junction, and angiogenesis (Figure 1).

In GSE198597, we found NK1R was significantly up-regulated in depression and belonged to the top-ranking sets as well. These differently expressed genes in depression were enriched in EMT, interferon response, bile acid metabolism, oxidative phosphorylation and angiogenesis, which was similar to the enrichment analysis of T1DM (Figure 2).

2 The overlapped genes in T1DM and depression constructed an interaction network

After differential expression analysis of GSE37450 and GSE198597, we found 97 overlapped genes that are differently expressed in both datasets (Figure 3A). The interaction network of these overlapped genes from STRING was depicted, and NK1R-related genes (Gal, Gad1, Foxp2, Lhx9, and Aldh1b1) in the network were extracted (Figures 3B, C). Then, Pearson analysis was performed to show the correlation among NK1R-related genes (Figures 3D, E). In addition, we constructed a heatmap of overlapped genes in each disease to show the expression pattern respectively (Figures 3F, G).

3 Enrichment analysis of overlapped genes

Furtherly, we performed GO enrichment analysis for overlapped genes. In the biological process, these genes were enriched in the regulation of cardiocyte differentiation, fat cell differentiation, and organ morphogenesis. In the cellular component, they were enriched in the adherens junction, basal plasma membrane, and extracellular matrix. As for molecule function, GDP binding, kinase binding, nuclear receptor activity, and transcription factor activity were found enriched by overlapped genes (Figures 4A–C). Then, we combined the expression matrix and GO enrichment analysis, constructing the interaction network between overlapped genes and GO terms (Figures 4D–I).

4 The NK-1R antagonist aprepitant promoted diabetic wound healing *in vivo*

To explore the potential therapeutic effect of NK-1R antagonist aprepitant for clinical treatment, we established a full-thickness diabetic wound model and used PBS, 200uM aprepitant, 500uM aprepitant, 1000uM aprepitant to treat the

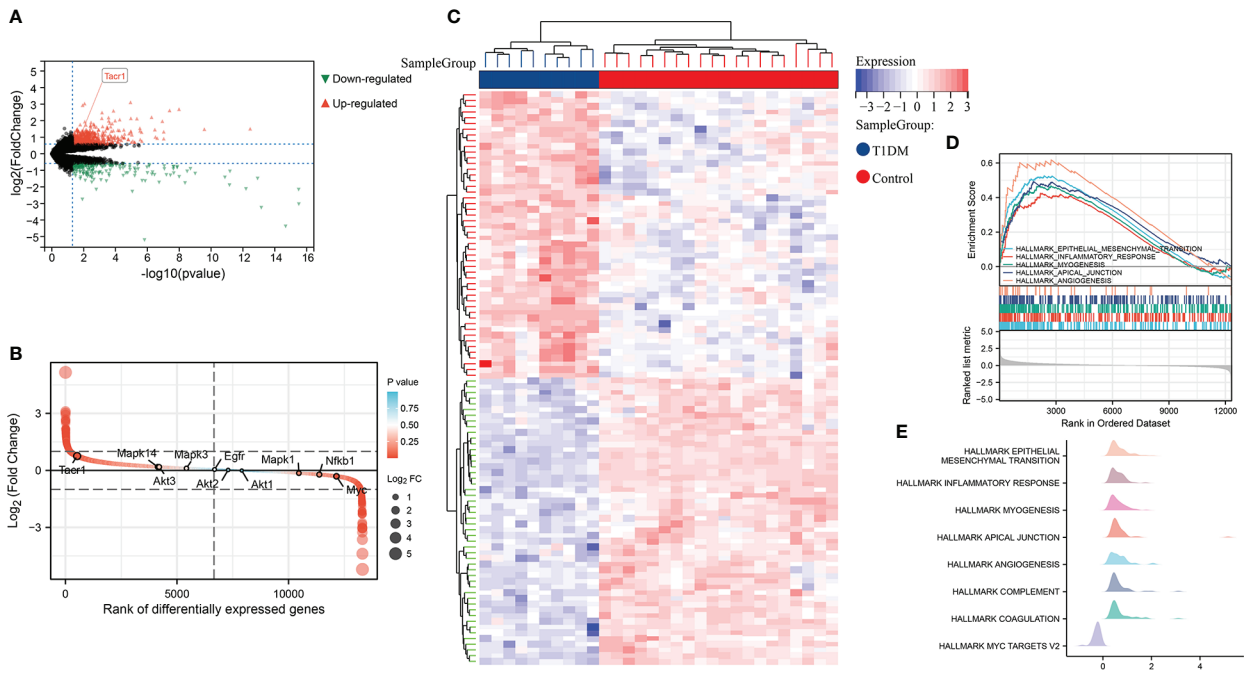

FIGURE 1
(A) Volcano plot of differential expression analysis in GSE37450 dataset. **(B)** Rank of differentially expressed genes in GSE37450 dataset. **(C)** Heatmap of differential expression analysis in GSE37450 dataset. **(D)** Enrichment score and the rank in ordered dataset of GSEA hallmark gene sets in GSE37450 dataset. **(E)** The distribution of gene expression in significant hallmark gene sets in GSE37450. X axis represents log2(Fold Change) of enriched genes.

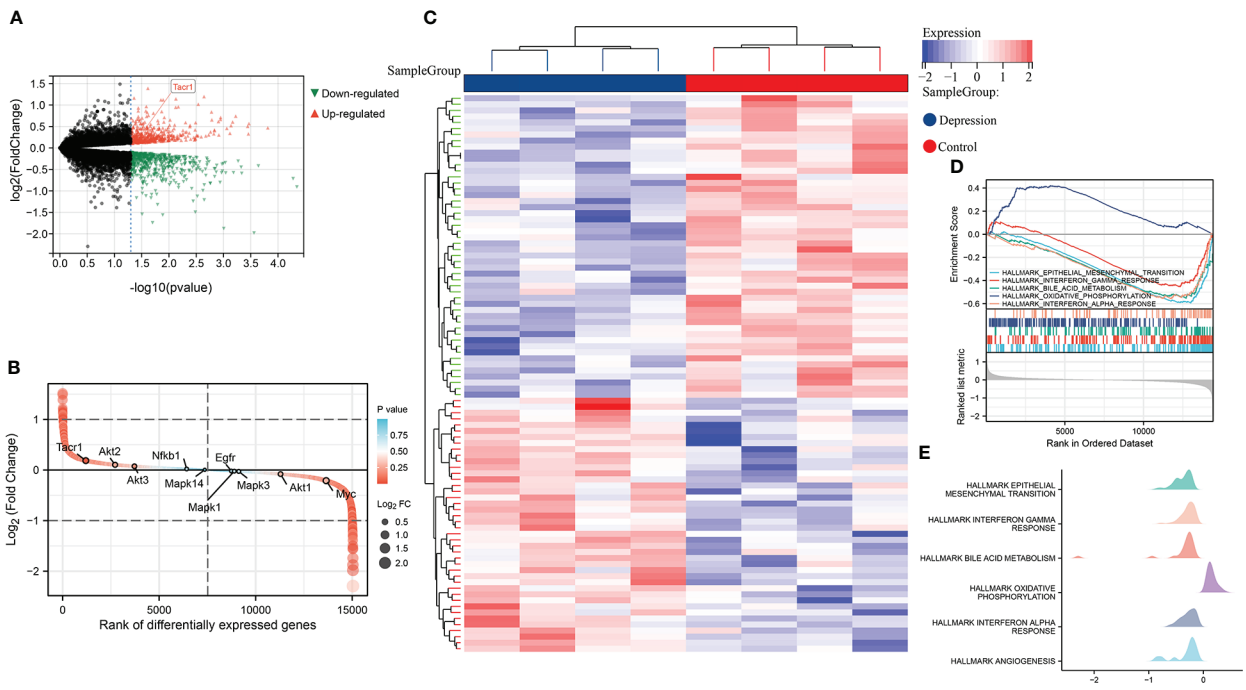

FIGURE 2
(A) Volcano plot of differential expression analysis in GSE198597 dataset. **(B)** Rank of differentially expressed genes in GSE198597 dataset. **(C)** Heatmap of differential expression analysis in GSE198597 dataset. **(D)** Enrichment score and the rank in ordered dataset of GSEA hallmark gene sets in GSE198597 dataset. **(E)** The distribution of gene expression in significant hallmark gene sets in GSE198597. X axis represents log2(Fold Change) of enriched genes.

diabetic mice (Figure 5A). The unclosed wound rate in mice treated with 1000uM aprepitant was the lowest in these different treated groups at days 0, 5, 10, and 15 post-wounding (Figures 5B, C). Moreover, the aprepitant-treated groups resulted in the recovery of body weights compared with controled group (Figure 5D). Besides, histological analyses were performed to investigate the wound repair efficiency in different treatment groups at day 15 post-operation. H&E staining analysis(5X,20X,40X) showed that 1000uM aprepitant-treated group exhibited the highest re-epithelialization rate among other groups (Figure 5E). We also observed the Masson staining analysis which demonstrated that the collagen deposition in the 1000uM aprepitant-treated group was significantly increased when compared to other groups (Figure 5F). CD31 is an indicator of blood vessels and very few blood vessels were observed in the wound tissues of the PBS group, while the treatment of 200uM, 500uM, and 1000uM groups improved vascular network formation (Figure 5G). Notably, the most CD31-positive blood vessels per field in CD31 immunostaining photographs (40X) was achieved in the 1000uM group (Figure 5H). On Day 15, we measured the mRNA level of GAD1, ALDH1B1, and FOXP2 in the wound skins. The results showed that the levels of GAD1, ALDH1B1, and FOXP2 in the 1000uM aprepitant group were reduced compared to the PBS, and 200uM groups (Figure 5I). The results of western blotting showed similar concentration-related trend as qRT-PCR (Figure 5J). These data indicated that aprepitant significantly accelerated diabetic wound healing by promoting wound re-epithelialization, collagen deposition and angiogenesis, with down-regulated GAD1, ALDH1B1, and FOXP2 expression in wounds.

Discussion

It is commonly acknowledged that T1DM results from the inflammatory response, exhibiting microvascular injury and damage to peripheral nerves (17). As a critical mediator between neurons and inflammation, NK1R is responsible for the release of proinflammatory cytokines such as CCL4, CXCL2, MCP-1, CCL5, and IL-8, which recruit monocytes, macrophages, and lymphocytes thus leading to the pathogenesis of various inflammatory diseases (18). Neuroimmune interactions with macrophages controlled islet destruction, indicating the control of neuroimmune interactions may represent a new therapeutic target for T1DM (19). Recent reports showed that targeting NK1R was effective in several diabetes-related diseases. Carlin et al. (15) found that the application of NK1R antagonist, and

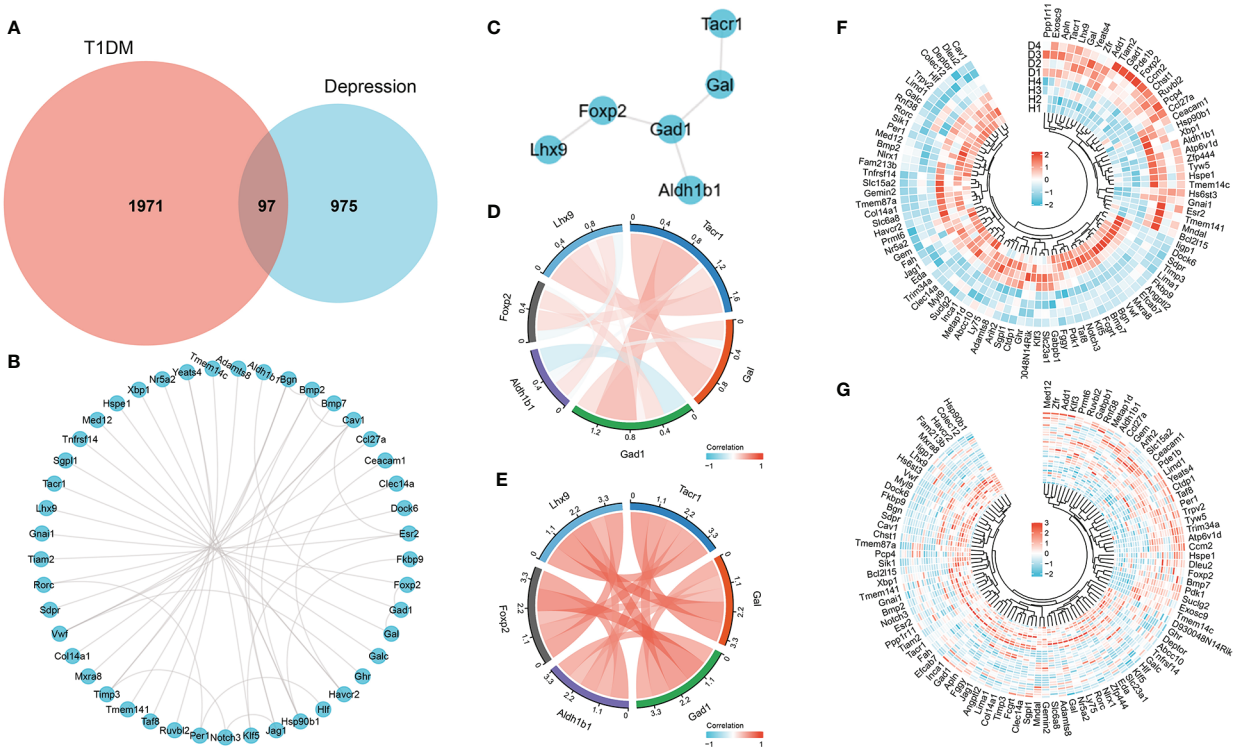

FIGURE 3
(A) Overlapped genes of differential expression analysis in both GSE37450 and GSE198597 dataset. **(B)** Interaction network of overlapped genes. **(C)** Interaction of NK1R-related genes in overlapped gene sets. **(D)** Pearson analysis of NK1R-related genes in overlapped gene sets in GSE37450 dataset. **(E)** Pearson analysis of NK1R-related genes in overlapped gene sets in GSE198597 dataset. **(F)** Heatmap of NK1R-related genes in overlapped gene sets in GSE37450 dataset. **(G)** Heatmap of NK1R-related genes in overlapped gene sets in GSE198597 dataset.

tradipitant clinically improved the patients with diabetic gastroparesis. Jeong et al. (20) described the effects of selective NK1R antagonist RP-67580 in diabetic atria. Although there are studies illustrating the association between NK1R and diabetic complications, e.g., corneal wound healing, fracture, and limb ischemia, evidence-based insight into the exact mechanisms were still lacking (14, 21, 22). As diabetic non-healing wounds and depression are highly correlated with chronic inflammation while NK1R plays a central role in the development of inflammation *via* angiogenesis, we hypothesized NK1R as a potential therapeutic target for both diseases (23).

Based on the results of the bioinformatics analysis, differential gene expression showed that NK1R was significantly upregulated in diabetes and depression, indicating a key role of NK1R in both diseases. According to hallmark gene sets in GSEA, differently expressed genes in diabetes were enriched in EMT, inflammatory response, and angiogenesis, which was also found highly correlated with depression, indicating the potentially shared mechanisms between the two diseases. Then, we performed GO analysis on overlapped genes to clarify the enrichment relationship between diabetes and depression. The results showed that these genes were enriched in organ morphogenesis, fat cell and cardiocyte differentiation, adherens junction, basal plasma membrane, extracellular matrix, GDP and kinase binding, nuclear receptor activity as well as a transcription factor.

To further explore the key proteins related to NK1R which affected the development of diabetes and depression, we conducted PPI analysis and identified the five NK1R-related genes: aldehyde dehydrogenase 1B1 (ALDH1B1), forkhead box P2 (FOXP2), galanin (GAL), glutamate decarboxylase 1 (GAD1) and LIM homeobox 9 (LHX9). Among the five aforementioned genes, GAL has been broadly studied along with the NK1R in neurons and found to interact with life stresses thus mediating depression and anxiety (24–26). Moreover, GAL also regulated insulin release, which was associated with T1DM development (27). ALDH1B1 was found upregulated in the injured pancreas after streptozotocin paradigms and showed an association with diabetes (28, 29). Li T et al. revealed the relationship between FOXP2 and depression (30). As to LHX9, the hypothalamic marker has been proven highly correlated with FOXP2 in patients with depression (30–33). Combined with the enrichment analysis, we provoked the hypothesis that the GAD1, ALDH1B1, and FOXP2 genes functioned with NK1R

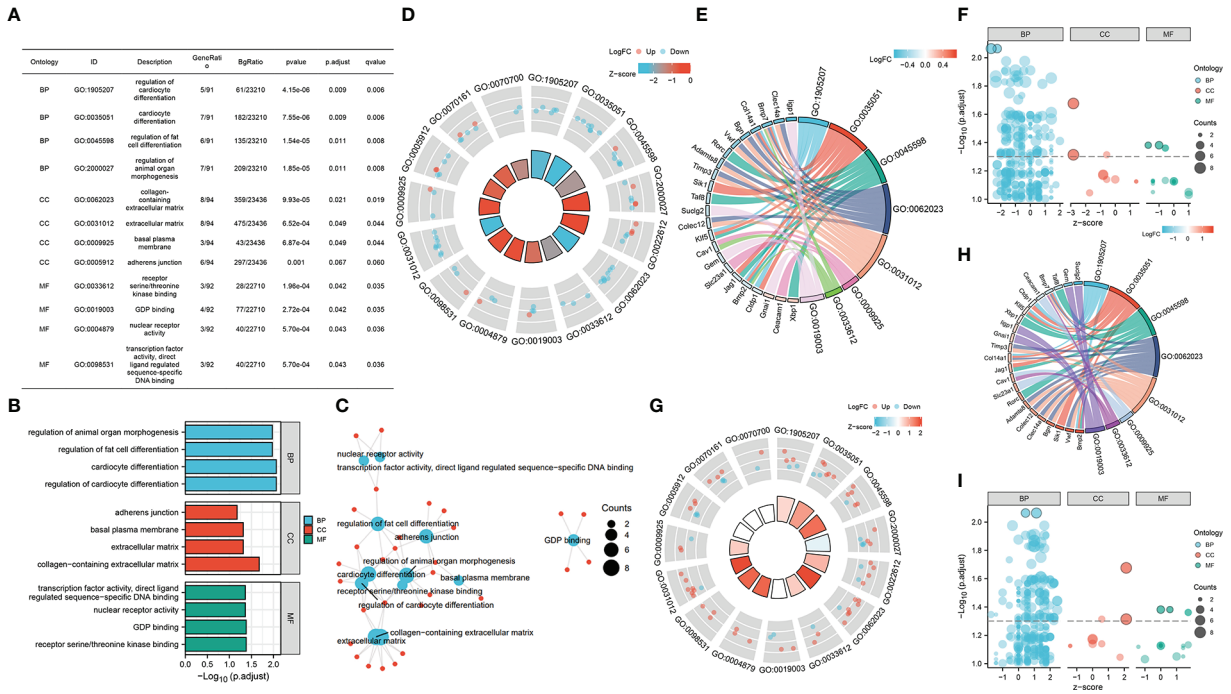

FIGURE 4
(A–C) GO enrichment analysis of overlapped gene sets. **(D–F)** GO enrichment analysis of overlapped gene sets based on GSE37450 expression matrix. **(G–I)** GO enrichment analysis of overlapped gene sets based on GSE198597 expression matrix.

in terms of angiogenesis, EMT, collagen deposition, and inflammation, while blockade of NK1R may be therapeutic not only for depression but also for the diabetic non-healing wound.

To further verify the hypothesis, C57BL/6 mice were generated as a murine model of a T1DM non-healing wound. Strikingly, we found that topically applied NK1R antagonist, aprepitant could promote the healing of the refractory diabetic wound in a concentration-related manner. qRT-PCR and western blotting were then used for the verification of selected related genes and proteins in the diabetic non-healing wound model. The mRNA level of GAD1, ALDH1B1 and FOXP2 was observed to downregulated in aprepitant-treated mice in a concentration-related and negatively-correlated manner. The expression of these proteins was proved to be downregulated with aprepitant and showed the same concentration-related manner as qRT-PCR. Versus the control group, the thickening epithelial layer and increased collagen deposition could be observed by H&E and Masson staining. CD31 immunohistochemistry showed that a high concentration of aprepitant could potentially increase neovascularization. These phenomenons provided compelling pieces of evidence that aprepitant could effectively promote the healing process of T1DM non-healing wounds through regulation of the aforementioned NK1R-related genes. The underlying mechanism is still controversial. Momen (34) contributed the aprepitant-related angiogenesis to MMP-2, MMP-9, VEGF, and VEGFR. On the other hand, regulation of EGFR, Akt, and SIRT1 by NK1R blockade was also considered beneficial in terms of re-epithelialization and collagen deposition (35–37).

To the best of our knowledge, our study was the first to utilize bioinformatics methods in detecting potential therapeutic targets in diabetic non-healing wound and depression. We explored the common mechanisms of the two diseases, analyzed roles of NK1R-related genes and verified the therapeutic effect of aprepitant. Although the related pathways and key molecules remain not entirely clear, our work provided promising evidences that blockage of the SP-NK1R pathway will downregulate the expression of ALDH1B1, FOXP2 and GAD1, which may be therapeutic for both diseases.

Besides, the neuroinflammation network plays an important role in both diseases, while NK1R could initiate neurogenic inflammation thus leading to neuronal damage (38–40). The release of inflammatory cytokines and the activation of CD8+ T cells contribute to pancreas injury, followed by vasodilation and increased permeability of the microvasculature caused by NK1R (2, 18). Consequently, rescuing the disrupted vascular endothelial cells and relieving neurogenic inflammation through the NK1R pathway stands as a promising therapeutic strategy. Our study also has some limitations. Due to lacking in

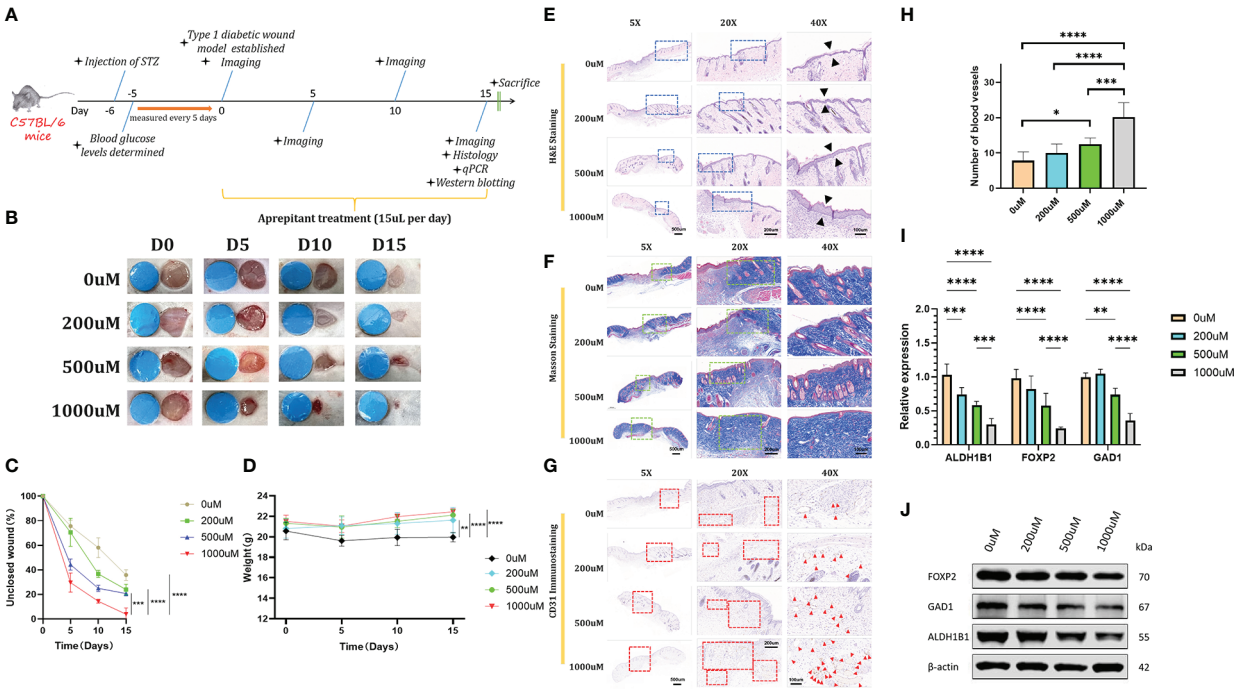

FIGURE 5
(A) Schematic timeline of diabetic wound formation and the following treatments. **(B, C)** Representative images and quantitative measurement of wounds on days 0, 5, 10, and 15 days. **(D)** Changes of body weights of mice after different treatments. **(E, F)** Representative H&E staining images and Masson staining images. **(G, H)** Representative CD31 immunostaining images after different treatments and the corresponding quantitative data of the CD31-positive blood vessels' numbers from respective staining images (40X). **(I)** qRT-PCR analysis of relative ALDH1B1, FOXP2, and GAD1 levels in different treated groups. **(J)** Expression of ALDH1B1, FOXP2, and GAD1 levels in different treated groups detected by western blotting analysis. Scale bars: 500μm for 5X, 200μm for 20X, and 100μm for 40X. n=6, ns: no significant, *p <.05, **p <.01, ***p <.001, ****p <.0001. Data were presented as mean ± SD. One-way ANOVA with Tukey *post-hoc* test was used.

feasible animal models with both diseases, further *in vivo* study for depression in T1DM mice is yet to be verified. Moreover, in-depth researches need to be carried out to reveal the underlying mechanisms and complex interplay between the two diseases.

Data availability statement

The datasets presented in this study can be found in online repositories. The names of the repository/repositories and accession number(s) can be found in the article/Supplementary Material.

Ethics statement

The animal study was reviewed and approved by Animal Experimentation Ethics Committee of the School of Medicine, Shanghai Jiao Tong University.

Author contributions

ML and HM performed data processing, animal experiments as well as statistical analysis, and were major contributors to writing the manuscript. SZ conducted the experiments and YP took part in the statistical analysis. LD helped in the data collection. YZ revised the manuscript. PM conceived and designed this study and revised the manuscript. All the authors read and approved the final manuscript.

Funding

This study was supported by the National Natural Science Foundation of China (grant number: 82172222, 81801918), the Outstanding Professional and Technical Leader Program of the Shanghai Municipal Science and Technology Commission(18XD1423700), the Shanghai Health Industry Clinical Research Special Project (20204Y0443), and the Cross Research Project of Ninth People's Hospital, Shanghai Jiao Tong University School of Medicine (JYJC202009), Shanghai Municipal Education Commission-Gaofeng Clinical Medicine Grant Support (Grant number:20152227).

Conflict of interest

The authors declare that the research was conducted in the absence of any commercial or financial relationships that could be construed as a potential conflict of interest.

Publisher's note

All claims expressed in this article are solely those of the authors and do not necessarily represent those of their affiliated organizations, or those of the publisher, the editors and the reviewers. Any product that may be evaluated in this article, or claim that may be made by its manufacturer, is not guaranteed or endorsed by the publisher.

Supplementary material

The Supplementary Material for this article can be found online at: https://www.frontiersin.org/articles/10.3389/fendo.2022.1077514/full#supplementary-material

References

1. Siddiqui AA, Siddiqui SA, Ahmad S, Siddiqui S, Ahsan I, Sahu K. Diabetes: Mechanism, pathophysiology and management-a review. *Int J Drug Dev Res* (2013) 5(2):0–.

2. Baltzis D, Eleftheriadou I, Veves A. Pathogenesis and treatment of impaired wound healing in diabetes mellitus: new insights. *Adv Ther* (2014) 31(8):817–36.

3. Greenhalgh DG. Wound healing and diabetes mellitus. *Clinics Plast surgery.* (2003) 30(1):37–45.

4. Jacobson AM, Samson JA, Weinger K, Ryan CM. Diabetes, the brain, and behavior: is there a biological mechanism underlying the association between diabetes and depression? *Int Rev Neurobiol* (2002) 51:455–79.

5. Prabhakar V, Gupta D, Kanade P, Radhakrishnan M. Diabetes-associated depression: the serotonergic system as a novel multifunctional target. *Indian J Pharmacol* (2015) 47(1):4.

6. Duarte-Silva E, de Melo MG, Maes M, Chaves Filho AJM, Macedo D, Peixoto CA. Shared metabolic and neuroimmune mechanisms underlying type 2 diabetes mellitus and major depressive disorder. *Prog Neuropsychopharmacol Biol Psychiatry* (2021) 111:110351. doi: 10.1016/j.pnpbp.2021.110351

7. Tsui H, Winer S, Chan Y, Truong D, Tang L, Yantha J, et al. Islet glia, neurons, and β cells: The neuroimmune interface in the pathogenesis of type 1 diabetes. *Ann New York Acad Sci* (2008) 1150(1):32–42. doi: 10.1196/annals.1447.033

8. Muñoz M, Coveñas R, Esteban F, Redondo M. The substance P/NK-1 receptor system: NK-1 receptor antagonists as anti-cancer drugs. *J biosciences.* (2015) 40(2):441–63.

9. Ebner K, Singewald GM, Whittle N, Ferraguti F, Singewald N. Neurokinin 1 receptor antagonism promotes active stress coping *via* enhanced septal 5-HT transmission. *Neuropsychopharmacology* (2008) 33(8):1929–41. doi: 10.1038/sj.npp.1301594

10. Schank JR, Heilig M. Chapter six - substance p and the neurokinin-1 receptor: The new CRF. In: Thiele TE, editor. *International review of neurobiology.* 136: Academic Press (2017) 151–75. doi: 10.1016/bs.irn.2017.06.008

11. Hargreaves R. Imaging substance p receptors (NK1) in the living human brain using positron emission tomography. *J Clin Psychiatry* (2002) 63(11):18–24.

12. Kramer MS, Cutler N, Feighner J, Shrivastava R, Carman J, Sramek JJ, et al. Distinct mechanism for antidepressant activity by blockade of central substance p receptors. *Science* (1998) 281(5383):1640–5. doi: 10.1126/science.281.5383.1640

13. Krishnan KRR. Clinical experience with substance p receptor (NK1) antagonists in depression. *J Clin Psychiatry* (2002) 63(11):25–9.

14. Wang X, Su N. Neurokinin-1-tachykinin receptor agonist promotes diabetic fracture healing in rats with type 1 diabetes *via* modulation of wnt/β-catenin signalling axis. *Saudi J Biol Sci* (2021) 28(4):2139–45. doi: 10.1016/j.sjbs.2021.02.026

15. Carlin JL, Lieberman VR, Dahal A, Keefe MS, Xiao C, Birznieks G, et al. Efficacy and safety of tradipitant in patients with diabetic and idiopathic gastroparesis in a randomized, placebo-controlled trial. *Gastroenterology* (2021) 160(1):76–87.e4. doi: 10.1053/j.gastro.2020.07.029

16. Zhu L, Titone R, Robertson DM. The impact of hyperglycemia on the corneal epithelium: molecular mechanisms and insight. *Ocular Surface.* (2019) 17 (4):644–54. doi: 10.1016/j.jtos.2019.06.007

17. Egan AM, Dinneen SF. What is diabetes? *Medicine* (2019) 47(1):1–4. doi: 10.1016/j.mpmed.2018.10.002

18. O'Connor TM, O'Connell J, O'Brien DI, Goode T, Bredin CP, Shanahan F. The role of substance p in inflammatory disease. *J Cell Physiol* (2004) 201(2):167–80. doi: 10.1002/jcp.20061

19. Christoffersson G, Ratliff SS, von Herrath MG. Interference with pancreatic sympathetic signaling halts the onset of diabetes in mice. *Sci Adv* (2020) 6(35): eabb2878. doi: 10.1126/sciadv.abb2878

20. Jeong Y, Lee S, Kim W. Substance P/neurokinin1 receptor is associated with the expression of cardiac stem/pluripotency-associated genes in diabetic right and left atria. Research Square (2021). doi: 10.21203/rs.3.rs-254561/v1

21. Dang Z, Avolio E, Albertario A, Sala-Newby GB, Thomas AC, Wang N, et al. Nerve growth factor gene therapy improves bone marrow sensory innervation and nociceptor-mediated stem cell release in a mouse model of type 1 diabetes with limb ischaemia. *Diabetologia* (2019) 62(7):1297–311. doi: 10.1007/s00125-019-4860-y

22. Yang L, Di G, Qi X, Qu M, Wang Y, Duan H, et al. Substance p promotes diabetic corneal epithelial wound healing through molecular mechanisms mediated *via* the neurokinin-1 receptor. *Diabetes* (2014) 63(12):4262–74. doi: 10.2337/db14-0163

23. Esteban F, Ramos-García P, Muñoz M, González-Moles MÁ. Substance p and neurokinin 1 receptor in chronic inflammation and cancer of the head and neck: A review of the literature. *Int J Environ Res Public Health* (2022) 19(1):375.

24. Spirovski D, Li Q, Pilowsky PM. Brainstem galanin-synthesizing neurons are differentially activated by chemoreceptor stimuli and represent a subpopulation of respiratory neurons. *J Comp Neurology.* (2012) 520(1):154–73. doi: 10.1002/cne.22723

25. Rana T, Behl T, Sehgal A, Singh S, Sharma N, Abdeen A, et al. Exploring the role of neuropeptides in depression and anxiety. *Prog Neuropsychopharmacol Biol Psychiatry* (2022) 114:110478. doi: 10.1016/j.pnpbp.2021.110478

26. Juhasz G, Hullam G, Eszlari N, Gonda X, Antal P, Anderson IM, et al. Brain galanin system genes interact with life stresses in depression-related phenotypes. *Proc Natl Acad Sci* (2014) 111(16):E1666–E73. doi: 10.1073/pnas.1403649111

27. Fang P, Yu M, Shi M, Bo P, Zhang Z. Galanin peptide family regulation of glucose metabolism. *Front Neuroendocrinology.* (2020) 56:100801. doi: 10.1016/j.yfrne.2019.100801

28. Ioannou M, Serafimidis I, Arnes L, Sussel L, Singh S, Vasiliou V, et al. ALDH1B1 is a potential stem/progenitor marker for multiple pancreas progenitor pools. *Dev Biol* (2013) 374(1):153–63. doi: 10.1016/j.ydbio.2012.10.030

29. Singh S, Chen Y, Matsumoto A, Orlicky DJ, Dong H, Thompson DC, et al. ALDH1B1 links alcohol consumption and diabetes. *Biochem Biophys Res Commun* (2015) 463(4):768–73. doi: 10.1016/j.bbrc.2015.06.011

30. Li T, Zeng Z, Zhao Q, Wang T, Huang K, Li J, et al. FoxP2 is significantly associated with schizophrenia and major depression in the Chinese han population. *World J Biol Psychiatry* (2013) 14(2):146–50. doi: 10.3109/15622975.2011.615860

31. Liu J, Merkle FT, Gandhi AV, Gagnon JA, Woods IG, Chiu CN, et al. Evolutionarily conserved regulation of hypocretin neuron specification by Lhx9. *Development* (2015) 142(6):1113–24. doi: 10.1242/dev.117424

32. Homman-Ludiye J, Kwan WC, de Souza MJ, Bourne JA. Full: Ontogenesis and development of the nonhuman primate pulvinar. *J Comp Neurology.* (2018) 526(17):2870–83. doi: 10.1002/cne.24534

33. Dalal J, Roh JH, Maloney SE, Akuffo A, Shah S, Yuan H, et al. Translational profiling of hypocretin neurons identifies candidate molecules for sleep regulation. *Genes Dev* (2013) 27(5):565–78. doi: 10.1101/gad.207654.112

34. Momen Razmgah M, Ghahremanloo A, Javid H, AlAlikhan A, Afshari A-R, Hashemy SI. The effect of substance p and its specific antagonist (aprepitant) on the expression of MMP-2, MMP-9, VEGF, and VEGFR in ovarian cancer cells. *Mol Biol Rep* (2022) 49(10):9307–14. doi: 10.1007/s11033-022-07771-w

35. Zhang S, Li K, Yu Z, Jun C, Zhang Z, Zhang Y, et al. Dramatic effect of botulinum toxin type a on hypertrophic scar: A promising therapeutic drug and its mechanism through the SP-NK1R pathway in cutaneous neurogenic inflammation. *Front Med* (2022) 520. doi: 10.3389/fmed.2022.820817

36. Backman LJ, Eriksson DE, Danielson P. Substance p reduces TNF-α-induced apoptosis in human tenocytes through NK-1 receptor stimulation. *Br J sports Med* (2014) 48(19):1414–20. doi: 10.1136/bjsports-2013-092438

37. Ceci L, Francis H, Zhou T, Giang T, Yang Z, Meng F, et al. Knockout of the tachykinin receptor 1 in the Mdr2–/–(Abcb4–/–) mouse model of primary sclerosing cholangitis reduces biliary damage and liver fibrosis. *Am J Pathology.* (2020) 190(11):2251–66. doi: 10.1016/j.ajpath.2020.07.007

38. Singh RB, Naderi A, Cho W, Ortiz G, Musayeva A, Dohlman TH, et al. Modulating the tachykinin: Role of substance p and neurokinin receptor expression in ocular surface disorders. *Ocular Surface* (2022) 25:142–53. doi: 10.1016/j.jtos.2022.06.007

39. Jayasimhan A, Mariño E. Dietary SCFAs, IL-22, and GFAP: The three musketeers in the gut–Neuro–Immune network in type 1 diabetes. *Front Immunol* (2019) 10:2429. doi: 10.3389/fimmu.2019.02429

40. Morris G, Berk M F, Carvalho A, Caso J R, Sanz Y, Maes M. The role of microbiota and intestinal permeability in the pathophysiology of autoimmune and neuroimmune processes with an emphasis on inflammatory bowel disease type 1 diabetes and chronic fatigue syndrome. *Curr Pharm design.* (2016) 22(40):6058–75. doi: 10.2174/1381612822666160914182822

frontiers | Frontiers in Endocrinology

TYPE Original Research
PUBLISHED 10 January 2023
DOI 10.3389/fendo.2022.1051374

OPEN ACCESS

EDITED BY
Xuebin Fu,
Ann &Robert H. Lurie Children's Hospital of Chicago,
United States

REVIEWED BY
Zhangyuan Yin,
Broad Institute, United States
Yuntian Guan,
University of Virginia, United States

*CORRESPONDENCE
Xiaolin Tang
xltang@cmu.edu.cn

SPECIALTY SECTION
This article was submitted to Diabetes: Molecular Mechanisms, a section of the journal Frontiers in Endocrinology

RECEIVED 22 September 2022
ACCEPTED 12 December 2022
PUBLISHED 10 January 2023

CITATION
Wang Y, Huang M, Xu W, Li F, Ma C and Tang X (2023) Calcitriol-enhanced autophagy in gingival epithelium attenuates periodontal inflammation in rats with type 2 diabetes mellitus. *Front. Endocrinol.* 13:1051374. doi: 10.3389/fendo.2022.1051374

Calcitriol-enhanced autophagy in gingival epithelium attenuates periodontal inflammation in rats with type 2 diabetes mellitus

Yanan Wang, Maoting Huang, Wanlin Xu, Fulong Li, Chunliang Ma and Xiaolin Tang*

Department of Periodontology, School and Hospital of Stomatology, China Medical University, Liaoning Provincial Key Laboratory of Oral Diseases, Shenyang, China

Type 2 diabetes mellitus (T2DM)-associated periodontitis is a common disease with high prevalence, associated with persistent infection and complicated manifestations. Calcitriol (1 alpha, 25-dihydroxyvitamin D3, 1,25D) is the active form of vitamin D that plays a protective role in immune regulation, bone metabolism, and inflammatory response. In this study, we constructed a T2DM model in rats by combining a high-fat diet with low-dose streptozotocin. The periodontitis model in rats was developed by ligation and *Porphyromonas gingivalis* (ATCC 33277) inoculation. Rats were randomly divided into five groups: non-diabetic blank, diabetic blank, diabetes with calcitriol treatment, diabetes with 3-methyladenine (3-MA) treatment, or diabetes with calcitriol and 3-MA treatment. The diabetic rats exhibited an intense inflammatory response and decreased autophagy compared with the non-diabetic rats. Intraperitoneal injection of calcitriol and autophagy inhibitor (3-MA) allowed us to explore the effect of calcitriol on inflammation in the gingival epithelium and the role of autophagy in this process. Treatment with calcitriol resulted in the decreased expression of NFκB-p65, p62/SQSTM1 and inflammatory response and increased expression of LC3-II/LC3-I. Application of 3-MA significantly suppressed autophagy, which was apparently retrieved by calcitriol. Antibacterial peptide (LL-37) is the only antimicrobial peptide in the cathelicidin family that is found in the human body, and it exhibits a broad spectrum of antibacterial activity and regulates the immune system. In the present study, our findings indicated that calcitriol-enhanced autophagy may attenuated periodontitis and the decrease of LL-37 was rescued by calcitriol treatment in the gingival epithelial cells of T2DM rats. Our study provides evidence for the application of calcitriol as an adjunctive treatment for T2DM-associated periodontitis.

KEYWORDS

type 2 diabetes mellitus, *Porphyromonas gingivalis*, calcitriol, LL-37, autophagy, rats model

Introduction

Diabetes mellitus is a metabolic disorder characterized by chronic hyperglycemia. It has the third highest health risk of disability and mortality after tumors and cardiovascular disease. Periodontitis is one of the most frequent complications of diabetes, especially type 2 diabetes mellitus (T2DM) (1). The clinical manifestations of periodontitis are periodontal inflammation and attachment loss (AL), which subsequently exacerbate alveolar bone resorption and tooth loss. The Global Burden of Diseases, Injuries, and Risk Factors Study 2017 (GBD 2017) estimated that severe periodontitis affects 11% of the global population (2, 3). The prevalence of periodontitis in diabetics is significantly higher than that in non-diabetics (17.3% vs 9%) (4). There is evidence that those with moderate-to-severe periodontitis have a significantly increased risk of incident T2DM (5). The impaired immune function of people with diabetes leads to impaired resistance against periodontal infection, which exacerbates alveolar bone loss and impairs tissue healing (6). Moreover, severe periodontitis aggravates insulin resistance, making achieving clinical stability in diabetes challenging (7). In summary, diabetics have intense clinical manifestations and poor therapeutic responsiveness. Therefore, it is essential to improve the clinical diagnosis and treatment efficacy of diabetes mellitus-associated periodontitis.

Vitamin D is an essential regulating hormone in the human body. It is converted into its active form, calcitriol (1 alpha, 25-dihydroxyvitamin D3, 1,25D), and circulates through the blood to target organs (8). Based on the effects of vitamin D on immune regulation, bone metabolism, and inflammatory response, the relationship between calcitriol and diabetes mellitus-associated periodontitis has been explored in several recent studies. Vitamin D deficiency increases the risk of periodontitis and the progressive destruction of periodontal tissues (9). Our previous and related studies reported that calcitriol can alleviate periodontal inflammation by inhibiting endogenous expression of IL-8 in human periodontal ligament cells (hPDLCs) and the expression of IL-8/IL-6 in hPDLCs induced by *Phorphyromonas gingivalis* lipopolysaccharide (10). Wang et al. (11) found that calcitriol attenuated experimental periodontitis through downregulation of TLR4 and JAK1/STAT3 signaling in diabetic mice. In human oral keratinocytes and a mouse model of T2DM, PTPN2 contributed to a decrease in periodontal inflammation *via* protein substrate dephosphorylation in the JAK1/STAT3 signaling pathway after calcitriol treatment (12). However, it remains unclear whether there are other mechanism involved in vitamin D-induced alleviation of periodontitis in T2DM. Thorough investigation of calcitriol and its involvement in inhibiting inflammation may help improve the treatment of diabetes mellitus-associated periodontitis.

Autophagy is a physiological process by which cells phagocytize their organelles or cytoplasm and degrade the cargo in lysosomes (13). It is a self-protective cellular catabolic pathway that is essential for cellular homeostasis, immune defense, and stress response (14). Autophagy plays an important role in the development of periodontitis. Increased expression of autophagy-related protein was found in PDLCs from individuals with periodontitis compared with healthy individuals (15). Park et al. (16) found that THP-1-derived macrophages eliminated *P. gingivalis* and restricted excessive inflammatory response by activating an autophagic response. Moreover, increased autophagy induced osteoclastogenesis and stimulated osteoclast-mediated bone resorption. However, the role of autophagy in periodontitis and its related mechanisms remain unclear.

Vitamin D can regulate the inflammatory response by promoting autophagy in various tissues. A study found that active vitamin D activated chondrocyte autophagy to reduce osteoarthritis (17). Wei et al. (18) discovered that vitamin D protected against myocardial damage, inflammation, and apoptosis by promoting autophagy. In addition, vitamin D has potential renoprotective effects in diabetic nephropathy *via* downregulation of mTOR gene expression, stimulation of autophagy, and antioxidant, anti-inflammatory, and hypotensive effects (19). In our previous study, we found that calcitriol significantly decreased the number of live *P. gingivalis* internalized into epithelial cells, monocytes, and macrophages by promoting autophagy (20, 21). Human cationic antimicrobial peptide 18 (hCAP18) is the only antimicrobial peptide in the cathelicidin family found in the human body. LL-37 is expressed in salivary glands, oral mucosa, and oral immune cells (22). We have previously found that LL-37 reduced the quantity of live *P. gingivalis* internalized into HaCaT cells by promoting autophagy, and a potential molecular pathway of LL-37-induced autophagy was indicated (23). However, the role of autophagy in the regulation of periodontal inflammatory response treated with vitamin D in diabetes mellitus-associated periodontitis remains unclear.

Our previous study found that the calcitriol treatment may inhibit the number of live *P. gingivalis* in KB cells and U-937 cells by promoting autophagy. But the effect of calcitriol on the inflammatory responses of gingival tissues with T2DM-associated periodontitis has been rarely studied, and the role of autophagy during the inflammatory process is still unclear. In this study, the model of experimental T2DM with periodontitis in rats was employed to investigate the effect of calcitriol treatment on the regulation of inflammation in the gingival tissues, especially in the epithelial cells. In addition, we also explored the possible roles of

autophagy and LL-37 during the process so as to provide further evidence for relevant mechanisms.

Materials and methods

Animals, bacterial strains, and grouping

Twenty male Sprague-Dawley rats (7 weeks old) were purchased from Beijing Vital River (Beijing, China). All rats were given free access to food and tap water and were caged on an auto-cycling 12-h light and 12-h dark cycle under specific pathogen-free conditions. The *P. gingivalis* ATCC 33277 strain, which is the most common putative pathogen involved in periodontitis, was originally obtained from the American Tissue Culture Collection (Maryland, USA) and stored at the Department of Oral Biology at China Medical University.

Rats were randomly divided into five groups: non-diabetic blank, diabetic blank, diabetes with calcitriol treatment, diabetes with 3-methyladenine (3-MA) treatment, or diabetes with calcitriol and 3-MA treatment. All experimental procedures were approved by the Animal Ethics Committee of China Medical University (KT2019040).

High-fat diet/streptozotocin-induced experimental type 2 diabetes model in rats

The rats in the diabetic groups consumed high-fat diet (HFD, HD001, 60% calories from fat) for 30 days. Then, they were fasted overnight before receiving intraperitoneal injection of a low dose of streptozotocin (STZ) (35 mg/kg), according to Srinivasan et al. (24) Three days after injection, random blood glucose (RBG) measurement was performed. The model was considered successful if the RBG was not less than 16.7 mmol/L.

Ligation/*P. gingivalis*-induced experimental periodontitis model in rats

The *P. gingivalis* ATCC 33277 strain was maintained anaerobically at 37°C on brain-heart infusion (BHI) solid medium (containing 5% sterilized and defibrinated sheep blood, 0.5% hemin, and 0.1% vitamin K). Then *P. gingivalis* was cultured in a liquid BHI medium for 16–18 h. After the type 2 diabetes model was established, 5-0 silk ligatures were ligated firmly and sub-gingivally around the left maxillary first molar to facilitate bacterial colonization; the right side was the self-control. Then, they were infected with 10^9 colony-forming units of live bacteria inoculated into the gingival sulci by a syringe three times at 2 days.

Calcitriol treatment and autophagy blocking

After the rat model was established, intraperitoneal injection of blank solvent (propylene glycol:water:ethyl glycol = 60:30:10), calcitriol solvent (2 μg/kg, Sigma, St. Louis, MO, USA), 3-MA solvent (15 mg/kg, Selleck, Texas, USA), and calcitriol + 3-MA solvent was performed for 1 week. All rats were sacrificed for subsequent experiments.

Micro-computed tomography and histological analysis

After stripping the attached gingival tissue, all maxillary teeth and alveolar bone fixed in 4% paraformaldehyde were subjected to scanning by a micro-computed tomography system.

The gingival samples were fixed with 4% paraformaldehyde for 24–48 hours, embedded, and sliced. The slices were prepared for hematoxylin and eosin (H&E) staining.

Immunohistochemical analysis

After being deparaffinized, rehydrated, and antigen retrieved, the sample slices were quenched with endogenous peroxidase and blocked. Then, sample slices were incubated with primary antibody overnight, including nuclear transcription factor-kappa B p65 (NFκB-p65, Immunoway, China, YT3107,1:200), microtubule-associated proteins 1A/1B light chain 3B (LC3B, Proteintech, China, 14600-1, 1:500), and antibacterial peptide LL-37 (LL-37, Cohesion Biosciences, England, CQA1065, 1:200). On the next day, the processes of secondary antibody binding, DAB, hematoxylin re-staining, dehydration, transparency, and sealing were performed to complete immunohistochemistry.

Western blot analysis

The gingival tissue was lysed with a RIPA lysis buffer supplemented with 1 mM PMSF. Then, samples were centrifuged at 12,000 rpm at 4 °C for 15 min in three freezing-melting cycles. Equal amounts of protein samples were separated by SDS-polyacrylamide gel electrophoresis and transferred onto a PVDF membrane by electro-blotting. The membranes were blocked with 5% BSA dissolved in Tris-buffered saline containing Tween (TBST), then incubated with primary antibodies at 4 °C overnight, including LC3B (1:1000), p62/SQSTM1 (GeneTex, America, GTX636328, 1:2000), NFκB-p65 (1:1000), GAPDH (Proteintech, China, 10494-1, 1:2000) and LL-37 (1:1000) at 4 °C. Membranes were incubated with a secondary antibody (Abbkine, America, A23220, 1:1000) in the dark for 1 h

at 37 °C. Images were obtained using the Infrared Fluorescence Scanning Imaging System (Odyssey CLx, LI-COR, USA).

Statistical analysis

All the experiments were conducted in triplicate. The data are presented as mean ± standard deviation (SD). The differences between two groups were assessed by unpaired *t* test, and differences among three or more groups were analyzed by one-way analysis of variance (ANOVA) using SPSS 22.0 (SPSS Inc., Chicago, IL, USA). $P < 0.05$ was considered statistically significant.

Results

Establishment of the experimental type 2 diabetes model in rats

As shown in the flow chart of operating processes (Figure 1A), we combined a high-fat diet (HFD) and low dose

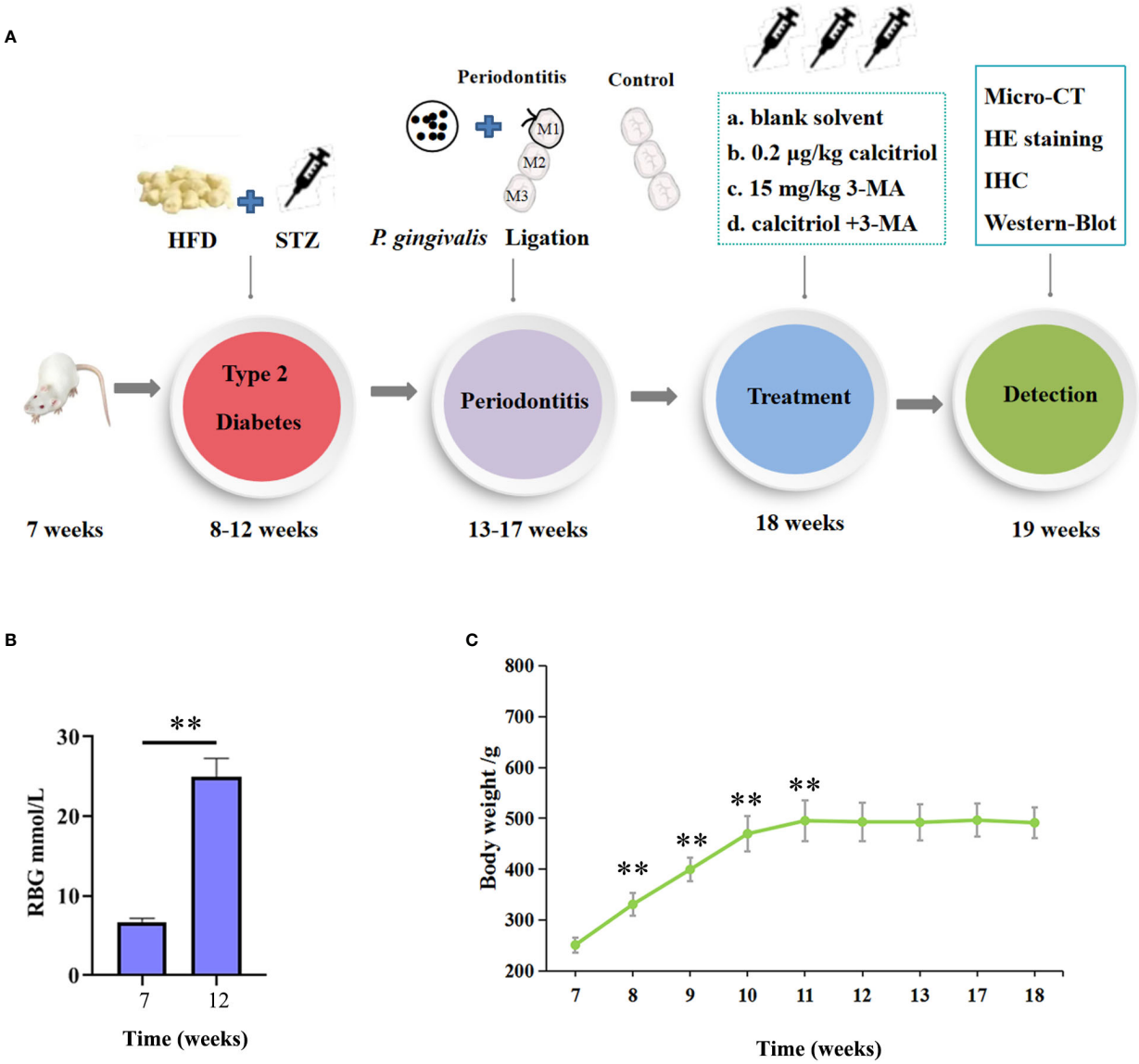

FIGURE 1
Establishment of the experimental type 2 diabetic model in rats. **(A)** The flow chart of the experimental design. HFD, High-Fat Diet; STZ, streptozotocin (35 mg/kg); HE, hematoxylin and eosin; IHC, immunohistochemical. **(B)** The random blood glucose (RBG) of the rats were measured. **(C)** Body weight of the diabetic rats were measured. The data were presented as the mean ± SD (n=4/group, $^{**}P$ <0.01, compared with 7 week).

of STZ to develop an experimental type 2 diabetes model in rats. After HFD and injection of STZ, the random blood glucose (RBG) of rats in our study ranged from 20.9 mmol/L to 28.2 mmol/L (Figure 1B). The RBG was not less than 16.7 mmol/L in diabetic rats, which indicated a successful model. The body weight of all rats was measured for 8 weeks. Body weight gradually increased for 4 weeks, and the rats exhibited a stable or slight decrease in body weight after intraperitoneal injection of STZ (Figure 1C). The changes in RBG and body weight in this study indicated the establishment of the experimental type 2 diabetes model in the rats.

Establishment of the experimental periodontitis model in rats

The maxillary bone samples were obtained after sacrifice. The inflammatory responses were observed in the gross specimen and *via* H&E staining of samples obtained individually from the control group and the periodontitis group (Figure 2A, B). As shown in the gross specimen (Figure 2A a; Figure 2B e), the distance from the cemento-enamel junction (CEJ) to the alveolar bone crest in the periodontitis group was remarkably longer than in the control group, indicating that alveolar bone resorption had occurred. Compared with H&E staining of gingival tissue from the control group, the location of the junctional epithelium in the periodontitis group, from CEJ to root, indicated AL (Figure 2A b, c; Figure 2B f, g). Moreover, more inflammatory cells and more severe vasodilatation was observed in the gingival tissue from the periodontitis group than the control group (Figure 2A d; Figure 2B h). The occurrence of AL, inflammatory cell infiltration, and severe vasodilatation indicated the establishment of the experimental periodontitis model in rats.

Diabetic rats with periodontitis showed more severe alveolar bone loss and intense gingival inflammatory response than non-diabetic rats

We performed Micro-CT of the maxillary bone and H&E staining of gingival tissues from non-DM control group (health

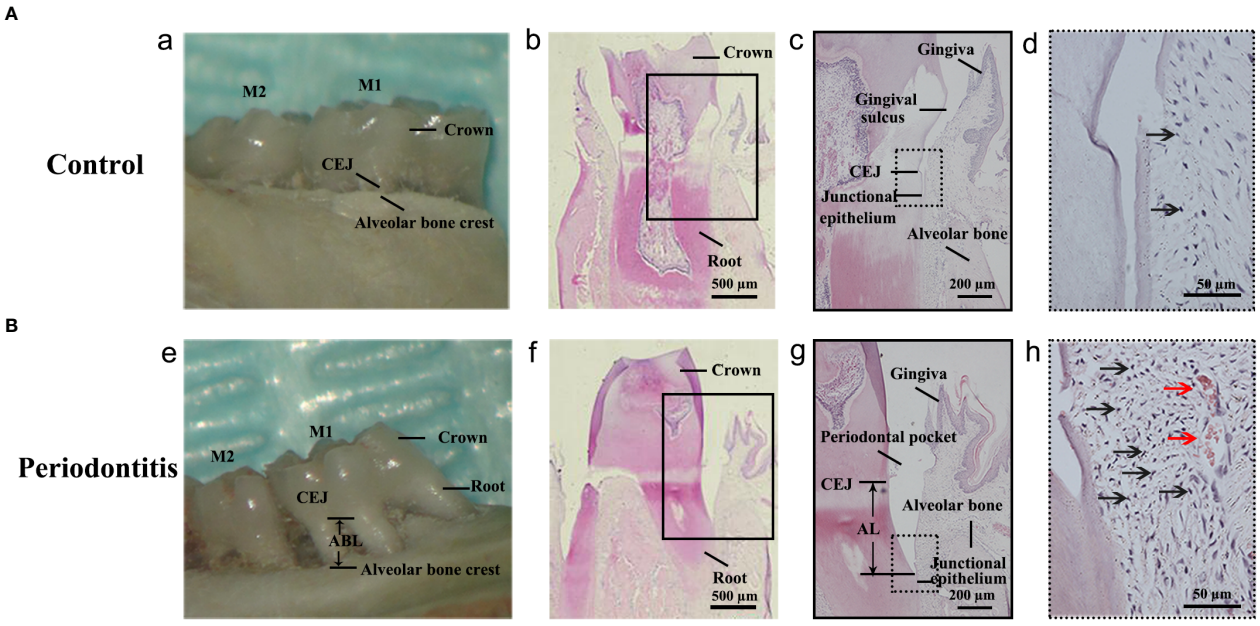

FIGURE 2
Establishment of the experimental periodontitis model in rats. **(A, B)** The figures presented the gross specimens and sections obtained individually from the control group and the periodontitis group. (a, e): As shown in the gross specimen, the distance from the cemento-enamel junction (CEJ) to the alveolar bone crest in the periodontitis group was remarkably longer than that in the control group, that is alveolar bone resorption occurred. (b, c): As shown in the section from the control group with hematoxylin and eosin (HE) staining, the junctional epithelium is located at the CEJ site. (f, g): The section from the periodontitis group shows that the junctional epithelium was located on the root, that is attachment loss (AL) occurred. (d, h): Compared with that from the control group, more inflammatory cells and more severe vasodilatation was observed in the gingival tissue from the periodontitis group. The black arrows in (d, h) indicates the inflammatory cell (especially neutrophile) infiltration. The red arrows in (h) indicates vasodilatation. M1, the maxillary first molar; M2, the maxillary second molar.

control without T2DM and periodontitis), non-DM periodontitis group (ligation/*P. gingivalis*- induced periodontitis but without T2DM), DM control group (high-fat diet and low dose of streptozotocin-induced T2DM but without periodontitis), and DM periodontitis group (combination periodontitis and T2DM) to explore the different inflammatory response in four groups. The overall morphology, as a reconstructed 3D model, exhibited a significantly higher degree of bone loss in diabetic rats than in non-diabetic rats (Figure 3A, B). H&E staining revealed epithelial rete peg elongation, inflammatory cell infiltration, disordered arrangement of subepithelial fibers, and vascular reaction in rats with diabetes mellitus-associated periodontitis (Figure 3C). The above data indicated that the diabetic rats with periodontitis showed more alveolar bone loss and intense gingival inflammatory responses.

Autophagy in gingival epithelium was attenuated in diabetic rats

Autophagy is usually assessed by detecting changes in LC3, LC3-II/LC3-I ratio and p62. The expression of LC3, LC3-II/LC3-I ratio and p62 in gingival epithelium of non-DM control group, non-DM periodontitis group, DM control group and DM periodontitis group were detected by immunohistochemical (IHC) and western blot. IHC staining showed the significantly decreasing expression of LC3 and western blot revealed the significantly decreasing expression of LC3 and LC3-II/LC3-I ratio and the increasing expression of p62 in the diabetic rats (Figure 4). The results indicated a marked decrease of autophagy in the diabetic gingival tissues, especially in the epithelial cells. Besides, autophagy was promoted in gingival tissues with periodontitis both in non-diabetic and diabetic rats.

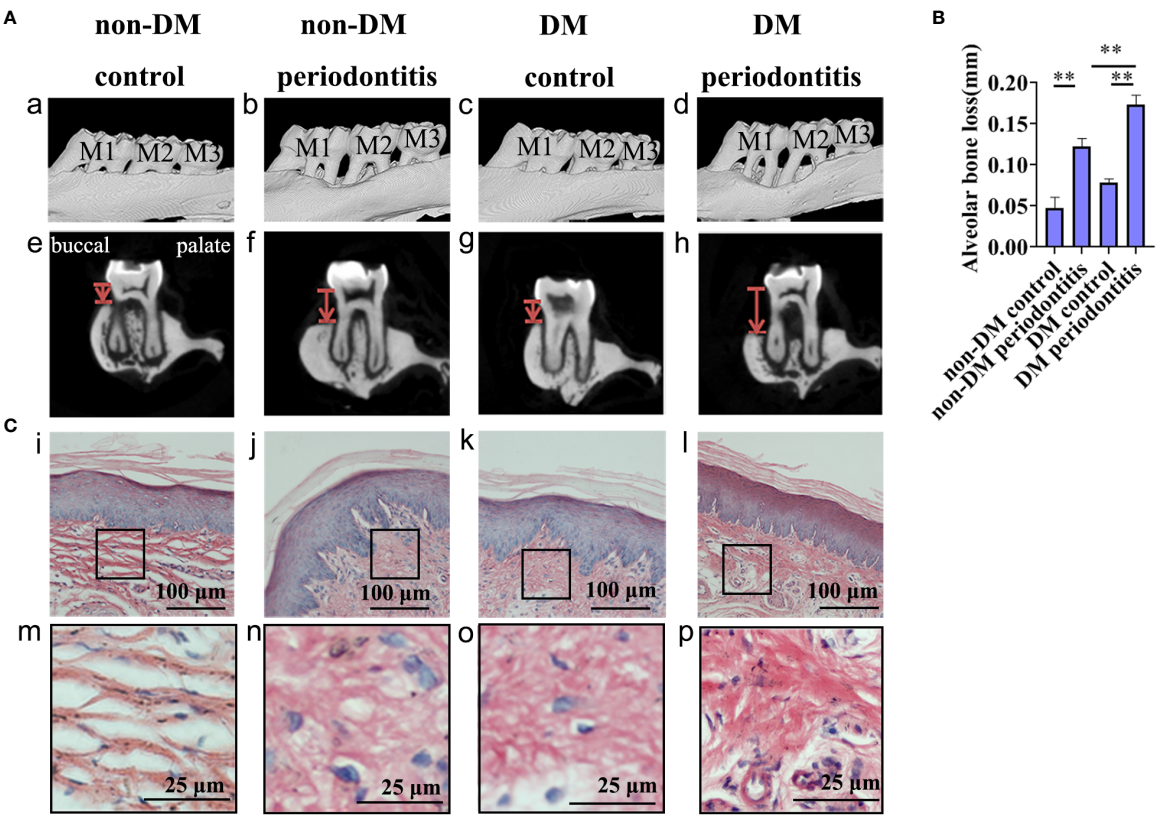

FIGURE 3
Diabetic rats with periodontitis showed more severe alveolar bone loss and intense gingival inflammatory response than non-diabetic rats. The figures present the micro-CT images and sections obtained individually from the non-DM control group, non-DM periodontitis group, DM control group and the DM periodontitis group. Non-DM control group, health control without type 2 diabetes mellitus (T2DM) and periodontitis; non-DM periodontitis group, ligation/*P. gingivalis*-induced periodontitis but without T2DM; DM control group, high-fat diet and low dose of streptozotocin-induced T2DM but without periodontitis; DM periodontitis group, combination periodontitis and T2DM. **(A)** Micro-computed tomography images of the maxillary first molars from (a-d). The distance between two red lines, cemento-enamel junction (CEJ) and the alveolar bone crest, represents the alveolar bone resorption (e-h). **(B)** Statistical analysis of the alveolar bone loss. Data are presented as mean ± SD (n=4) and are shown in the bar graphs, repeated 3 times (***P* <0.01, compared with the control group or the non- DM group). **(C)** Hematoxylin and eosin staining of sections (i-p).

10.3389/fendo.2022.1051374

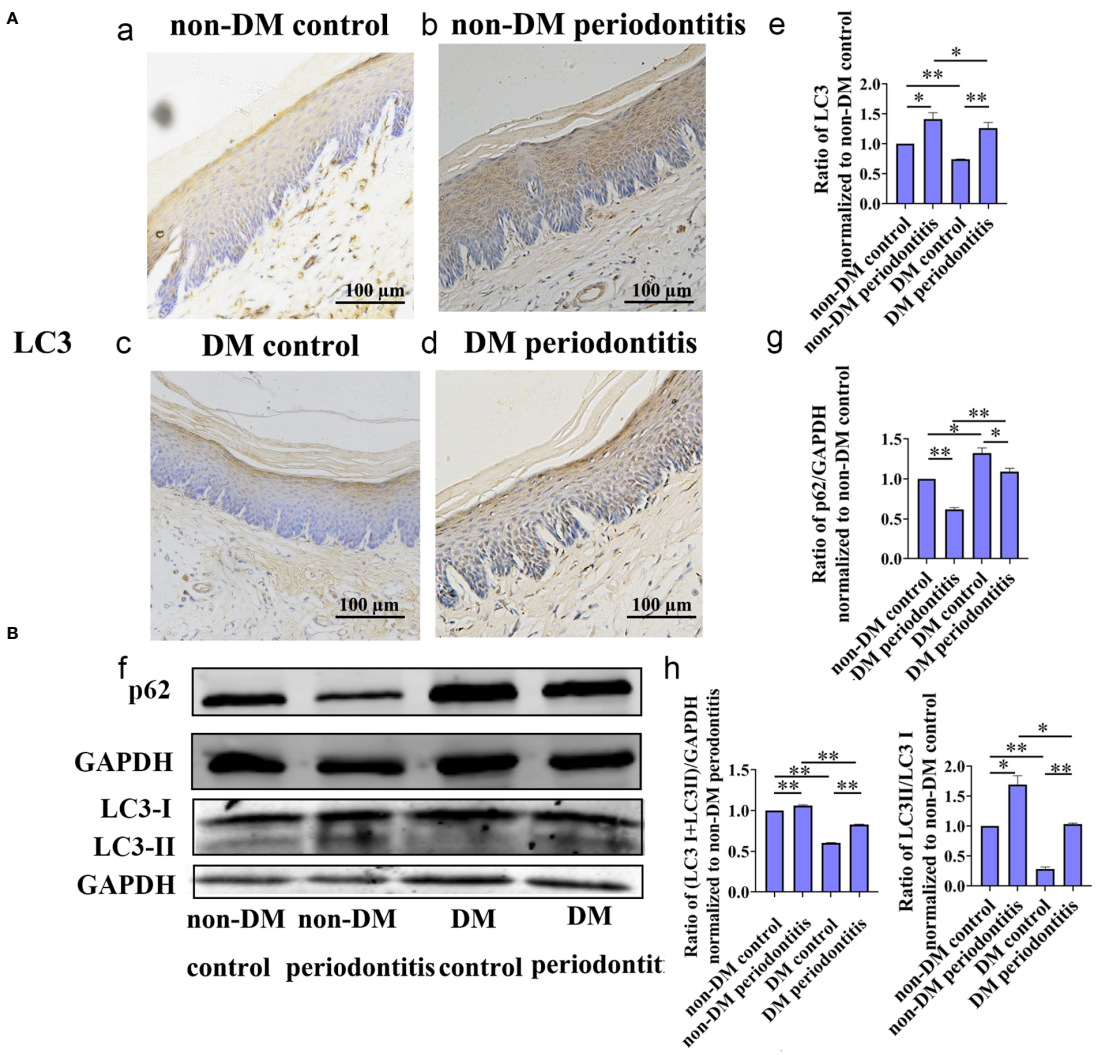

FIGURE 4
Autophagy in gingival epithelium was attenuated in diabetic rats. The expression of autophagy-related protein of gingival epithelium in non-DM control group, non-DM periodontitis group, DM control group and the DM periodontitis group were detected. Non-DM control group, health control without type 2 diabetes mellitus (T2DM) and periodontitis; non-DM periodontitis group, ligation/*P. gingivalis*-induced periodontitis but without T2DM; DM control group, high-fat diet and low dose of streptozotocin-induced T2DM but without periodontitis; DM periodontitis group, combination periodontitis and T2DM. **(A)** Immunohistochemical (IHC) staining and semi-quantitative analysis of the expression of LC3 in the gingival epithelium of the four groups (a-e). **(B)** Western Blot reveals the expression of LC3 and p62 in four groups (f-h). All data are presented as mean ± SD (n = 3) relative to non- DM control are shown in bar graphs (**P* <0.05, ***P* <0.01).

Calcitriol attenuated the gingival epithelium inflammatory responses in diabetic rats by promoting autophagy

To study the intrinsic mechanism underlying autophagy, the diabetic rats with periodontitis were randomly divided into blank group (propylene glycol: water: ethyl glycol=60:30:10), calcitriol group (2 μg/kg), 3-MA group (15 mg/kg) and calcitriol + 3-MA group. After intraperitoneal injections for 1 week, we harvested the gingival tissues following sacrifice of the rats. IHC staining was performed to evaluate the expression of inflammatory response-related proteins (NFκB-p65) and autophagy- related proteins (LC3) in the gingival epithelium (Figure 5A). Western blot was performed to detect the expression of LC3, LC3-II/LC3-I, p62 and NFκB-p65 (Figure 5C). HE staining was performed to observe the inflammatory response in the subepithelial fiber (Figure 5B). We observed that the expression of NFκB-p65 and p62 was alleviated by treatment with calcitriol (Figure 5A f-j; Figure 5C o, p, r). Furthermore, the expression of LC3 and LC3-II/LC3-I ratio were significantly elevated (Figure 5A a-e; Figure 5C o, q). Following intraperitoneal injection of 3-MA, the level of LC3 and LC3-II/LC3-I ratio were decreased (Figure 5A a-e; Figure 5C o, q), the

expression of p62 and NFκB-p65 were increased (Figure 5A f-j; Figure 5C o, p, r), indicating marked suppression of autophagy. Autophagy suppression of 3-MA was apparently retrieved by calcitriol.

Decrease of LL-37 in the gingival epithelial cells of T2DM rats, which was rescued by calcitriol treatment

Based on our previous study on LL-37-induced autophagy, we further detected the expression of LL-37 in diabetics. IHC staining was performed to assess the expression of LL-37 in the gingival epithelium of non-DM control group, non-DM periodontitis group, DM control group and DM periodontitis group (Figure 6A). We observed a lower expression of LL-37 in the diabetic rats compared with non-diabetic rats and LL-37 was promoted in gingival tissues with periodontitis both in non-diabetic and diabetic rats (Figure 6A a-h; Figure 6C r).

We further explored the role of LL-37 in calcitriol-enhanced autophagy in diabetics rats with periodontitis, which randomly divided into blank group, calcitriol group, 3-MA group and calcitriol + 3-MA group (Figure 6B, C). We observed that the expression of LL-37 was increased by treatment with calcitriol

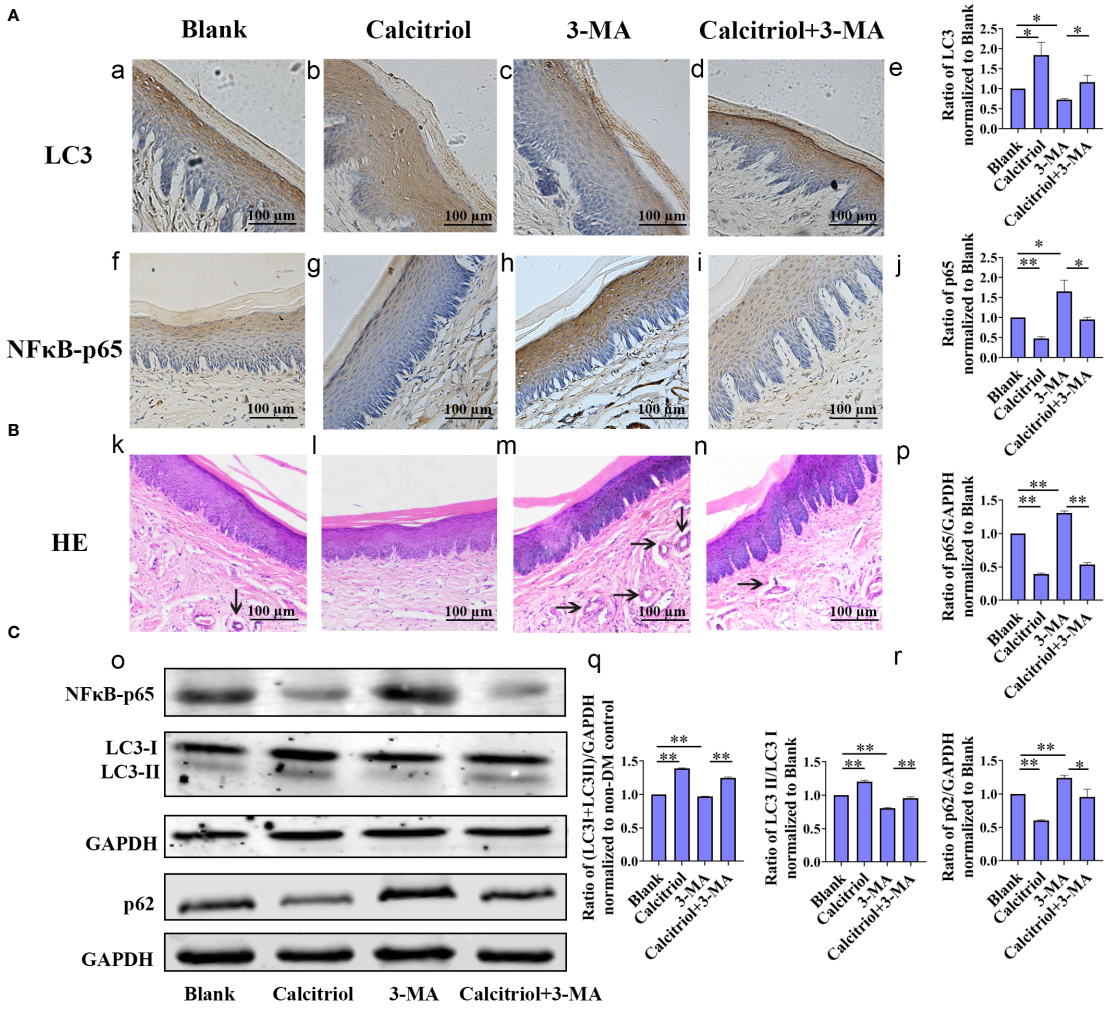

FIGURE 5
Calcitriol attenuated the gingival epithelium inflammatory response in diabetic rats by promoting autophagy. The diabetic rats with periodontitis were randomly divided into blank group (propylene glycol: water: ethyl glycol=60:30:10), calcitriol group (2 μg/kg), 3-MA group (15 mg/kg) and calcitriol + 3-MA group. They received intraperitoneal injections for 1 week. **(A)** The expression of LC3 (a-e) and NFκB-p65 (f-j) in the gingival epithelium of the four groups were detected by IHC staining. **(B)** HE staining showed the inflammatory response in the subepithelial fiber of the four groups (k-n). **(C)** The expression of NFκB-p65, LC3-II/LC3-I and p62 in the gingival epithelium of the four groups were detected by western-blot (o-r). Semi-quantitative analysis of IHC and western-blot were performed by gray density analysis. All data are presented as mean ± SD (n = 3) relative to blank group are shown in bar graphs (*P <0.05, **P <0.01).

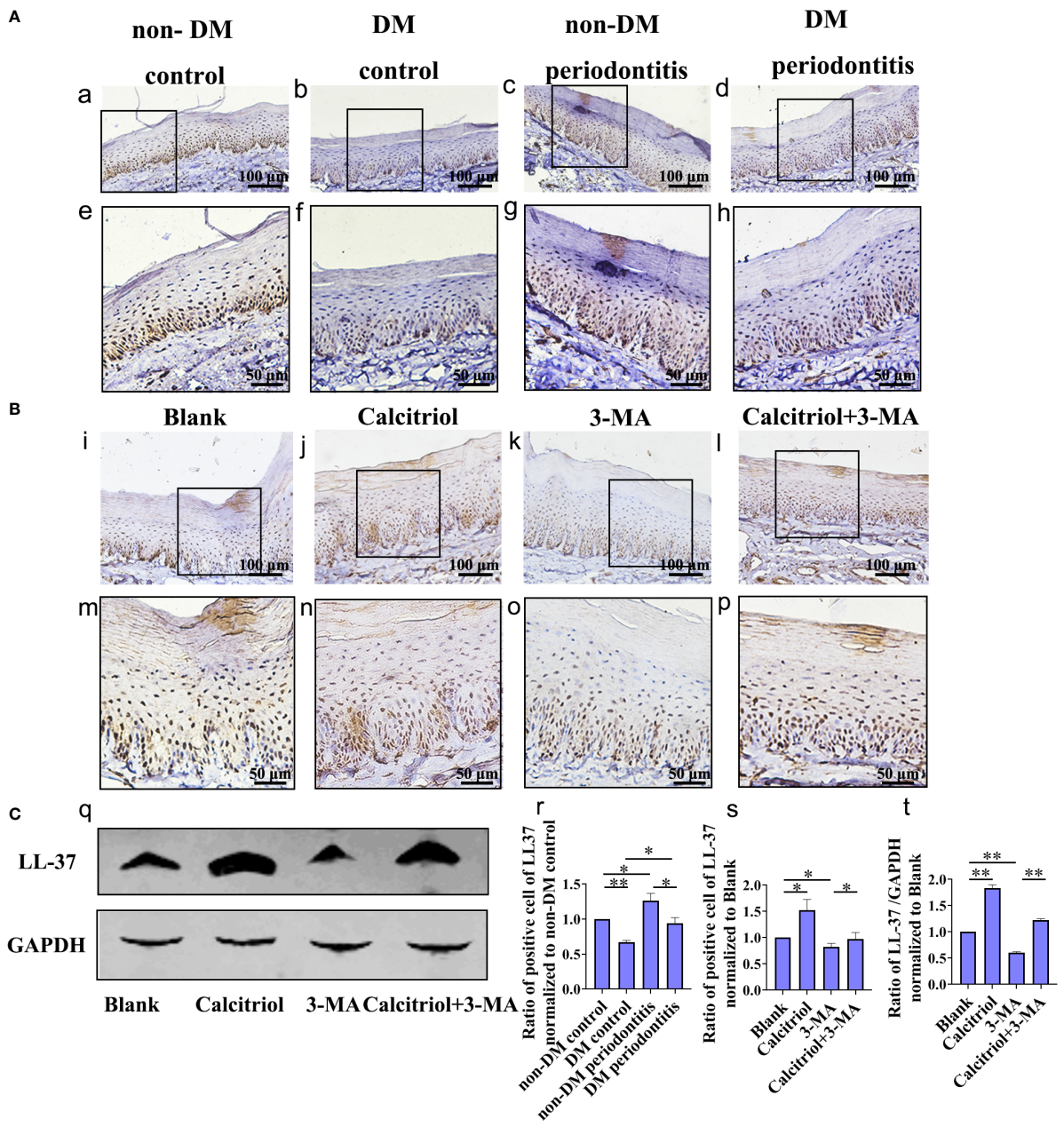

FIGURE 6
Decrease of LL-37 in the gingival epithelial cells of T2DM rats, which was rescued by calcitriol treatment. **(A)** IHC staining of the gingival epithelium obtained individually from the non-DM control group, non-DM periodontitis group, DM control group and the DM periodontitis group (a-h, r). Non-DM control group, health control without type 2 diabetes mellitus (T2DM) and periodontitis; non-DM periodontitis group, ligation/*P. gingivalis*-induced periodontitis but without T2DM; DM control group, high-fat diet and low dose of streptozotocin-induced T2DM but without periodontitis; DM periodontitis group, combination periodontitis and T2DM. **(B)** IHC staining of the LL-37 expression in the gingival epithelium of different groups (i-p, s). The diabetic rats with periodontitis were randomly divided into blank group (propylene glycol: water: ethyl glycol=60:30:10), calcitriol group (2 μg/kg), 3-MA group (15 mg/kg) and calcitriol + 3-MA group. **(C)** Western Blot reveals the expression of LL-37 in four groups (q) analysis of the LL-37 expression in the gingival epithelium (t). All data are presented as mean ± SD (n = 3) relative to non-DM and blank group are shown in bar graphs (**P* <0.05, ***P* <0.01, compared with the blank group).

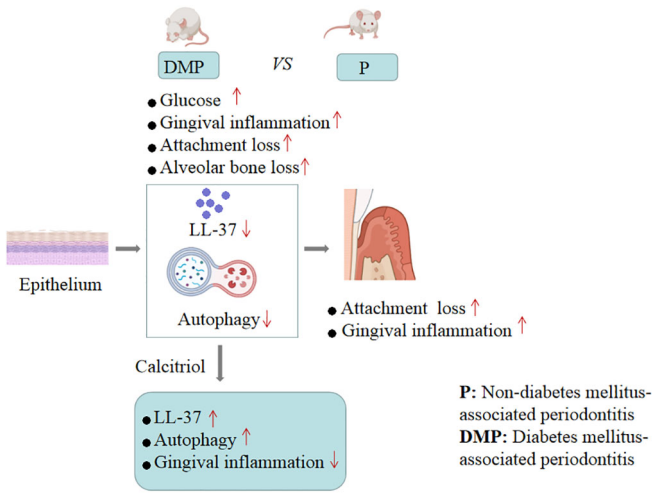

FIGURE 7
Mechanism schema diagram.

(Figure 6B j, n; Figure 6C q, s, t). In contrast, LL-37 expression decreased following intraperitoneal injection of 3-MA (Figure 6B k, o; Figure 6C q, s, t). LL-37-mediated suppression of 3-MA was apparently retrieved by calcitriol treatment (Figure 6B l, p; Figure 6C q, s, t).

Discussion

Autophagy plays an important role in maintaining general homeostasis, but the specific function and mechanism of autophagy in T2DM-associated periodontitis is not clear. In our study, we employed rats with T2DM and periodontitis to explore the effect of calcitriol on the regulation of periodontal inflammation and the role of autophagy in this process. We found the defective autophagy and increased inflammation in the gingival tissues, especially in the epithelial cells of T2DM rats than non-diabetic rats. Additionally, calcitriol attenuated the gingival inflammatory responses in diabetic rats by promoting autophagy and LL-37 may be involved in this process.

Previous studies have demonstrated elevated inflammation in diabetic rats, which was confirmed by our study. The accumulation of ubiquitinated proteins in islet β cells (25, 26) and advanced glycation end product (AGE)-induced ROS (27, 28) cause the increasing inflammation. In the T2DM rats induced by HFD for 4-6 weeks combined with STZ injection (30-35 mg/kg), higher level of serum glucose and homeostatic model assessment-insulin resistance (HOMA-IR) were observed (29–31). However, the high-dose STZ (>50 mg/kg) injection can induce type 1 diabetes according the studies (32–34). In our experiment, we used HFD combined low-dose STZ (35 mg/kg) injection to establish T2DM rats, which is frequently used (24, 29–31). After HFD + STZ injection, the RBG of rats in our study ranged from 20.9 mmol/L to 28.2 mmol/L. The periodontitis model was established by ligation and *P. gingivalis* inoculation. Accumulation of plaque around the ligature and persistent infection with *P. gingivalis* can cause inflammatory infiltration, which leads to the destruction of periodontal tissues (35). Micro-CT and H&E staining revealed alveolar bone loss and inflammatory cell infiltration, which indicated a successful periodontitis model. IHC staining revealed the increased expression of NFκB-p65 in diabetic rats. NFκB-p65 is closely related to the expression of various pro-inflammatory mediators (36). Therefore, in this study, the experimental model established in rats with T2DM and periodontitis was successful and reliable.

This study revealed that the periodontitis condition induced a more severe inflammatory response in the gingival epithelium of diabetic rats than non-diabetic rats. Moreover, blocking of autophagy further aggravated the inflammation. Moderate autophagy plays a crucial role in general homeostasis by phagocytizing and degrading cargo (37). In our study, autophagy was interrupted with 3-MA. Consequently, we observed a decreased expression of autophagy flux, while the inflammatory response increased significantly. These data indicated that autophagy in the gingival epithelium of diabetic rats may decrease, which may weaken the degradation of inflammatory factors and in turn aggregate the periodontal inflammatory process.

In addition, this study revealed low expression of autophagy in the gingival epithelium of diabetic rats, which is rarely

reported. The synthesis and processing of LC3 is increased during autophagy, making it a key readout of autophagy levels in cells (38). p62/SQSTM1 serves as an essential adaptor to identify and deliver specific organelles and protein aggregates to autophagosome for degradation (39). The detection of p62 turnover assay is reliable for autophagy flux assay (38). It has been reported that autophagy may play a protective role by clearing the aggregates of ubiquitinated proteins resulting from hyperglycemia in insulin-expressing β cells (25). Bachar-Wikstrom et al. (26) reported that large aggregates of autophagy and increased expression of LC3 was observed in pancreatic β cells of diabetic rats. High glucose was found to increase protein oxidation and trigger autophagy in MC3T3-E1 cells (40). In contrast, the expression of autophagic hallmarks (Beclin-1 and LC3), and numbers of autophagolysosomes was decreasing, and the expression of p62 was increasing in the diabetic hearts (41). The results of our study showed decreased expression of LC3-II/LC3-I and increased expression of p62 *via* IHC and western blot analysis, which indicated the insufficient autophagy in the gingival tissues of diabetic rats. However, the relevant mechanism should be explored further in the future.

Vitamin D can decrease the level of inflammation in diabetics (11, 12). However, the role of autophagy in the above process has not been reported. The present study revealed increasing autophagy and decreasing inflammation in rats gingival tissues treated with calcitriol, especially in the gingival epithelium. Meanwhile, calcitriol could attenuate the upregulation of NFκB-p65 and inflammatory response caused by autophagy inhibitor in our study. Similarly, vitamin D can protect against osteoarthritis, myocardial damage, and diabetic nephropathy by promoting autophagy (17–19). Vitamin D has been shown to increase the expression of LC3 and Beclin-1, suppress apoptosis, and alleviate insulitis in pancreatic β cells of diabetic mice (42). Therefore, we hypothesized that calcitriol may decrease periodontal inflammation by promoting autophagy and degrading inflammatory factors.

Our previous study indicated that LL-37 might promote autophagy of keratinocytes to reduce the quantities of live *P. gingivalis* (23). The results of this study revealed that expression of LL-37 was lower in the gingival epithelium of rats with T2DM compared with rats without T2DM, but LL-37 was promoted in gingival tissues with periodontitis both in non-diabetic and diabetic rats.

Turkoglu et al. (43) reported the increased levels of GCF LL-37 in patients with periodontitis. Furthermore, we found that calcitriol promoted LL-37 expression while increasing autophagy. Wang et al. (44) demonstrated that vitamin D played an important role in antimicrobial cutaneous immunity when identifying a vitamin D response element (VDRE) in the promoter region of the cathelicidin LL-37 gene. Soon thereafter, other groups confirmed that cathelicidin constituted a direct target of vitamin D in keratinocytes (45). Yuk et al. (46) indicated that calcitriol induced autophagy in human monocytes *via* LL-37, which activated transcription of Beclin-1 and Atg5. Nilsson et al. (47) reported that LL-37 antagonize pro-inflammatory cytokines produced by lipopolysaccharide- stimulated PDL cells, so we speculated the reducing of LL-37 after the application of 3-MA may be due to the consuming of LL-37 to neutralize excessive inflammatory factors in our study. In the present study, the decrease of LL-37 may be the specific manifestation in the gingival tissues with the severe periodontal inflammatory response induced by T2DM. Furthermore, calcitriol may promote the expression of LL-37 to take part in the inflammatory response of periodontitis in T2DM rats. However, the possible mechanism on the above process have not been clarified and need further study.

In conclusion, our findings provided evidence that calcitriol-enhanced autophagy positively attenuates periodontal inflammation and the decrease of LL-37 was rescued by calcitriol treatment in the gingival epithelial cells of T2DM rats (Figure 7). We will continue to study potential mechanisms to provide evidence for the application of calcitriol as an adjunctive treatment for T2DM-associated periodontitis.

Data availability statement

The raw data supporting the conclusions of this article will be made available by the authors, without undue reservation.

Ethics statement

The animal study was reviewed and approved by Animal Ethics Committee of China Medical University (KT2019040).

Author contributions

XT, YW designed the study. YW performed the experiments with the help from XT, WX and FL. YW wrote the final manuscript. XT, MH and CM revised the manuscript. All authors contributed to the article and approved the submitted version.

Funding

The present work was supported by the 2021 Annual Scientific Research Funding Project of the Educational Department of Liaoning Province (Key Project, LJKZ0782), the National Natural Science Foundation of China (81670999) and Shenyang Youth Science and Technology Innovation Talent

Support Project supported by Shenyang Science and Technology Bureau (RC170520).

Conflict of interest

The authors declare that the research was conducted in the absence of any commercial or financial relationships that could be construed as a potential conflict of interest.

Publisher's note

References

1. Wu CZ, Yuan YH, Liu HH, Li SS, Zhang BW, Chen W, et al. Epidemiologic relationship between periodontitis and type 2 diabetes mellitus. *BMC Oral Health* (2020) 20(1):204. doi: 10.1186/s12903-020-01180-w

2. James SL, Abate D, Abate KH, Abay SM, Abbafati C, Abbasi N, et al. Global, regional, and national incidence, prevalence, and years lived with disability for 354 diseases and injuries for 195 countries and territories, 1990-2017: a systematic analysis for the global burden of disease study 2017. *Lancet* (2018) 392 (10159):1789–858. doi: 10.1016/S0140-6736(18)32279-7

3. Jiao J, Jing W, Si Y, Feng X, Tai B, Hu D, et al. The prevalence and severity of periodontal disease in mainland China: Data from the fourth national oral health survey (2015-2016). *J Clin Periodontol* (2021) 48(2):168–79. doi: 10.1111/jcpe.13396

4. Thorstensson H, Hugoson A. Periodontal disease experience in adult long-duration insulin-dependent diabetics. *J Clin Periodontol* (1993) 20(5):352–8. doi: 10.1111/j.1600-051x

5. Winning L, Patterson CC, Neville CE, Kee F, Linden GJ. Periodontitis and incident type 2 diabetes: a prospective cohort study. *J Clin Periodontol* (2017) 44 (3):266–74. doi: 10.1111/jcpe.12691

6. Duarte PM, Bezerra JP, Miranda TS, Feres M, Chambrone L, Shaddox LM. Local levels of inflammatory mediators in uncontrolled type 2 diabetic subjects with chronic periodontitis. *J Clin Periodontol* (2014) 41(1):11–8. doi: 10.1111/jcpe.12179

7. Blasco-Baque V, Garidou L, Pomié C, Escoula Q, Loubieres P, Le Gall-David S, et al. Periodontitis induced by porphyromonas gingivalis drives periodontal microbiota dysbiosis and insulin resistance *via* an impaired adaptive immune response. *Gut* (2017) 66(5):872–85. doi: 10.1136/gutjnl-2015-309897

8. Hoe E, Nathanielsz J, Toh ZQ, Spry L, Marimla R, Balloch A, et al. Anti-inflammatory effects of vitamin d on human immune cells in the context of bacterial infection. *Nutrients* (2016) 8(12):806. doi: 10.3390/nu8120806

9. Botelho J, Machado V, Proença L, Delgado AS, Mendes JJ. Vitamin d deficiency and oral health: A comprehensive review. *Nutrients* (2020) 12(5):1471. doi: 10.3390/nu12051471

10. Tang X, Pan Y, Zhao Y. Vitamin d inhibits the expression of interleukin-8 in human periodontal ligament cells stimulated with porphyromonas gingivalis. *Arch Oral Biol* (2013) 58(4):397–407. doi: 10.1016/j.archoralbio.2012.09.010

11. Wang Q, Li H, Xie H, Fu M, Guo B, Ding Y, et al. 25-hydroxyvitamin D3 attenuates experimental periodontitis through downregulation of TLR4 and JAK1/STAT3 signaling in diabetic mice. *J Steroid Biochem Mol Biol* (2013) 135:43–50. doi: 10.1016/j.jsbmb.2013.01.008

12. Zhang P, Zhang W, Zhang D, Wang M, Aprecio R, Ji N, et al. 25-hydroxyvitamin D(3) -enhanced PTPN2 positively regulates periodontal inflammation through the JAK/STAT pathway in human oral keratinocytes and a mouse model of type 2 diabetes mellitus. *J Periodontal Res* (2018) 53(3):467–77. doi: 10.1111/jre.12535

13. Shibutani ST, Saitoh T, Nowag H, Münz C, Yoshimori T. Autophagy and autophagy-related proteins in the immune system. *Nat Immunol* (2015) 16 (10):1014–24. doi: 10.1038/ni.3273

14. Høyer-Hansen M, Nordbrandt SP, Jäättelä M. Autophagy as a basis for the health-promoting effects of vitamin d. *Trends Mol Med* (2010) 16(7):295–302. doi: 10.1016/j.molmed.2010.04.005

15. Otomo C, Metlagel Z, Takaesu G, Otomo T. Structure of the human ATG12~ATG5 conjugate required for LC3 lipidation in autophagy. *Nat Struct Mol Biol* (2013) 20(1):59–66. doi: 10.1038/nsmb.2431

16. Park MH, Jeong SY, Na HS, Chung J. Porphyromonas gingivalis induces autophagy in THP-1-derived macrophages. *Mol Oral Microbiol* (2017) 32(1):48–59. doi: 10.1111/omi.12153

17. Kong C, Wang C, Shi Y, Yan L, Xu J, Qi W. Active vitamin d activates chondrocyte autophagy to reduce osteoarthritis *via* mediating the AMPK-mTOR signaling pathway. *Biochem Cell Biol* (2020) 98(3):434–42. doi: 10.1139/bcb-2019-0333

18. Wei YX, Dong SM, Wang YY, Zhang P, Sun MY, Wei YX, et al. Autophagy participates in the protection role of 1,25-dihydroxyvitamin D3 in acute myocardial infarction *via* PI3K/AKT/mTOR pathway. *Cell Biol Int* (2021) 45 (2):394–403. doi: 10.1002/cbin.11495

19. Khodir SA, Samaka RM, Ameen O. Autophagy and mTOR pathways mediate the potential renoprotective effects of vitamin d on diabetic nephropathy. *Int J Nephrol* (2020) 2020:7941861. doi: 10.1155/2020/7941861

20. Hu X, Niu L, Ma C, Huang Y, Yang X, Shi Y, et al. Calcitriol decreases live porphyromonas gingivalis internalized into epithelial cells and monocytes by promoting autophagy. *J Periodontol* (2020) 91(7):956–66. doi: 10.1002/JPER.19-0510

21. Niu L, Chen S, Yang X, Ma C, Pan C, Wang H, et al. Vitamin d decreases porphyromonas gingivalis internalized into macrophages by promoting autophagy. *Oral Dis* (2021) 27(7):1775–88. doi: 10.1111/odi.13696

22. Murakami M, Ohtake T, Dorschner RA, Gallo RL. Cathelicidin antimicrobial peptides are expressed in salivary glands and saliva. *J Dent Res* (2002) 81(12):845–50. doi: 10.1177/154405910208101210

23. Yang X, Niu L, Pan Y, Feng X, Liu J, Guo Y, et al. LL-37-Induced autophagy contributed to the elimination of live porphyromonas gingivalis internalized in keratinocytes. *Front Cell Infect Microbiol* (2020) 10:561761. doi: 10.3389/fcimb.2020.561761

24. Srinivasan K, Viswanad B, Asrat L, Kaul CL, Ramarao P. Combination of high-fat diet-fed and low-dose streptozotocin-treated rat: a model for type 2 diabetes and pharmacological screening. *Pharmacol Res* (2005) 52(4):313–20. doi: 10.1016/j.phrs.2005.05.004

25. Kaniuk NA, Kiraly M, Bates H, Vranic M, Volchuk A, Brumell JH. Ubiquitinated-protein aggregates form in pancreatic beta-cells during diabetes-induced oxidative stress and are regulated by autophagy. *Diabetes* (2007) 56 (4):930–9. doi: 10.2337/db06-1160

26. Bachar-Wikstrom E, Wikstrom JD, Kaiser N, Cerasi E, Leibowitz G. Improvement of ER stress-induced diabetes by stimulating autophagy. *Autophagy* (2013) 9(4):626–8. doi: 10.4161/auto.23642

27. Hamann C, Kirschner S, Günther KP, Hofbauer LC. Bone, sweet bone–osteoporotic fractures in diabetes mellitus. *Nat Rev Endocrinol* (2012) 8(5):297–305. doi: 10.1038/nrendo.2011.233

28. Leslie WD, Rubin MR, Schwartz AV, Kanis JA. Type 2 diabetes and bone. *J Bone Miner Res* (2012) 27(11):2231–7. doi: 10.1002/jbmr.1759

29. Cui X, Qian DW, Jiang S, Shang EX, Zhu ZH, Duan JA. Scutellariae radix and coptidis rhizoma improve glucose and lipid metabolism in T2DM rats *via* regulation of the metabolic profiling and MAPK/PI3K/Akt signaling pathway. *Int J Mol Sci* (2018) 19(11):3634. doi: 10.3390/ijms19113634

30. Chen GM, Hu N, Liu L, Xie SS, Wang P, Li J, et al. Pharmacokinetics of verapamil in diabetic rats induced by combination of high-fat diet and streptozotocin injection. *Xenobiotica* (2011) 41(6):494–500. doi: 10.3109/00498254.2011.558933

31. Zhang C, Deng J, Liu D, Tuo X, Xiao L, Lai B, et al. Nuciferine ameliorates hepatic steatosis in high-fat diet/streptozocin-induced diabetic mice through a PPARα/PPARγ coactivator-1α pathway. *Br J Pharmacol* (2018) 175(22):4218–28. doi: 10.1111/bph.14482

32. Kim JH, Kim AR, Choi YH, Kim A, Sohn Y, Woo GH, et al. Intermittent PTH administration improves alveolar bone formation in type 1 diabetic rats with periodontitis. *J Transl Med* (2018) 16(1):70. doi: 10.1186/s12967-018-1438-2

33. Zhu Y, Jia Y, Wang Y, Xu J, Chai Y. Impaired bone regenerative effect of exosomes derived from bone marrow mesenchymal stem cells in type 1 diabetes. *Stem Cells Transl Med* (2019) 8(6):593–605. doi: 10.1002/sctm.18-0199

34. Romaní-Pérez M, Outeiriño-Iglesias V, Moya CM, Santisteban P, González-Matías LC, Vigo E, et al. Activation of the GLP-1 receptor by liraglutide increases ACE2 expression, reversing right ventricle hypertrophy, and improving the production of SP-a and SP-b in the lungs of type 1 diabetes rats. *Endocrinology* (2015) 156(10):3559–69. doi: 10.1210/en.2014-1685

35. Lin P, Niimi H, Ohsugi Y, Tsuchiya Y, Shimohira T, Komatsu K, et al. Application of ligature-induced periodontitis in mice to explore the molecular mechanism of periodontal disease. *Int J Mol Sci* (2021) 22(16):8900. doi: 10.3390/ijms22168900

36. Wang Z, Wang G, Wang Y, Liu Q, Li H, Xie P, et al. Omp31 of brucella inhibits NF-κB NFκB-p65 signaling pathway by inducing autophagy in BV-2 microglia. *Neurochem Res* (2021) 46(12):3264–72. doi: 10.1007/s11064-021-03429-4

37. Greabu M, Giampieri F, Imre MM, Mohora M, Totan A, Pituru SM, et al. Autophagy, one of the main steps in periodontitis pathogenesis and evolution. *Molecules* (2020) 25(18):4338. doi: 10.3390/molecules25184338

38. Klionsky DJ, Abdalla FC, Abeliovich H, Abraham RT, Acevedo-Arozena A, Adeli K, et al. Guidelines for the use and interpretation of assays for monitoring autophagy. *Autophagy* (2012) 8(4):445–544. doi: 10.4161/auto.19496

39. Jeong SJ, Zhang X, Rodriguez-Velez A, Evans TD, Razani B. p62/SQSTM1 and selective autophagy in cardiometabolic diseases. *Antioxid Redox Signal* (2019) 31(6):458–71. doi: 10.1089/ars.2018.7649

40. Bartolomé A, López-Herradón A, Portal-Núñez S, García-Aguilar A, Esbrit P, Benito M, et al. Autophagy impairment aggravates the inhibitory effects of high glucose on osteoblast viability and function. *Biochem J* (2013) 455(3):329–37. doi: 10.1042/BJ20130562

41. Tong J, Lai Y, Yao YA, Wang XJ, Shi YS, Hou HJ, et al. Qiliqiangxin rescues mouse cardiac function by regulating AGTR1/TRPV1-mediated autophagy in STZ-induced diabetes mellitus. *Cell Physiol Biochem* (2018) 47(4):1365–76. doi: 10.1159/000490822

42. Wang Y, He D, Ni C, Zhou H, Wu S, Xue Z, et al. Vitamin d induces autophagy of pancreatic β-cells and enhances insulin secretion. *Mol Med Rep* (2016) 14(3):2644–50. doi: 10.3892/mmr.2016.5531

43. Turkoglu O, Emingil G, Eren G, Atmaca H, Kutukculer N, Atilla G. Gingival crevicular fluid and serum hCAP18/LL-37 levels in generalized aggressive periodontitis. *Clin Oral Investig* (2017) 21(3):763–9. doi: 10.1007/s00784-016-1834-z

44. Wang TT, Nestel FP, Bourdeau V, Nagai Y, Wang Q, Liao J, et al. Cutting edge: 1,25-dihydroxyvitamin D3 is a direct inducer of antimicrobial peptide gene expression. *J Immunol* (2004) 173(5):2909–12. doi: 10.4049/jimmunol.173.5.2909

45. Gombart AF, Borregaard N, Koeffler HP. Human cathelicidin antimicrobial peptide (CAMP) gene is a direct target of the vitamin d receptor and is strongly up-regulated in myeloid cells by 1,25-dihydroxyvitamin D3. *FASEB J* (2005) 19 (9):1067–77. doi: 10.1096/fj.04-3284com

46. Yuk JM, Shin DM, Lee HM, Yang CS, Jin HS, Kim KK, et al. Vitamin D3 induces autophagy in human monocytes/macrophages *via* cathelicidin. *Cell Host Microbe* (2009) 6(3):231–43. doi: 10.1016/j.chom.2009.08.004

47. Nilsson BO. Mechanisms involved in regulation of periodontal ligament cell production of pro-inflammatory cytokines: Implications in periodontitis. *J Periodontal Res* (2021) 56(2):249–255. doi: 10.1111/jre.12823

Frontiers in Endocrinology

Explores the endocrine system to find new therapies for key health issues

The second most-cited endocrinology and metabolism journal, which advances our understanding of the endocrine system. It uncovers new therapies for prevalent health issues such as obesity, diabetes, reproduction, and aging.

Discover the latest Research Topics

See more →

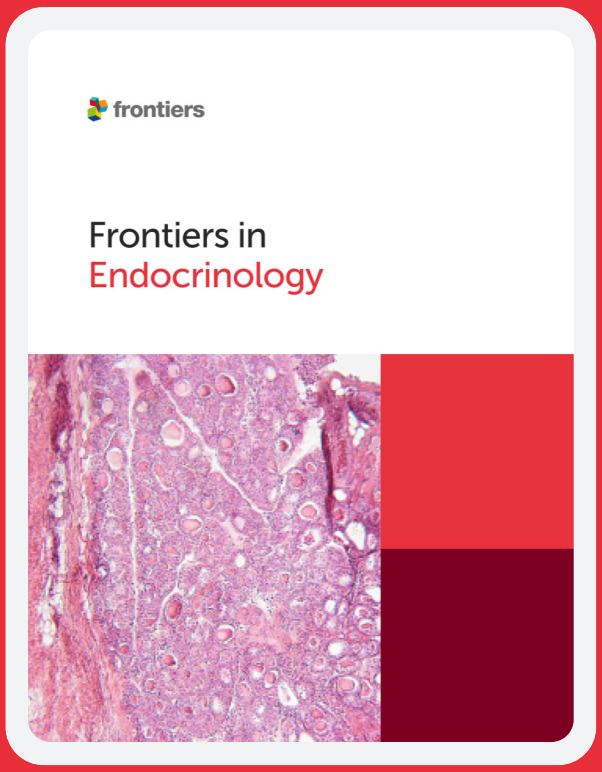

Frontiers

Avenue du Tribunal-Fédéral 34
1005 Lausanne, Switzerland
frontiersin.org

Contact us

+41 (0)21 510 17 00
frontiersin.org/about/contact